

**Towards Understanding the Pathway for Hydrogen Sulfide Metabolism**

By Scott L. Melideo

July 2015

A Dissertation Presented to the Faculty of Drexel University College of Medicine  
in partial fulfillment of the Requirements for the Degree of  
Doctor of Philosophy in Biochemistry



---

Patrick Loh, Ph.D.  
Professor  
Department of Biochemistry &  
Molecular Biology



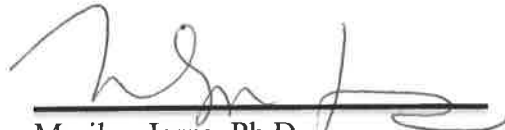
---

Simon Cocklin, Ph.D.  
Assistant Professor  
Department of Biochemistry &  
Molecular Biology



---

Alexander Mazin, Ph.D.  
Professor  
Department of Biochemistry &  
Molecular Biology



---

Marilyn Jorns, Ph.D.  
Professor  
Department of Biochemistry &  
Molecular Biology



---

Craig Leach, Ph.D.  
Manager, Biology  
The Pipeline Futures Group R&D  
Alternative Discovery & Development  
GlaxoSmithKline

**Towards Understanding the Pathway for Hydrogen Sulfide Metabolism**

By Scott L. Melideo

August 2015

A Dissertation Presented to the Faculty of Drexel University College of Medicine in  
partial fulfillment of the Requirements for the Degree of  
Doctor of Philosophy in Biochemistry



© Copyright 2015  
Scott L. Melideo. All Rights Reserved

## Acknowledgements

I would like to first and foremost thank my extended and immediate family for all their love and support during my entire time as a student. To my parents Beth and Leon Melideo and my grandma, Concetta Melideo, thank you for always being there for me day or night, I do not think we could be any closer. Also to my grandfather, Ralph Melideo, I know you if you were still alive, you would have shown me the same support. To my girlfriend, Deanna Shelly, thank you for your love, support, and positive attitude during this final stage of my Ph.D. and the start of my life after school. I would also like to say thank you to all my friends who have helped me during my time in college or just let me vent for hours on end over the years, I am truly grateful. To my tennis friends, thank you all for giving me a reason to go outside. To Tim Foley (my mentor from The University of Scranton) thank you for all your support and advice not only during my time at Scranton but at Drexel as well. Also without you I would have never discovered my passion for science and gotten a Ph.D. To my committee Pat Loll (chair and program director), Alex Mazin, Simon Cocklin, and Craig Leach thank you for your support and guidance during my thesis. To Michael R. Jackson, without you being in the lab over my entire time as a Ph.D. candidate I do not think I would have made it without your support and guidance. Also thank you for our non-science talk to help make it through the long days. Lastly, to Marilyn Jorns, one of the smartest individuals I know, thank you for giving me the opportunity to rotate and then join your lab for my thesis work. Your lab has become my home more so than my apartment over for the last five years and words cannot describe my gratitude.



## Table of Contents

List of Tables .....	ix
List of Illustrations .....	xi
Abstract .....	xiv
Chapter 1: Introduction .....	1
1.1 Biosynthesis of hydrogen sulfide .....	1
1.2 Mammalian metabolism of hydrogen sulfide .....	2
1.3 Previously proposed pathways for hydrogen sulfide metabolism .....	2
1.4 Sulfide:quinone Oxidoreductase .....	4
1.4.1 Background, classification and general purification .....	4
1.4.2 <i>Acidithiobacillus ferrooxidans</i> SQOR .....	6
1.4.3 <i>Aquifex aeolicus</i> SQOR .....	10
1.4.4 <i>Acidianus ambivalens</i> SQOR .....	14
1.4.5 <i>Rhodobacter capsulatus</i> SQOR .....	16
1.4.6 <i>Oscillatoria limnetica</i> SQOR .....	18
1.4.7 <i>Geobacillus stearothermophilus</i> SQOR .....	19
1.4.8 <i>Pseudomonas putida</i> SQOR .....	21
1.4.9 <i>Schizosaccharomyces pombe</i> SQOR .....	21
1.4.10 <i>Arenicola marina</i> SQOR .....	23
1.5 Hydrogen sulfide signaling .....	24
1.6 Diseases associated with abnormal hydrogen sulfide levels .....	25
1.6.1 Hydrogen sulfide's role in cardiovascular health and pathology .....	26
1.6.2 Hydrogen sulfide's other physiological roles .....	27

1.7 Summary .....	29
Chapter 2: Human sulfide:quinone oxidoreductase catalyzes the first step in hydrogen sulfide metabolism and produces a sulfane sulfur metabolite .....	36
2.1 Abstract .....	36
2.2 Introduction .....	37
2.3 Experimental procedures .....	38
2.3.1 Materials .....	38
2.3.2 Expression of human SQOR in <i>Escherichia coli</i> .....	38
2.3.3 Purification of recombinant human SQOR .....	39
2.3.4 Flavin analysis .....	41
2.3.5 Activity and protein assays .....	41
2.3.6 Product analysis .....	42
2.3.7 Spectroscopy .....	43
2.4 Results .....	43
2.4.1 Expression and purification of recombinant human SQOR .....	43
2.4.2 Sulfide oxidation with cyanide as the acceptor of the sulfane sulfur .....	45
2.4.3 Identification of a putative physiological acceptor of the sulfane sulfur .....	45
2.4.4 Sulfide oxidation in the absence of cyanide or sulfite .....	46
2.4.5 Identification of the sulfide oxidation product formed in the “acceptor-free” reaction .....	47
2.4.6 Effect of pH on catalysis by human SQOR .....	50
2.4.7 Steady-state kinetic parameters for sulfide oxidation by SQOR with different acceptors of the sulfane sulfur .....	51
2.4.8 Anaerobic reduction of SQOR with sulfide .....	52

2.5 Discussion .....	53
2.5.1 Role of SQOR in the biosynthesis of thiosulfate .....	54
2.5.2 Mechanism of SQOR catalysis .....	57
2.5.3 Concluding remarks .....	59
Chapter 3: Biosynthesis of a central intermediate in hydrogen sulfide metabolism by a novel human sulfurtransferase and its yeast ortholog .....	72
3.1 Abstract .....	72
3.2 Introduction .....	73
3.3 Experimental procedures .....	76
3.3.1 Materials .....	76
3.3.2 Expression of yeast RDL1 in <i>Escherichia coli</i> .....	76
3.3.3 Purification of recombinant yeast RDL1 .....	77
3.3.4 Expression of Human TSTD1 Isoforms 1, 2 and 3 in <i>E. coli</i> .....	78
3.3.5 Purification of recombinant human TSTD1 Isoforms 1, 2, and 3 .....	79
3.3.6 Protein assays .....	80
3.3.7 Catalytic assays with thiosulfate as sulfane sulfur donor and glutathione as acceptor .....	80
3.3.8 Effect of sulfur dioxygenase on catalytic assays with glutathione and thiosulfate .....	81
3.3.9 Steady-state kinetic analysis of the thiosulfate:glutathione sulfurtransferase reaction .....	81
3.3.10 Sulfurtransferase reactions with <i>p</i> -toluenethiosulfonate as sulfane sulfur donor and glutathione as acceptor .....	81
3.3.11 Substitution of glutathione by alternate small molecule acceptors in sulfurtransferase reactions with thiosulfate as sulfane sulfur donor .....	82

3.3.12 Mutation of the single cysteine in yeast RDL1 or human TSTD1 Isoform 1 .....	82
3.3.13 Detection of cysteine persulfide in yeast RDL1 or human TSTD1	83
3.4 Results .....	83
3.4.1 Use of bioinformatics to identify potential candidate gene(s) for yeast thiosulfate sulfurtransferase .....	83
3.4.2 Expression and purification of recombinant yeast RDL1 .....	84
3.4.3 Does recombinant yeast RDL1 exhibit thiosulfate:glutathione sulfurtransferase activity .....	84
3.4.4 Use of bioinformatics to identify a potential candidate gene for human thiosulfate sulfurtransferase .....	85
3.4.5 Expression and purification of recombinant human TSTD1 Isoforms 1, 2, and 3 .....	86
3.4.6 Do human TSTD1 Isoforms 1, 2, and/or 3 exhibit thiosulfate:glutathione sulfurtransferase activity .....	87
3.4.7 Use of sulfur dioxygenase to distinguish between thiosulfate:glutathione sulfurtransferase versus thiosulfate reductase activity .....	88
3.4.8 Steady-state kinetics of the yeast RDL1 or human TSTD1 reaction with thiosulfate and glutathione in the presence of sulfur dioxygenase .....	89
3.4.9 Reaction of yeast RDL1 or human TSTD1 with a chromogenic substrate as an alternate sulfane sulfur donor .....	90
3.4.10 Reaction of yeast RDL1 or human TSTD1 with alternate sulfane sulfur acceptors .....	92
3.4.11 Role of the single cysteine residue in yeast RDL1 or human TSTD1 .....	93
3.4.12 Identification of bacterial SDO-TSTD1 fusion proteins .....	94
3.4.13 Are human-like SQORs found in bacteria that express SDO-TSTD1 fusion proteins .....	96
3.5 Discussion .....	97

3.5.1 Functional interaction between human SDO and human TSTD1 or yeast RDL1 .....	99
3.5.2 Phylogenetic association of human TSTD1 and human SDO .....	101
3.5.3 Concluding remarks .....	102
3.6 Acknowledgments.....	102
Chapter 4: Characterization of the SDO-TSTD1 fusion enzyme from <i>Nitrosococcus oceani</i> .....	118
4.1 Introduction.....	118
4.2 Experimental procedure .....	121
4.2.1 Materials .....	121
4.2.2 Expression of wild type and mutant Noc_2007 .....	122
4.2.3 Purification of recombinant wild type and mutant fusion protein .....	123
4.2.4 Protein assay .....	124
4.2.5 Iron analysis .....	124
4.2.6 Producing glutathione persulfide .....	125
4.2.7 Catalytic assays of Noc_2007 using an oxygen electrode .....	125
4.2.8 TST catalytic assay of Noc_2007 mutants using a sulfite discontinuous assay .....	126
4.3 Results.....	126
4.3.1 Purification and iron analysis of recombinant <i>Nitrosococcus oceani</i> SDO-TSTD1 fusion protein .....	126
4.3.2 Mutagenesis of the TSTD1 Domain .....	128
4.3.3 Mutagenesis of the SDO Domain .....	129
4.3.4 Is the TSTD1 domain of the fusion protein bidirectional? .....	130
4.4 Discussion .....	131

Chapter 5: Discussion and future directions .....	138
Appendices.....	144
Appendix 1: Supplemental Figures for Chapter 2 .....	144
Appendix 2: Supplemental Figures and Tables for Chapter 3 .....	149
Appendix 3: Supplemental Figure for Chapter 4.....	160
List of References .....	162
Vita.....	182

### List of Tables

Table 1.1 Properties of SQORs from different organisms.....	30
Table 2.1 Purification of Recombinant SQOR from <i>E. coli</i> .....	60
Table 2.2 Spectral and Catalytic Properties of Recombinant Human SQOR.....	61
Table 2.3 Stoichiometry of Products formed in the SQOR Reaction with Different Acceptors of the Sulfane Sulfur .....	61
Table 2.4 Effect of pH on Sulfide Oxidation by SQOR with Different Acceptors of the Sulfane Sulfur .....	62
Table 2.5 Steady-state Kinetic Parameters for Three Reactions Catalyzed by Human SQOR .....	63
Table 3.1 Potential Candidate Genes for Yeast Thiosulfate Sulfurtransferase.....	103
Table 3.2 Steady-State Kinetic Parameters for Thiosulfate:Glutathione Sulfurtransferase Reactions Catalyzed by Yeast RDL1 or Human TSTD1	104
Table 3.3 BLASTp Search of the NCBI Database of Human Proteins Using Yeast RDL1 as the Query Sequence .....	105
Table 3.4 Apparent Steady-State Kinetic Parameters Observed for Yeast RDL1 or Human TSTD1 Reactions with Various Sulfane Sulfur Acceptors and Thiosulfate as Donor.....	106
Table 3.5 Detection of Cysteine Persulfide in RDL1 or TSTD1 Isolated by Gel Filtration after Reaction with Thiosulfate.....	106
Table 3.6 BLASTp Search of the NCBI Database of Human Proteins Using Bacterial Fusion Proteins as the Query Sequence .....	107
Table 4.1. Primers Used for Mutagenesis of <i>Noc_2007</i> .....	134
Table 4.2 Ratio of Iron to Enzyme.....	134
Table 4.3 Rate of Wild Type and Mutant <i>Noc_2007</i> Compared to Human TSTD1 and SDO Enzymes .....	135

Table 4.4 SDO Reaction: Determining the Mole Ratio of a Mole of Oxygen Consumed to a Mole of Glutathione Persulfide for Human SDO and Wild Type and Cys322Ser of Noc_2007 .....	135
Appendix 2 Table 1 Primers used for PCR reaction.....	149
Appendix 2 Table 2 BLASTp Search of the Bacterial Proteomes that Contain SDO-TSTD1 Fusion Proteins Using Human SQOR as the Query Sequence .....	150



## List of Illustrations

Scheme 1.1 Proposed catalytic mechanism of <i>Acidithiobacillus ferrooxidans</i> SQOR .....	31
Scheme 1.2 Proposed catalytic mechanism of <i>Aquifex aeolicus</i> SQOR.....	32
Scheme 1.3 Proposed catalytic mechanism of <i>Acidianus ambivalens</i> SQOR .....	33
Scheme 1.4 Proposed catalytic mechanism of <i>Rhodobacter capsulatus</i> SQOR .....	34
Scheme 1.5 Proposed catalytic mechanism of <i>Arenicola marina</i> SQOR.....	35
Scheme 2.1 Proposed pathways for H <sub>2</sub> S metabolism in (i) Glutathione-Depleted Cells or Mitochondria (path A) and (ii) Untreated Cells or Intact Animals (paths A and B).....	64
Scheme 2.2 The catalytic mechanism proposed for SQOR is indicated by the steps (1-5) enclosed within the dotted rectangle.....	65
Figure 2.1 Expression of recombinant human SQOR .....	66
Figure 2.2 Absorption spectra of native and denatured SQOR .....	67
Figure 2.3 Effect of sulfite on the spectral course of SQOR catalytic assays .....	68
Figure 2.4 Reaction of sulfite with the sulfur oxidation product formed during the apparent “acceptor-free” oxidation of sulfide by SQOR .....	69
Figure 2.5 Effect of pH on the rate of sulfide oxidation observed with SQOR in the presence or absence of sulfite or cyanide .....	70
Figure 2.6 Anaerobic reaction of SQOR with sulfide and CoQ <sub>1</sub> .....	71
Scheme 3.1 Proposed scheme for mammalian hydrogen sulfide metabolism.....	109
Figure 3.1 Purification of recombinant yeast RDL1 .....	110
Figure 3.2 Steady-state kinetic analysis of the thiosulfate:glutathione sulfurtransferase reaction catalyzed by recombinant yeast RDL1 .....	111
Figure 3.3 Purification of recombinant human TSTD1 isoform 1 with a cleavable N-terminal His-SUMO tag .....	112

Figure 3.4 Steady-state kinetic analysis of the thiosulfate:glutathione sulfurtransferase reaction catalyzed by recombinant human TSTD1 .....	113
Figure 3.5 Effect of human SDO on thiosulfate:glutathione sulfurtransferase reactions catalyzed by human TSTD1 or yeast RDL1 .....	114
Figure 3.6 Reaction of recombinant yeast RDL1 or human TSTD1 with <i>p</i> -toluenethiosulfonate ( $p\text{-Tol-SO}_2\text{S}^-$ ) and glutathione as sulfane sulfur donor and acceptor, respectively .....	115
Figure 3.7 The active site loop and putative catalytic cysteine in RDL1 and TSTD1 ....	116
Figure 3.8 Phylogenetic tree of SQOR homologs .....	117
Figure 4.1 Sequence alignment of human SDO or human TSTD1 with the N-terminal SDO-like or the C-terminal TSTD1-like domain, respectively, in Noc_2007 .....	136
Figure 4.2 Expression of recombinant <i>Nitrosococcus</i> oceanii Noc_2007 .....	137
Appendix 1 Figure 1 The nucleotide sequence of the synthetic gene used to express recombinant SQOR (upper case) is compared with the original gene sequence (lower case) .....	144
Appendix 1 Figure 2 Spectral course of sulfide oxidation by SQOR in the presence of cyanide and $\text{CoQ}_1$ .....	145
Appendix 1 Figure 3 Reaction of dithiothreitol (DTT) with the sulfur oxidation product formed during the apparent “acceptor-free” oxidation of sulfide by SQOR .....	146
Appendix 1 Figure 4 Spectral course of sulfide oxidation by SQOR in the presence of glutathione and $\text{CoQ}_1$ .....	147
Appendix 1 Figure 5 Effect of sulfide concentration on the observed rate of reduction of $\text{CoQ}_1$ .....	148
Appendix 2 Figure 1 The nucleotide sequence of the synthetic gene used to express recombinant TSTD1 isoform 1 (upper case) is compared with the original gene sequence (lower case) .....	151
Appendix 2 Figure 2 The nucleotide sequence of the synthetic gene used to express recombinant TSTD1 isoform 2 (upper case) is compared with the original gene sequence (lower case).....	152
Appendix 2 Figure 3 The nucleotide sequence of the synthetic gene used to express recombinant TSTD1 isoform 3 (upper case) is compared with the original gene sequence	

(lower case). The top line shows the amino acid sequence of isoform 3.....	153
Appendix 2 Figure 4 Alignment of human TSTD1 isoforms. Amino acids encoded across a splice junction and cysteines are highlighted in yellow and red, respectively.....	154
Appendix 2 Figure 5 Purification of recombinant human TSTD1 isoform 2 with a cleavable N-terminal His-SUMO tag.....	155
Appendix 2 Figure 6 Purification of recombinant human TSTD1 isoform 3 with a cleavable N-terminal His- SUMO tag.....	156
Appendix 2 Figure 7 Spectral properties of p-toluenethiosulfonate (p-Tol-SO <sub>2</sub> S <sup>-</sup> ) and p-toluenesulfonite (p- Tol-SO <sub>2</sub> <sup>-</sup> ).....	157
Appendix 2 Figure 8 Multiple sequence alignment of selected SDO-TSTD1 bacterial fusion proteins. The black box marks a poorly conserved, variable length linker (9 to 52 amino acids) between the N-terminal SDO-like domain (230 or 231 amino acids) and the C-terminal TSTD1-like domain (96 to 105 amino acids).....	158
Appendix 2 Figure 9 Multiple sequence alignment of human SDO or human TSTD1 with the N-terminal SDO-like or the C-terminal TSTD1-like domain, respectively, in selected bacterial SDO-TSTD1 fusion proteins.....	159
Appendix 3 Figure 1 The nucleotide sequence of the synthetic gene used to express recombinant Noc_2007 (upper case) is compared with the original gene sequence (lower case) .....	160

**Abstract**

Toward Understanding the Metabolic Pathway of Hydrogen Sulfide

Scott L. Melideo

Mentor: Marilyn Schuman Jorns, PhD

Hydrogen sulfide ( $H_2S$ ) is the most recently identified member of a small family of labile biological signaling molecules, termed gasotransmitters, which includes nitric oxide and carbon monoxide.  $H_2S$  is the only gasotransmitter that is enzymatically metabolized a process that occurs in the mitochondria.  $H_2S$  needs to be tightly regulated because it is toxic at high concentrations and leads to physiological defects at low concentrations. For example, a genetic defect that affects the metabolic pathway of  $H_2S$  is ethylmalonic encephalopathy, a fatal disorder that is characterized by extremely high levels of  $H_2S$ . On the other hand, animal model studies provide compelling evidence for a functional association between abnormally low levels of  $H_2S$  and cardiovascular disease. In light of  $H_2S$ 's critical role, the goal of this thesis was to identify and characterize two human enzymes that are proposed to comprise part of the metabolic pathway of  $H_2S$  in mammals: Sulfide:quinone oxidoreductase (SQOR) and thiosulfate:glutathione sulfurtransferase (TST).

The present study postulates that human sulfide:quinone oxidoreductase (SQOR), a membrane-bound enzyme, catalyzes the first step in the mitochondrial metabolism of  $H_2S$ . The reaction involves a two-electron oxidation of  $H_2S$  to  $S^0$  (sulfane sulfur) and uses coenzyme Q as an electron acceptor. The fact that SQOR is a membrane-associated

protein has made its expression and isolation challenging. We successfully purified and characterized human SQOR. Cyanide, sulfite, or sulfide can act as the sulfane sulfur acceptor in reactions that produce thiocyanate, thiosulfate, or a putative sulfur analog of hydrogen peroxide ( $\text{H}_2\text{S}_2$ ), respectively. Thiosulfate is a known intermediate in the oxidation of  $\text{H}_2\text{S}$  within animals and the major product formed in glutathione-depleted cells or mitochondria. Importantly, oxidation of  $\text{H}_2\text{S}$  by SQOR with sulfite as the sulfane sulfur acceptor is rapid and highly efficient at physiological pH ( $k_{\text{cat}}/K_{\text{m},\text{H}_2\text{S}} = 2.9 \times 10^7 \text{ M}^{-1} \text{ s}^{-1}$ ). We propose that this highly efficient oxidation of  $\text{H}_2\text{S}$  by SQOR is the predominant source of the thiosulfate in mammalian tissues and that sulfite is the physiological acceptor of the sulfane sulfur. Our proposal opposes an alternative hypothesis that glutathione is an acceptor of the sulfane sulfur, which we have compelling evidence against.

The discovery that sulfite was the physiological acceptor of the sulfane sulfur and SQOR produced thiosulfate, led us to postulate a role in  $\text{H}_2\text{S}$  metabolism for a TST that transfers the sulfane sulfur of thiosulfate to glutathione producing  $\text{GSS}^-$  and sulfite. We postulate that the TST links together the SQOR and sulfur dioxygenase (SDO) steps in the pathway because it consumes the thiosulfate from the SQOR reaction and produces glutathione persulfide ( $\text{GSS}^-$ ), a substrate required for SDO. Although an active TST enzyme had been found in yeast, attempts by other laboratories to isolate and characterize the mammalian enzyme have been unsuccessful.

We also discovered genes that encode for human and yeast TST (TSTD1 and RDL1, respectively). We demonstrated that  $\text{GSS}^-$  was released into solution and consumed by SDO. Additionally,  $\text{GSS}^-$  is a potent inhibitor of TSTD1 and RDL1, as

judged by initial rate accelerations and  $\geq 25$ -fold lower  $K_m$  values for glutathione observed in the presence of SDO. Our studies support the conclusion that TST is the missing link between the SQOR and SDO reactions.

The discovery of bacterial proteins that are fusions of SDO and TSTD1 provides phylogenetic evidence of the association of these enzymes. We successfully purified and characterized the fusion protein from *Nitrosococcus oceani* encoded by the gene *Noc\_2007*. We showed that operationally, the fusion is a glutathione-dependent thiosulfate dioxygenase, which is the TST reaction followed by the SDO reaction. The thiosulfate dioxygenase reaction requires one mole of thiosulfate in the presence of oxygen to produce two moles of sulfite with a catalytic amount of glutathione. Lastly, the TST reaction is the apparent rate-limiting step in the thiosulfate dioxygenase reaction.

From this study, we propose a new pathway for  $H_2S$  metabolism, which opens the door to future research.



## Chapter 1: Introduction

### 1.1 Biosynthesis of hydrogen sulfide

Hydrogen sulfide is the newest gasotransmitter, a family of gases that diffuse through membranes and act as biological signaling molecules. Nitric oxide (NO) and carbon monoxide (CO) are the only other known gasotransmitters. Their half-life can be on the order of seconds to minutes. Hydrogen sulfide exists in three forms:  $\text{H}_2\text{S}$ ,  $\text{HS}^-$  (the predominant species at physiological pH) and  $\text{S}^{2-}$ . For brevity, we will refer to the total pool as  $\text{H}_2\text{S}$  or sulfide.  $\text{H}_2\text{S}$  was initially regarded as the least important gasotransmitter, however the publication of more than 250 reviews on  $\text{H}_2\text{S}$  within the last few years has proved otherwise.  $\text{H}_2\text{S}$  is the only gasotransmitter that is enzymatically metabolized. Although the pathway for  $\text{H}_2\text{S}$  metabolism is poorly understood, the three major biological sources of  $\text{H}_2\text{S}$  are well characterized.  $\text{H}_2\text{S}$  biosynthesis enzymes, cystathionine  $\beta$ -synthase (CBS) and cystathionine  $\gamma$ -lyase (CSE) were originally discovered as part of the transsulfuration pathway. CBS produces  $\text{H}_2\text{S}$  in a condensation reaction requiring cysteine and homocysteine and is the main producer of  $\text{H}_2\text{S}$  in the brain. CSE is the major producer of  $\text{H}_2\text{S}$  from cysteine in peripheral tissues. Another source of  $\text{H}_2\text{S}$  production from cysteine is a pathway involving cysteine aminotransferase and 3-mercaptopyruvate sulfurtransferase (1). Although,  $\text{H}_2\text{S}$  has physiological effects within mammals and plants, only the effects in mammals will be discussed. For more information on  $\text{H}_2\text{S}$ 's role within plants please see a recent review by Hancock and Whiteman (2).



## 1.2 Mammalian metabolism of hydrogen sulfide

When radiolabeled  $\text{H}_2\text{S}$  ( $\text{H}_2\text{S}^{35}$ ) is injected subcutaneously in mammals,  $\text{H}_2\text{S}$  is oxidized into radiolabeled organic sulfur compounds that are removed from the animal through the urine (3). One of those compounds, sulfate, produced by the oxidation of sulfite by sulfite oxidase, is the major product of  $\text{H}_2\text{S}$  metabolism within the liver (4). Sulfite oxidase was originally studied because of its role in the oxidative degradation pathway of cysteine and methionine (5). Moreover, thiosulfate ( $\text{SSO}_3^{2-}$ ), is a known intermediate in the metabolic pathway of  $\text{H}_2\text{S}$  to sulfate ( $\text{SO}_4^{2-}$ ) and is found within animals and perfused liver (4, 6-11). Thiosulfate is not only an intermediate in the pathway but can be a major product as shown within the colon of mammals, a tissue that must detoxify large amounts of  $\text{H}_2\text{S}$  that are produced by sulfate-reducing bacteria (12, 13). Furthermore,  $\text{H}_2\text{S}$  oxidation to sulfate or thiosulfate has been shown to be dependent on glutathione (4, 7).

## 1.3 Previously proposed pathways for hydrogen sulfide metabolism

Hildebrandt and Grieshaber proposed a pathway for the metabolism of  $\text{H}_2\text{S}$  to thiosulfate in mammals and invertebrates based upon the knowledge at that time (14). The first step in the proposed mitochondrial metabolism of  $\text{H}_2\text{S}$  is catalyzed by sulfide:quinone oxidoreductase (SQOR), an inner mitochondrial membrane-bound enzyme with a flavin adenine dinucleotide (FAD) cofactor, which catalyzes a two-electron oxidation of  $\text{H}_2\text{S}$  to sulfane sulfur ( $\text{S}^0$ ) using coenzyme Q as the electron acceptor (14-16). Reduced coenzyme Q can then be shunted to the electron transport chain, making  $\text{H}_2\text{S}$  the only inorganic compound in mammals that can produce ATP via the electron transport chain (17). Within mammals SQOR requires an acceptor for the

sulfane sulfur, which was at the time unknown. Cyanide has been used as a substitute because it is known to be an acceptor of sulfane sulfur and produces thiocyanate, which can easily be quantified (14, 18-20). Hildebrandt and Grieshaber postulated that glutathione ( $\text{GS}^-$ ) is the physiological acceptor of the sulfane sulfur producing glutathione persulfide ( $\text{GSS}^-$ ) for the next step in the pathway (14).

Hildebrandt and Grieshaber postulated that the second enzyme in the metabolism of  $\text{H}_2\text{S}$  is catalyzed by sulfur dioxygenase (SDO). SDO is a mitochondrial matrix enzyme, requiring oxygen to catalyze the four-electron oxidation of the sulfane sulfur in glutathione persulfide ( $\text{GSS}^-$ ) to produce sulfite ( $\text{SO}_3^{2-}$ ) and glutathione (14, 21, 22). Human SDO belongs to a superfamily of enzymes called dioxygen-activating mononuclear non-heme iron(II) enzymes that require a 2-His-1-carboxylate facial triad for iron binding (23, 24). Mutations of the enzyme have been linked to ethylmalonic encephalopathy, a disease associated with high levels of  $\text{H}_2\text{S}$  and thiosulfate (for more information on ethylmalonic encephalopathy see, section 1.6 Diseases associated with abnormal  $\text{H}_2\text{S}$  levels) (22, 25). SDO activity has also been detected within bacteria (26, 27).

Hildebrandt and Grieshaber postulated that the third step requires a sulfur transferase, rhodanese (thiosulfate:cyanide sulfurtransferase) (14). In the "forward" direction rhodanese catalyzes the transfer of the sulfane sulfur on thiosulfate to cyanide producing thiocyanate and sulfite. In their pathway, Hildebrandt and Grieshaber postulate that rhodanese operates in the "reverse" direction by catalyzing the conversion of glutathione persulfide and sulfite to thiosulfate and glutathione (14).

Thiosulfate is a final product of H<sub>2</sub>S metabolism in the pathway postulated by Hildebrandt and Grieshaber. However, these authors also propose a two-step process for the conversion of thiosulfate to sulfate, involving a thiosulfate reductase and sulfite oxidase (14). The thiosulfate reductase will catalyze the transfer of the sulfane sulfur from thiosulfate to glutathione producing sulfite and glutathione persulfide. In a non-enzymatic reaction, the glutathione persulfide generated by the thiosulfate reductase is thought to react with glutathione to produce H<sub>2</sub>S and oxidize glutathione (GSSG). The sulfite product will be oxidized to sulfate by sulfite oxidase.

## **1.4 Sulfide:quinone Oxidoreductase**

### **1.4.1 Background, classification and general purification**

This section contains a background on SQORs, followed by a summary of their classification, and then a detailed review of selected SQORs. SQOR as mentioned above, is a membrane-associated mitochondria protein. The fact that SQOR is a membrane-associated protein has made it challenging to express and isolate the enzyme. The enzyme was first isolated from *O. limnetica* and identified as a flavoprotein because it contained a FAD cofactor (28-30). Since then, SQOR has been studied in many organisms ranging from lugworm to bacteria (19, 31-34). Some SQORs bind the FAD cofactor covalently, a feature shared by approximately 10% of known flavoproteins (35). The FAD in eukaryotic SQORs was postulated to be covalently attached to a conserved tyrosine residue (15). SQORs are part of the flavoprotein disulfide reductase superfamily (36). Within this superfamily SQORs are classified as group 1 enzymes which includes lipamide dehydrogenase, glutathione reductase, trypanothione reductase, and mycothione reductase (36). The group 1 enzymes have a super secondary structural

element called a Rossmann fold, which is commonly found in FAD and NAD(P) containing proteins. These enzymes not only require the FAD, but also a cysteine-cysteine disulfide bridge for a second redox-active center (15, 36). A notable difference between SQORs and the group 1 enzymes of flavoprotein disulfide reductase superfamily is that sulfide replaces NADPH as the electron donor.

Originally, SQORs were divided into three types based on the evolutionary origin of the gene found in bacteria and eukaryotes (37). Currently there are only three known crystal structures of SQOR, all from bacteria: (i) *Aquifex aeolicus*, (ii) *Acidianus ambivalens*, and (iii) *Acidithiobacillus ferrooxidans* (32-34). Recently, Marco et al. divided SQORs into 5 types (Type I-V) based on sequence fingerprints, in addition to an unclassified group (Type VI); Pham et al. proposed a similar classification system (38). From Marco et al.'s classification Type I enzymes contain a loop region that blocks the active site from the bulk solvent allowing for sulfide specificity and a C-terminus amphipathic helix with an elongated loop (15). The *A. aeolicus* and *A. ferrooxidans*, SQORs, for which the structures are known for are both Type I enzymes. Type II SQORs are found in some bacteria, pathogens, and all eukaryotes, except for plants (15, 18). Type III enzymes are found in green sulfur bacteria and Archaea; their physiological role in these organisms is currently unknown (15). Type IV enzymes are classified by five elongated loops throughout the protein. Type V SQORs have an elongated capping loop and a shorter C-terminus compared to Type I (15). The *A. ambivalens* SQOR, the third known structure, is a Type V SQOR.

The majority of groups that have purified SQOR have used detergents to solubilize the enzyme from the membrane (19, 28, 31, 32, 39-43). Interestingly, the *A.*

*ferrooxidans* SQOR did not require detergent for purification (33, 44, 45). Some groups have been able to detect SQOR activity within isolated mitochondria and thylakoids (14, 28, 46). Thylakoids are compartments that are bound to the membrane of cyanobacteria and the location of photosynthesis (light-dependent step). SQOR activity is typically measured under anaerobic conditions by monitoring the reduction of a quinone substrate, such as decylubiquinone. As mentioned above, mammalian SQORs require an acceptor for the sulfane sulfur, a feature apparently shared with other type II SQORs. In addition to mammalian SQORs, Type II enzymes include SQORs from lower eukaryotes and some bacteria. Unlike bacterial Type II enzymes, other types of bacterial SQORs do not appear to require an acceptor for the sulfane sulfur. Instead, these bacterial SQORs produce sulfane sulfur in the form of polysulfide chains or cyclooctasulfur rings (elemental sulfur, S<sub>8</sub>). Table 1.1 summarizes some properties reported for SQORs from various organisms. A detailed discussion of the results summarized in table 1.1 with selected SQORs is presented in sections 1.4.2-1.4.10.

#### **1.4.2 *Acidithiobacillus ferrooxidans* SQOR**

SQOR from *A. ferrooxidans*, a chemolithotrophic, iron-oxidizing bacterium, is a Type I SQOR that has been recently characterized and crystallized (33, 42, 44, 45). It is believed that these bacteria couple sulfide oxidation with carbon dioxide fixation, the process of converting inorganic carbon to organic carbon (47). In a study prior to isolating *A. ferrooxidans* SQOR, Kamimura's group showed that there was SQOR activity within isolated membranes (48). In a subsequent study, Kamimura's group succeeded in isolating natural SQOR without detergent. The purified enzyme had a molecular weight (MW) of 47 kDa (42, 48). The optimal pH for the enzymatic activity

was 7.0 (42). Zhang and Weiner, determined a similar pH optimum of 6.5-7.0 with recombinant SQOR (45).

Recombinant *A. ferrooxidans* SQOR was overexpressed in *E. coli* and isolated without detergent, as with the natural enzyme (45). With the recombinant enzyme, the FAD was determined to be non-covalently bound with greater than 95% of the FAD being released into solution (45). The spectrum of the purified enzyme exhibited two flavin absorption peaks, at 379 and 448 nm.

In the same study, mutagenesis was conducted to help elucidate the enzymatic mechanism. A common feature of Type I SQORs is three conserved cysteines. From sequence alignments the three conserved cysteine residues within *A. ferrooxidans* SQOR were hypothesized to be, Cys128, Cys160, and Cys356. The three residues were mutated along with two-conserved histidine residues (His 198 and His132) (33, 45). All five residues had significantly lower SQOR activity compared to the wild type enzyme, confirming their importance for activity (45).

To further elucidate the mechanism, stopped-flow experiments were performed to characterize the reductive half-reaction, by monitoring the reduction of the FAD visible absorption maximum at 448 nm for the wild type and mutant enzymes. The observed rate for the wild type enzyme with excess sulfide was almost 2-fold faster than when monitoring decylubiquinone reduction. The Cys128 and His132Ala mutations did not affect the FAD reductive half-reaction. The Cys160 and Cys356 mutations did not catalyze the FAD reductive half-reaction. These results show that Cys160 and Cys356 are required for the FAD reductive half-reaction and presumably comprise the redox-active

disulfide bridge. The His198 mutation catalyzed the FAD reductive half-reaction but its activity compared to the wild type enzyme was approximately 4-fold lower.

A crystal structure was also solved for *A. ferrooxidans* SQOR (33, 44). The recombinant enzyme was purified for crystallography under the same protocol used to isolate the enzyme for kinetic studies (33, 44, 45). The solved crystal structure had a resolution of 2.3 Å (33). For determining the structure of SQOR, two different crystal structures were used: (i) in the detergent dodecyl-maltoside and (ii) without detergent (33). In the solved crystal the enzyme forms a dimer. Each monomer contains two-consecutive Rossmann folds and two amphipathic helices at the C-terminus, which are most likely required for anchoring the enzyme within the membrane (33). Dimerization of SQOR occurs via the hydrophobic interactions at the C-terminus, which is observed with the other known structures of *A. aeolicus* and *A. ambivalens* SQOR (33).

Because the monomers are joined at the same hydrophobic region that interacts with the membrane, Cherney et al. proposed a slightly different structure based on the enzyme's binding energy,  $\Delta G^\circ$ , when it would be associated with the membrane (33). According to this model, the amphipathic helices are embedded  $\sim 20$  Å within the membrane; the FAD ring is located at the membrane-cytoplasm interface. This is to be expected, because the FAD transfers the electrons from soluble H<sub>2</sub>S to an insoluble quinone, located within the membrane. As shown biochemically by denaturing the enzyme, the FAD was non-covalently bound to the enzyme in the crystal structure. Located within the first Rossmann fold, the FAD prosthetic group is stabilized by van der Waals forces, electrostatic interactions, and hydrogen bonding with the enzyme (33). Even though there is a second Rossmann fold, a second molecule of FAD (or NAD)

cannot bind because there is a loop that prevents binding. The two cysteines (Cys160 and Cys356) that comprise the redox-active disulfide bridge are located on the re side of the FAD isoalloxazine ring, parallel to the ring, and  $\sim 5$  Å away from the ring (33).

The structure was also solved with bound decylubiquinone. Within the structure there are pockets, two of which contain the FAD cofactor and the decylubiquinone. Additionally, there is a channel that is proposed to allow for sulfide to enter the active site from the bulk solution. The redox-active disulfide bridge as expected, has access to the sulfide channel, with Cys356 closer to the bulk solvent. The decylubiquinone has its hydrophilic ring positioned within the enzyme near the si face of the isoalloxazine ring and its hydrophobic aliphatic chain pointed out, near the part of SQOR that is predicted to be within the membrane.

Zhang and Weiner, proposed a catalytic mechanism for sulfide oxidation by SQOR (Scheme 1.1). In the proposed mechanism the disulfide bridge is presumably between Cys356 and Cys160. Additionally, the third conserved cysteine residue, Cys128, exists as a protein-bound persulfide,  $\text{Cys128SS}^-$ , in the resting enzyme. The first step, involves a nucleophilic attack of sulfide at Cys356, forming a protein-bound persulfide,  $\text{Cys356SS}^-$  and the thiolate form of Cys160 (45). For the second step, the persulfide attacks the C(4a) position of the isoalloxazine ring forming a covalent FAD 4a-adduct. In the third step, there is a nucleophilic attack of  $\text{Cys160S}^-$  at the sulfur atom in the 4a-adduct, resulting in the formation of a trisulfide bridge ( $\text{Cys160S-SSCys356}$ ) and reduced FAD ( $\text{FADH}_2$ ). For the fourth step, the  $\text{FADH}_2$  is oxidized to FAD by transferring the electrons to ubiquinone forming ubiquinol. These four steps are repeated seven more times to form an octasulfur ring. The octasulfur ring is released by the nucleophilic attack



of Cys128SS<sup>-</sup> (the third conserved cysteine residue), forming a trisulfide bond with Cys160 (Cys128SSSCys160) (step 5). In the last step, Cys356 attacks the gamma sulfur on Cys160 regenerating the disulfide bridge and Cys128SS<sup>-</sup> persulfide (step 6).

### 1.4.3 *Aquifex aeolicus* SQOR

SQOR from *A. aeolicus* is another Type I SQOR that has been crystalized (49). *A. aeolicus* is a hyperthermophilic bacterium, which lives in environments of 60 °C and above. Additionally, it is a chemolithoautotrophic bacterium that does not require light as an energy source; instead, it obtains its energy from inorganic compounds including H<sub>2</sub>S. *A. aeolicus* SQOR activity was originally detected in isolated membranes (46). The observed activity was temperature dependent; the activity of the enzyme increased with increasing temperature (46). To determine how tightly SQOR associated with the membrane, Nubel et al. solubilized the membrane with sodium bromide or thesitol, a non-ionic detergent. They observed that thesitol solubilized active SQOR, releasing it from the membrane (46). For isolation of *A. aeolicus* SQOR, membranes were solubilized in dodecyl-maltoside (49, 50). After solubilization the dodecyl-maltoside was exchanged for Zwittergent 3-10 (49).

The purified enzyme was determined to be monomer, ~47 kDa, with SDS-PAGE. In the presence of a covalent cross linker, the purified enzyme also ran as a dimer (~ 94 kDa) and trimer (~141 kDa) (49). To determine the oligomeric state of SQOR in solution, Marcia et al. performed native PAGE, analytical size-exclusion chromatography (SEC), and sedimentation velocity analytical ultracentrifugation (SV-AUC) (51). The MW of SQOR based on native gels without detergent was ~150 kDa. However, in the presence of dodecyl-maltoside the MW was 250 kDa and with dodecyl-maltoside and

deoxycholate the MW was ~75 kDa (51). This shows that detergents can affect the protein-protein interactions, making it hard to determine the predominant oligomer state of SQOR in solution. The MW of SQOR in solution from the analytical SEC and SV-AUC was ~120 and 160 ( $\pm 10\%$ ) kDa respectively. From these experiments they determine that *A. aeolicus* SQOR can be a monomer, dimer, or trimer, depending on the solution's conditions of the purified sample (34, 51).

In a crystallographic study with *A. aeolicus* SQOR, the solved crystal structure had a resolution of ~2.15 Å and was a trimer (34). The enzyme for these studies was purified using the same method used to characterize the enzyme. Similar to *A. ferrooxidans* SQOR, *A. aeolicus* SQOR has two amphipathic helices located at the C-terminus, that are postulated to anchor the enzyme to the membrane. Additionally, there are two Rossmann folds, with only one containing a FAD cofactor. The FAD is covalently attached to Cys124 via the methyl group at the C(8) position of the FAD isoalloxazine ring [C(8m)]. Cys124 thought is too far away for a direct covalent linkage. Marcia et al. propose that because Cys124 is too far away that in solution there must be a conformational change that brings Cys124 closer to the C(8m) position (34). However, from structural analysis performed by Marcia et al. there does not seem to be evidence for that degree of flexibility (51). Importantly, there is a heavy atom between Cys124 and the C(8m) position of the FAD, that they propose to be a sulfur that forms a protein-bound persulfide (Cys124SS<sup>-</sup>) and allows for the formation of the covalent C(8m) adduct [Cys124S-S-C(8m) position of the FAD ring].

Surface analysis of the protein revealed, negativity and positively charged surface areas near the Rossmann folds and on the opposite side to the Rossmann folds,

respectively. Additionally, on the surface there was a hydrophobic area on each monomer. It is the hydrophobic area on the monomers that most likely interacts with the membrane and forms the trimer. They calculate that the trimer is embedded  $\sim 12$  Å within the membrane.

When decylubiquinone was crystallized with the enzyme, the hydrophobic portion was facing the solvent and the ring was inside the enzyme, on the si face of the FAD ring. Membrane insertion is postulated to help trimerization of the monomers. Additionally, insertion into the membrane prevents the reduction of oxidants other than ubiquinone by protecting the si face from soluble oxidants, such as, NAD(P)H. They would not be able to enter the active site since the si face of the FAD is facing the membrane (34). Located on the re face of the FAD ring is a cavity that contains the three conserved cysteines (Cys124, Cys156, Cys347). The cavity is connected to the bulk solvent by a channel that allows for sulfide to enter the active site. Located at the opening of the channel is a valine residue (Val 294) that is conserved in Type I SQORs and has been shown to play an important role in activity (41).

Marcia et al. proposed an enzymatic reaction from the structural analysis (Scheme 1.2) (34). Their proposed mechanism is similar to what has already been described for the *A. ferrooxidans* SQOR. The residues that are postulated to comprise the redox disulfide bridge are Cys156 and Cys347. However, within the solved structure they are too far away to form a disulfide bridge. Instead, Marcia et al. determined by using an electron density map, that a cyclooctasulfur ring is covalently bound to Cys156 persulfide (Cys156SS<sup>-</sup>). Marcia et al. proposed two different mechanisms assuming that the

interaction between the persulfide on Cys124 (the third conserved cysteine), Cys124SS<sup>-</sup> and the FAD is either (i) static or (ii) dynamic (34).

For the mechanism with a static interaction between Cys124SS<sup>-</sup> and the C(8m) position of the FAD, the first step involves a nucleophilic attack by sulfide at Cys156 forming a protein-bound persulfide (Cys156SS<sup>-</sup>) and the thiolate form of Cys347 (Scheme 1.2). The protein-bound persulfide forms a charge-transfer complex intermediate with the C(4a) position of the FAD ring (step 1) followed by the formation of a covalent FAD 4a-adduct, with the persulfide (step 2). For the third step, Cys347S<sup>-</sup> attacks the sulfur atom in the 4a-adduct, forming a trisulfide bridge (Cys347S-SSCys156) and reduced FAD (FADH<sub>2</sub>). During the fourth step, the FADH<sub>2</sub> is oxidized back to FAD by reducing ubiquinone to ubiquinol. After the formation of a eight sulfur atom chain on Cys347, the chain is transferred to Cys156SS<sup>-</sup> and in the process closes on its self forming a cyclooctasulfur that is bound to Cys156, through a trisulfide bridge (Cys156SS-S<sub>8</sub>ring) intermediate before being released into solution. Lastly, the sulfur ring is released into solution when the thiolate on Cys347 attacks the sulfane sulfur on Cys156. This step results in the formation of a trisulfide bridge (Cys347S-SSCys156), which is the same intermediate produced after step 4 (Scheme 1.2). The other postulated mechanism, is similar except that there is no 4a-adduct intermediate.

For the second mechanism the first step is a nucleophilic attack by the thiolate on Cys156 on the sulfur atom in the C(8m) adduct forming a trisulfide bridge (Cys156S-SSCys124) intermediate and reduced FAD (FADH<sub>2</sub>) (similar to step 3 in scheme 1.2.). Next sulfide attacks the trisulfide bridge forming two protein bound persulfides, Cys156SS<sup>-</sup> and Cys124SS<sup>-</sup>. The persulfide, Cys124SS<sup>-</sup> attacks the C(8m) position on the

FAD reforming the C(8m) adduct. During this step the sulfane sulfur on Cys156SS<sup>-</sup> is transferred to Cys347, the residue that the polysulfide chain grows on. After the formation of a eight sulfur atom chain, the chain is transferred to Cys156SS<sup>-</sup> and in the process closes on its self forming a cyclooctasulfur that is bound to Cys156, through a trisulfide bridge (Cys156SS-S<sub>8</sub>ring) intermediate before being released into solution (similar to scheme 1.2 step 5). Lastly, the sulfur ring is released into solution resulting in a protein bound persulfide, Cys156SS<sup>-</sup>.

#### **1.4.4 *Acidianus ambivalens* SQOR**

*A. ambivalens* SQOR is a Type V SQOR, with a solved crystal structure. *A. ambivalens* SQOR's DNA is more than 70% different compared to the Type I *A. ferrooxidans* SQOR (32, 33). *A. ambivalens* is a thermoacidophilic archaeon that belongs to the order of *Sulfolobales* and its optimal growth conditions are at 85 °C and pH 2 (52, 53). Originally, a proteolytically cleaved form of the enzyme was classified as a type II NADH dehydrogenase because it exhibited NADPH oxidase activity (MW of 43 kDa) (54-56). However, the enzyme name was changed from NADPH oxidase to SQOR because the natural full-length enzyme exhibited only SQOR activity (32). Isolation of the full-length natural enzyme followed a similar method to that which was used to isolate the truncated SQOR (32). Isolation of SQOR required a solubilization step with dodecyl-maltoside to release it from the membrane. To confirm the purity of the full-length protein, mass spectrometry and SDS-PAGE were conducted. Unlike SQOR from *A. aeolicus*, *A. ambivalens* SQOR was a monomer in solution, with a MW of ~48 kDa determined by SEC. The enzyme had a covalently bound FAD and a typical FAD spectrum with absorption peaks at 350 and 454 nm (32). Because *A. ambivalens* is a

thermoacidophilic bacterium, SQOR activity with respect to temperature was tested. SQOR activity increased with temperature from 25 to 70 °C and had an optimal pH of ~6. SQOR activity was similar with decylubiquinone and caldariella quinone, the natural quinone within *A. ambivalens*.

The structure of *A. ambivalens* SQOR solved by Brito et al. is similar to *A. ferrooxidans* and *A. aeolicus* SQORs (32). The FAD is bound to one of the two Rossmann folds. A loop extending through the second fold prevents NAD(P) from binding. The FAD is covalently bound to the protein via a thioether bond between C(8m) and Cys129 (one of the three conserved cysteine residues). The residues Cys178 and Cys350 comprise the redox-active disulfide bridge and are located on the re face of the FAD. In proximity to the disulfide are two aspartic residues, Asp215 and Asp353, which are postulated to stabilize H<sub>2</sub>S by hydrogen bonding. The hydrogen bonding is between the carboxylate on each aspartate side chain and the hydrogen atoms on H<sub>2</sub>S causing the sulfur atom to be a stronger nucleophile. Crystal structures have not been obtained with a bound quinone. It is presumed that the large cavity on the si face of the FAD is the quinone binding site. Within the cavity there is a hydrophilic region adjacent to the isoalloxazine ring suitable for the hydrophilic quinone ring of caldariella quinone. As with the other two known SQOR structures, *A. ambivalens* SQOR is hypothesized to interact with the membrane with the amphipathic helix located at the C-terminus (32). It is worth noting, that no helix was observed in the crystal structure; the last 53 residues were disordered and could not be visualized (32).

From the structural analysis, Brito et al. postulated a mechanism for *A. ambivalens* SQOR (Scheme 1.3) (32). The first step, involves a nucleophilic attack by

sulfide at Cys350, forming Cys350SS<sup>-</sup> persulfide and the thiolate form of Cys178. This results in the formation of a charge-transfer complex between the sulfane sulfur on the persulfide and the C(4a) position on the FAD ring (step 2). This is followed by the formation of a 4a-adduct with the persulfide (step 3). Cys178S<sup>-</sup> attacks the sulfur atom in the 4a-adduct producing a trisulfide bridge (Cys350SS-SCys178) and FADH<sub>2</sub> (step 4). FADH<sub>2</sub> is oxidized back to FAD by reducing caldariella quinone to a quinol (step 5). A second molecule of sulfide enters the active site and the above process is repeated until the polysulfide chain becomes too large. It is proposed that the longest chain that can grow on Cys350 is five sulfur atoms. For step six, the chain is released when the sulfur atom on Cys178 attacks the gamma sulfur on Cys350 regenerating the disulfide bridge.

#### **1.4.5 *Rhodobacter capsulatus* SQOR**

*R. capsulatus* is a purple “non-sulfur” bacterium, containing a Type I SQOR, which has a MW of ~48 kDa, and is located in the periplasm. The enzymatic reaction for this SQOR produces a soluble polysulfide chain rather than elemental sulfur. Next soluble polysulfide chains that have been released by SQOR are transported outside the cell where through a series of steps requiring a metal ion are deposited as elemental sulfur (S<sub>8</sub>,ring) (yellowish in color) (41, 57). What makes *R. capsulatus* unique is that this phenomenon is normally observed with green sulfur bacteria (58). Prior to the isolation of SQOR, it was known that *R. capsulatus* could enzymatically oxidize H<sub>2</sub>S, under dark conditions within the chromatophores (vesicles that reflect light) in a reaction requiring ubiquinone (59, 60). *R. capsulatus* strains expressing either wild type SQOR or mutations of the conserved cysteine residues were grown on sulfide plates; to determine if the mutations affected the growth of the bacterium. To create the mutant strains,

transposon (which is DNA that can move within the genome) mutagenesis was performed via a conjugative method called triparental mating (41, 61). Transposon mutagenesis is when a transposon is inserted into a gene, which renders the translated protein inactive. Triparental mating requires a bacterium, which assists in the transfer of the plasmid of interest from one bacterium to another. None of the three mutants were able to grow on the sulfide plates (41).

Griesbeck et al. expressed recombinant *R. capsulatus* SQOR in *E. coli* and solubilized the enzyme using thesitol to release it from the membrane (41). The spectrum of the purified enzyme exhibited two flavin absorption peaks at ~375 and ~450 nm. As observed with mostly other SQORs, the recombinant *R. capsulatus* SQOR had a pH optimum of ~6.5. Cyanide was shown to inhibit SQOR activity (40).

To confirm the three-conserved cysteine residues (Cys127, Cys159, and Cys353) mutagenesis was conducted. A mutation was also made to a conserved valine (Val300), which is believed to be critical for SQOR activity (41, 62, 63). Additionally, two conserved histidines (His131 and His 196) were mutated, which are proposed to help in the transfer of electrons from FADH<sub>2</sub> to a quinone (41, 62, 63). As expected the cysteine mutations lost more than 98% of their enzymatic activity. The Val300, His131, and His196 all had a significant decrease in activity. Additionally, the Val300 mutation caused a ~5-fold increase in the K<sub>m</sub> for decylubiquinone. The His131 and His196 mutations had a significant loss in activity and caused a shift in the optimal pH from ~6.5 to ~4.5 and 6.2 respectively. The low activity observed even at the optimal pH could be due to the unfavorable acidic conditions for the enzyme (41).



Spectral studies showed that both the wild type and Val300 mutant enzyme catalyzed the reduction of FAD (to FADH<sub>2</sub>). Additionally, the FADH<sub>2</sub> was oxidized to FAD and the quinone was reduced to quinol. The three-cysteine mutations could not catalyze the reduction of FAD. With the histidine mutations, FAD was still reduced to FADH<sub>2</sub>. However, FADH<sub>2</sub> was not oxidized back to FAD with the addition of decylubiquinone. The observed spectral changes with the histidine mutants showed that they helped facilitated the oxidation of FADH<sub>2</sub> to FAD and the reduction of the quinone to quinol.

From the experimental data, Griesbeck et al. postulated a mechanism for *R. capsulatus* SQOR (Scheme 1.4) (41). They postulate that the disulfide bridge between Cys159 and Cys127 is in equilibrium with a disulfide bridge between Cys127 and Cys353. The first step in the catalytic mechanism involves a nucleophilic attack by sulfide at Cys353 forming a protein-bound persulfide (Cys353SS<sup>-</sup>). Next, a second molecule of sulfide reacts with the sulfane sulfur on the persulfide forming a polysulfide (H<sub>2</sub>S<sub>2</sub>) that is released into solution and the thiolate on Cys159, forms a charge-transfer complex at C(4a) position within the FAD ring (step 2). For the third step, Cys159 forms a covalent 4a-adduct, intermediate. Next, the thiolate on Cys127 attacks the sulfur atom on the 4a-adduct producing a disulfide bridge between Cys159 and Cys127 and FAD is reduced to FADH<sub>2</sub> (step 4). The last step is the oxidation of FADH<sub>2</sub> to FAD, reducing the quinone to quinol (step 5).

#### **1.4.6 *Oscillatoria limnetica* SQOR**

The *O. limnetica* SQOR, is a Type I SQOR that was one of the first ones characterized. Within *O. limnetica* thylakoids it was first discovered that H<sub>2</sub>S in the

presence of light can induce NADPH and ATP production through the cytochrome  $b_6f$  complex (part of the electron transport chain) (30). When *O. limnetica* were grown in the dark,  $H_2S$  oxidation via the addition of a quinone caused the reduction of NADP to NADPH. Under dark conditions it was hypothesized that there was a SQOR transferring the electrons from  $H_2S$  to the electron transport chain (29). Ariel et al. successfully isolated and characterized *O. limnetica* SQOR from the thylakoids (28). In order to isolate a sufficient amount of the natural enzyme *O. limnetica* bacteria were “induced” with sulfide (28, 29). SQOR was isolated from thylakoid membranes by solubilization with dodecyl-maltoside. The SQOR had a MW of ~57 kDa and exhibited a typical flavin spectrum with absorption peaks at 373 and 461 nm. The enzymatic assay monitored the reduction of plastoquinone-1, which is an analog of plastoquinone, a natural substrate for *O. limnetica* SQOR. It is worth noting that, Bronstein et al. were able to express this SQOR recombinantly in *E. coli* along with a SQOR from another cyanobacteria, *Aphanothece halophytica* (64). While the enzymes were not isolated, they showed that the enzymes were localized to the membrane (64).

#### **1.4.7 *Geobacillus stearothermophilus* SQOR**

*Geobacillus stearothermophilus* formally known as *Bacillus stearothermophilus*, is a thermophilic bacterium found in many environments (40, 65, 66). The *b-hmt2* gene encodes for a SQOR, which most likely is a Type II SQOR. SQOR was expressed naturally in *G. stearothermophilus* and recombinantly in *E. coli*. For purification the membranes were solubilized with Triton X-100 to isolate active SQOR. The purified enzyme had a MW of ~40 kDa. Shibata et al. stated that the absorbance spectrum of the denatured enzyme exhibited a typical flavin spectrum (but not shown) (40). Activity

assays were performed by monitoring the reduction of decylubiquinone or 2,3-dimethyl-1,4-naphthoquinone, which is a water soluble analog of menaquinone, a natural quinone in *G. stearothermophilus* (40). SQOR activity was similar with decylubiquinone or 2,3-dimethyl-1,4-naphthoquinone as the electron acceptor. Importantly, in assays with the addition of cyanide (as an acceptor of the sulfane sulfur) and phosphatidylcholine there was an over 700-fold rate increase in SQOR activity. Additionally, there was a decrease in the  $K_m$  value for sulfide. The Type II SQORs do not produce polysulfide chains or cyclooctasulfur rings and require an acceptor of the sulfane sulfur. This work supports the notation that *G. stearothermophilus* SQOR is a Type II SQOR.

The postulated mechanism for this SQOR is significantly different compared to the other bacterial SQORs because there is an acceptor of the sulfane sulfur. The similarities are that there is a redox-active disulfide bridge and after the reduction of FAD the electrons are transferred to a quinone. A possible mechanism for *G. stearothermophilus* is similar to the one that is proposed for *Arenicola marina* SQOR in scheme 1.5 (Cys 1 corresponds to *A. marina* Cys387 and Cys2 corresponds to Cys208). For the proposed mechanism Cys1 and Cys 2 comprise the redox-active disulfide bridge (Cys1 and Cys2, numbers do not correspond to their location in the protein sequence). The first step involves a nucleophilic attack by sulfide at Cys1, forming a persulfide (Cys1SS<sup>-</sup>) and a thiolate (Cys2). Next, cyanide reacts with the sulfane sulfur, on the persulfide Cys1SS<sup>-</sup> forming thiocyanate. This is followed by, nucleophilic attack of Cys2 at the C(4a) position of the FAD ring producing a covalent 4a-adduct (similar to scheme 1.5 step 3). The disulfide bridge is regenerated by nucleophilic attack by the thiolate on Cys1 at the sulfur atom on the 4a-adduct. During this step there is a two-electron

reduction of FAD to FADH<sub>2</sub> (same as scheme 1.5 step 4). Lastly, FADH<sub>2</sub> transfers its electrons to a quinone forming a quinol and regenerating FAD (same as scheme 1.5 step 5).

#### **1.4.8 *Pseudomonas putida* SQOR**

*Pseudomonas putida* gene PP0053, encodes for a putative Type II SQOR homolog. *P. putida* is a saprotrophic bacterium, which are known to break down dead organic matter within the soil. Prior studies showed that *P. putida* could remove H<sub>2</sub>S from water at a pH optimum between 6 and 8 (67). The optimal pH for most known SQORs is ~6.5-7.0. Natural *P. putida* SQOR localized to the membrane (39). When the *P. putida* gene PP0053 was inactivated via insertional mutagenesis, no SQOR activity was detected in *P. putida*. The protein was also expressed recombinantly in *E. coli*. For purification, SQOR was solubilized with the detergent, Triton X-100, to release it from the membrane (39). The purified enzyme had a MW of ~43 kDa and a typical flavin absorption spectrum with peaks at 372 and 452 nm. In the presence of cyanide there is an increase in SQOR activity and a decrease in the K<sub>m</sub> value for sulfide, which is similar to *G. stearothermophilus* SQOR, another Type II bacterial SQOR. (39).

#### **1.4.9 *Schizosaccharomyces pombe* SQOR**

*Schizosaccharomyces pombe* is a Type II SQOR. The postulated *S. pombe* gene that encodes for SQOR is called heavy metal tolerance 2 (*Hmt2*). Mutations to the gene resulted in the organism becoming hypersensitive to heavy metals (31, 68). The amino acid sequence has 35%, 20%, 38% identity to lugworm, *R. capsulatus* and a human SQOR (at the time this had not been studied) respectively (31). All eukaryotic SQORs

are Type II, which have the disulfide bridge as Type Is but lack the conserved third cysteine residue (51).

*S. pombe* SQOR localized to the mitochondria. Recombinant *S. pombe* SQOR was expressed in *E. coli* and solubilized with Triton X-100 to release it from the membrane (31). The solubility of *S. pombe* SQOR could be enhanced if the solution was increased to a pH of 11. This enhancement of solubility at pH 11 has also been observed with other peripheral membrane proteins (31). The recombinant SQOR had a MW of ~52 and ~50 kDa. The 50 kDa MW protein could be due to it being truncated (ie. protein degradation). It was postulated by Marcia et al. that in eukaryotic SQORs the FAD would be covalently bound to a conserved tyrosine residue (15). However, for recombinant *S. pombe* SQOR the FAD was noncovalently bound. The spectrum of the purified enzyme exhibited two flavin absorption peaks at 375 and 455 nm and the ratio of FAD to protein was ~1:3. The low ratio may reflect the loss of FAD through purification (31). Enzymatic activity was determined by measuring the reduction of coenzyme Q<sub>2</sub>, an analog of coenzyme Q, a natural quinone (31). Weghe and Ow determined a mole ratio of 1:1 for sulfide consumed to reduced coenzyme Q<sub>2</sub>, meaning that the sulfide is oxidized to sulfane sulfur because two electrons are required to fully reduce coenzyme Q<sub>2</sub> (31). Activity was detected in yeast mitochondria in the presence of cyanide. Additionally, in assays containing cyanide, cyanide lowered the K<sub>m</sub> value for sulfide (unpublished data) (18). This is also observed with, *Arenicola marina*, *P. putida*, and *G. stearothermophilus* SQORs, which like *S. pombe* SQOR, are Type II SQORs.

#### 1.4.10 *Arenicola marina* SQOR

Another eukaryotic Type II SQOR that has been studied is from *A. marina*, commonly known as lugworm (19). Lugworm SQOR has a 45%, 35% and 23% amino acid sequence identity to human, *S. pombe* and *R. capsulatus* SQORs respectively (19). Lugworms are found in marine sediments that can contain up to 2 mM H<sub>2</sub>S (19). H<sub>2</sub>S oxidization has been shown to be localized to the mitochondria and produce equimolar amounts of thiosulfate (11, 69). SQOR activity was the highest within the mitochondrial matrix (14). Cyanide was required to observe SQOR activity with decylubiquinone and sulfide. In the assay with mitochondria, the amount of sulfide consumed was equal to the amount of thiocyanate produced. The formation of thiocyanate in the enzymatic assay occurs from the transfer of the sulfane sulfur in sulfide to cyanide (19).

Theissen and Martin expressed lugworm SQOR recombinantly in *Saccharomyces cerevisiae*, which lacks its own SQOR (19). SQOR was isolated from the mitochondrial membrane by solubilization with Triton X-100. The purified SQOR had a MW of ~47 kDa; and information regarding the FAD content of the preparation was not provided (19). The Asp342 is conserved within eukaryotic SQORs and postulated to be required for FAD binding (19). Mutation to Asp342 caused a significant decrease in SQOR activity.

For observing enzymatic activity of lugworm SQOR cyanide was required. Enzymatic assays replacing cyanide with thioredoxin exhibited thioredoxin-dependent activity, however, the activity was significantly lower than with cyanide. SQOR activity was optimal at a pH of 9, which is higher than the 6.5-7.0 for the bacterial enzymes. The cysteine residues, Cys208 and Cys387, were identified from sequence alignments as the

conserved cysteines that comprise the disulfide bridge. Mutations of the cysteines exhibited no detectable SQOR activity. Conserved histidines, His86 and His299 were identified as possible residue to promote quinone binding and reduction. These two residues along with the proposed active-site base, Glu159, were mutated. Mutations to His86, His299, and Glu159 exhibited no detectable SQOR activity.

From the biochemical data an enzymatic mechanism was proposed (Scheme 1.5) (19). The first step involves a nucleophilic attack by sulfide at Cys387 forming a protein bound persulfide, Cys387SS<sup>-</sup>. Next, cyanide reacts with the sulfane sulfur on Cys387SS<sup>-</sup>, forming thiocyanate. This is followed by, nucleophilic attack of Cys208S<sup>-</sup> at the C(4a) position of the FAD ring producing a covalent 4a-adduct (step 3). The thiolate on Cys387 will attack the sulfur atom in the 4-adduct producing the original disulfide bridge and FADH<sub>2</sub> (step 4). Lastly, the electrons from FADH<sub>2</sub> are transferred to a quinone reducing it to a quinol and regenerating FAD (step 5).

### **1.5 Hydrogen sulfide signaling**

The emerging signaling mechanism for H<sub>2</sub>S is protein sulfhydration. In this process, a sulfur atom is covalently attached to a cysteine residue to produce a persulfide derivative (CysSS<sup>-</sup>). Many proteins in mammals have been shown to undergo sulfhydration including: actin, tubulin, transcription factor NF- $\kappa$ B, and the ATP-sensitive potassium channel (K<sub>ATP</sub> channel), which is a key regulator of heart activity, smooth muscle tone, insulin secretion, and neurotransmitter release (70-74). Sulfhydration is believed to occur not only in mammals but in invertebrates too (75, 76). Invertebrates can live in habitats in which H<sub>2</sub>S concentrations can be as high as 1-2 mM (19, 75). As a result most of these invertebrates have sulfide-hemeprotein interactions to aid in the

transport of the  $H_2S$  to symbiotic bacteria, which will oxidize the  $H_2S$  (75). For a review of  $H_2S$  signaling see reference (77).

### **1.6 Diseases associated with abnormal hydrogen sulfide levels**

Ethylmalonic encephalopathy is an autosomal recessive disease that results in extremely elevated levels of  $H_2S$ . The disease is caused by a defect in the gene (*ETHE1*) that encodes for SDO and results in death within the first decade of life (22, 25). Many of the known abnormalities in these patients can be attributed to the toxic effects of  $H_2S$ . Ethylmalonic encephalopathy patients and the mouse model exhibit elevated urinary excretion of ethylmalonic acid, a biochemical indicator of short-chain acyl-CoA dehydrogenase deficiency.

Ulcerative colitis is a type of inflammatory bowel disease, in colonic epithelia cells. Associated with this disease is a block in the  $\beta$ -oxidation of short chain fatty acids (78). This impairment of fatty acid metabolism is also observed with ethylmalonic encephalopathy patients. The excessive levels of  $H_2S$  in patients with ulcerative colitis is proposed to be due to sulfate-reducing bacteria in the large intestine or impairment in the metabolism of  $H_2S$  (79, 80). This disease can be recapitulated when cells are exposed to millimolar levels of sulfide (78). The removal of  $H_2S$  by the colon has been shown to be a result of the metabolic pathway where thiosulfate is the main product, even though cells have the ability to remove  $H_2S$  by methylation (12, 80). For more information on  $H_2S$ 's role in ulcerative colitis see reference (79).

Down syndrome patients have an extra copy of the *CBS* gene that encodes for CBS, the enzyme that produces  $H_2S$  in the brain. As a result CBS is enriched in the brains of Down's patients (81). These patients exhibit a 300% increase in the brain's expression



of CBS as well as numerous symptoms, such as elevated levels of sulfhemoglobin consistent with the overproduction of H<sub>2</sub>S. It has been suggested that the chronically elevated levels of H<sub>2</sub>S may contribute to the progressive decrease in the mental abilities of Down syndrome children who exhibit near normal intelligence at birth (82-85).

Alzheimer's disease is the most common form of dementia for which there is currently no cure or prevention method. Alzheimer's disease is related to damage of the hippocampus where the loss of memory is a result of a deficiency in long-term potentiation (86). Long-term potentiation helps in neuronal plasticity, which facilitates learning and memory and has been shown to be dependent on the activation of the N-methyl-D-aspartate (NMDA) receptor (87). The NMDA receptor is activated by H<sub>2</sub>S (88, 89). In patients with Alzheimer's disease H<sub>2</sub>S levels are severely decreased due to low CBS activity caused by low levels of S-adenosyl-L-methionine, an activator of the enzyme (90, 91). In Alzheimer's disease mice models, a H<sub>2</sub>S donor has been shown to increase learning and memory (92). For comprehensive reviews on sulfide's role in the nervous system see references (93, 94).

### **1.6.1 Hydrogen sulfide's role in cardiovascular health and pathology**

H<sub>2</sub>S protects against ischemia/reperfusion injury, mediates vasodilation, promotes angiogenesis, and inhibits plaque formation (atherogenesis) (95-98). Sulfide's role in pre- and post- ischemia/reperfusion injury has been extensively studied ranging from animal models to renal transplants (96, 99-102). For example, a H<sub>2</sub>S donor had protective effects during reperfusion.

Hypertension in mice has been shown to be associated with a deficiency in H<sub>2</sub>S. CSE<sup>-/-</sup> mice develop age-dependent hypertension (95). This was reversed with a H<sub>2</sub>S

donor (95). Hypertension was also shown in rats when they were administered an inhibitor of CSE (103). H<sub>2</sub>S causes a decrease in blood pressure via sulfhydrylation of the K<sub>atp</sub> channels and not the voltage-dependent K<sup>+</sup> channels (72, 104-106).

H<sub>2</sub>S is an endogenous stimulator of angiogenesis (97). Papapetropoulos et al. showed that H<sub>2</sub>S promotes angiogenesis via K<sub>atp</sub> channels and inhibition of the channels mitigated the effects of H<sub>2</sub>S (97). Additionally, H<sub>2</sub>S promotes new blood vessel formation via activation of the MAPK/Erk pathway (97, 107). Along with promoting angiogenesis H<sub>2</sub>S can also affect atherosclerosis. Compared to wild type mice, CSE<sup>-/-</sup> mice fed an atherogenic diet, develop atherosclerotic lesions and plaque formation (108). H<sub>2</sub>S has subsequently become a therapeutic target of interest (109). For a review on H<sub>2</sub>S's effects on atherosclerosis see reference (110).

H<sub>2</sub>S has been shown to mediate oxygen sensing within the carotid body (111). The carotid body is a cluster of receptors and cells that monitor oxygen levels along with carbon dioxide, pH, and temperature. CSE<sup>-/-</sup> mice compared to wild type mice had a decreased overall response to hypoxia (12 % O<sub>2</sub>) (111). Under hypoxia within the carotid body it is postulated that H<sub>2</sub>S activates the L-type high voltage-gated calcium channels (111). Another possible mechanism for oxygen sensing is via the calcium-activated potassium channel (112). This is critical because calcium influx into glomus cells are important for carotid body activation during hypoxia (113). For a review on H<sub>2</sub>S's role as an oxygen sensor see reference (114).

### **1.6.2 Hydrogen sulfide's other physiological roles**

Within a small concentration window H<sub>2</sub>S will act as an anti-cancer therapeutic agent (115). Studying H<sub>2</sub>S's effects on cancer, Lee et al. showed that continuous

exposure of a slow releasing H<sub>2</sub>S compound caused intercellular acidification, leading to apoptosis of breast cancer cells (116). In non-cancer breast cell lines there were no effects in cell survival (116). As stated above H<sub>2</sub>S can promote angiogenesis under hypoxia conditions (97). Angiogenesis can be upregulated in cancers because of their rapid growth, and large nutrient requirements. Szabo et al. demonstrated that CBS is upregulated in colon cancer (117). Chattopadhyay et al. studied many different cancer cell lines and found that H<sub>2</sub>S-releasing non-steroidal anti-inflammatory drugs (HS-NSAIDs) inhibited cell growth (118). HS-NSAIDs are a new anti-inflammatory drug class containing both nitric oxide and H<sub>2</sub>S releasing moieties (119). For reviews on HS-NSAIDs' treating cancer and general drug design with H<sub>2</sub>S see references (120, 121).

Recently Hine et al. looked into the effects of H<sub>2</sub>S on dietary restriction. They showed that when mice are on a restricted diet there was an increase in H<sub>2</sub>S levels (122). By measuring the protein concentration of CSE and CBS, Predmore et al. further proved the idea that over time in rats, caloric restriction will alter H<sub>2</sub>S signaling, with tissue specific affects (123).

*Caenorhabditis elegans* exposed continuously to a low concentration of H<sub>2</sub>S in the atmosphere before early development lived longer compared to *C. elegans* grown under a normal atmosphere (124). If the animals were placed in a H<sub>2</sub>S atmosphere after early development then there was no increase in their life span (124). It appears that there are other factors besides exposure to H<sub>2</sub>S related to the life span of the animals. For more information about H<sub>2</sub>S's therapeutic benefits related to aging see reference (125).

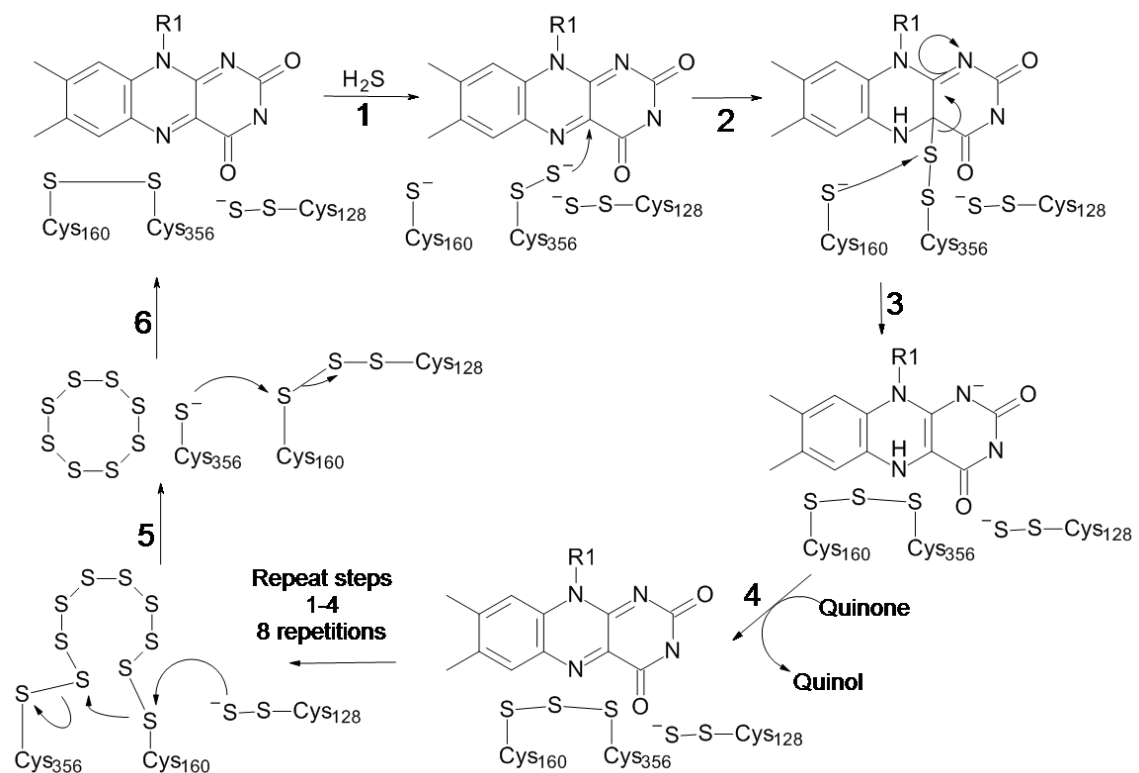
## 1.7 Summary

H<sub>2</sub>S is the third known gasotransmitter similar to nitric oxide and carbon monoxide. It is the only gasotransmitter that is enzymatically degraded. Although originally believed to be toxic to animals it is now understood that it plays an important role within mammals ranging from high blood pressure to a neuroprotectant and modulator. H<sub>2</sub>S has also been associated with diseases including, Down syndrome and Alzheimer's disease.

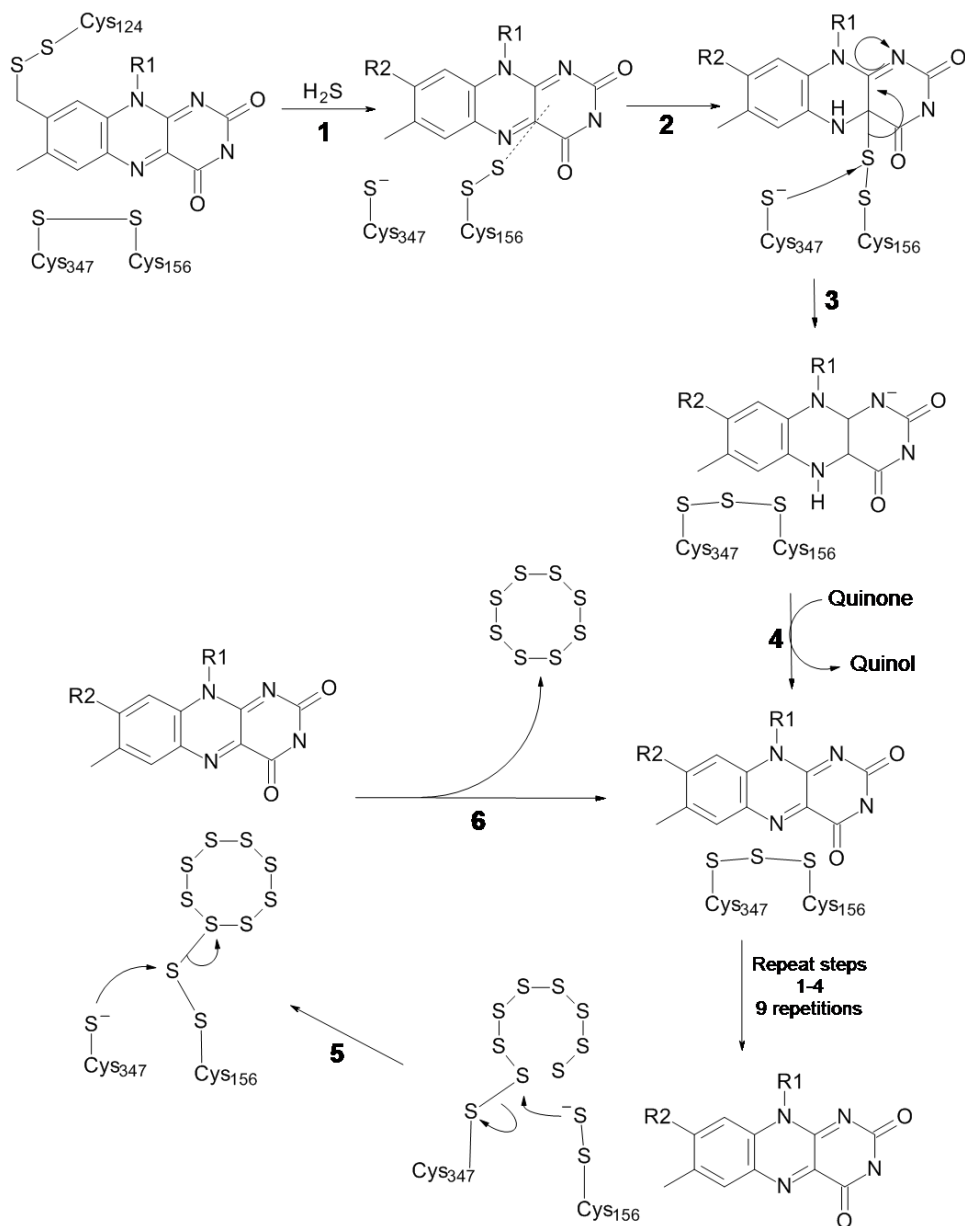
The goal of this thesis is to enhance the understanding of the metabolic pathway of H<sub>2</sub>S. To achieve this we first characterized recombinant human SQOR. SQOR is a mitochondria membrane-associated flavoprotein. The fact that SQOR is membrane-associated made it difficult to express properly folded and functional enzyme. After an extensive screening process we determined that 1,2-diheptanoyl-sn-glycero-3-phosphocholine was the optimal detergent for solubilization. Unlike most bacterial SQORs, eukaryotic and bacterial Type II SQORs require an acceptor of the sulfane sulfur. We discovered that sulfite was the physiological acceptor in a reaction that produced thiosulfate. This discovery lead us to postulate a role in H<sub>2</sub>S metabolism for a thiosulfate sulfurtransferase (TST), which can transfer the sulfane sulfur of thiosulfate to glutathione producing GSS<sup>-</sup> and sulfite. We postulate that the TST links together the SQOR and SDO steps in the pathway because it consumes thiosulfate from the SQOR reaction and produces glutathione persulfide, a substrate required for SDO. Moreover, we identified and characterized the genes for the yeast and human TST. We demonstrated that the TST produced glutathione persulfide, which was released into solution and consumed by SDO. Further supporting the coupling of the TST and SDO reactions was

the discovery of a bacterial fusion protein containing both a TST domain and a SDO domain. Our findings provide new insight into the metabolic pathway of H<sub>2</sub>S.

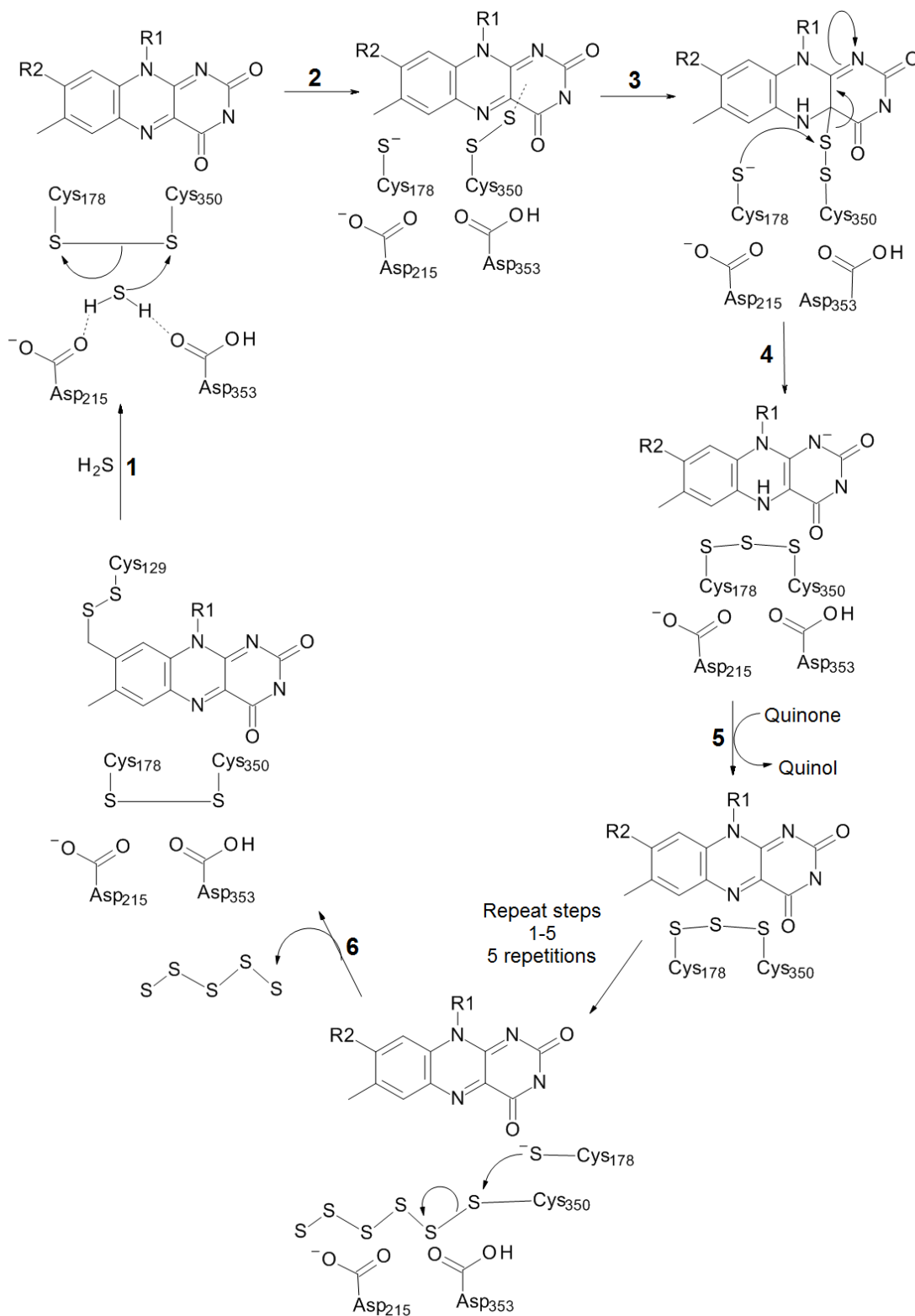
Organism	Type	Cyanide Effect	Flavoprotein	FAD covalent or noncovalently bound
<i>A. ferrooxidans</i> <sup>(42, 45)</sup>	I	ND	Yes	Noncovalent
<i>A. aeolicus</i> <sup>(49)</sup>	I	ND	Yes	Covalent
<i>O. limnetica</i> <sup>(28)</sup>	I	ND	Yes	ND
<i>R. capsulatus</i> <sup>(40, 41)</sup>	I	Inhibits	Yes	ND
<i>A. marina</i> <sup>(19)</sup>	II	Required	ND	ND
<i>G. stearothermophilus</i> <sup>(40)</sup>	II	Increases activity and decrease K <sub>m</sub> for sulfide	Yes	ND
<i>P. putida</i> <sup>(39)</sup>	II	Activates and reduces the K <sub>m</sub> for sulfide	Yes	ND
Rat <sup>(14)</sup>	II	Required	ND	ND
<i>S. pombe</i> <sup>(18, 31)</sup>	II	Activates and reduces the K <sub>m</sub> for sulfide	Yes	Noncovalent
<i>A. ambivalens</i> <sup>(32)</sup>	V	Inhibits	Yes	Covalent



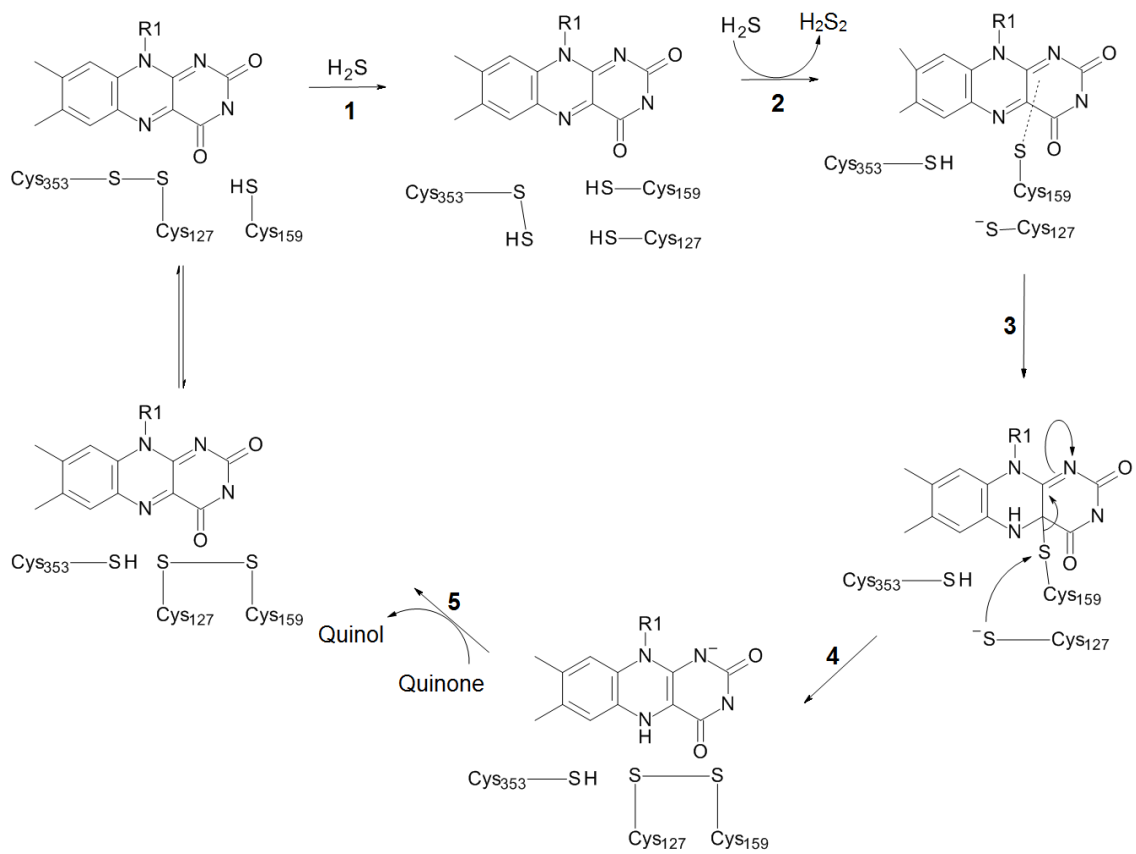
**Scheme 1.1** Proposed catalytic mechanism of *Acidithiobacillus ferrooxidans* SQOR. The proposed mechanism is modified from reference (45). For an explanation go to section 1.4.2.



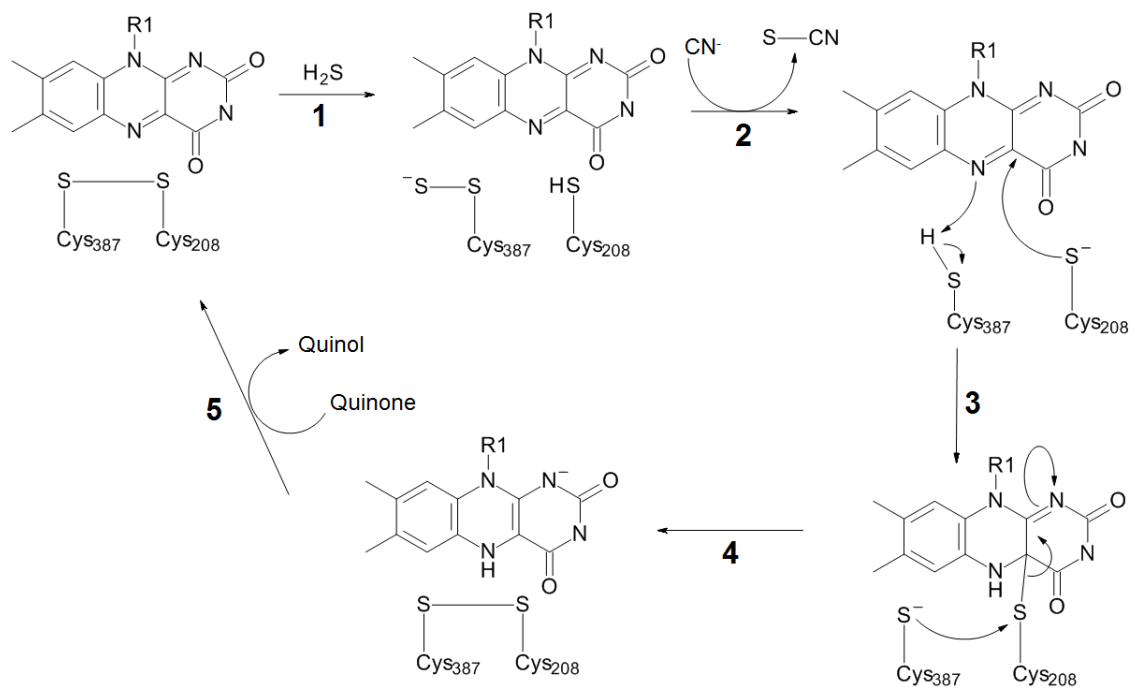
**Scheme 1.2** Proposed catalytic mechanism of *Aquifex aeolicus* SQOR. The proposed mechanism is modified from reference (49). For an explanation go to section 1.4.3.







**Scheme 1.4** Proposed catalytic mechanism of *Rhodobacter capsulatus* SQOR. The proposed mechanism is modified from reference (41). For an explanation go to section 1.4.5.



**Scheme 1.5** Proposed catalytic mechanism of *Arenicola marina* SQOR. The proposed mechanism is modified from reference (19). For explanation go to section 1.4.10.

## Chapter 2: Human sulfide:quinone oxidoreductase catalyzes the first step in hydrogen sulfide metabolism and produces a sulfane sulfur metabolite

Adapted from Michael R. Jackson, Scott L. Melideo, and Marilyn Schuman Jorns  
Biochemistry, 2012

### 2.1 Abstract

Sulfide:quinone oxidoreductase (SQOR) is a membrane-bound enzyme that catalyzes the first step in the mitochondrial metabolism of H<sub>2</sub>S. Human SQOR is successfully expressed at low temperature in *Escherichia coli* by using an optimized synthetic gene and cold-adapted chaperonins. Recombinant SQOR contains noncovalently bound FAD and catalyzes the 2-electron oxidation of H<sub>2</sub>S to S<sup>0</sup> (sulfane sulfur) using CoQ<sub>1</sub> as electron acceptor. The prosthetic group is reduced upon anaerobic addition of H<sub>2</sub>S in a reaction that proceeds via a long-wavelength absorbing intermediate ( $\lambda_{\text{max}} = 673 \text{ nm}$ ). Cyanide, sulfite, or sulfide can act as the sulfane sulfur acceptor in reactions that: (i) exhibit pH optima at 8.5, 7.5 and 7.0, respectively; and (ii) produce thiocyanate, thiosulfate, or a putative sulfur analog of hydrogen peroxide (H<sub>2</sub>S<sub>2</sub>), respectively. Importantly, thiosulfate is a known intermediate in the oxidation of H<sub>2</sub>S by intact animals and the major product formed in glutathione-depleted cells or mitochondria. H<sub>2</sub>S oxidation by SQOR with sulfite as the sulfane sulfur acceptor is rapid and highly efficient at physiological pH ( $k_{\text{cat}}/K_{\text{m H}_2\text{S}} = 2.9 \times 10^7 \text{ M}^{-1} \text{ s}^{-1}$ ). A similar efficiency is observed with cyanide, a clearly artificial acceptor, at pH 8.5 whereas a 100-fold lower value is seen with sulfide as acceptor at pH 7.0. The latter reaction is unlikely to occur in healthy individuals but may become significant under certain pathological conditions. We propose that sulfite is the physiological acceptor of the sulfane sulfur and

that the SQOR reaction is the predominant source of the thiosulfate produced during H<sub>2</sub>S oxidation by mammalian tissues.

## 2.2 Introduction

Hydrogen sulfide is the most recently identified member of a small family of labile biological signaling molecules, termed gasotransmitters, which includes nitric oxide and carbon monoxide. Mitochondrial metabolism of H<sub>2</sub>S is coupled to the synthesis of ATP (126). The first step of this pathway is catalyzed by sulfide:quinone oxidoreductase (SQOR), a poorly characterized inner mitochondrial membrane-bound flavoenzyme that is ubiquitously expressed in animals and also found in some lower eukaryotes (14, 15, 18, 19, 31, 127). SQOR catalyzes a 2-electron oxidation of H<sub>2</sub>S to sulfane sulfur (S<sup>0</sup>) using coenzyme Q as electron acceptor. The enzyme also appears to require an acceptor for the sulfane sulfur. Cyanide has been used *in vitro* as a substitute for the currently unknown acceptor (14, 18, 19). The sulfane sulfur produced in the SQOR reaction is a metabolic precursor of substrates for better-characterized downstream enzymes, such as sulfite oxidase. The identity of the sulfane sulfur-containing product of the SQOR reaction is necessary to address a major gap in our understanding of the mitochondrial pathway(s) for H<sub>2</sub>S metabolism. It is worth noting that a sulfane sulfur donor is required for conversion of cysteine to thiocysteine, suggesting that a possible link may exist between H<sub>2</sub>S metabolism and signaling.

SQOR has been purified from several bacteria (32-34). Unlike eukaryotic SQOR, the bacterial homologs produce sulfane sulfur in the form of polysulfide chains or cyclooctasulfur rings and do not require an acceptor molecule. Characterization of eukaryotic SQOR has proved far more challenging, as judged by difficulties encountered

in attempts to isolate recombinant forms of the lugworm or yeast enzyme (19, 31). In this paper, we describe the expression and characterization of human SQOR and the identification of the previously unknown physiological acceptor of the sulfane sulfur. Our studies suggest the enzyme may produce the sulfur analog of hydrogen peroxide ( $H_2S_2$ ) under conditions where the physiological acceptor is limiting. To our knowledge, this is the first successful purification of a eukaryotic SQOR.

## **2.3 Experimental procedures**

### **2.3.1 Materials**

Sodium sulfite was obtained from Fluka. Potassium cyanide was purchased from Fisher. Sodium sulfide was obtained from Alfa Aesar.  $CoQ_1$  was purchased from Sigma-Aldrich. Glutathione was obtained from Acros. DHPC was purchased from Avanti Polar Lipids. Isopropyl  $\beta$ -D-thiogalactopyranoside was purchased from Gold Biotechnology. Restriction enzymes and T4 DNA ligase were obtained from New England Biolabs. PFU turbo was obtained from Agilent Technologies. PCR mix was purchased from Amresco.

### **2.3.2 Expression of human SQOR in *Escherichia coli***

A synthetic version of the gene encoding human SQOR (*sqrdl*) was obtained from Blue Heron Biotechnology, Inc. (Bothell, WA). The synthetic gene (i) contained a single Met in place of an N-terminal mitochondrial-targeting presequence (41 amino acids)<sup>1</sup>; (ii) was optimized for expression in *E. coli*; and (iii) was flanked by unique *NdeI* and *XhoI* sites, a feature achieved by introducing a silent mutation to remove of an internal *NdeI* site. (See Appendix 1 Figure 1 of the Supporting Information for the sequence of the synthetic gene). The synthetic gene was subcloned between the *NdeI* and *XhoI* sites of plasmid

---

<sup>1</sup>Hauska, G., personal communication

pET23a (Novagen) to yield plasmid pET23a\_MATopzSQOR. A pACYC-based plasmid (pCPN10/60) was isolated from ArcticExpress (DE3) Competent Cells (Agilent Technologies). Plasmid pCPN10/60 contains genes (*cpn10*, *cpn60*) for cold-adapted chaperonins from *Oleispira antarctica* (Cpn10, Cpn60) and a gentamycin-resistance gene. Plasmid pET23a\_MATopzSQOR was used to transform *E. coli* BL21 (DE3) cells to ampicillin resistance. Plasmid pCPN10/60 was then used to transform BL21 (DE3)/pET23a\_MATopzSQOR cells to gentamycin resistance. A starter culture was prepared by overnight growth of *E. coli* BL21 (DE3)/pET23a\_MATopzSQOR/pCPN10/60 cells at 37 °C in LB media containing gentamycin (20 µg/mL) and ampicillin (100 µg/mL). The starter culture was used to inoculate TB media containing the same two antibiotics. Cells were grown with shaking in 2 L flasks containing 500 mL of media at 15 °C until the  $A_{595}$  reached 1.1. SQOR expression was induced with isopropyl β-D-thiogalactopyranoside (0.5 mM). Cells were harvested 20 h after induction. The cell pellets (~100 g from 9 L of culture) were stored at -80 °C.

### **2.3.3 Purification of recombinant human SQOR**

All steps of the purification were conducted at 4 °C. Cell pellets (~50 g) were thawed and suspended in 75 mL of Tris-acetate buffer, pH 7.6 containing 0.5 M sucrose and 0.1 mM EDTA. The cell suspension was mixed with lysozyme (0.5 mg/mL) plus a cocktail of nucleases and protease inhibitors (DNAase, 20 µg/mL; RNAase, 20 µg/mL; 5 mM magnesium sulfate; soybean trypsin inhibitor, 12.6 µg/mL; aprotinin, 2 µg/mL; phenylmethanesulfonyl fluoride, 25 µM/mL; and tosyllysine chloromethylketone, 3 µg/mL). The suspension was incubated with stirring for 20 min and then sonicated (Branson Model 350, power setting = 6, duty cycle = 40%) for a total of 450 s in 30-s

intervals, separated by 30-s cooling periods. Cell debris was removed by centrifugation at low speed (10 min at 10,000 g). Membrane-bound SQOR is found in the supernatant which contains membrane fragments generated during sonication. The low speed supernatant was diluted 1:1 with 50 mM potassium phosphate buffer, pH 7.4, containing 1% DHPC, 10% glycerol, and a cocktail of protease inhibitors and DNAase, as described above. The sample was incubated for 2 h on a rocking platform shaker to solubilize SQOR and then centrifuged at 120,000 g for 1 h. The high speed supernatant was collected and its buffer was modified to contain 200 mM Tris-HCl, pH 8.0, 200 mM sodium chloride and 40 mM imidazole. The high speed supernatant was loaded onto a 5-mL HiTrap IMAC column (GE Healthcare), previously equilibrated with 40 mM Tris-HCl buffer, pH 8.0, containing 150 mM sodium chloride and 40 mM imidazole-HCl. The column was washed with 50 mM Tris-HCl buffer, pH 8.0, containing 150 mM sodium chloride, 10% glycerol, 80 mM imidazole-HCl and 0.05% DHPC. SQOR was eluted with 50 mM Tris-HCl buffer, pH 8.0, containing 150 mM sodium chloride, 10% glycerol, 160 mM imidazole-HCl and 0.1% DHPC and stored at -80 °C. For the final step of the purification, eight batches of IMAC-purified SQOR obtained from ~400 g of cells were thawed, pooled, and dialyzed for 2 h versus a ~200-fold excess of Tris-HCl buffer, pH 8.0, containing 50 mM sodium chloride and 5% glycerol. The sample was centrifuged for 10 min at 30,000 g. The supernatant was loaded onto a 50-mL HiLoad 26/10 Q Sepharose High Performance anion exchange column (GE Healthcare), previously equilibrated with 50 mM Tris-HCl buffer, pH 8.0, containing 2% glycerol and 0.03% DHPC. The column was washed with 50 mM Tris-HCl buffer, pH 8.0, containing 2% glycerol, 100 mM sodium chloride, and 0.06% DHPC (buffer A). SQOR was eluted with

a 100 mL linear gradient formed with each of buffer A and buffer B (50 mM Tris-HCl buffer, pH 8.0, containing 2% glycerol, 1.0 M sodium chloride, and 0.06% DHPC ).

SQOR-containing fractions were pooled, concentrated using a 10 K Macrosep Advance Centrifugal Device (Pall Life Sciences), and stored in aliquots at -80 °C.

#### **2.3.4 Flavin analysis**

SQOR was denatured by heating for 5 min at 100 °C. The flavin was separated from the denatured protein by microfiltration (VWR Centrifugal Filter) and identified as FAD, as previously described (128). The stoichiometry of flavin incorporation and the extinction coefficient of SQOR at 451 nm were determined after denaturation of the enzyme with 3 M guanidine hydrochloride, as described by Wagner et al. (129).

#### **2.3.5 Activity and protein assays**

Except as indicated, assays were conducted under anaerobic conditions at 25 °C using a cuvette (Spectrocell) with a screw-cap equipped with a Teflon-silicon membrane. Buffers used to prepare stock solutions of sodium sulfide, sodium sulfite or potassium cyanide were bubbled with argon for at least 20 min. Sodium sulfite and sodium cyanide ( $\leq 2$  mM) stock solutions were prepared directly in the assay buffer. To prepare more concentrated sodium cyanide solutions, a 1 M solution of the substrate was neutralized to the desired pH with monobasic potassium phosphate and then diluted with assay buffer. Stock solutions of sodium sulfide were prepared in 50 mM potassium carbonate/bicarbonate buffer, pH 9.6, containing 250 mM EDTA. The sulfide concentration was determined based on its absorbance at 230 nm ( $\epsilon = 7200 \text{ M}^{-1}\text{cm}^{-1}$ ) (130). Stock solutions of CoQ<sub>1</sub> were prepared in DMSO. Reagents were added to the cuvette using argon-purged gas-tight Hamilton syringes. Cuvettes containing buffer,



CoQ<sub>1</sub>, and, where indicated, sulfite or cyanide, were incubated at 25 °C for 2 min. An aliquot of SQOR was added, and the reaction was initiated immediately thereafter by addition of sodium sulfide. Reaction rates were determined by monitoring the reduction of CoQ<sub>1</sub> at 278 nm ( $\Delta\epsilon_{\text{ox-red}} = 12,000 \text{ M}^{-1} \text{ cm}^{-1}$ ) and are corrected for the corresponding blank rate observed in the absence of SQOR. The value for  $\Delta\epsilon_{\text{ox-red}}$  was determined using the reported extinction coefficient for oxidized CoQ<sub>1</sub> ( $\epsilon_{278} = 14,500 \text{ M}^{-1} \text{ cm}^{-1}$ ) and the absorption spectrum of reduced CoQ<sub>1</sub> ( $\lambda_{\text{max}} = 287 \text{ nm}$ ;  $\epsilon_{287} = 3340 \text{ M}^{-1} \text{ cm}^{-1}$ ) observed 2 s after addition of sodium sulfide to assays containing sodium sulfite and a large excess of SQOR (131). Unless otherwise indicated, the concentration of SQOR used in steady-state kinetic studies was estimated based on the absorbance of the enzyme at 451 nm ( $\epsilon = 11,500 \text{ M}^{-1} \text{ cm}^{-1}$ ).

Enzyme activity during purification was monitored using a routine assay that contained 100 mM potassium phosphate buffer, pH 7.5, 0.5 mM EDTA, 80  $\mu\text{M}$  CoQ<sub>1</sub>, 600  $\mu\text{M}$  sodium sulfite and 200  $\mu\text{M}$  sodium sulfide. Similar rates were observed in control studies when assays at these substrate concentrations were performed under aerobic or anaerobic conditions. Accordingly, the routine assay is conducted using aerobic buffer and uncapped 1-mL cuvettes. Stock solutions of sodium sulfide and sodium sulfite are, however, prepared and stored on ice under anaerobic conditions. During enzyme purification, protein was determined using the Pierce BCA (Bicinchoninic Acid Assay) Protein Assay Kit.

### 2.3.6 Product analysis

To determine the sulfide oxidation product formed in the presence of sulfite, assays were conducted at 25 °C in 25 mM Tris-HCl, pH 8.0, containing 400  $\mu\text{M}$  sodium

sulfide, 1.0 mM sodium sulfite, and 77.6 or 194  $\mu\text{M}$  CoQ<sub>1</sub>. Reactions were monitored at 278 nm until reduction of CoQ<sub>1</sub> was complete. Aliquots were then withdrawn and analyzed for thiosulfate by cold cyanolysis in the presence of copper chloride, as previously described (132). To determine the product of sulfide oxidation generated in the presence of cyanide, assays were conducted at 25 °C in 100 mM potassium carbonate buffer, pH 9.0, containing 0.5 mM EDTA, 400  $\mu\text{M}$  sodium sulfide, 1.0 mM potassium cyanide, and 277  $\mu\text{M}$  CoQ<sub>1</sub>. Aliquots were withdrawn when reduction of CoQ<sub>1</sub> was complete and analyzed for thiocyanate according to the procedure described by Wood (133). The product of sulfide oxidation produced in the absence of sulfite or cyanide was characterized as described in Results.

### **2.3.7 Spectroscopy**

All spectral data were recorded using an Agilent Technologies 8453 diode array spectrophotometer. The reaction of substrate amounts of SQOR with sulfide was monitored under anaerobic conditions at 4 °C using screw-cap cuvettes. Reaction buffer containing 50 mM sarcosine was bubbled with argon for 20 min prior to addition of SQOR and an “oxygen sponge” (0.74  $\mu\text{M}$  monomeric sarcosine oxidase, ~10 U/mL of catalase). The samples were incubated for at least 20 min at 4 °C to scavenge trace amounts of oxygen prior to reaction with sulfide. Anaerobic stock solutions of sarcosine and sulfide were prepared similar to that described above.

## **2.4 Results**

### **2.4.1 Expression and purification of recombinant human SQOR**

Major barriers are frequently encountered when attempting to produce even modest amounts of a functional, recombinant, membrane-bound mammalian protein like

SQOR. In an attempt to overcome these obstacles, we surveyed a wide range of expression vectors, prokaryotic, and eukaryotic host cells, and growth conditions. We succeeded in expressing mature SQOR (47 kDa) in *Escherichia coli* by using a synthetic version of the human gene that lacked the N-terminal mitochondrial-targeting presequence and had been optimized for expression in *E. coli*. The synthetic gene was subcloned into plasmid pET23a to introduce a C-terminal (His)<sub>6</sub>-tag. *E. coli* BL21 (DE3) cells were sequentially transformed with the resulting SQOR expression plasmid and a second compatible (pACYC-based) plasmid containing two genes for cold-adapted chaperonins (134). SQOR is expressed as a catalytically active, membrane-bound protein when the clone harboring both plasmids is grown at 15 °C, conditions that minimize inclusion body formation. Optimal solubilization of SQOR was achieved using 0.5% 1,2-diheptanoyl-*sn*-glycero-3-phosphocholine (DHPC), a mild, short-chain, phospholipid detergent (135). The solubilized enzyme was purified to >95% homogeneity (Figure 2.1) in two steps by using metal (Ni<sup>2+</sup>) affinity and anion exchange chromatography (Table 2.1).

Recombinant human SQOR is stable and contains an approximately stoichiometric amount of FAD (Table 2.2). The enzyme exhibits a typical flavoprotein visible absorption spectrum with peaks at 451 and 385 nm and a pronounced shoulder at 473 nm that is eliminated upon denaturation with guanidine hydrochloride (Figure 2.2). The yellow flavin color of the denatured enzyme is recovered in the filtrate obtained after microfiltration. The data indicate that FAD is noncovalently bound to human SQOR. The results fail to support a proposal that the coenzyme would be covalently attached to a highly conserved tyrosine residue in eukaryotic SQOR's (15).

### 2.4.2 Sulfide oxidation with cyanide as the acceptor of the sulfane sulfur

An initial assessment of the catalytic activity of human SQOR was performed at pH 8.0 in assays containing cyanide as the acceptor of the sulfane sulfur and CoQ<sub>1</sub>, a water soluble ubiquinone derivative, as the electron acceptor. Sulfide oxidation is readily detected under these conditions by monitoring the reduction of CoQ<sub>1</sub> at 278 nm ( $k_{\text{cat app}} = 82 \pm 6 \text{ s}^{-1}$ ) (Table 2.2). The reaction is accompanied by the formation of a stoichiometric amount of thiocyanate (Table 2.3), as observed with rat and lugworm SQOR (14, 19). The rate of sulfide oxidation observed with human SQOR is about 20-fold faster than reported for lugworm SQOR under similar conditions ( $k_{\text{cat app}} = 4.5 \text{ s}^{-1}$ ) (19).

### 2.4.3 Identification of a putative physiological acceptor of the sulfane sulfur

The reaction with cyanide is clearly not biologically relevant. A clue regarding the possible physiological acceptor of the sulfane sulfur in the SQOR reaction was provided by an intriguing metabolic abnormality exhibited by patients suffering from ethylmalonic encephalopathy and the corresponding mouse model. The patients and the knockout mice harbor a defective gene, *ETHE1*, that codes for sulfur dioxygenase (SDO) (22). This enzyme produces sulfite by catalyzing the oxidation of the sulfane sulfur in glutathione persulfide (GSS<sup>-</sup>) (14, 22). Wild-type levels of SQOR activity are observed with liver homogenates from *Ethe1*<sup>-/-</sup> knockout mice in assays using cyanide as the acceptor of the sulfane sulfur. Nevertheless, both the mice and the ethylmalonic encephalopathy patients exhibit extremely high, toxic, levels of H<sub>2</sub>S (22). The observed impairment of H<sub>2</sub>S metabolism suggested that sulfite might be the physiological acceptor of the sulfane sulfur in the SQOR reaction.

Indeed, we discovered that human SQOR would readily oxidize sulfide in assays

containing sulfite in place of cyanide. The rate of sulfide oxidation in the presence of 600  $\mu\text{M}$  sulfite ( $k_{\text{cat app}} = 251 \pm 9 \text{ s}^{-1}$ ) is 3-fold faster than observed for the reaction with 1.0 mM cyanide in an otherwise identical assay at pH 8.0 (Table 2.2). Significantly, the reaction with sulfite is accompanied by the formation of a stoichiometric amount of thiosulfate (Table 2.3). The results show that sulfite can act as the acceptor of the sulfane sulfur produced during sulfide oxidation by SQOR. It is noteworthy that numerous studies have shown that the observed product, thiosulfate, plays a central role in mammalian metabolism of  $\text{H}_2\text{S}$ , as will be discussed.

#### **2.4.4 Sulfide oxidation in the absence of cyanide or sulfite**

Studies with rat and lugworm SQOR lead us to expect that sulfide oxidation by human SQOR would be difficult to detect in the absence an acceptor for the sulfane sulfur, such as cyanide (14, 19). However, we found that sulfide oxidation by human SQOR is readily detectable in assays containing only sulfide and  $\text{CoQ}_1$ . The observed rate of sulfide oxidation in this apparently “acceptor-free” reaction at pH 8.0 ( $k_{\text{cat app}} = 18.5 \pm 0.9 \text{ s}^{-1}$ ) is, however, considerably slower than seen for the reaction in the presence of sulfite or cyanide (13.6- or 4.5-fold, respectively) (Table 2.2). It is worth noting that a similar “acceptor-free” reaction has been detected with yeast SQOR (31).

Various groups have postulated that SQOR might use glutathione as the acceptor of the sulfane sulfur in a reaction that would produce  $\text{GSS}^-$ , the persulfide substrate for SDO (14, 22). In a preliminary test of this hypothesis, we sought to determine whether glutathione could accelerate the rate of sulfide oxidation by human SQOR, as observed with sulfite or cyanide. However, we found that the rate of sulfide oxidation in the presence of 1 mM glutathione was, within experimental error, identical to that observed

for the “acceptor-free” reaction with only sulfide and CoQ<sub>1</sub> (Table 2.2).

#### **2.4.5 Identification of the sulfide oxidation product formed in the “acceptor-free” reaction**

A working mechanism for SQOR catalysis predicts that turnover of the enzyme will occur only in the presence of an acceptor for the sulfane sulfur, as will be discussed. The putative “acceptor-free” reaction would appear to be incompatible with this mechanism, unless sulfide itself can act as the sulfane sulfur acceptor. In this case, the “acceptor-free” reaction should produce hydrogen disulfide, H<sub>2</sub>S<sub>2</sub>, the sulfur analog of hydrogen peroxide. The pK<sub>a</sub> values estimated for hydrogen disulfide (pK<sub>a1</sub> = 5.0; pK<sub>a2</sub> = 9.7) suggest that the compound will exist predominantly as the monoanion, HS<sub>2</sub><sup>-</sup>, at pH 8.0 (136). The absorption spectrum of hydrogen disulfide is highly sensitive to its protonation state. The unionized H<sub>2</sub>S<sub>2</sub> molecule exhibits a maximum at 258 nm whereas a maximum at 358 nm is estimated for the dianion, S<sub>2</sub><sup>-2</sup>. The dramatic 100-nm bathochromic shift caused by the removal of two protons is attributed to resonance delocalization of electrons in the dianion that are localized to S-H σ bonds in the neutral molecule (137, 138). Intermediate spectral properties are expected for the monoanion, HS<sub>2</sub><sup>-</sup>, but, to our knowledge, have not previously been described.

Based on the above considerations, we hypothesized that the “acceptor-free” SQOR reaction would generate the monoanion of hydrogen disulfide at pH 8.0, a species likely to absorb in the near-UV region. Evidence to evaluate this hypothesis was sought by monitoring the spectral course of assays conducted in the presence or absence of sulfite or cyanide. The reaction in the presence of 400 μM sulfite results in a progressive loss of the intense absorption band of oxidized CoQ<sub>1</sub> at 278 nm and its tail of absorbance

at longer wavelengths ( $\lambda > 300$  nm). The end of the reaction is signaled by the appearance of a stable, relatively weak absorption band at 287 nm due to reduced CoQ<sub>1</sub> (Figure 2.3a). A single minimum at 272 nm is seen in difference spectra calculated by subtracting the final spectrum of reduced CoQ<sub>1</sub> from spectra observed during the reaction (data not shown). It is worth noting that similar kinetics are observed for the decrease in absorbance at 272 or 317 nm (Figure 2.3a, inset).

The same spectral course is observed for assays containing 1.0 mM cyanide instead of sulfite (see Appendix 1 Figure 2 of the Supporting Information). A striking difference is, however, observed when assays are conducted in the absence of sulfite or cyanide. In this case, the loss of the 278 nm absorption band of oxidized CoQ<sub>1</sub> is accompanied by the formation of a species absorbing in the 300 to 400 nm region (Figure 2.3b). The corresponding difference spectra exhibit a minimum at 272 nm and a maximum at 317 nm (data not shown). Except for a small initial lag, the increase in absorbance at 317 nm exhibits kinetics similar to that observed for the decrease in absorbance at 272 nm (Figure 2.3b, inset).

Hydrogen disulfide should readily react with nucleophiles, such as sulfide or cyanide, as judged by results obtained with other persulfides (133). To investigate its chemical reactivity, the near-UV absorbing product was generated by allowing the “acceptor-free” SQOR assay with limiting CoQ<sub>1</sub> to proceed until complete reduction of CoQ<sub>1</sub>. Subsequent addition of 400  $\mu$ M sulfite results in a rapid loss of the absorbance attributed to the putative hydrogen disulfide product in a reaction that is complete in less than 5 min. The spectrum observed at the end of the sulfite reaction coincides with that expected for reduced CoQ<sub>1</sub> (Figure 2.4). The final spectrum was subtracted from the

spectrum observed prior to sulfite addition. The resulting difference spectrum exhibits maxima at 269 and 315 nm (Figure 2.4, inset). The maximum at 315 nm falls within the range expected for the hydrogen disulfide monoanion. A similar reaction is observed when sulfite is replaced with cyanide. However, a considerably higher cyanide concentration (56 mM) is required to achieve a comparable reaction rate (data not shown). The observed difference in the reactivity of the two nucleophiles is attributed to the fact that only a small amount of the added cyanide (<5%) will exist as the reactive cyanide anion in solution at pH 8.0 ( $pK_a = 9.31$ ) whereas most of the sulfite (>90%) will be present as the reactive  $SO_3^{2-}$  dianion ( $pK_a = 6.9$ ) at this pH.

In addition to nucleophiles, hydrogen disulfide is expected to be consumed by thiols in a reduction reaction that produces  $H_2S$  ( $\lambda_{max} = 230$  nm) (130, 133). Accordingly, studies were conducted to determine whether dithiothreitol (DTT) or glutathione, could reduce the product formed in the “acceptor-free” SQOR reaction. In fact, the near-UV absorbance of the product was eliminated within 15 min after addition of 1 mM DTT (see Appendix 1 Figure 3 of the Supporting Information) or 1 mM glutathione (data not shown). The reaction of hydrogen disulfide with DTT is expected to generate an organic persulfide intermediate,  $HS-CH_2-(CHOH)_2-CH_2-SS^-$ , that will undergo a rapid intramolecular reaction to produce oxidized DTT and  $H_2S$ . We reasoned that a slower intermolecular reaction might permit detection of the persulfide intermediate formed with glutathione,  $GSS^-$  ( $\lambda_{max} = \sim 340$  nm) (139). However,  $GSS^-$  was not detected in the glutathione reaction which exhibited a spectral course very similar to that observed with DTT.

Addition of 1 mM glutathione to SQOR assays containing only sulfide and  $CoQ_1$



did not affect the rate of sulfide oxidation (see Table 2.2). The spectral course of these assays is, however, very similar to that seen in the presence of sulfite or cyanide (see Appendix 1 Figure 4 of the Supporting Information). The observed reduction of the near UV-absorbing product with thiols can account for the failure to detect formation of this species when SQOR assays are conducted in the presence of glutathione.

#### 2.4.6 Effect of pH on catalysis by human SQOR

We sought to evaluate the catalytic efficiency of SQOR with different sulfane sulfur acceptors by comparing sulfide oxidation rates under optimal conditions for each acceptor, including reaction pH. A bell-shaped pH-activity profile is observed for sulfide oxidation with cyanide as the sulfane sulfur acceptor. The reaction exhibits an optimum at pH 8.5 (Figure 2.5a). The data could be fitted to a double ionization titration curve (eq. 1).

$$V_{\text{obs}} = \frac{[\text{H}^+]^2 V_{\text{AH}_2} + [\text{H}^+] K_1 V_{\text{AH}} + K_1 K_2 V_{\text{A}}}{K_1 K_2 + [\text{H}^+] K_1 + [\text{H}^+]^2} \quad (\text{eq. 1})$$

The results indicate that maximal activity is observed when one group is unprotonated ( $\text{AH}_2 \rightleftharpoons \text{AH} + \text{H}^+$ ) ( $\text{pK}_{1\text{ app}}$ ) and a second group is protonated ( $\text{AH} \rightleftharpoons \text{A} + \text{H}^+$ ) ( $\text{pK}_{2\text{ app}}$ ) (Table 2.4). A similar optimum at moderately alkaline pH (9.0) is observed for the lugworm SQOR reaction with cyanide (19). Sulfide oxidation by human SQOR with sulfite as the sulfane sulfur acceptor also exhibits a bell-shaped pH-activity profile. However, the optimum is at pH 7.5, close to physiological pH and one pH unit lower than observed for the cyanide reaction (Figure 2.5a). The values estimated for  $\text{pK}_{1\text{ app}}$  and  $\text{pK}_{2\text{ app}}$  in the reaction with sulfite exhibit a similar shift to more acidic pH (Table 2.4). The “acceptor-free” SQOR reaction exhibits a pH optimum at 7.0 (Figure 2.5b) and apparent

$pK_a$  values that are most similar to those observed for the reaction with sulfite (Table 2.4).

#### **2.4.7 Steady-state kinetic parameters for sulfide oxidation by SQOR with different acceptors of the sulfane sulfur**

Turnover of SQOR with each acceptor was monitored at the pH optimum determined for the reaction. The reactions with sulfite or cyanide involve three different substrates. Steady-state kinetics parameters for such reactions can be estimated by varying the concentration of one substrate at a fixed, saturating concentration of the other two substrates (140). We found that reaction rates with sulfite or cyanide as acceptor exhibit an expected hyperbolic dependence on the concentration of each of the three varied substrates ( $k_{cat\ app} = k_{cat}[S]/(K_m + [S])$ ). Values obtained for  $k_{cat}$  with either acceptor are independent of the nature of the varied substrate (Table 2.5). Interestingly, the turnover rate observed with sulfite at pH 7.5 is, within experimental error, identical to that observed with cyanide at pH 8.5, as judged by comparing the average values obtained for  $k_{cat}$  with the two acceptors ( $k_{cat\ avg} = 370 \pm 14$  and  $345 \pm 11\ s^{-1}$ , respectively). The apparent  $K_m$  observed for sulfite is 4-fold smaller than observed for cyanide. However, very similar apparent  $K_m$  values for sulfide and  $CoQ_1$  are obtained with either acceptor.

The reaction with sulfide as the sulfane sulfur acceptor is essentially an oxidative dimerization of two identical substrates. According to a steady-state equation derived for this type of reaction (eq. 2), the velocity observed at a fixed saturating concentration of  $CoQ_1$  should not exhibit a simple hyperbolic dependence on the concentration of sulfide except under the limiting condition where  $[sulfide] \gg K_{m1}$  (141, 142).

$$V_{\text{obs}} = \frac{V_{\text{max}}}{1 + (K_{m2}/[S]) ( 1 + (K_{m1} / [S]))} \quad (\text{eq. 2})$$

In fact, the latter is observed when the sulfide concentration is varied in the range from 40 to 2100  $\mu\text{M}$  (see Appendix 1 Figure 5 of the Supporting Information). Measurements at higher sulfide concentrations were not possible owing to prohibitively high blank rates. The apparent  $K_m$  obtained for sulfide in this reaction ( $315 \pm 28 \mu\text{M}$ ) is about 25-fold larger than observed with sulfite or cyanide as the sulfane sulfur acceptor (Table 2.5). The high  $K_m$  value precluded studies at a fixed saturating sulfide concentration and a variable concentration of CoQ<sub>1</sub>. The turnover rate estimated for the reaction with sulfide as sulfane sulfur acceptor ( $k_{\text{cat}} = 65 \pm 2 \text{ s}^{-1}$ ) exhibits a relatively modest decrease (6-fold) compared with values obtained for the reactions with sulfite or cyanide. The catalytic efficiency of the reaction with sulfide as acceptor is, however, more than 100-fold lower than observed with sulfite or cyanide, as judged by values calculated for the ratio,  $k_{\text{cat}}/K_m$  H<sub>2</sub>S (Table 2.5).

#### **2.4.8 Anaerobic reduction of SQOR with sulfide**

Anaerobic reaction of SQOR with 1 or 2 equivalents of sulfide results in the rapid formation of an intermediate that exhibits a moderately intense long-wavelength absorption band that is centered at 673 nm and extends out to nearly 900 nm, accompanied by a loss of ~35% of the absorbance of the oxidized enzyme at 451 nm (Figure 2.6, curve 1). The SQOR intermediate undergoes a slow isosbestic conversion to a reduced species that exhibits a maximum at 365 nm, a plateau around 450 nm, and a tail of absorbance extending into the long-wavelength region (Figure 2.6, curve 6). The conversion of the intermediate to the final reduced product exhibits apparent first-order

kinetics (Figure 2.6, inset). However, the observed rate of this reaction ( $k = 4.1 \pm 0.2 \times 10^{-3} \text{ s}^{-1}$ ) is more than four orders of magnitude slower than rates observed for turnover of SQOR with sulfite, cyanide, or sulfide as the sulfane sulfur acceptor. The possible identity and catalytic significance of the two species observed during reaction of SQOR with sulfide will be discussed. Immediate oxidation of the reduced enzyme is observed upon addition of CoQ<sub>1</sub> (Figure 2.6, curve 7). The re-oxidized enzyme exhibits a similar absorption band at 450 nm but enhanced absorbance in the 380 nm region as compared with untreated enzyme. The basis for the latter difference is unclear.

## 2.5 Discussion

Human SQOR is expressed in *E. coli* at low temperature as a catalytically active membrane-bound protein, an outcome dependent on the use of a synthetic gene optimized for expression in a prokaryotic host and the assistance of cold-adapted bacterial chaperonins. Solubilized SQOR is readily purified to produce a stable homogenous holoenzyme that contains a nearly stoichiometric amount of noncovalently bound FAD. SQOR is one of a small group of mammalian membrane-bound proteins that have been successfully expressed in *E. coli*. A similar approach may facilitate the expression of other intrinsic mammalian proteins.

Recombinant SQOR catalyzes the 2-electron oxidation of H<sub>2</sub>S using CoQ<sub>1</sub> as electron acceptor and one of three different nucleophiles (cyanide, sulfite, or sulfide) as the acceptor of the sulfane sulfur in reactions that exhibit pH optima at 8.5, 7.5 and 7.0, respectively. The reaction with cyanide is accompanied by the formation of a stoichiometric amount of thiocyanate. Our studies confirm the nucleophile's ability to act as an artificial acceptor for eukaryotic SQOR, in agreement with results obtained with rat

and lugworm SQOR (14, 19). The reaction with sulfite produces thiosulfate, a known intermediate in H<sub>2</sub>S metabolism. The product of the reaction with sulfide as acceptor has been tentatively identified as hydrogen disulfide, H<sub>2</sub>S<sub>2</sub>, on the basis of its near-UV absorption and reactivity with nucleophiles and thiol reductants. The effect of the acceptor on the catalytic efficiency of H<sub>2</sub>S oxidation can be assessed by comparison of values obtained for  $k_{\text{cat}}/K_{\text{m H}_2\text{S}}$  at the pH optimum of each reaction. The catalytic efficiency observed with sulfite at physiological pH ( $2.9 \times 10^7 \text{ M}^{-1} \text{ s}^{-1}$ ) is similar to that observed with cyanide at moderately alkaline pH ( $3.1 \times 10^7 \text{ M}^{-1} \text{ s}^{-1}$ ) whereas a 100-fold lower value is seen with sulfide ( $2.1 \times 10^5 \text{ M}^{-1} \text{ s}^{-1}$ ). The reaction with sulfide as the acceptor is unlikely to occur in healthy individuals but may become significant under certain pathological conditions. We propose that sulfite is the biological acceptor, as discussed below.

### **2.5.1 Role of SQOR in the biosynthesis of thiosulfate**

Thiosulfate is the major product of H<sub>2</sub>S oxidation by: (i) isolated mitochondria; (ii) hepatocytes depleted of glutathione; and (iii) the colon in intact animals where large quantities of H<sub>2</sub>S are produced by sulfate-reducing bacteria (9, 12, 14, 143). Oxidation of thiosulfate to sulfate: (i) requires a glutathione-dependent thiosulfate reductase and sulfite oxidase (5, 144) and (ii) is observed when isolated mitochondria are supplemented with glutathione and with untreated hepatocytes (9, 143). Additionally, the elegant experiments of Koj et al. (144) and Szczepkowski et al. (8) support a central role for thiosulfate as a key intermediate in the oxidation of H<sub>2</sub>S by perfused liver and intact animals.

We propose that thiosulfate biosynthesis occurs in the first step of H<sub>2</sub>S oxidation

in a reaction catalyzed by SQOR with sulfite as the acceptor of the sulfane sulfur. Our studies with the recombinant human enzyme show that the reaction is rapid and highly efficient at physiological pH. In fact, the observed efficiency of SQOR is just 4-fold lower than reported for carbonic anhydrase, one of the most potent known catalysts ( $k_{\text{cat}}/K_m = 1.2 \times 10^8 \text{ M}^{-1} \text{ s}^{-1}$ ) (145). Rhodanese is a mitochondrial enzyme best known for its ability to utilize thiosulfate as a source of sulfane sulfur in the production of thiocyanate (20). Hildebrandt and Grieshaber postulated that thiosulfate is produced from  $\text{GSS}^-$  and sulfite in an alternate rhodanese reaction (14). However, thiosulfate formation with human SQOR is more than 2 orders of magnitude faster than the rate of thiosulfate formation observed with bovine or rat rhodanese ( $k_{\text{cat app}} = 2.3$  or  $0.22 \text{ s}^{-1}$ , respectively). Furthermore, the sluggish rhodanese reaction is unlikely to effectively compete with the much faster rate of  $\text{GSS}^-$  oxidation observed with SDO ( $k_{\text{cat app}} = 51 \text{ s}^{-1}$ )<sup>2</sup>. Finally, it is worth noting that inhibitors of SQOR reduce the production of thiosulfate from  $\text{H}_2\text{S}$  by mouse colon (146). Overall, the results strongly implicate the SQOR reaction as the predominant source of thiosulfate produced during  $\text{H}_2\text{S}$  oxidation by mammalian tissues.

Thiosulfate is the major product of  $\text{H}_2\text{S}$  oxidation in glutathione-depleted cells or mitochondria. Formation of 1 mol of thiosulfate requires an 8-electron oxidation of 2 mol of  $\text{H}_2\text{S}$ . A 4-step pathway can account for the observed conversion of  $\text{H}_2\text{S}$  to thiosulfate under these conditions (Scheme 2.1, path A). Steps 1 and 4 are catalyzed by SQOR. The thiosulfate produced in step 1 is likely to act as the substrate for a sulfur transferase (ST) that regenerates the sulfite consumed in step 1 and produces  $\text{GSS}^-$ . The latter undergoes a 4-electron oxidation reaction catalyzed by SDO (step 3) that produces the sulfite required

---

<sup>2</sup> Jackson, M. R. and Jorns, M. S., unpublished observations.

for step 4 and regenerates the glutathione consumed in step 2. The ST and SDO reactions are likely to be tightly coupled to prevent decomposition of  $\text{GSS}^-$ , a labile metabolite (22)<sup>3</sup>. The pathway is largely short-circuited by the absence of SDO in ethylmalonic encephalopathy patients owing to their impaired ability to produce sulfite. The resulting greatly elevated  $\text{H}_2\text{S}$  levels will promote  $\text{H}_2\text{S}$  oxidation by SQOR in an alternate reaction that uses sulfide as acceptor and produces hydrogen disulfide instead of thiosulfate. Hydrogen disulfide is, however, likely to be reduced by glutathione in a futile cycle that regenerates  $\text{H}_2\text{S}$  and causes oxidative stress by depleting the mitochondrial pool of reduced glutathione. In this regard it is noteworthy that N-acetylcysteine, an antioxidant and glutathione precursor, has been shown to reduce the severity of the pathology exhibited by ethylmalonic encephalopathy patients (147).

It is known that thiosulfate can be converted to sulfate in a glutathione-dependent pathway involving the sequential action of thiosulfate reductase (TSR) and sulfite oxidase (SO) (5, 7) (Scheme 2.1, path B). The operation of both paths A and B in the presence of glutathione means that two pairs of enzymes, SQOR/SO and ST/TSR, will compete for substrates (sulfite and thiosulfate, respectively) that are common to both pathways. Interestingly, SQOR and SO exhibit nearly identical catalytic efficiencies for sulfite utilization, as judged by values obtained for  $k_{\text{cat}}/K_{\text{m sulfite}}$  ( $2.1 \times 10^6$  and  $2.4 \times 10^6 \text{ M}^{-1} \text{ s}^{-1}$ , respectively) (148). Its inner mitochondrial membrane location may favor sulfite utilization by SQOR because reaction with SO requires transport of the metabolite from the matrix to the intermembrane space. However, the availability of  $\text{H}_2\text{S}$  is likely to play

---

<sup>3</sup>SDO has been reported to form a complex with rhodanese. The ST that produces  $\text{GSS}^-$  is, however, currently unknown.

a decisive role in the partitioning of sulfite between the two pathways. Consistent with this hypothesis, elevated urinary excretion of thiosulfate is observed under conditions associated with elevated H<sub>2</sub>S levels, such as Down's syndrome (82), environmental exposure to H<sub>2</sub>S gas (149), and ethylmalonic encephalopathy (22). A minor cysteine catabolic pathway is thought to provide the sulfite required to generate the elevated urinary thiosulfate observed in ethylmalonic encephalopathy patients (22, 150)<sup>4</sup>. The partitioning of thiosulfate is clearly regulated by the availability of glutathione, probably because 2 mol of glutathione are consumed by the TSR reaction in path B whereas only catalytic amounts are required for the ST-SDO reaction in path A.

### 2.5.2 Mechanism of SQOR catalysis

SQOR exhibits homology with flavoprotein disulfide oxidoreductases, such as glutathione reductase and flavocytochrome c sulfide dehydrogenase (15). These enzymes utilize a Cys-S-S-Cys disulfide bridge as a redox center in addition to flavin. Human SQOR contains two cysteine residues (Cys201, Cys379) that are: (i) conserved in all eukaryotic homologs (15); and (ii) essential for catalytic activity<sup>5</sup>. Cys201 aligns with the "proximal" cysteine of the redox-active disulfide in flavocytochrome c sulfide dehydrogenase, i.e., the cysteine closer to the C(4a) position of FAD (151). By analogy with mechanisms observed for other members of the flavoprotein disulfide oxidoreductase family (152), we propose that the SQOR reaction is initiated by nucleophilic attack of HS<sup>-</sup> (the predominant H<sub>2</sub>S form at physiological pH) at the distal

---

<sup>4</sup> Cysteine sulfinic acid, produced from cysteine by cysteine dioxygenase, is mainly (70-90%) converted to hypotaurine. However, a small amount of this metabolite may undergo transamination to produce β-sulfinylpyruvate, a compound that spontaneously decomposes to pyruvate and sulfite.

<sup>5</sup>Melideo, S. L. and Jorns, M. S. unpublished observations.



cysteine, Cys379, to produce an intermediate containing: (i) a protein-bound persulfide, Cys<sub>379</sub>SS<sup>-</sup> and (ii) a charge-transfer (CT) complex of FAD with Cys<sub>201</sub>S<sup>-</sup> or Cys<sub>379</sub>SS<sup>-</sup> (Scheme 2.2, step 1). Nucleophilic attack of Cys<sub>201</sub>S<sup>-</sup> at the C(4a) position of the flavin ring produces a covalent flavin adduct, 4a-adduct I (step 2). Reaction of this intermediate with a nucleophilic acceptor of the sulfane sulfur (N:) generates an intermediate, 4a-adduct II, containing the thiolate form of Cys379 (step 3). Nucleophilic attack of Cys<sub>379</sub>S<sup>-</sup> at the sulfur atom in the 4a-adduct produces an intermediate containing 1,5-dihydroFAD plus the original disulfide (EFAD<sub>red</sub>/disulfide) (step 4). The catalytic cycle is completed upon transfer of electrons from EFAD<sub>red</sub>/disulfide to coenzyme Q (step 5).

Consistent with the proposed mechanism, turnover of SQOR requires an acceptor (N:) that may be sulfite, cyanide or HS<sup>-</sup>, and produces an expected sulfane sulfur-containing product, thiosulfate, thiocyanate or hydrogen disulfide, respectively. An intermediate that exhibits a long-wavelength absorption band, centered at 673 nm and extending out to nearly 900 nm, is detected immediately after mixing SQOR with sulfide under anaerobic conditions. Blue neutral flavin radicals absorb in the long-wavelength region but exhibit maxima at shorter wavelengths and negligible absorbance at 700 nm (153). On the other hand, CT complexes with oxidized or 1,5-dihydroflavins exhibit maxima in the long-wavelength region that can vary over a wide range (>500 to ~800 nm), depending on the difference in the 1-electron reduction potential of the donor and acceptor (154-157). The absorption spectrum of the SQOR intermediate is consistent with a CT complex of the oxidized flavin with Cys<sub>201</sub>S<sup>-</sup> or Cys<sub>379</sub>SS<sup>-</sup> that may be in equilibrium with 4a-adduct I. Studies to further characterize this intermediate are in progress.

The SQOR intermediate is slowly converted to a reduced species that exhibits a

maximum at 365 nm, a broad shoulder around 450 nm, and a tail of absorbance at  $\lambda > 500$  nm. The spectral properties of this species are highly suggestive of a 1,5-dihydroflavin complex with a CT acceptor. The complex is, however, formed at a rate that is much slower than turnover, indicating that it is not a kinetically competent intermediate. We propose that a slow rearrangement of 4a-adduct I produces a CT complex of 1,5-dihydroFAD with thiocystine, Cys<sub>379</sub>SSSCys<sub>201</sub> (Scheme 2.2, step 6). The reaction does not require a sulfane sulfur acceptor but does produce a species, EFAD<sub>red</sub>/thiocystine, that could react with coenzyme Q to generate EFAD<sub>ox</sub>/thiocystine (Scheme 2.2, step 7). Step 7 can account for the reaction observed when the reduced species is mixed with CoQ<sub>1</sub>. It is worth noting that thiocystine is postulated as a catalytic intermediate in the oxidative polymerization of sulfide that is observed with prokaryotic SQOR's (32-34).

### 2.5.3 Concluding remarks

H<sub>2</sub>S is a signaling molecule with multiple physiological functions but also a highly toxic substance that must be tightly regulated to avoid potential adverse effects, such as inhibition of cytochrome oxidase and mitochondrial respiration. The highly efficient SQOR reaction will rapidly convert H<sub>2</sub>S to thiosulfate, a non-toxic metabolite and known intermediate in the mitochondrial oxidation of the gasotransmitter. Nevertheless, the observed metabolism of H<sub>2</sub>S to sulfate via a thiosulfate intermediate appears somewhat convoluted compared with a hypothetical 3-step pathway in which H<sub>2</sub>S is directly converted to GSS<sup>-</sup> and then sequentially oxidized to sulfite and sulfate (H<sub>2</sub>S  $\Rightarrow$  GSS<sup>-</sup>  $\Rightarrow$  SO<sub>3</sub><sup>-2</sup>  $\Rightarrow$  SO<sub>4</sub><sup>-2</sup>). The alternative route is, of course, ruled out by the fact that glutathione does not act as an acceptor of the sulfane sulfur in the SQOR reaction.

However, the comparison suggests that the more convoluted metabolism of H<sub>2</sub>S via a thiosulfate intermediate may have evolved because the metabolite plays an important role in H<sub>2</sub>S signaling. Thus, the zero-valent sulfur in thiosulfate may provide a source of the sulfane sulfur that is required for sulfhydration of cysteine residues in proteins and/or act as an intracellular storage site from which H<sub>2</sub>S can be readily mobilized by a thiosulfate reductase. Unraveling the myriad aspects of H<sub>2</sub>S signaling will clearly require additional studies.

<b>Table 2.1</b> Purification of Recombinant SQOR from <i>E. coli</i> <sup>a</sup>				
Purification step	Total activity (U) <sup>b</sup>	Total protein (mg)	Specific activity (U/mg)	Yield (%)
High speed supernatant	32,200	27,600	1.17	100
IMAC	11,100	89.8	124	34.5
Q Sepharose	8,330	14.3	581	25.9
<sup>a</sup> SQOR was purified from ~400 g of cells, as detailed in Experimental Procedures. <sup>b</sup> A unit of activity is defined as the formation of 1 μmol of reduced CoQ <sub>1</sub> at 25°C using a routine aerobic assay, as described in Experimental Procedures.				

<b>Table 2.2</b> Spectral and Catalytic Properties of Recombinant Human SQOR	
$\lambda_{\text{max}}$	451, 385, and 277 nm
$\epsilon_{451}$	11,500 M <sup>-1</sup> cm <sup>-1</sup>
$A_{280}/A_{451}$	9.24
mol FAD/mol protein	0.82
-----	
catalytic activity	$k_{\text{cat app}}$ (s <sup>-1</sup> ) <sup>a</sup>
-----	
HS <sup>-</sup> + CN <sup>-</sup> + CoQ <sub>1</sub>	82 ± 6
HS <sup>-</sup> + SO <sub>3</sub> <sup>-2</sup> + CoQ <sub>1</sub>	251 ± 9
HS <sup>-</sup> + CoQ <sub>1</sub>	18.5 ± 0.9
HS <sup>-</sup> + GSH + CoQ <sub>1</sub>	19 ± 3
<p><sup>a</sup>Reaction rates were measured at 25 °C by monitoring CoQ<sub>1</sub> reduction at 278 nm in anaerobic 100 mM potassium phosphate buffer, pH 8.0, containing 0.5 mM EDTA, 200 μM sulfide, 80 μM CoQ<sub>1</sub>, and, where indicated, 600 μM sulfite, 1.0 mM cyanide or 1 mM glutathione (GSH).</p>	

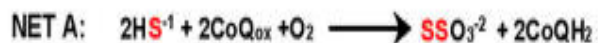
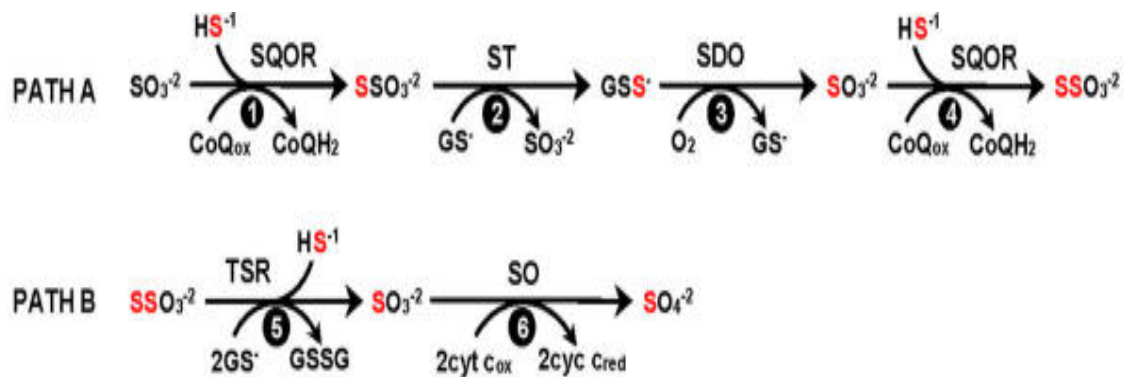
<b>Table 2.3</b> Stoichiometry of Products formed in the SQOR Reaction with Different Acceptors of the Sulfane Sulfur <sup>a</sup>			
Acceptor	[CoQ <sub>1</sub> ] (μM)	[Product] (μM)	
		thiosulfate	thiocyanate
cyanide	277		243 ± 6
sulfite	77.6	77.4	
	194	182	
<p><sup>a</sup>Assays were conducted in the presence of a limiting amount of CoQ<sub>1</sub>, 400 μM sulfide, and 1.0 mM cyanide or 1.0 mM sulfite, as described in Experimental Procedures. Aliquots were withdrawn when reduction of CoQ<sub>1</sub> was complete and analyzed for thiocyanate or thiosulfate using previously described methods (132, 133)</p>			

**Table 2.4** Effect of pH on Sulfide Oxidation by SQOR with Different Acceptors of the Sulfane Sulfur<sup>a</sup>

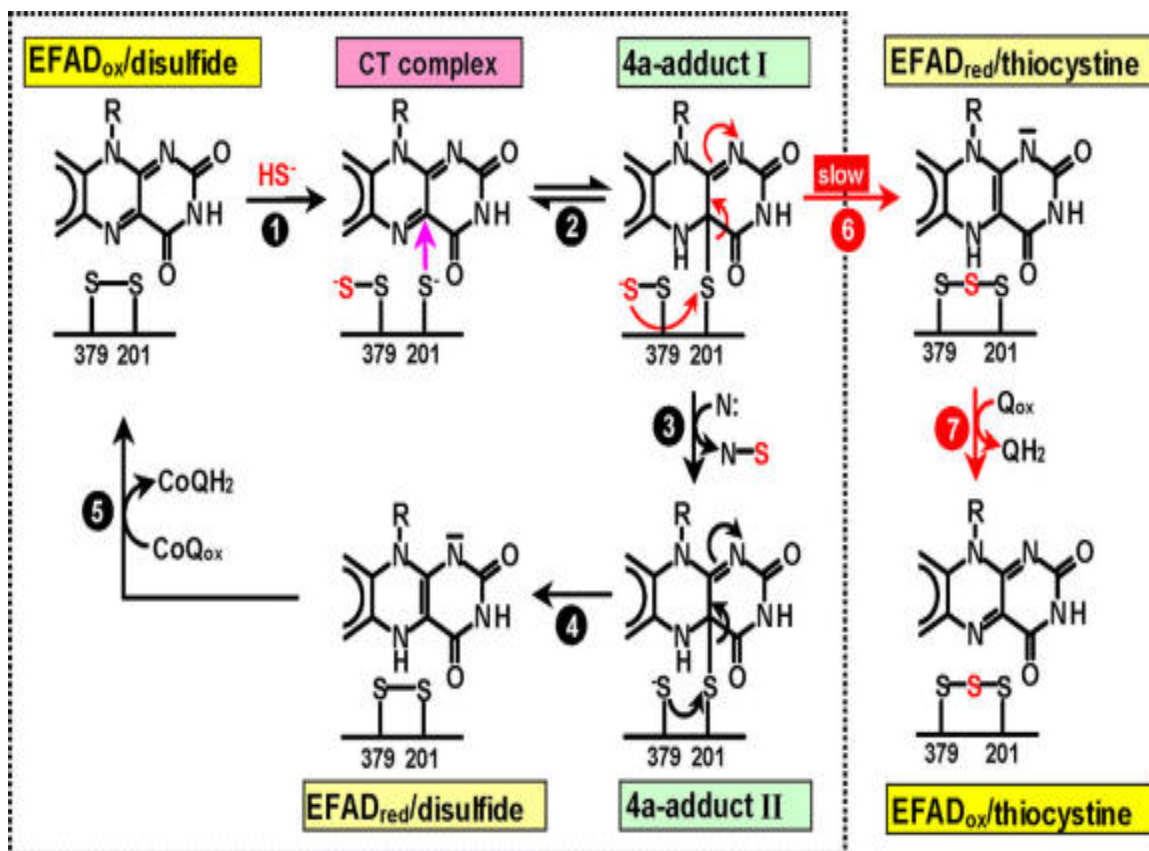
acceptor	pH optimum	$pK_{1\text{ app}}$	$pK_{2\text{ app}}$
cyanide	8.5	$7.6 \pm 0.3$	$9.6 \pm 0.4$
sulfite	7.5	$6.3 \pm 0.2$	$8.4 \pm 0.1$
sulfide	7.0	$5.9 \pm 0.1$	$8.22 \pm 0.09$

<sup>a</sup>Parameters were determined as described in the legend to Figure 2.5.

<b>Table 2.5</b> Steady-state Kinetic Parameters for Three Reactions Catalyzed by Human SQOR <sup>a</sup>				
sulfide + sulfite + CoQ <sub>1</sub> ⇒ thiosulfate + CoQ <sub>1</sub> H <sub>2</sub>				
Variable substrate	Fixed substrates <sup>b</sup>	K <sub>m</sub> (μM)	k <sub>cat</sub> (s <sup>-1</sup> )	k <sub>cat</sub> /K <sub>m</sub> (M <sup>-1</sup> s <sup>-1</sup> )
sulfide	sulfite, CoQ <sub>1</sub>	13 ± 3	379 ± 20	2.9 ± 0.6 × 10 <sup>7</sup>
sulfite	sulfide, CoQ <sub>1</sub>	174 ± 20	368 ± 14	2.1 ± 0.3 × 10 <sup>6</sup>
CoQ <sub>1</sub>	sulfide, sulfite	19 ± 2	364 ± 8	1.9 ± 0.2 × 10 <sup>7</sup>
sulfide + cyanide + CoQ <sub>1</sub> ⇒ thiocyanate + CoQ <sub>1</sub> H <sub>2</sub>				
Variable substrate	Fixed substrates <sup>c</sup>	K <sub>m</sub> (μM)	k <sub>cat</sub> (s <sup>-1</sup> )	k <sub>cat</sub> /K <sub>m</sub> (M <sup>-1</sup> s <sup>-1</sup> )
sulfide	cyanide, CoQ <sub>1</sub>	10.9 ± 0.7	343 ± 9	3.1 ± 0.2 × 10 <sup>7</sup>
cyanide	sulfide, CoQ <sub>1</sub>	650 ± 80	330 ± 12	5.1 ± 0.7 × 10 <sup>5</sup>
CoQ <sub>1</sub>	sulfide, cyanide	14 ± 2	360 ± 13	2.7 ± 0.3 × 10 <sup>7</sup>
2 sulfide + CoQ <sub>1</sub> ⇒ hydrogen disulfide + CoQ <sub>1</sub> H <sub>2</sub>				
Variable substrate	Fixed substrate <sup>d</sup>	K <sub>m</sub> (μM)	k <sub>cat</sub> (s <sup>-1</sup> )	k <sub>cat</sub> /K <sub>m</sub> (M <sup>-1</sup> s <sup>-1</sup> )
sulfide	CoQ <sub>1</sub>	315 ± 28	65 ± 2	2.1 ± 0.2 × 10 <sup>5</sup>
<sup>a</sup> Apparent K <sub>m</sub> values for the variable substrate were determined at saturating concentrations of the fixed substrates or at concentrations that yielded the maximum possible reaction rate in cases where excess substrate inhibition was observed. All measurements were made in buffers containing 0.5 mM EDTA at 25 °C. Reactions with sulfite, cyanide or sulfide as the sulfane sulfur acceptor were conducted in 100 mM potassium phosphate pH 7.5, 100 mM potassium pyrophosphate pH 8.5 or 100 mM potassium phosphate pH 7.0, respectively. <sup>b</sup> Measurements were made at the following fixed substrate concentrations: 83 μM sulfide, 99 μM CoQ <sub>1</sub> , and 2000 μM sulfite. <sup>c</sup> Measurements were made at the following fixed substrate concentrations: 47 μM sulfide, 72.5 μM CoQ <sub>1</sub> and 6000 μM cyanide. <sup>d</sup> Measurements were made at 66.2 μM CoQ <sub>1</sub> .				



**Scheme 2.1** Proposed pathways for H<sub>2</sub>S metabolism in: (i) glutathione-depleted cells or mitochondria (path A) and (ii) untreated cells or intact animals (paths A + B). ST, sulfur transferase; SDO, sulfur dioxygenase; TSR, thiosulfate reductase; SO, sulfite oxidase.



**Scheme 2.2** The catalytic mechanism proposed for SQOR is indicated by the steps (1-5) enclosed within the dotted rectangle. The complex formed in step 1 may involve CT interaction with Cys<sub>201</sub>S<sup>-</sup>, as indicated, or with Cys<sub>379</sub>SS<sup>-</sup> (not shown). Step 6 is postulated to account for a slow step observed during the anaerobic reaction of the enzyme with sulfide, as discussed in the text.



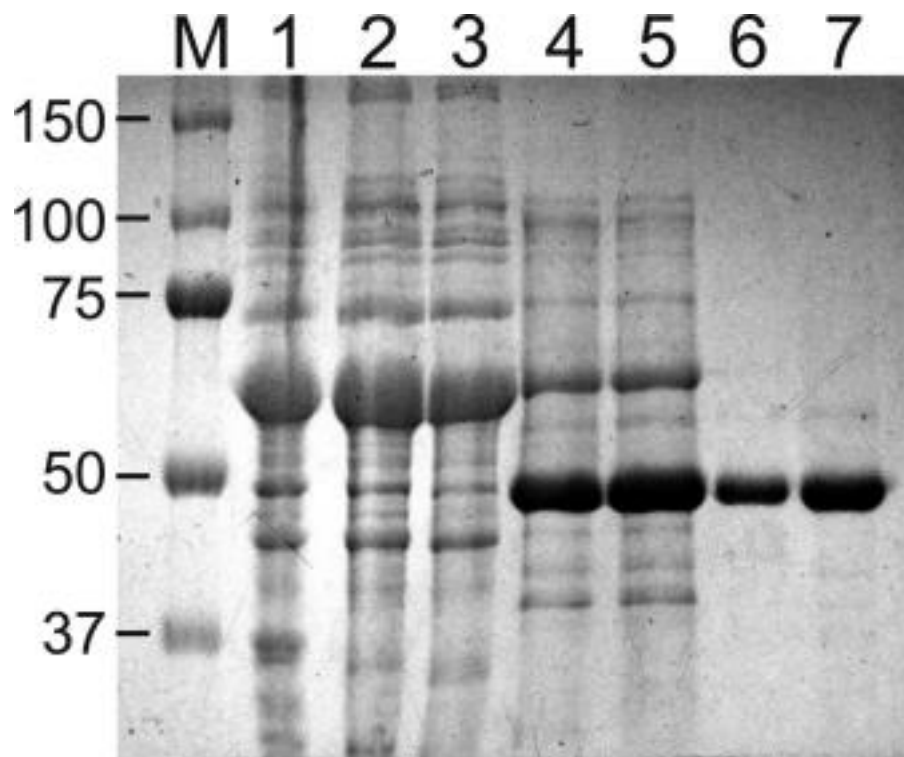


**Figure 2.1** Expression of recombinant human SQOR. The SDS-12% polyacrylamide gel was stained for protein with ProSieve Blue Protein Staining Solution (Lonza). Molecular markers are shown in lane M. Lane 1, crude cell lysate; lane 2, high speed supernatant; lane 3, IMAC wash; lane 4, IMAC eluate; lane 5, dialyzed IMAC eluate; lane 6, Q Sepharose eluate; lane 7, concentrated Q Sepharose eluate.

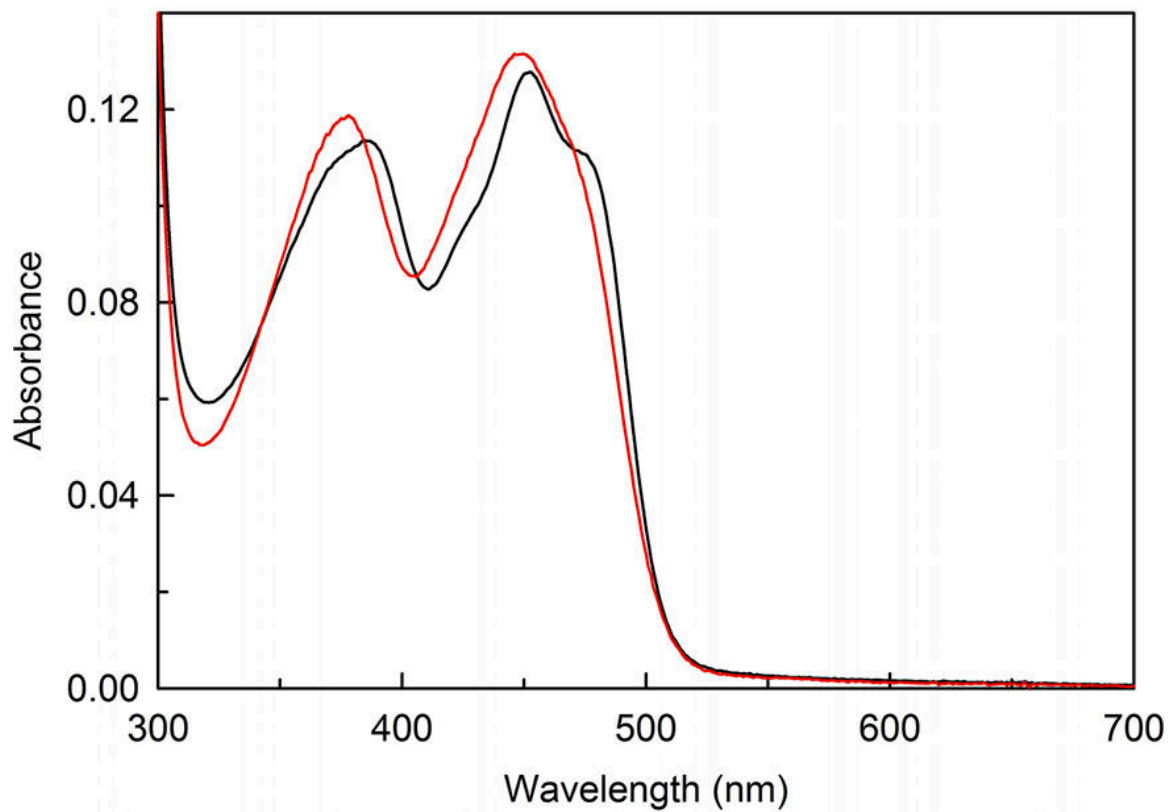


**Figure 2.2** Absorption spectra of native and denatured SQOR. The black curve is the absorption spectrum of SQOR in 100 mM potassium phosphate buffer, pH 7.4, containing 0.04% DHPC. The red curve was recorded after denaturation with 3 M guanidine hydrochloride.

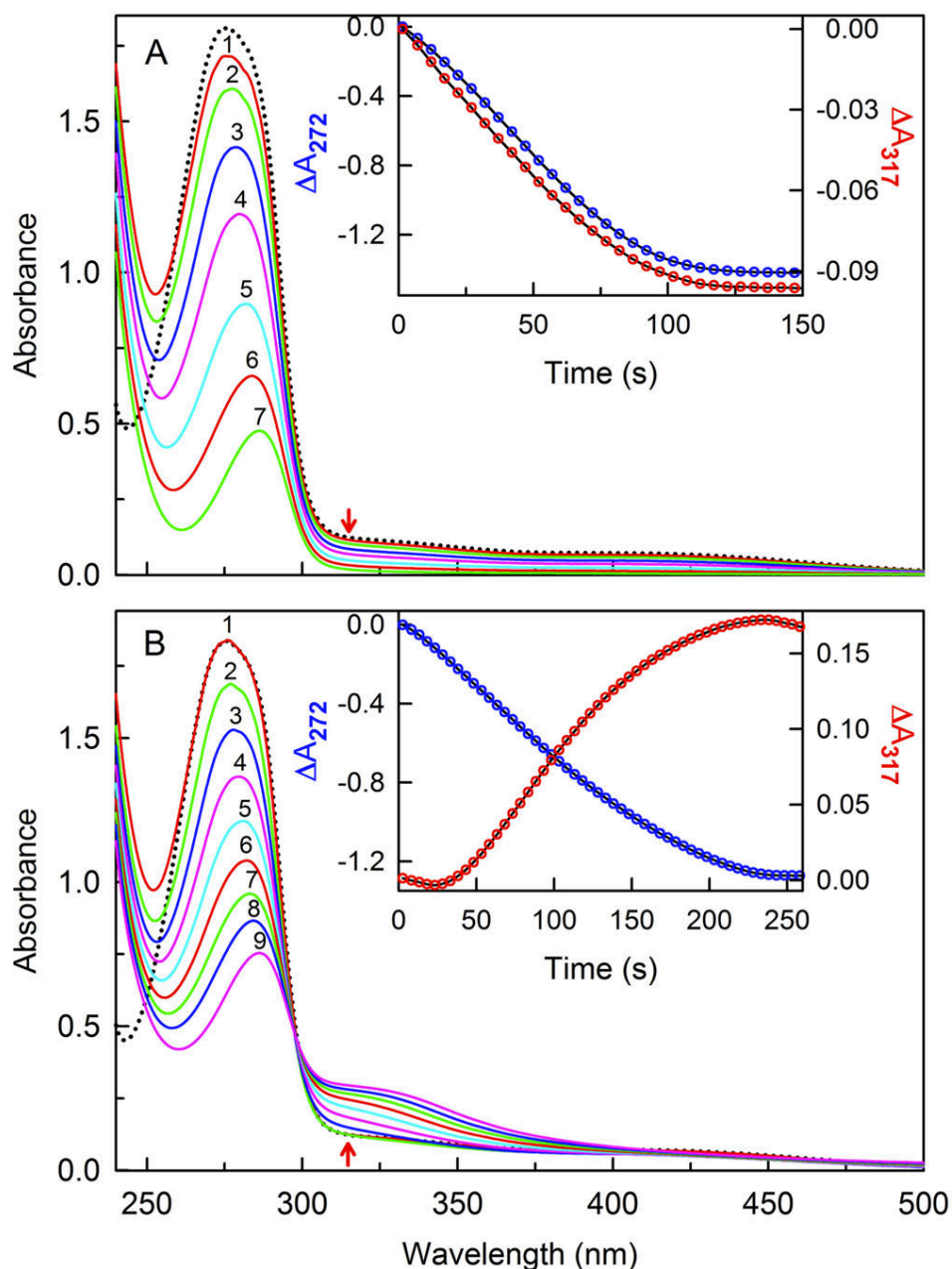


**Figure 2.3** Effect of sulfite on the spectral course of SQOR catalytic assays. Reactions were conducted in 100 mM potassium phosphate, pH 8.0, containing 0.5 mM EDTA at 25 °C in the presence (panel A) or absence (panel B) of sulfite. Red arrows indicate the direction of the spectral changes observed at  $\lambda > 300$  nm. Panel A: The dotted black line was recorded before addition of 300  $\mu$ M sulfide to an assay mixture containing 160  $\mu$ M CoQ<sub>1</sub>, 400  $\mu$ M sulfite and 7.2 nM SQOR. Curves 2 to 7 were recorded 1.4, 12, 27, 42, 62, 82, and 132 s, respectively, after sulfide addition. Panel B: The dotted black line was recorded before addition of 300  $\mu$ M sulfide to an assay mixture containing 160  $\mu$ M CoQ<sub>1</sub> and 35.6 nM SQOR. Curves 1 to 9 were recorded 2.6, 33.2, 58.2, 88.2, 108, 133, 158, 183, and 233 s, respectively, after sulfide addition. The inset in each panel shows the time course of absorbance changes at 272 and 317 nm plotted according to the left and right y-axes, respectively.

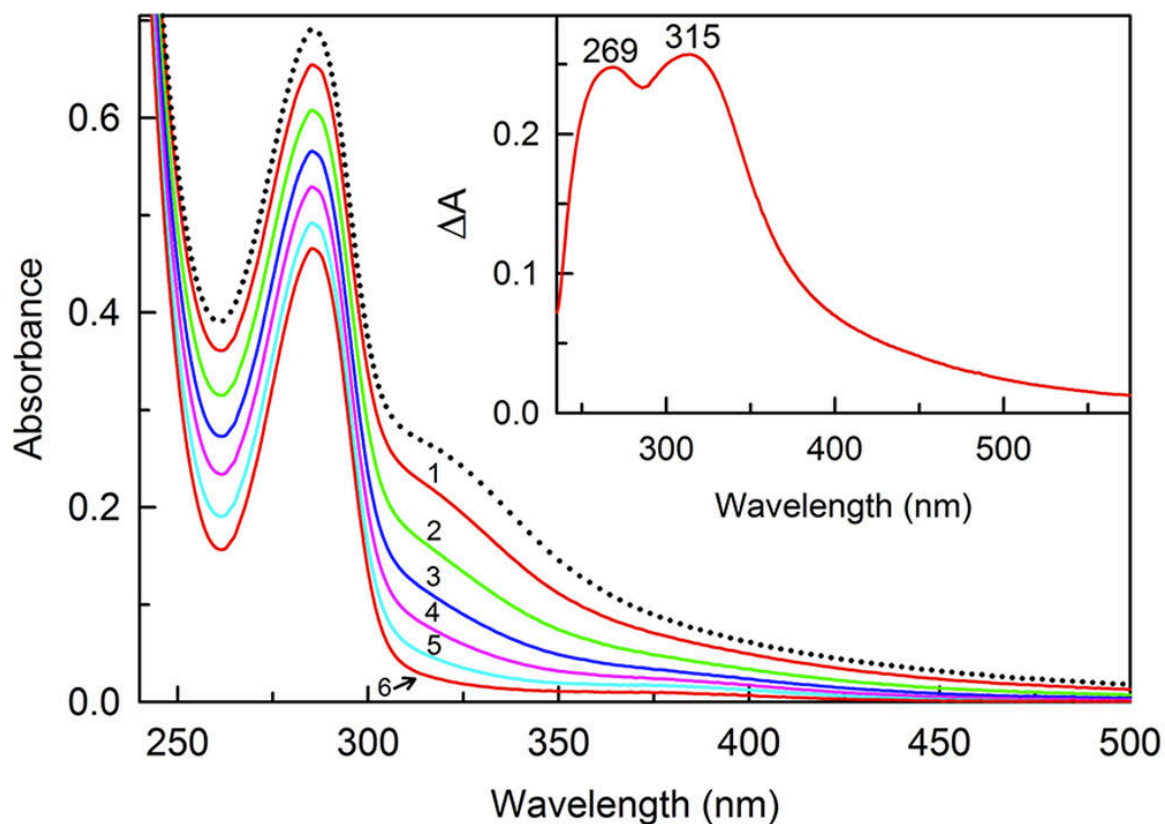


**Figure 2.4** Reaction of sulfite with the sulfur oxidation product formed during the apparent “acceptor-free” oxidation of sulfide by SQOR. Reactions were conducted in 100 mM potassium phosphate, pH 8.0, containing 0.5 mM EDTA at 25 °C. The dotted black line was recorded after maximal formation of the sulfur oxidation product in an assay mixture containing 300 μM sulfide, 160 μM CoQ<sub>1</sub> and 35.6 nM SQOR. Curves 1 to 6 were recorded 22, 42, 62, 92, and 292 s, respectively, after addition of 400 μM sulfite. The inset shows a difference spectrum calculated by subtracting the spectrum observed at the end of the sulfite reaction from the spectrum observed before sulfite addition.

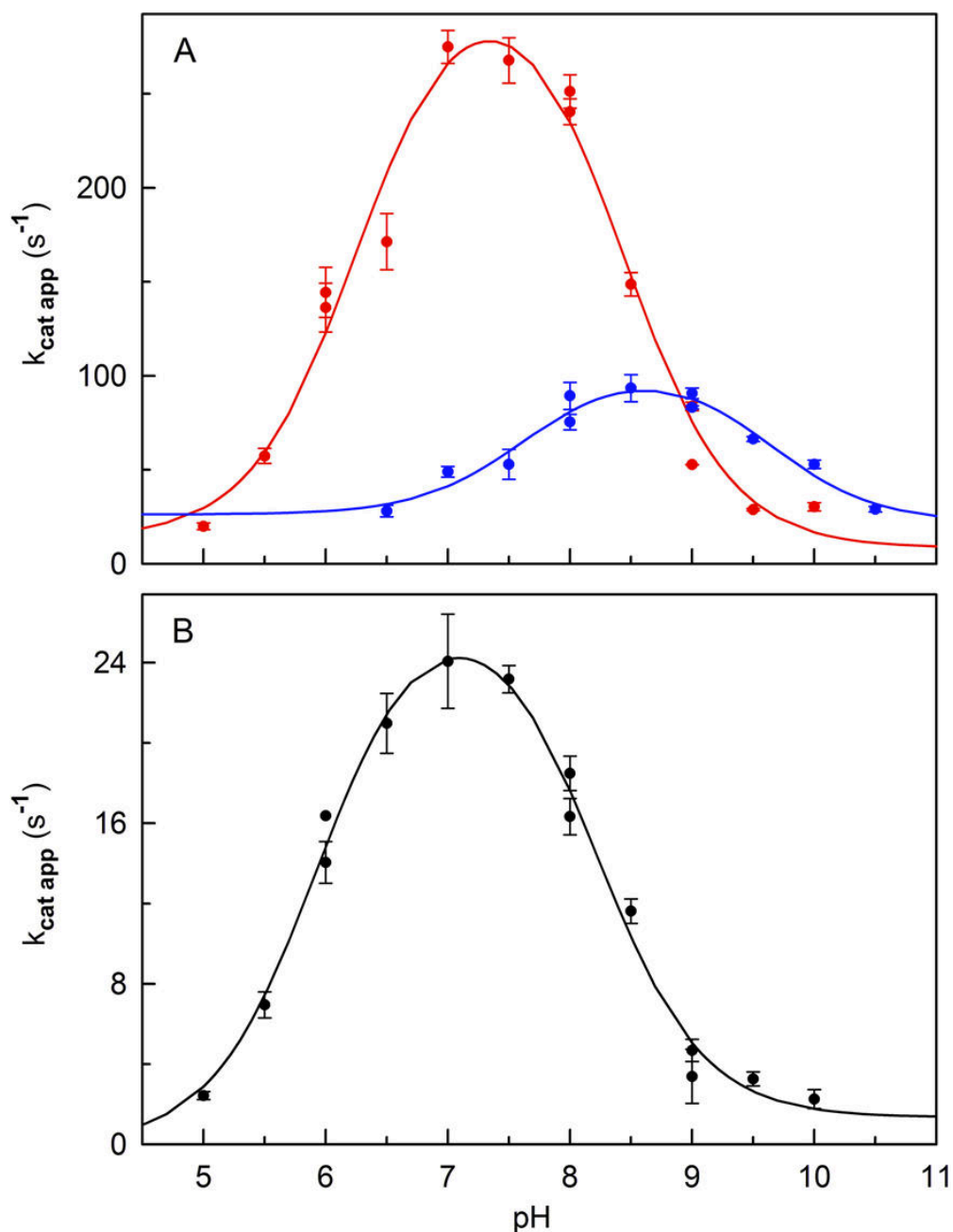


**Figure 2.5** Effect of pH on the rate of sulfide oxidation observed with SQOR in the presence or absence of sulfite or cyanide. The red and blue curves in panel A were obtained for the reactions in the presence of sulfite or cyanide respectively. Panel B shows the results obtained for the reaction in the absence of sulfite and cyanide. Reactions were monitored at 25 °C by measuring the reduction of CoQ<sub>1</sub> at 278 nm, as described in Experimental Procedures. Assays contained 200  $\mu$ M sulfide, 80  $\mu$ M CoQ<sub>1</sub> and, where indicated, 600  $\mu$ M sulfite or 1.0 mM cyanide. All reactions contained 0.5 mM EDTA plus one of the following buffers: 100 mM potassium citrate, pH 5 to 6; 100 mM potassium phosphate, pH 6 to 8; 100 mM potassium pyrophosphate, pH 8 to pH 9; 100 mM potassium carbonate/bicarbonate, pH 9 to 10.5. The solid lines were obtained by fitting equation 1 to the data (filled circles).

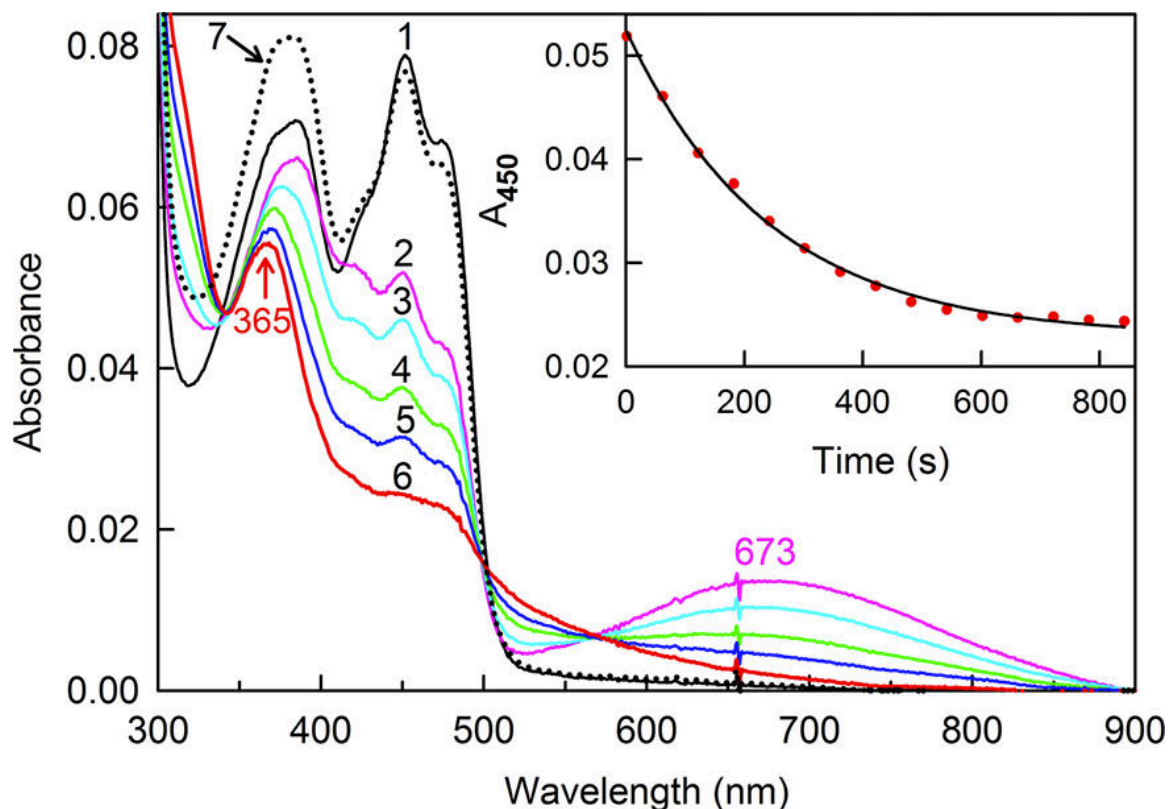


**Figure 2.6** Anaerobic reaction of SQOR with sulfide and CoQ<sub>1</sub>. Curve 1 is the absorption spectrum of 6.82 μM SQOR in anaerobic 25 mM Tris-HCl buffer, pH 8.0 at 4°C. Curves 2 to 6 were recorded 0, 1, 3, 5, and 14 min, respectively, after addition of 16.4 μM sulfide. Curve 7 (dotted line) was recorded 1 min after addition of 17.5 μM CoQ<sub>1</sub>. The inset shows a plot of the absorbance decrease at 450 nm observed after sulfide addition. The black line was obtained by fitting a single exponential equation ( $y = Ae^{-kt} + B$ ) to the data (red circles). Similar results were obtained in a separate experiment upon addition of 1.1 equivalents of sulfide (data not shown).

### Chapter 3: Biosynthesis of a central intermediate in hydrogen sulfide metabolism by a novel human sulfurtransferase and its yeast ortholog

Adapted from Scott L. Melideo, Michael R. Jackson, and Marilyn Schuman Jorns

Biochemistry 2014

#### 3.1 Abstract

Human sulfide:quinone oxidoreductase (SQOR) catalyzes the conversion of H<sub>2</sub>S to thiosulfate, the first step in mammalian H<sub>2</sub>S metabolism. SQOR's inability to produce the glutathione persulfide (GSS<sup>-</sup>) substrate for sulfur dioxygenase (SDO) suggested that a thiosulfate:glutathione sulfurtransferase (TST) was required to provide the missing link between the SQOR and SDO reactions. Although TST could be purified from yeast, attempts to isolate the mammalian enzyme were not successful. We used bioinformatic approaches to identify genes likely to encode human TST (*TSTD1*) and its yeast ortholog (*RDL1*). Recombinant TSTD1 and RDL1 catalyze a predicted thiosulfate-dependent conversion of glutathione to GSS<sup>-</sup>. Both enzymes contain a rhodanese homology domain and a single catalytically essential cysteine, which is converted to cysteine persulfide upon reaction with thiosulfate. GSS<sup>-</sup> is a potent inhibitor of TSTD1 and RDL1, as judged by initial rate accelerations and  $\geq 25$ -fold lower  $K_m$  values for glutathione observed in the presence of SDO. The combined action of GSS<sup>-</sup> and SDO is likely to regulate the biosynthesis of the reactive metabolite. SDO drives to completion *p*-toluenethiosulfonate:glutathione sulfurtransferase reactions catalyzed by TSTD1 and RDL1. The thermodynamic coupling of the irreversible SDO and reversible TST

reactions provides a model for the physiologically relevant reaction with thiosulfate as the sulfane donor. The discovery of bacterial Rosetta stone proteins that comprise fusions of SDO and TSTD1 provides phylogenetic evidence for the association of these enzymes. The presence of adjacent bacterial genes encoding SDO-TSTD1 fusion proteins and human-like SQORs suggests these prokaryotes and mammals exhibit strikingly similar pathways for H<sub>2</sub>S metabolism.

### 3.2 Introduction

H<sub>2</sub>S is the only gasotransmitter that is enzymatically metabolized and the only inorganic compound that can be used by mammalian mitochondria to generate ATP (126). H<sub>2</sub>S metabolism is particularly important because the gasotransmitter is a Janus-faced molecule that can exhibit toxic effects at supraphysiological concentrations. The first step in the mitochondrial metabolism of H<sub>2</sub>S is catalyzed by sulfide:quinone oxidoreductase (SQOR), an inner mitochondrial membrane-bound flavoenzyme that catalyzes a two-electron oxidation of H<sub>2</sub>S to sulfane sulfur (S<sup>0</sup>) using coenzyme Q as an electron acceptor (14-16, 158). The enzyme also requires an acceptor for the sulfane sulfur. Recently, the Jorns lab successfully expressed human SQOR as a membrane-bound protein in *Escherichia coli* and identified sulfite (SO<sub>3</sub><sup>-2</sup>) as the physiological acceptor of the sulfane sulfur (158). This reaction produces thiosulfate (SSO<sub>3</sub><sup>-2</sup>) (Scheme 3.1, step 1), a known intermediate in the oxidation of H<sub>2</sub>S to sulfate by animals or perfused liver (7-9). Thiosulfate is also a major product of H<sub>2</sub>S metabolism by colon, a tissue that must detoxify large amounts of H<sub>2</sub>S produced by sulfate-reducing bacteria (12, 13).



The identification of thiosulfate as the product of the SQOR reaction requires a major revision of previously suggested pathways for the downstream metabolism of the gasotransmitter (1, 14). We propose that thiosulfate acts as a substrate for a glutathione-dependent thiosulfate sulfurtransferase (TST) (Scheme 3.1, step 2). The TST reaction produces glutathione persulfide ( $\text{GSS}^-$ ) and also regenerates the sulfite consumed in step 1.  $\text{GSS}^-$  is a known substrate for sulfur dioxygenase (SDO), an enzyme that catalyzes a 4-electron oxidation of the sulfane sulfur in  $\text{GSS}^-$  to produce sulfite (Scheme 3.1, step 3) (14, 21, 22). The last step of  $\text{H}_2\text{S}$  metabolism may proceed via one of two competing alternative reactions, a scenario that can account for observed tissues differences in the final product. In one path, the sulfite produced in step 3 undergoes a 2-electron oxidation catalyzed by sulfite oxidase (SO) using cytochrome c as electron acceptor to produce sulfate (Scheme 3.1, step 4). This path results in an overall 8-electron oxidation of 1 mol of  $\text{H}_2\text{S}$  to sulfate, the major product of  $\text{H}_2\text{S}$  metabolism in liver. Alternatively, the sulfite produced in step 3 may be further metabolized by SQOR (Scheme 3.1, step 5). This path achieves an overall 8-electron oxidation of 2 mol of  $\text{H}_2\text{S}$  to 1 mol of thiosulfate, the major metabolic product observed in colon. SQOR and SO exhibit nearly identical catalytic efficiencies for sulfite utilization ( $k_{\text{cat}}/K_{\text{m sulfite}} = 2.11 \times 10^6$  and  $2.4 \times 10^6 \text{ M}^{-1} \text{ s}^{-1}$ , respectively), suggesting that the availability of  $\text{H}_2\text{S}$  is likely to play a key role in the partitioning of sulfite between the two competing reactions (148, 158). Consistent with this hypothesis, elevated urinary excretion of thiosulfate is observed under conditions that result in pathologically high levels of  $\text{H}_2\text{S}$  (e.g, Down's syndrome, sub-lethal environmental exposure to  $\text{H}_2\text{S}$  gas, ethylmalonic encephalopathy and in patients affected by sulfite oxidase deficiency (22, 82, 149, 159). The ability to rapidly convert  $\text{H}_2\text{S}$  to

thiosulfate is forcefully illustrated by the large increase in blood thiosulfate levels (up to 200-fold) that is observed in fatal cases of H<sub>2</sub>S poisoning where death occurs virtually instantaneously, before thiosulfate can be detected in the urine (160).

The proposed (scheme 3.1) is consistent with key features observed for mammalian metabolism of H<sub>2</sub>S, including the known catalytic properties of SQOR, SDO and SO. Little information is, however, currently available regarding the postulated TST. Operationally, TST can be defined as an enzyme that uses thiosulfate to produce sulfite in a glutathione-dependent reaction. The same operational definition has been used in studies with enzymes referred to as thiosulfate reductases (TRs), a nomenclature that implies that the reactions also generate H<sub>2</sub>S and oxidized glutathione (GSSG) (eq. 3) (144, 161-163).



For simplicity, an enzyme that satisfies the operational definition described above will be referred to as a TST with the understanding that additional studies are required to justify the rigorous use of this terminology.

Although TST activity is readily detected in liver extracts, attempts to isolate the mammalian enzyme have not been successful (144, 164). On the other hand, a TST was purified from *Saccharomyces cerevisiae* more than 30 years ago; the corresponding gene was not, however, identified (161-163). In this paper, we have used bioinformatics approaches to successfully identify the genes that encode the yeast TST (*RDL1*) and the corresponding human ortholog (*TSTD1*). We provide definitive evidence to show that the yeast and human enzymes act as genuine TSTs that synthesize and release GSS<sup>-</sup> into solution. We present biochemical evidence for the functional interaction of human SDO

with the novel human TST and its yeast ortholog. Our discovery of bacterial Rosetta stone proteins that comprise fusions of human SDO and human TST provides phylogenetic evidence for the association of the two enzymes.

### **3.3 Experimental procedures**

#### **3.3.1 Materials**

All enzymes required for ligation-independent cloning were purchased from New England Biolabs. Isopropyl  $\beta$ -D-1-thiogalactopyranoside (IPTG) was purchased from Gold Biotechnology. Thiosulfate, glutathione, D,L-homocysteine, coenzyme A and D,L-dihydrolipoic acid were purchased from Sigma-Aldrich. Potassium cyanide and dithiothreitol (DTT) were obtained from Fisher. L-Cysteine was obtained from Amresco. Potassium *p*-toluenethiosulfonate was purchased from TCI scientific.

#### **3.3.2 Expression of yeast RDL1 in *Escherichia coli***

PCR was used to amplify the *RDL1* gene from *Saccharomyces cerevisiae* genomic DNA (EMD chemicals). The reactions were conducted using Taq polymerase (Qiagen) and primers (see Appendix 2 Table 1) designed to introduce unique *NdeI* and *XhoI* restriction sites, as previously described (165). The Topo TA Cloning® kit (Invitrogen) was used to insert the PCR product into the pCR®2.1-TOPO vector for blue/white screening. The screening was conducted using One Shot® TOP10 *E. coli* cells, supplied with the kit, as the host cell. Plasmid DNA from a white colony was digested with *NdeI* and *XhoI* to yield a desired 420 bp fragment that was subcloned between the *NdeI* and *XhoI* sites of plasmid pET21b (Novagen). The resulting plasmid, pET21b\_rdl1, was used to transform *E. coli* BL21(DE3) cells to ampicillin resistance and sequenced across the insert (Genewiz, Inc.). A starter culture of *E. coli*

BL21(DE3)/pET21b\_rd11 cells was prepared by overnight growth at 37 °C in LB medium containing ampicillin (100 µg/mL) and used to inoculate 2.5 L flasks containing 1 L of TB medium supplemented with ampicillin (100 µg/mL). Cells were grown with shaking at 30 °C. Expression of yeast RDL1 was induced with IPTG (0.1 mM) when the cell density reached  $A_{595} \sim 0.6$ . Cells were harvested 4 h after induction (~ 20 g from 3 L) and stored at -80 °C.

### **3.3.3 Purification of recombinant yeast RDL1**

The enzyme was purified at 4 °C by a modification of a previously described protocol (165). Cells (10 g) were suspended in 15 mL of 20 mM Tris-HCl, pH 8.0, containing 150 mM NaCl and 20 mM imidazole-HCl. The cell suspension was mixed with a nuclease/protease inhibitor cocktail (20 µg/mL DNAase, 20 µg/mL RNAase, 5 mM magnesium sulfate, 12.6 µg/mL soybean trypsin inhibitor, 2 µg/mL aprotinin, 25 µg/mL phenylmethanesulfonyl fluoride, and 3 µg/mL tosyllysine chloromethylketone). The cells were disrupted by sonication. Cell debris was removed by centrifugation (10,000 g, 10 min). The supernatant was mixed with 10 mL of Ni affinity matrix (Talon affinity resin, Qiagen), previously equilibrated with buffer A (20 mM Tris-HCl, pH 8.0, containing 500 mM NaCl, 20 mM imidazole-HCl), and rocked gently for 1 h. The mixture was poured into a column, which was washed with 4 column volumes of buffer A. Yeast RDL1 was eluted using a 120 mL linear gradient from 20 to 250 mM imidazole, which was formed with buffer A and buffer B (20 mM Tris-HCl, pH 8.0, containing 500 mM NaCl, and 250 mM imidazole-HCl). The eluate was dialyzed against 50 mM Tris-HCl, pH 8.0, containing 50 mM NaCl and 5% (w/v) glycerol. The supernatant, obtained

after centrifugation (30,000 g, 10 min), was concentrated using a 5K Macrosep Advance Centrifugal Device (Pall Life Sciences) and then stored in aliquots at -80 °C.

### 3.3.4 Expression of Human TSTD1 Isoforms 1, 2 and 3 in *E. coli*

A synthetic version of the human gene for each isoform, which had been optimized for expression in *E. coli*, was obtained from Blue Heron Biotechnology, Inc. (Bothell, WA) (see Appendix 2 figures 1, 2, 3 for the sequences of synthetic genes). Ligation-independent cloning was used to add a cleavable (His)<sub>6</sub>-SUMO tag to the N-terminus of each synthetic gene. The cloning was conducted by using the PCR primers listed in Appendix 2 Table 1, plasmid pETHSUL (gift from Dr. Patrick Loll), and a protocol similar to that described by Weeks et al. (166). The resulting constructs for isoforms 1, 2 and 3 (pETHSUL\_tstd1IF1, pETHSUL\_tstd1IF2, and pETHSUL\_tstd1IF3, respectively) were used to transform *E. coli* BL21(DE3) cells to ampicillin resistance and sequenced across each insert (Genewiz, Inc.).

For expression of isoform 1, a starter culture of *E. coli* BL21(DE3)/pETHSUL\_tstd1IF1 cells was prepared by an overnight growth at 37 °C in LB medium containing ampicillin (100 µg/mL) and used to inoculate 2 L flasks containing 1 L of the same medium. Cells were grown with shaking at 37 °C. Expression of (His)<sub>6</sub>-SUMO-tagged isoform 1 was induced with 0.5 mM IPTG when the cell density reached A<sub>595</sub> ~ 0.6. Cells were harvested 2 h after induction (~ 35 g of cells from 15 L) and stored at -80 °C.

A similar procedure was used for expression of isoform 2 or 3 except that *E. coli* cells (BL21(DE3)/pETHSUL\_tstd1IF2 or BL21(DE3)/pETHSUL\_tstd1IF3, respectively) were induced with 0.5 mM IPTG at A<sub>595</sub> ~ 0.6 and harvested 3 h post induction. The yield

of cells was similar to that obtained with isoform 1 (isoform 2, 33 g from 18 L; isoform 3, 31 g from 15 L).

### 3.3.5 Purification of recombinant human TSTD1 Isoforms 1, 2, and 3

The same procedure was used to purify each isoform, except as noted. All steps were conducted at 4 °C, following a modification of a previously described generic protocol (166). Cells (20 g) were suspended in 35 mL of 25 mM Tris-HCl, pH 8.0, containing 500 mM NaCl, 10% (w/v) glycerol, and 8 mM imidazole-HCl. The cell suspension was mixed with a nuclease/protease inhibitor cocktail, as described above. The cells were disrupted by sonication. Cell debris was removed by centrifugation (39,000 g, 10 min). The supernatant was mixed with 10 mL of Ni affinity matrix (Talon affinity resin, Qiagen), previously equilibrated with buffer C (25 mM Tris-HCl, pH 8.0, containing 500 mM NaCl, 10% (w/v) glycerol, 2 mM thiosulfate, and 8 mM imidazole-HCl) and rocked gently for 1 h. The mixture was poured into a column, which was washed with 4 column volumes of buffer C. The (His)<sub>6</sub>-SUMO-tagged TSTD1 isoforms were eluted with a 20 mL linear gradient from 8 to 250 mM imidazole, which was formed with buffer C and buffer D [25 mM Tris-HCl, pH 8.0, containing 500 mM NaCl, 10% (w/v) glycerol, 2 mM thiosulfate, and 250 mM imidazole-HCl]. (In the case of isoform 3, the column eluate was centrifuged (30,000 g, 10 min) to remove a small precipitate.) The peptide bond between the (His)<sub>6</sub>-SUMO tag and the N-terminus of each TSTD1 isoform was cleaved using the UD1 domain of the *S. cerevisiae* Ulp1 peptidase (0.5 % , v/v), an engineered SUMO-specific protease containing a C-terminal (His)<sub>6</sub> tag (166) (gift from Dr. Simon Cocklin). After a 6 h incubation with gentle rocking at 4 °C, the reaction mixture was dialyzed against 2 changes of a ~ 60-fold excess of buffer C.

The supernatant obtained after centrifugation (30,000 g, 10 min) was applied to the Ni affinity matrix column described above, which had been re-equilibrated with buffer C. Tag-free TSTD1 isoforms do not bind to the matrix and are recovered in the column flow-through. The purified isoforms were dialyzed against 50 mM Tris-HCl, pH 8.0, containing 50 mM NaCl, 2 mM thiosulfate, and 5% (w/v) glycerol and then centrifuged (30,000 g, 10 min). The supernatants were stored in aliquots at -80 °C.

### 3.3.6 Protein assays

Protein concentration during enzyme purification was assessed by using a Nano Drop 2000 spectrometer (Thermo Scientific). All other absorbance measurements were made using an Agilent Technologies 8453 diode array spectrophotometer. The concentration of purified RDL1 ( $\epsilon_{280} = 25,440 \text{ M}^{-1} \text{ cm}^{-1}$ ) and purified TSTD1 isoforms 1, 2 and 3 ( $\epsilon_{280} = 11,460, 11,460$  and  $9970 \text{ M}^{-1} \text{ cm}^{-1}$ , respectively) was determined using extinction coefficients calculated using the ProParam tool (<http://web.expasy.org/protparam/>).

### 3.3.7 Catalytic assays with thiosulfate as sulfane sulfur donor and glutathione as acceptor

TST activity during enzyme purification was monitored using a sulfite endpoint assay, similar to that previously described (163). Briefly, reactions were initiated by addition of enzyme to assays containing 50 mM Tris-acetate, pH 9.0, 20 mM thiosulfate, and 20 mM glutathione at 37 °C in a final volume of 500  $\mu\text{L}$ . Assays were quenched after 2 min by addition of mercuric chloride to a final concentration of 115 mM and centrifuged. The supernatant was assayed for sulfite by using a *p*-rosaniline colorimetric assay ( $\epsilon_{570} = 35,300 \text{ M}^{-1} \text{ L}^{-1}$ ).

### 3.3.8 Effect of sulfur dioxygenase on catalytic assays with glutathione and thiosulfate

Assays were conducted at 37 °C in 50 mM Tris-acetate, pH 9.0 or at 25 °C in 50 mM potassium/sodium phosphate, pH 8.0 in the presence of 20 mM thiosulfate and 2.4 or 20 mM glutathione. Reactions in the presence or absence of SDO were initiated by addition of glutathione, quenched after 2 min, and assayed for sulfite formation, as described above. Recombinant human SDO was expressed in *E. coli* BL21(DE3)/pMW172ETHE and purified similar to that previously described (22). Plasmid pMW172ETHE was obtained as a gift from Valeria Tiranti.

### 3.3.9 Steady-state kinetic analysis of the thiosulfate:glutathione sulfurtransferase reaction

Steady-state kinetic studies were performed by using the sulfite endpoint assay. Studies were conducted at 37 °C in 50 mM Tris-acetate, pH 9.0 in the absence or presence of SDO, as indicated. Steady-state kinetic parameters were estimated by fitting an equation for a sequential mechanism (eq. 4, A = thiosulfate, B = glutathione) to the data.

$$V = \frac{k_{\text{cat}}[A][B]}{K_{\text{ia}}K_{\text{b}} + K_{\text{a}}[B] + K_{\text{b}}[A] + [A][B]} \quad (\text{eq. 4})$$

### 3.3.10 Sulfurtransferase reactions with *p*-toluenethiosulfonate as sulfane sulfur donor and glutathione as acceptor

Reactions using *p*-toluenethiosulfonate (*p*-Tol-SO<sub>2</sub>S<sup>-</sup>) as sulfane sulfur donor were conducted using 2 mm cuvettes at 25 °C in 50 mM potassium/sodium phosphate buffer, pH 8.0. Reaction progress was monitored by following the disappearance of *p*-Tol-SO<sub>2</sub>S<sup>-</sup> at 242 nm ( $\Delta\epsilon_{242} = 5080 \text{ M}^{-1} \text{ cm}^{-1}$ ), as described in the text. The data are not corrected for absorbance changes due to the conversion of reduced glutathione to glutathione



persulfide, which are likely to be small, as judged by the similar extinction coefficients determined for reduced and oxidized glutathione ( $\epsilon_{242} = 540 \text{ M}^{-1}$  and  $410 \text{ M}^{-1} \text{ cm}^{-1}$ , respectively). Reactions were conducted in the absence or presence of human SDO, as indicated.

### **3.3.11 Substitution of glutathione by alternate small molecule acceptors in sulfurtransferase reactions with thiosulfate as sulfane sulfur donor**

Apparent steady-state kinetic parameters for reactions in which glutathione was replaced with other thiols (cysteine, coenzyme A, DTT) or cyanide were determined by varying the acceptor concentration at a fixed, saturating concentration of thiosulfate and by varying the thiosulfate concentration at a fixed, saturating concentration of the acceptor. Reactions were conducted at  $37^\circ\text{C}$  in 50 mM Tris-acetate, pH 9.0, and were initiated by addition of yeast RDL1 or human TSTD1. Reaction rates with thiol acceptors were determined by monitoring sulfite formation in an endpoint assay, as described above. Reaction rates with cyanide were determined by using a thiocyanate endpoint assay, similar to that previously described (20). Briefly, reactions were quenched by the addition of 5% formaldehyde; thiocyanate was measured based on the formation of a red complex upon addition of an acidic solution of ferric nitrate ( $\epsilon_{460} = 4300 \text{ M}^{-1} \text{ cm}^{-1}$ ).

### **3.3.12 Mutation of the single cysteine in yeast RDL1 or human TSTD1 Isoform 1**

PCR site-directed mutagenesis was used to replace Cys98 in yeast RDL1 or Cys79 in human TSTD1 isoform 1 with Ala or Ser. PCR reactions were conducted using pET21b\_rd11 or pETHSUL\_tstd1IF1 as template, PCR Mix (Amresco®), Pfu turbo DNA polymerase (Agilent Technologies), and the primers listed in Appendix 2 Table 1. After treatment with *DpnI* (New England Bio Labs) to remove template DNA, the PCR

products were used to transform *E. coli* BL21(DE3) cells to ampicillin resistance and sequenced across the insert (Genewiz, Inc.). Transformants harboring the mutant plasmids (pEt21b\_rdl1\_C98A, pET21b\_rdl1\_C98S, pETHSUL\_tstd1 C79A # 6, pETHSUL\_tstd1 C79S # 1) were used to express and purify the enzyme variants, following the same procedures described for the corresponding wild-type enzymes.

### **3.3.13 Detection of cysteine persulfide in yeast RDL1 or human TSTD1**

Enzyme samples were incubated for 10 min on ice with 2 mM thiosulfate and then subjected to gel filtration at 4°C on a Sephadex G-15 column equilibrated with 50 mM potassium phosphate buffer, pH 7.5. The protein concentration in the gel eluate was estimated based on the absorbance at 280 nm. The persulfide concentration in the untreated eluate and in samples incubated for 10 min at room temperature with 7 mM glutathione and 1.2 µM SDO was determined using the cold cyanolysis method, as previously described (133).

## **3.4 Results**

### **3.4.1 Use of bioinformatics to identify potential candidate gene(s) for yeast thiosulfate sulfurtransferase**

Yeast TST is a ~17,000 Da protein that exhibits an isoelectric point of 5.1 and contains a single cysteine residue, as judged by properties observed for the natural enzyme isolated from *S. cerevisiae* more than 30 years ago (163). We sought to identify potential candidate gene(s) for yeast TST by searching the *S. cerevisiae* genomic database (<http://www.yeastgenome.org>) for entries annotated as sulfurtransferases, a term used to describe enzymes that transfer a sulfane sulfur atom from a donor substrate to a thiophilic acceptor molecule. This search retrieved two genes of unknown function

(*RDL1* and *RDL2*) plus seven other genes of known function (*TUM1*, *UBA4*, *YCH1*, *NFS1*, *LIP5*, *BIO2*, *SLM3*) (Table 3.1). An additional gene of known function (*OAC1*) was retrieved using thiosulfate as the search term. Searches performed using other terms (e.g., rhodanese, rhodanese-like protein, sulfur transfer, thiosulfate cyanide transsulfurase, thiosulfate reductase) did not identify any additional candidate genes. Except for *RDL1*, all of the retrieved genes could be eliminated as potential candidates for yeast TST on the basis of the isoelectric point, molecular weight and/or the cysteine content of the corresponding gene product (Table 3.1). On the other hand, the protein encoded by the *RDL1* gene (RDL1) contains a single cysteine and exhibits other properties (MW 15.4 kDa, pI = 5.9) remarkably similar to those reported for the natural TST purified from yeast.

### **3.4.2 Expression and purification of recombinant yeast RDL1**

We used PCR to amplify the *RDL1* gene from yeast genomic DNA. The PCR product was subcloned into plasmid pET21b to introduce a C-terminal His-tag. Recombinant RDL1 is highly expressed in *E. coli* and readily isolated by metal affinity chromatography (Figure 3.1). A typical preparation yields 50 mg of purified RDL1 from 10 g of cells.

### **3.4.3 Does recombinant yeast RDL1 exhibit thiosulfate:glutathione sulfurtransferase activity**

The standard TST assay is performed at pH 9, the optimum observed with the natural yeast enzyme (163). This assay is initiated by addition of enzyme to reaction mixtures containing 20 mM thiosulfate and 20 mM glutathione. The reaction is quenched after a specified time when sulfite formation is measured using a colorimetric assay.

Using this assay, we found that RDL1 catalyzed the formation of sulfite in a reaction that exhibits a linear dependence on time and enzyme concentration (data not shown).

A complete steady-state kinetic analysis of the reaction catalyzed by RDL1 was conducted by measuring turnover rates at various concentrations of thiosulfate and glutathione. Double reciprocal plots of reaction rate versus thiosulfate at different concentrations of glutathione or versus glutathione at different concentrations of thiosulfate are linear and intersect to the left of the  $y$ -axis, just above the  $x$ -axis (Figure 3.2A, 2B). The observed intersecting line kinetics are in agreement with results obtained in previous studies with TST isolated from yeast (163). Recombinant RDL1 exhibits a 10-fold faster limiting turnover rate ( $k_{\text{cat}}$ ) but other steady-state kinetic parameters are nearly identical to values reported for the natural enzyme isolated from yeast (Table 3.2). The lower turnover rate observed for the natural enzyme is probably attributable to stability problems encountered during the multiple steps required to purify TST from yeast (163). The results provide compelling evidence that the *RDL1* gene encodes yeast TST.

#### **3.4.4 Use of bioinformatics to identify a potential candidate gene for human thiosulfate sulfurtransferase**

A BLASTp search of the human genome database using RDL1 as the query sequence retrieved a single promising candidate gene (*TSTD1*, thiosulfate sulfurtransferase rhodanese-like domain containing 1) for the human ortholog of yeast TST (Table 3.3). The *TSTD1* gene contains four exons and is annotated as having three splice variants (RefSeq mRNAs). The predicted protein isoforms (TSTD1 isoforms 1, 2, and 3) differ in size (115, 74, and 109 amino acids, respectively) but share a common

core of 55 amino acids that contains the single cysteine residue found in each isoform (Appendix 2 figure 4). The TSTD1 isoforms exhibit about 34% identity (~52% similarity) with yeast RDL1<sup>6</sup>. The rank ordering of the TSTD1 isoforms by the BLAST algorithm (1 >> 3 > 2) is based on the calculated Expect value (E) (see Table 3.3) which takes into account both the number of conserved residues and the length of the RDL1 query sequence that overlaps with each human isoform.

### **3.4.5 Expression and purification of recombinant human TSTD1 Isoforms 1, 2, and 3**

The mRNA for the top-ranking isoform 1 contains all four of the exons in the *TSTD1* gene. We obtained a synthetic version of the corresponding cDNA that had been optimized for expression of isoform 1 in *E. coli*. The synthetic gene was subcloned into plasmid pET21b to introduce a C-terminal (His)<sub>6</sub> tag. The resulting construct was then used to transform *E. coli* BL21(DE3) cells, following a strategy similar to that used to successfully express recombinant RDL1. However, no expression of TSTD1 isoform 1 was observed in cell lysates produced under a range of growth conditions, as judged by SDS-PAGE analysis. In an attempt to overcome this difficulty, we introduced a (His)<sub>6</sub>-SUMO tag at the N-terminus of the synthetic gene. The (His)<sub>6</sub>-SUMO-TSTD1 isoform 1 fusion protein is highly expressed in *E. coli* (Figure 3.3, lane 2) and readily purified by metal affinity chromatography (Figure 3.3, lane 5). Quantitative cleavage of the fusion protein is achieved by digestion with a SUMO-specific protease (Figure 3.3, lanes 6, 7). Rechromatography of the digest on a metal affinity column yields pure, tag-free TSTD1

---

<sup>6</sup> Calculated values were obtained in pairwise local sequence alignments using EMBOSS Water ([http://www.ebi.ac.uk/Tools/psa/emboss\\_water/](http://www.ebi.ac.uk/Tools/psa/emboss_water/)).

isoform 1 (Figure 3.3, lanes 8, 10). We obtained 90 mg of TSTD1 isoform 1 from 20 g of cells.

The mRNA for the smallest isoform 2 lacks exon 2 but contains the other three exons of the *TSTD1* gene. A different exon is missing in the mRNA that encodes isoform 3 (exon 4). Additionally, intron 3 is retained in the mRNA for isoform 3 and encodes a predicted decapeptide at the C-terminus of the protein (see Appendix 2 figure 4).

Isoforms 2 and 3 were successfully expressed as SUMO fusion proteins and readily isolated, as described in Experimental Procedures and shown in Appendix 2 figures 5 and 6. We obtained 68 mg of TSTD1 isoform 2 and 54 mg of TSTD1 isoform 3 from 20 g of cells.

#### **3.4.6 Do human TSTD1 Isoforms 1, 2, and/or 3 exhibit thiosulfate:glutathione sulfurtransferase activity**

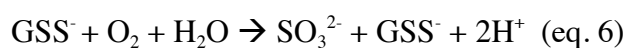
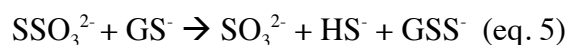
A survey was conducted using the standard TST assay to determine whether activity could be detected with any of the human TSTD1 isoforms. Isoform 1 was found to catalyze the conversion of thiosulfate to sulfite in a glutathione-dependent reaction that exhibits a linear dependence on time and enzyme concentration (data not shown). In contrast, neither of the other two TSTD1 isoforms exhibits detectable TST activity. The results with isoform 2 suggest that the peptide encoded by exon 2 is essential for the activity observed with isoform 1. The absence of activity with isoform 3 may reflect the loss of the peptide encoded by exon 4 and/or the translation of retained intron 3. It is worth noting that catalytically inactive isoforms are known to exhibit a regulatory function in metabolism (167). This intriguing possibility is, however, beyond the scope of

the current investigation. Instead, our studies have focused on isoform 1, as described below.

A complete steady-state kinetic analysis of the thiosulfate:glutathione sulfurtransferase reaction catalyzed by TSTD1 isoform 1 was conducted at pH 9.0 (37°C). Double reciprocal plots of reaction rate versus thiosulfate or versus glutathione intersect to the left of the y-axis, just above the x-axis (Figure 3.4), as observed with yeast RDL1. The human enzyme exhibits catalytic parameters fairly similar to RDL1, except that turnover is ~25-fold slower (Table 3.2). The results show that the *TSTD1* gene encodes the human ortholog of yeast TST. The catalytically active isoform 1 will henceforth be referred to as human TSTD1.

#### **3.4.7 Use of sulfur dioxygenase to distinguish between thiosulfate:glutathione sulfurtransferase versus thiosulfate reductase activity**

TSTs and TRs both catalyze the glutathione-dependent conversion of thiosulfate to sulfite. The TST reaction is, however, accompanied by the formation of a stoichiometric amount of glutathione persulfide (GSS<sup>-</sup>). Formation of GSS<sup>-</sup> as a product is a feature that uniquely distinguishes between TSTs (eq. 5) versus TRs (eq. 3). SDO catalyzes the oxidation of the sulfane sulfur in GSS<sup>-</sup> to produce sulfite (eq. 6). Consequently, addition of SDO to assays containing thiosulfate and glutathione should cause a 2-fold increase in the rate of sulfite formation observed with an authentic TST (eq. 5 + 6) whereas the rate observed with a TR should be unaffected.



Indeed, a 2-fold increase in the rate of sulfite formation is observed with TSTD1 or RDL1 upon addition of excess SDO to the standard TST assay (pH 9, 37 °C) which contains 20 mM thiosulfate and 20 mM glutathione (Figure 3.5A). A very similar effect is observed in assays containing the same substrate concentrations but conducted at a lower pH and temperature (pH 8.0, 25 °C) (Figure 3.5B). However, much larger rate increases (4- to 9-fold) are observed upon addition of SDO to assays containing 2.4 mM glutathione. The greater than anticipated rate enhancements at the lower glutathione concentration are observed in assays with TSTD1 or RDL1 at pH 9 or pH 8 (Figure 3.5). The observed increase in the rate of sulfite formation in SDO-coupled assays at 2.4 mM glutathione corresponds to a 2- to 4.5-fold increase in the rate of the sulfurtransferase reaction (eq. 5).

The results provide definitive evidence that TSTD1 and RDL1 are authentic TSTs that catalyze the formation of  $\text{GSS}^-$  as a product that is released into solution (eq. 5). The data also indicate the  $\text{GSS}^-$  is a potent inhibitor of both the human and yeast enzymes. The fact that inhibition by  $\text{GSS}^-$  is observed at lower but not higher glutathione concentrations suggests that the product acts as a competitive inhibitor with respect to glutathione.

### **3.4.8 Steady-state kinetics of the yeast RDL1 or human TSTD1 reaction with thiosulfate and glutathione in the presence of sulfur dioxygenase**

Intersecting line double-reciprocal plots are obtained for the yeast RDL1 reaction in the presence of SDO (Figure 3.2C and 2D), as observed in the absence of SDO. The presence of SDO results in a 25-fold decrease in the  $K_m$  value obtained for glutathione whereas only modest changes are observed for other steady-state kinetic parameters



(Table 3.2). A complete steady-state kinetic analysis of the TSTD1 reaction in the presence of SDO is not possible owing to a large decrease in the  $K_m$  value for glutathione ( $< 0.04$  mM). It is worth noting that SDO causes only minor changes in the TSTD1 turnover rate or the  $K_m$  for thiosulfate, as judged by apparent steady-state kinetic parameters obtained by varying the concentration of thiosulfate at a saturating concentration of glutathione (Table 3.2). The decreased  $K_m$  value for glutathione observed with RDL1 or TSTD1 in the presence of SDO is consistent with the hypothesis that  $GSS^-$  is a potent competitive inhibitor with respect to glutathione.

### **3.4.9 Reaction of yeast RDL1 or human TSTD1 with a chromogenic substrate as an alternate sulfane sulfur donor**

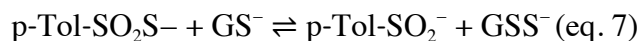
*p*-Toluenethiosulfonate ( $p\text{-Tol-SO}_2\text{S}^-$ ) is more a reactive sulfane sulfur donor than thiosulfate (168). The compound exhibits a moderately intense absorption band in the UV region ( $\epsilon_{242} = 6760 \text{ M}^{-1} \text{ cm}^{-1}$ ) that is lost upon transfer of the sulfane sulfur to an acceptor and formation of *p*-toluenesulfinate ( $p\text{-Tol-SO}_2^-$ ) (Appendix 2 figure 7) (169).

Consequently, the reaction with  $p\text{-Tol-SO}_2\text{S}^-$  as sulfane donor can be monitored by measuring the disappearance of the substrate at 242 nm ( $\Delta\epsilon_{242} = 5080 \text{ M}^{-1} \text{ cm}^{-1}$ ). This continuous spectrophotometric assay is less cumbersome than the fixed time point assay used to monitor sulfite formation with thiosulfate as donor.

To minimize the blank rate with the more reactive donor, assays with  $p\text{-Tol-SO}_2\text{S}^-$  and glutathione are conducted at a lower pH and temperature (pH 8.0, 25 °C) than the standard TST assay with thiosulfate as donor (pH 9.0, 37 °C). Human TSTD1 and yeast RDL1 exhibit  $p\text{-Tol-SO}_2\text{S}^-$ :glutathione sulfurtransferase activity; the observed initial rates of these reactions are directly proportional to the enzyme concentration (Figure 3.6A and

6B). Apparent turnover rates for the TSTD1 and RDL1 reactions were estimated from the slopes of these plots ( $k_{\text{cat app}} = 96 \pm 5 \text{ s}^{-1}$  and  $104 \pm 3 \text{ s}^{-1}$ , respectively). It is worth noting that replacing thiosulfate with p-Tol-SO<sub>2</sub>S<sup>-</sup> appears to eliminate the difference in the turnover rate of the human and yeast enzymes that is observed with the less reactive donor (see Table 3.2).

A 2.3- or 2.0-fold increase in the initial rate of p-Tol-SO<sub>2</sub>S<sup>-</sup> disappearance is observed when assays with RDL1 or TSTD1, respectively, are conducted in the presence of SDO (Figure 3.6C and 6D). The observed rate enhancements are similar to those seen in assays at the same glutathione concentration (2.4 mM) with thiosulfate as the sulfane sulfur donor. In addition to the effect on initial rates, SDO causes a dramatic change in the extent of the reactions observed with p-Tol-SO<sub>2</sub>S<sup>-</sup>. In the absence of SDO, the reactions with RDL1 and TSTD1 appear to be complete in about 200 s, as judged by the observed plateau in the progress curves (Figure 3.6C and 6D, curve 2). However, the maximal  $\Delta A_{242}$  observed with either enzyme is only 50% of that expected for complete consumption of p-Tol-SO<sub>2</sub>S<sup>-</sup>, as indicated by the dotted lines (curve 4) in Figure 3.6C and 6D. The observed progress curves suggested that the reactions may have reached equilibrium after 200 s (eq. 7).



Consistent with this hypothesis, a quantitative conversion of p-Tol-SO<sub>2</sub>S<sup>-</sup> to p-Tol-SO<sub>2</sub><sup>-</sup> is observed when GSS<sup>-</sup> is oxidatively decomposed, as judged by the reaction traces obtained for the RDL1 and TSTD1 reactions in the presence of SDO (Figure 3.6C and 6D, curve 3).

### **3.4.10 Reaction of yeast RDL1 or human TSTD1 with alternate sulfane sulfur acceptors**

We investigated the specificity of yeast RDL1 and human TSTD1 with respect to the sulfane sulfur acceptor by determining whether alternate acceptors could substitute for glutathione. We surveyed four physiologically relevant thiols and two nonphysiological compounds in reactions conducted at pH 9.0 with thiosulfate as the sulfane sulfur donor. Activity was observed with RDL1 or TSTD1 using L-cysteine, coenzyme A, DTT, or cyanide as the acceptor. No activity was, however, detected with D,L-homocysteine or D,L-dihydrolipoic acid.

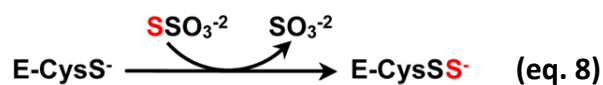
Apparent steady-state kinetic parameters for reactions observed with different acceptors were determined by varying the acceptor concentration in the presence of a saturating concentration of thiosulfate and vice versa. The observed velocities exhibit a hyperbolic dependence on the concentration of the varied substrate except for the reaction with RDL1 when thiosulfate is varied at a saturating concentration of coenzyme A. In this case, a sigmoidal dependence on the thiosulfate concentration is observed. Varying the nature of the acceptor causes only modest changes ( $\leq 3.5$ -fold) in the apparent turnover rate or the  $K_m$  for thiosulfate, as judged by results obtained for the RDL1 or TSTD1 reactions with glutathione and four alternate acceptors (Table 3.4). Similar  $K_m$  values are observed for L-cysteine and glutathione with RDL1 or TSTD1. The  $K_m$  value obtained for coenzyme A with RDL1 or TSTD1 is, however, 40- or 20-fold lower, respectively, than the  $K_m$  value observed for glutathione. The potential significance of the observed  $K_m$  values will be discussed.

### 3.4.11 Role of the single cysteine residue in yeast RDL1 or human TSTD1

Yeast RDL1 and human TSTD1 exhibit a signature motif characteristic of a rhodanese homology domain (RHOD). This alpha beta fold domain is found in other sulfurtransferases and is also observed in the crystal structure of RDL1, which was determined as part of a structural genomics initiative and published in an online database (3D1P.pdb). An invariant cysteine occupies the first position of a six-amino acid active site loop observed in other RHOD-containing sulfurtransferases (170). The single cysteine in yeast RDL1 (Cys98) occupies the same location within an active site loop found in the crystal structure of the protein (Figure 3.7, top panel). A sequence alignment indicates that the putative catalytic cysteine and three other residues in the active site loop of yeast RDL1 are conserved in human TSTD1 (Figure 3.7, bottom panel).

To evaluate the possible catalytic role of Cys98 in yeast RDL1 and Cys79 in human TSTD1, we mutated each residue to Ala or Ser. The mutations did not affect protein expression. However, each of the purified mutant enzymes was found to be catalytically inactive. The results provide compelling evidence that the single cysteine in the yeast and human enzymes is catalytically essential. In contrast, Chancey and Westley concluded that the cysteine was not required for catalysis by the yeast enzyme based on the failure of iodoacetate to inactivate the enzyme (162). Unfortunately, the postulated site of iodoacetate incorporation was not identified in this study.

The mutagenesis results suggested that catalysis by yeast RDL1 and human TSTD1 might occur via a double-displacement mechanism involving transfer of the sulfane sulfur from thiosulfate to the active site cysteine (eq. 8) and subsequent reaction of the persulfide-containing intermediate with glutathione (eq. 9).



Evidence to evaluate this hypothesis was sought by determining whether cyanolyzable sulfur could be detected in enzyme isolated by gel filtration after a short incubation with thiosulfate. We found that about 10 or 20% of the cysteine in the column eluate of RDL1 or TSTD1, respectively, is present as cysteine persulfide. The persulfide is largely eliminated upon incubation of the isolated intermediates with glutathione in the presence of SDO, which was included to oxidize the cyanolyzable sulfur in the GSS<sup>-</sup> product (Table 3.5).

#### 3.4.12 Identification of bacterial SDO-TSTD1 fusion proteins

Rosetta Stone proteins are fusion proteins consisting of two non-homologous proteins that are found as separate proteins in another genome. The fusion is thought to be maintained by selection because it facilitates a functional interaction between proteins, such as the kinetic coupling of consecutive enzymes in a pathway (170). Six bacterial proteins were previously classified as fusions of SDO with rhodanese, a thiosulfate:cyanide sulfurtransferase encoded by the *TST* gene (22, 171). The functional interaction between human TSTD1 and human SDO observed in the present study led us to question the validity of this assignment. Accordingly, we performed BLASTp searches of the human genome database using each of the putative SDO-rhodanese fusion proteins as the query sequence. Contrary to the previous classification, TSTD1 was the top scoring BLAST hit for the C-terminal domain in all six proteins (Table 3.6, entries 2, 4, 10, 11, 14, 15). Furthermore, rhodanese was not found among the lower scoring BLAST

hits for the C-terminal domain. On the other hand, SDO was the highest scoring BLAST hit for the N-terminal domain in each query sequence. The results indicate that all six bacterial proteins are more appropriately classified as fusions of SDO and TSTD1.

We reasoned that the six SDO-TSTD1 fusion proteins might be part of a larger group of homologous Rosetta Stone proteins. To evaluate this hypothesis, the fusion protein from *Methylobacter tundripaludum* (Table 3.6, entry 4) was used as the query sequence in a BLASTp search against all non-redundant GenBank CDS translations, with the maximum number of target sequences set to 500. The search retrieved 116 bacterial proteins that exhibit 96-99% coverage with the query sequence and low E values ( $3e^{-65}$  and  $9e^{-165}$ ), properties expected for homologs of the *M. tundripaludum* SDO-TSTD1 fusion protein. The group of 116 retrieved proteins included each of the six previously identified SDO-TSTD1 fusion proteins. The remainder of the 500 retrieved sequences are SDO homologs that align only with the N-terminal domain of the query fusion protein (60-66% query coverage) with E values between  $1e^{-65}$  to  $6e^{-109}$ . We performed BLASTp searches against the human genome using query sequences from a selected subset of the 116 hits that included no more than one representative species from within each genus. Satisfyingly, SDO and TSTD1 were the highest scoring BLAST hits obtained for the N- and C-terminal domains, respectively, in each tested query. The newly identified fusion proteins were rank-ordered with respect to the E values obtained for the TSTD1 hits; those exhibiting E values  $\leq 6e^{-04}$  are listed in Table 3.6.

### 3.4.13 Are human-like SQORs found in bacteria that express SDO-TSTD1 fusion proteins

H<sub>2</sub>S and thiosulfate are the most abundant reduced inorganic sulfur species in the environment (172). Bacteria that express SDO-TSTD1 fusion proteins might utilize exogenously derived thiosulfate as the substrate for the TSTD1 reaction. Alternatively, these bacteria might contain human-like SQORs that initiate the oxidation of H<sub>2</sub>S and produce an endogenous source of thiosulfate for the TSTD1 reaction, analogous to that proposed for mammalian H<sub>2</sub>S metabolism (see Scheme 3.1).

The proteomes of twelve of the thirteen bacteria that harbor top scoring SDO-TSTD1 fusion proteins are available in the NCBI database (Table 3.6, entries 1-10, 12-13). We conducted BLASTp searches of these proteomes using human SQOR as the query sequence. The searches identified SQOR homologs in eleven of the twelve searchable proteomes (Appendix 2 Table 2). Complete genomic data are available for two of the eleven bacteria that contain both SQOR and SDO-TSTD1 fusion proteins (*N. oceani*, *N. watsonii*); whole-genome shotgun contigs are available for the other nine bacteria. The genes for SQOR and the SDO-TSTD1 fusion protein in *N. oceani* and *N. watsonii* are transcribed in the same direction and separated by just 73 nucleotides. Although not predicted to lie in the same operon, the genes for the two proteins in *N. oceani* are considered to be functionally related as part of a regulon cluster, according to MicrobesOnline (<http://www.microbesonline.org/operons/>). Genomic distances could also be determined in four other bacteria where the genes for SQOR and the SDO-TSTD1 fusion protein were found within the same contig. In these cases, the genes were separated by 21 to 246 nucleotides (Appendix 2 Table 2).

Seven of the eleven identified bacterial SQORs, including the *N. oceani* and *N. watsonii* enzymes, exhibit high similarity to human SQOR ( $E \leq 5e^{-90}$ ) (see Appendix 2 Table 2). SQORs have been classified into six types (15). A phylogenetic tree shows that the seven top-scoring bacterial enzymes cluster with type II SQORs, a category that includes all known eukaryotic SQORs and a subset of prokaryotic enzymes (Figure 8). The lower-scoring hits include one that clusters with type I bacterial SQORs and three that did not cluster with representatives of other known types of bacterial SQORs (not shown).

### 3.5 Discussion

The first step in mammalian H<sub>2</sub>S metabolism was previously postulated to produce the GSS<sup>-</sup> substrate for SDO, an enzyme thought to catalyze the second step in the pathway (1, 14). This hypothesis was contradicted by the discovery that glutathione does not act as an acceptor of the sulfane sulfur generated during H<sub>2</sub>S oxidation by human SQOR. Instead, SQOR catalyzes the oxidative conversion of H<sub>2</sub>S to thiosulfate, a reaction in which sulfite acts as the sulfane sulfur acceptor from an enzyme persulfide intermediate ( $E\text{-CysSS}^- + \text{SO}_3^{-2} \Rightarrow E\text{-CysS}^- + \text{SSO}_3^{-2}$ ) (158). The inability of SQOR to produce GSS<sup>-</sup> led others to suggest that SDO might directly oxidize the sulfane sulfur in the persulfide intermediate ( $E\text{-CysSS}^- + \text{O}_2 + \text{H}_2\text{O} \Rightarrow E\text{-CysS}^- + \text{SO}_3^{-2} + 2\text{H}^+$ ) (21). However, human SDO cannot replace sulfite in the SQOR reaction, as judged by its inability to accelerate the slow rate of H<sub>2</sub>S oxidation observed in the absence of sulfite<sup>7</sup>. Similar negative results were obtained with coenzyme A, which was tested because the corresponding persulfide is an alternate, albeit poor, substrate for SDO (21). The results

---

<sup>7</sup> K. Acharya and M. S. Jorns, unpublished observations.



strongly suggested that a thiosulfate:glutathione sulfurtransferase was required to provide the missing link between the SQOR and SDO reactions.

Although TST could be purified from *S. cerevisiae*, attempts to isolate the mammalian enzyme were not successful (144, 161-164). We used bioinformatic approaches to identify the genes that encode human TST (*TSTD1*) and its yeast ortholog (*RDL1*). Both genes produce small RHOD-containing proteins. Recombinant yeast RDL1 catalyzes the glutathione-dependent conversion of thiosulfate to sulfite in a reaction that proceeds via a ternary complex mechanism and exhibits steady-state kinetic parameters similar to those reported for the natural yeast enzyme (163). The human *TSTD1* gene contains four exons and has three splice variants. TSTD1 isoform 1 is produced from a transcript that contains all four exons and exhibits TST activity; the smaller TSTD1 isoforms are catalytically inactive. TSTD1 (isoform 1) exhibits steady-state kinetic parameters similar to RDL1, except that turnover of the human enzyme is ~25-fold slower. Proteomics studies indicate that human TSTD1 is highly expressed in various tissues, including liver and heart (173, 174). Data for the individual isoforms is unavailable except in tumor cell lines where only isoform 1 is detected by Western blotting (175).

Yeast RDL1 and human TSTD1 contain a single cysteine (Cys98 and Cys79, respectively) that is catalytically essential, as judged by the loss of activity observed when the cysteines are replaced by serine or alanine. The detection of albeit modest amounts of cysteine persulfide in the human or yeast enzyme isolated after reaction with thiosulfate suggests that catalysis occurs via a double-displacement mechanism involving the formation of a cysteine persulfide-containing intermediate (see eqs. 6-7), as observed

with other RHOD-containing sulfurtransferases (176-179). Formation of the persulfide intermediate may be rate-limiting during catalysis by human TSTD1, as judged by the substantial increase in turnover rate observed when thiosulfate is replaced by a more reactive sulfane donor,  $p\text{-Tol-SO}_2\text{S}^-$ . Coenzyme A and L-cysteine can act as alternate sulfane sulfur acceptors for the yeast and mammalian enzymes. Human TSTD1 exhibits  $K_m$  values for glutathione and coenzyme A that are below or within the normal range reported for the concentrations of these thiols in animal cells (180, 181). The  $K_m$  value obtained for L-cysteine is, however, an order of magnitude higher than the L-cysteine level in liver cells (182). The results suggest that coenzyme A, but not L-cysteine, may be a possibly significant alternate acceptor for TSTD1 in mammalian cells. It is worth noting that coenzyme A persulfide is the only currently known alternate (albeit poor) substrate for human SDO (21).

### **3.5.1 Functional interaction between human SDO and human TSTD1 or yeast RDL1**

The operational definition of a TST as an enzyme that catalyzes a glutathione-dependent conversion of thiosulfate to sulfite does not distinguish between an authentic TST that produces  $\text{GSS}^-$  as a product versus a TR that catalyzes a glutathione-dependent reduction of thiosulfate to sulfite plus  $\text{H}_2\text{S}$ . Definitive evidence that TSTD1 and RDL1 are authentic TSTs is provided by studies, which show that the reaction product is oxidized by human SDO, as evidenced by an expected doubling of the rate of sulfite formation upon addition of SDO to assays at saturating glutathione<sup>8</sup>. The greater than

---

<sup>8</sup> Oxidation of  $\text{GSS}^-$  by SDO is also detectable by measuring oxygen consumption using an oxygen electrode-based TSTD1-SDO coupled assay (S. L. Melideo and M. S. Jorns, unpublished observations).

expected rate accelerations observed when SDO is added to assays at lower glutathione concentrations indicates that  $\text{GSS}^-$  is an inhibitor of both the yeast and human enzymes. The presence of SDO results in a  $\geq 25$ -fold decrease in the  $K_m$  value obtained for glutathione with RDL1 or TSTD1, suggesting that  $\text{GSS}^-$  is a potent competitive inhibitor with respect to glutathione. SDO also enhances the initial rate of glutathione-dependent sulfurtransferase reactions observed with  $p\text{-Tol-SO}_2\text{S}^-$  as the sulfane sulfur donor. The observed inhibition of the TST reactions by  $\text{GSS}^-$ , which is circumvented in the presence of human SDO, provide an apparent mechanism to regulate mammalian  $\text{GSS}^-$  biosynthesis and prevent the accumulation of a highly reactive metabolite.

The reactions observed with  $p\text{-Tol-SO}_2\text{S}^-$  and TSTD1 or RDL1 in the absence of SDO reach equilibrium when about 50% of the substrate has been consumed. A quantitative conversion of  $p\text{-Tol-SO}_2\text{S}^-$  to  $p\text{-Tol-SO}_2^-$  is, however, observed when  $\text{GSS}^-$  is oxidatively decomposed in the presence of SDO. The ability of human SDO to drive the reaction with a reactive sulfane sulfur donor to completion provides a paradigm for the thermodynamic coupling of the irreversible SDO reaction with the less favorable, but physiologically relevant, sulfurtransferase reaction with thiosulfate as sulfane donor.

The effect of SDO on the extent of the reaction with  $p\text{-Tol-SO}_2\text{S}^-$  is similar to that reported in a previous study with the natural yeast TST for the effect of cyanide on the extent of a reaction observed with glutathione and benzenethiosulfonate ( $\text{Ph-SO}_2\text{S}^-$ ) (161). However, the authors attributed the observed formation of a stoichiometric amount of thiocyanate to the reaction of cyanide with  $\text{GSS}^-$  that had been released into solution. This interpretation is rendered problematic by the fact that cyanide is an alternate substrate for yeast TST, as shown by results obtained in the present study and in a

previous survey of the thiosulfate:cyanide sulfurtransferase activity exhibited by RHOD-containing yeast proteins (165).

### 3.5.2 Phylogenetic association of human TSTD1 and human SDO

Using bioinformatic approaches, we identified a group of bacterial SDO-TSTD1 fusion proteins that includes six members previously misclassified as SDO-rhodanese fusions. The C-terminal TSTD1-like domain in the fusion proteins is connected to the N-terminal SDO-like domain by a variable length linker region (Appendix 2 figure 8). Catalytically important residues and signature motifs are conserved between the respective bacterial domains and human TSTD1 or SDO, as judged by multiple sequence alignments of the bacterial domains with the human proteins (Appendix 2 figure 9). The phylogenetic data reinforce the biochemical evidence obtained for the functional interaction of human TSTD1 and SDO.

It is worth noting that at least some of the bacteria that express SDO-TSTD1 fusion proteins also contain an adjacent gene that encodes a human-like SQOR. The results suggest that these organisms metabolize H<sub>2</sub>S via a pathway that is strikingly similar to the first three steps proposed for mammalian H<sub>2</sub>S metabolism (see Scheme 3.1)<sup>9</sup>. The metabolic similarity is not surprising from an evolutionary perspective given that the genes for H<sub>2</sub>S metabolism were acquired by eukaryotic cells from an endosymbiotic bacterial ancestor. Nevertheless, bacteria and mammals exhibit considerable divergence with respect to the role of H<sub>2</sub>S metabolism. Bacterial metabolism of environmental H<sub>2</sub>S provides an important source of energy and reducing equivalents.

---

<sup>9</sup> The SDO-TSTD1 fusion proteins may also function in the bacterial oxidation of environmental thiosulfate, providing an alternative to the widely distributed Sox (sulfur oxidizing) system (172)

In contrast, the primary physiological significance of H<sub>2</sub>S metabolism in mammals is closely tied to the acquired role of endogenously produced H<sub>2</sub>S as an important signaling molecule.

### 3.5.3 Concluding remarks

In summary, we describe a novel human sulfurtransferase that catalyzes the formation of a central intermediate in mammalian H<sub>2</sub>S metabolism. We propose that human TSTD1 constitutes the hitherto missing link between the reactions catalyzed by SQOR and SDO. The biosynthesis of glutathione persulfide by human TSTD1 provides a rare example of a mammalian enzyme that catalyzes the biosynthesis of a reactive sulfane sulfur donor that is released into solution. A recent study show that a reactive sulfane sulfur donor is produced by two other mammalian enzymes (cystathionine β-synthase, cystathionine γ-lyase), which catalyze the conversion of cystine to cysteine persulfide (183). In this regard, it is worth noting that glutathione persulfide and polysulfides have been found to mediate protein sulhydrylation (184, 185). It has recently been suggested that persulfides and other reactive sulfane sulfur donors may be the actual signaling molecules that implement many of the biological effects previously attributed to H<sub>2</sub>S (184, 185). Additional studies are clearly required to evaluate the intriguing possibility that H<sub>2</sub>S metabolism may have an unanticipated direct role in H<sub>2</sub>S signaling.

### 3.6 Acknowledgments

For their generous gifts of plasmids and other reagents (shown in parentheses) we thank Drs. Patrick Loll (plasmid pETHSUL), Simon Cocklin (UD1 domain of the *S. cerevisiae* Ulp1 peptidase), and Valeria Tiranti (plasmid pMW172ETHE). We also thank Nadish Goyal for initial studies on yeast RDL1.

<b>Table 3.1</b> Potential Candidate Genes for Yeast Thiosulfate Sulfurtransferase <sup>a</sup>					
Function	Gene		Molecular Weight (Da)	Isoelectric Point (pI)	Cysteine Residues
	Name	Location			
thiosulfate sulfurtransferase <sup>b</sup>	unknown	unknown	~17,000	5.1	1
unknown	<i>RDL1</i>	YOR285W	15,413	5.91	1
unknown	<i>RDL2</i>	YOR286W	16,697	9.65	1
thiolation tRNA	<i>TUM1</i>	YOR251C	34,219	5.71	4
thiolation tRNA	<i>UBA4</i>	YHR111W	49,361	6.12	13
phosphatase	<i>YCH1</i>	YGR203W	17,248	7.01	2
thiolation tRNA, iron-sulfur cluster biogenesis	<i>NFS1</i>	YCL017C	54,467	8.35	6
lipoic acid biosynthesis	<i>LIP5</i>	YOR196C	46,247	9.55	10
biotin biosynthesis	<i>BIO2</i>	YGR286C	41,884	8.76	10
thiolation tRNA	<i>SLM3</i>	YDL033C	47,049	8.72	6
mitochondrial inner membrane transporter <sup>c</sup>	<i>OAC1</i>	YKL120W	35,153	10.37	3

<sup>a</sup>Unless otherwise noted, genes were retrieved by searching the *S. cerevisiae* genome database (<http://www.yeastgenome.org>) for entries that contained the term “sulfurtransferase” in the gene annotation/description. <sup>b</sup>Data reported by Uhteg and Westley for the enzyme isolated from *S. cerevisiae* (163). <sup>c</sup>Gene retrieved using “thiosulfate” as the search term.

<b>Table 3.2</b> Steady-State Kinetic Parameters for Thiosulfate:Glutathione Sulfurtransferase Reactions Catalyzed by Yeast RDL1 or Human TSTD1 <sup>a</sup>					
Enzyme	SDO ( $\mu\text{M}$ )	$K_m$ glutathione (mM)	$K_m$ thiosulfate (mM)	$K_i$ thiosulfate (mM)	$k_{\text{cat}}$ ( $\text{s}^{-1}$ )
Natural yeast TST <sup>b</sup>	0	2.9	3.7	10	6.4
Yeast RDL1	0	$4.6 \pm 0.9$	$2.0 \pm 0.5$	$7 \pm 2$	$68 \pm 6$
Human TSTD1	0	$1.0 \pm 0.2$	$14 \pm 2$	$37 \pm 13$	$2.7 \pm 0.1$
Yeast RDL1	1.8	$0.2 \pm 0.05$	$7.6 \pm 0.6$	$54 \pm 18$	$94 \pm 3$
Human TSTD1 <sup>c</sup>	0.8	$< 0.04$	$10.7 \pm 0.5$	nd	$1.83 \pm 0.04$

<sup>a</sup>Reactions were conducted at 37 °C in 50 mM Tris-acetate buffer, pH 9.0 in the absence or presence of SDO, as indicated. Unless otherwise noted, steady-state kinetic parameters were obtained upon fitting eq. 4 to the data. Values for  $k_{\text{cat}}$  are determined based on the rate of sulfite formation; data obtained in the presence of SDO are corrected for fact that the coupled reaction converts 1 mol of thiosulfate into 2 mol of sulfite (eq. 5 + 6). <sup>b</sup>Data for the natural TST isolated from *S. cerevisiae*, as reported by Uhteg and Westley (163). <sup>c</sup>Apparent steady-state kinetic parameters for the TSTD1 reaction in the presence of SDO were estimated by varying the concentration of thiosulfate at a saturating concentration of glutathione (2 mM).

<b>Table 3.3</b> BLASTp Search of the NCBI Database of Human Proteins Using Yeast RDL1 as the Query Sequence							
Gene	Description	Isoform <sup>a</sup>	Max Score	Total Score	Query Cover (%)	E Value	Identity (%)
<i>TSTD1</i>	thiosulfate sulfurtransferase/rhodanese domain-containing protein 1	1 (115 aa)	58.5	58.5	63	9e-11	34
		3 (109 aa)	50.1	50.1	53	7e-08	36
		2 (74 aa)	43.9	43.9	43	7e-06	34
<i>TSTD3</i>	thiosulfate sulfurtransferase/rhodanese domain-containing protein 3		35.8	35.8	47	0.011	30
<i>TSTD2</i>	3-mercaptopyruvate sulfurtransferase		33.5	33.5	53	0.22	28
<i>TST</i>	rhodanese		33.1	33.1	53	0.30	26
<p><sup>a</sup>The listed TSTD1 isoforms are encoded by mRNA transcripts with a CCDS (consensus coding sequence) identifier indicative of a well-understood and validated coding sequence. The number of amino acids (aa) in each isoform is shown in parentheses. Isoforms predicted by automated computational analysis or conceptual translation are not shown.</p>							



**Table 3.4** Apparent Steady-State Kinetic Parameters Observed for Yeast RDL1 or Human TSTD1 Reactions with Various Sulfane Sulfur Acceptors and Thiosulfate as Donor<sup>a</sup>

acceptor	yeast RDL1			human TSTD1		
	K <sub>m</sub> (mM)		k <sub>cat</sub> (s <sup>-1</sup> )	K <sub>m</sub> (mM)		k <sub>cat</sub> (s <sup>-1</sup> )
	thiosulfate	acceptor		thiosulfate	acceptor	
glutathione	3.1 ± 0.3	5.6 ± 0.8	60 ± 2 (60 ± 3)	11 ± 1	1.7 ± 0.3	1.91 ± 0.06 (1.9 ± 0.1)
cysteine	5.5 ± 0.7	2.9 ± 0.3	49 ± 4 (45 ± 1)	10.4 ± 0.7	2.5 ± 0.2	1.67 ± 0.04 (2.25 ± 0.05)
coenzyme A	4.3 ± 0.8	0.15 ± 0.05	29 ± 3 (21 ± 2)	36 ± 3	0.09 ± 0.01	1.53 ± 0.06 (1.32 ± 0.05)
DTT	3.9 ± 0.6	0.16 ± 0.03	27 ± 1 (40 ± 2)	14 ± 2	0.12 ± 0.02	2.8 ± 0.1 (2.82 ± 0.07)
cyanide	4.0 ± 0.4	2.6 ± 0.3	38 ± 1 (36 ± 1)	12 ± 1	0.22 ± 0.02	2.41 ± 0.08 (2.05 ± 0.06)

<sup>a</sup>Apparent steady-state kinetic parameters were determined at 37°C in 50 mM Tris-acetate buffer, pH 9.0, by varying the thiosulfate concentration at a saturating concentration of the acceptor and by varying the acceptor concentration at a saturating concentration of thiosulfate. The values obtained for k<sub>cat</sub> by varying the acceptor concentration are shown in parentheses.

**Table 3.5** Detection of Cysteine Persulfide in RDL1 or TSTD1 Isolated by Gel Filtration after Reaction with Thiosulfate<sup>a</sup>

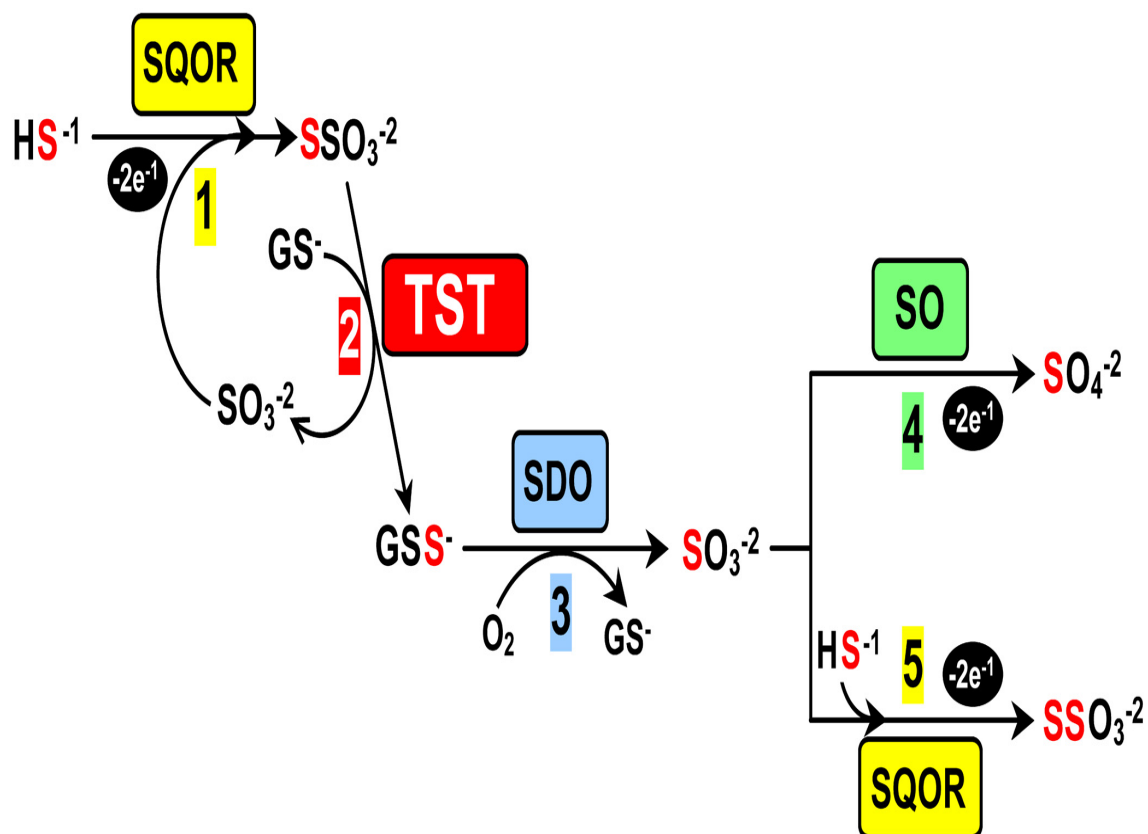
Enzyme	Persulfide Content (%)	
	As Isolated	GSH-treated
RDL1	8.9 ± 0.8	1.3 ± 0.8
TSTD1	19 ± 2	3.4 ± 0.8

<sup>a</sup>Samples were isolated and analyzed as described in Experimental Procedures.

**Table 3.6** BLASTp Search of the NCBI Database of Human Proteins Using Bacterial Fusion Proteins as the Query Sequence<sup>a</sup>

Bacterial Query Sequence (GenBank accession number)		C-terminal TSTD1-like Domain				N-terminal ETHE1 (SDO)-like domain			
		Human Gene	Query Cover (%)	E Value	Identity (%)	Human Gene	Query Cover (%)	E Value	Identity (%)
1	<i>Nitrosococcus oceani</i> (WP_011330831.1)	<i>TSTD1</i>	26	3e <sup>-11</sup>	33	<i>ETHE1</i>	63	9e <sup>-75</sup>	52
2	<i>Nitrosococcus watsonii</i> (WP_013220760.1) <sup>b</sup>	<i>TSTD1</i>	26	2e <sup>-08</sup>	34	<i>ETHE1</i>	63	3e <sup>-73</sup>	51
3	<i>Methylocella silvestris</i> (WP_012591638.1)	<i>TSTD1</i>	26	3e <sup>-08</sup>	28	<i>ETHE1</i>	65	2e <sup>-70</sup>	49
4	<i>Methylobacter tundripaludum</i> (WP_006892756.1) <sup>b</sup>	<i>TSTD1</i>	26	2e <sup>-07</sup>	31	<i>ETHE1</i>	62	2e <sup>-68</sup>	50
5	<i>Methylomicrobium album</i> (WP_005371248.1)	<i>TSTD1</i>	26	9e <sup>-07</sup>	33	<i>ETHE1</i>	63	9e <sup>-69</sup>	49
6	<i>Methyloglobulus morosus</i> (WP_023495230.1)	<i>TSTD1</i>	25	2e <sup>-06</sup>	31	<i>ETHE1</i>	60	2e <sup>-65</sup>	48
7	<i>Methylocystis rosea</i> (WP_018407856.1)	<i>TSTD1</i>	25	5e <sup>-06</sup>	31	<i>ETHE1</i>	66	3e <sup>-63</sup>	46
8	<i>Methylosarcina fibrata</i> (WP_020565272.1)	<i>TSTD1</i>	24	8e <sup>-06</sup>	30	<i>ETHE1</i>	63	1e <sup>-67</sup>	49
9	<i>Bradyrhizobiacae bacterium</i> (WP_009737228.1)	<i>TSTD1</i>	25	1e <sup>-05</sup>	29	<i>ETHE1</i>	65	2e <sup>-64</sup>	47

10	<i>Afipia broomeae</i> (WP_00602173 9.1) <sup>b</sup>	<i>TSTD1</i>	24	4e <sup>-05</sup>	33	<i>ETHE1</i>	65	1e <sup>-63</sup>	47
11	<i>γ-proteobacterium HTCC2148</i> (WP_00722949 1.1) <sup>b</sup>	<i>TSTD1</i>	23	1e <sup>-04</sup>	36	<i>ETHE1</i>	64	5e <sup>-80</sup>	54
12	<i>Rhizobium giardinii</i> (WP_01833015 2.1)	<i>TSTD1</i>	26	2e <sup>-04</sup>	32	<i>ETHE1</i>	66	7e <sup>-64</sup>	46
13	<i>Mesorhizobium amorphae</i> (WP_00620352 3.1)	<i>TSTD1</i>	26	6e <sup>-04</sup>	28	<i>ETHE1</i>	66	9e <sup>-67</sup>	48
14	<i>Polaromonas sp. JS666</i> (WP_01148570 3.1) <sup>b</sup>	<i>TSTD1</i>	29	0.005	30	<i>ETHE1</i>	60	5e <sup>-33</sup>	37
15	<i>Burkholderia cepacia</i> (WP_01490086 9.1) <sup>b</sup>	<i>TSTD1</i>	21	0.31	29	<i>ETHE1</i>	64	3e <sup>-87</sup>	59
<p>*Results are shown for the highest scoring BLAST hit in the human genome that aligns with the C- or N-terminal domain in the bacterial query sequence. <sup>b</sup>Proteins previously classified as fusions of SDO with rhodanese (22, 171).</p>									



**Scheme 3.1** Proposed scheme for mammalian hydrogen sulfide metabolism. SQOR, sulfide:quinone oxidoreductase; TST, thiosulfate:glutathione sulfurtransferase; SDO, sulfur dioxygenase; SO, sulfite oxidase

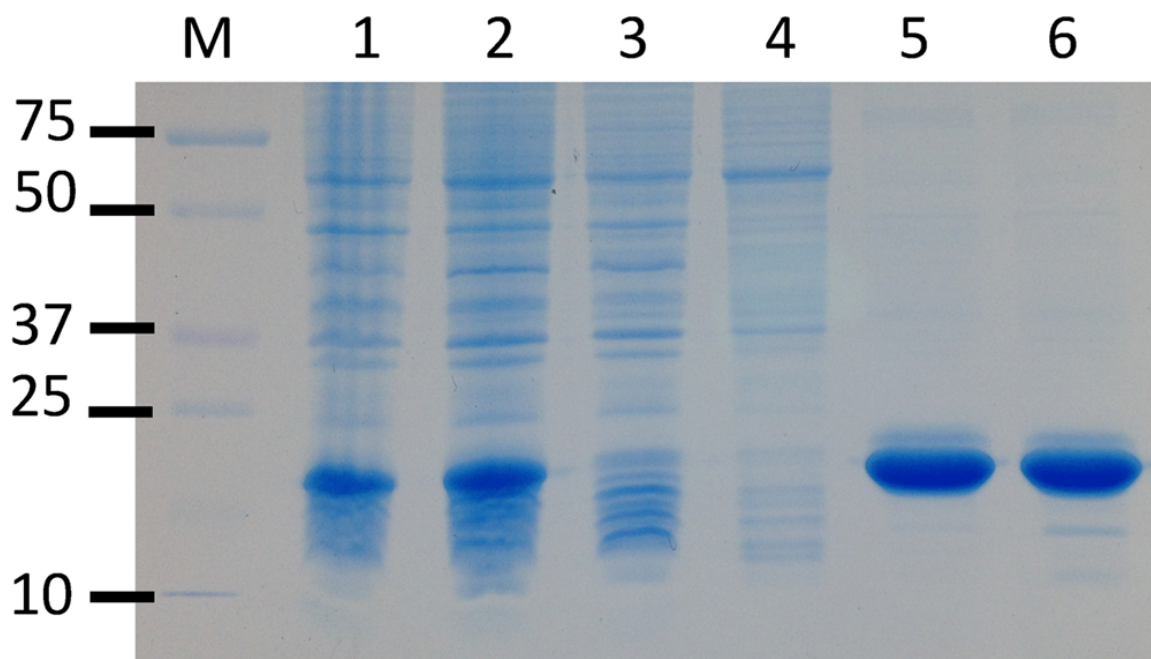


**Figure 3.1** Purification of recombinant yeast RDL1. The SDS 12% polyacrylamide gel was stained for protein with ProSieve Blue Protein Staining Solution (Lonza); lane M, molecular markers; lane 1, whole cell lysate; lane 2, low speed supernatant; lane 3, Ni affinity column flow-through; lane 4, Ni affinity column wash; lane 5, Ni affinity column eluate; lane 6, dialyzed and concentrated Ni affinity column eluate.

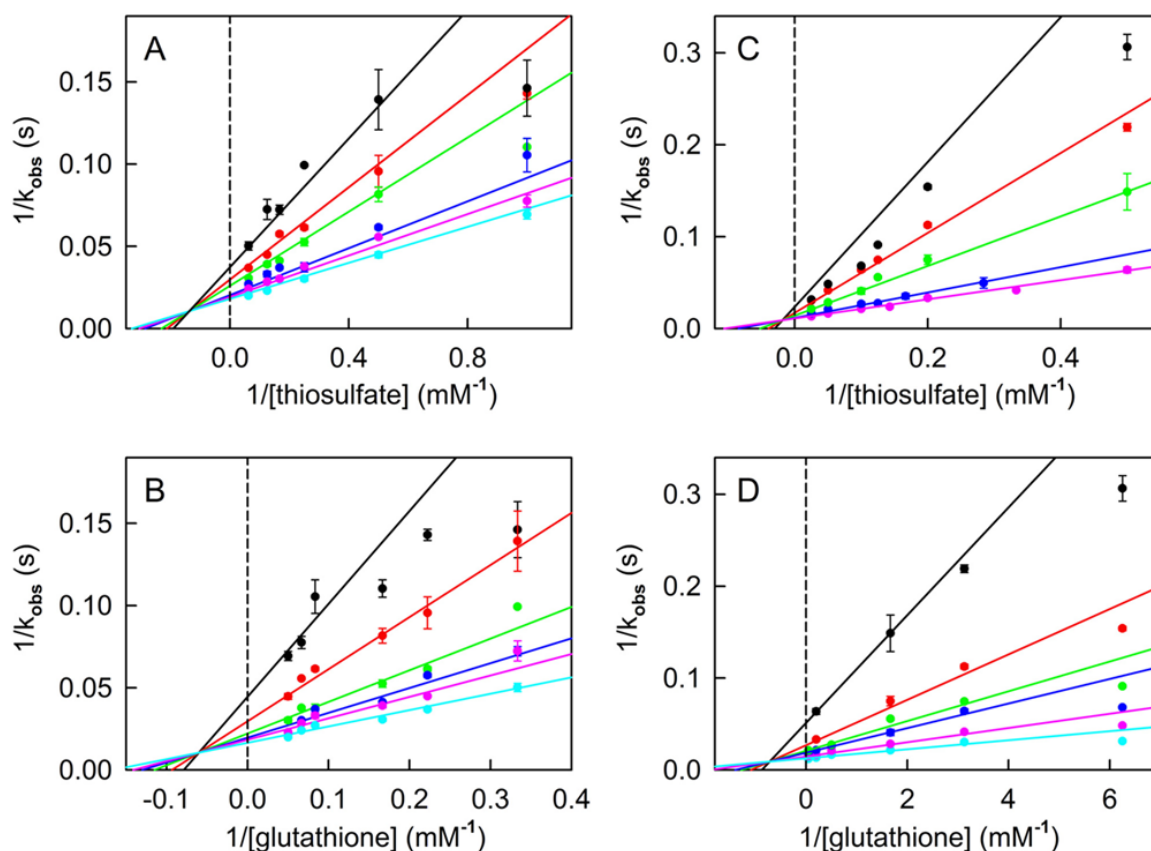


**Figure 3.2** Steady-state kinetic analysis of the thiosulfate:glutathione sulfurtransferase reaction catalyzed by recombinant yeast RDL1. Reactions were conducted at 37 °C in 50 mM Tris-acetate buffer, pH 9.0, containing 0 (panels A, B) or 1.8  $\mu\text{M}$  SDO (panels C, D). Panel A: Data obtained with 3.0, 4.5, 6.0, 12.0, 15.0, and 20.0 mM glutathione are shown by the black, red, green, blue, magenta, and cyan circles, respectively. Panel B: Data obtained with 1.0, 2.0, 4.0, 6.0, 8.0, and 16.0 mM thiosulfate are shown by the black, red, green, blue, magenta, and cyan circles, respectively. Panel C: Data obtained with 0.16, 0.32, 0.6, 2, and 15 mM glutathione are shown by the black, red, green, blue, and magenta circles, respectively. Panel D: Data obtained with 2, 5, 8, 10, 20, and 40 mM thiosulfate are shown by the black, red, green, blue circles, magenta, and cyan circles, respectively. The solid lines in panels A to D were obtained by fitting eq. 4 to the data.

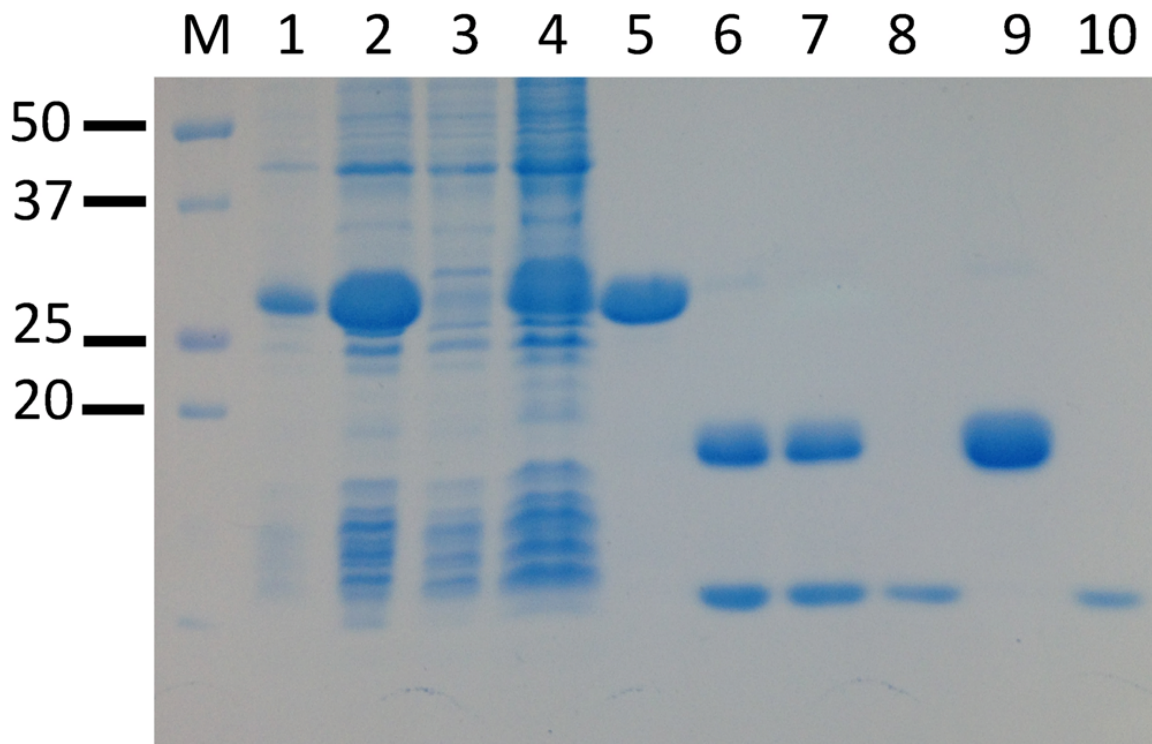


**Figure 3.3** Purification of recombinant human TSTD1 isoform 1 with a cleavable N-terminal His-SUMO tag. The SDS 12% polyacrylamide gel was stained for protein with ProSieve Blue Protein Staining Solution (Lonza); lane M, molecular markers. lane 1, crude cell lysate; lane 2, low speed supernatant; lane 3, Ni affinity column flow-through; lane 4, Ni affinity column wash; lane 5, Ni affinity column eluate; lane 6, Ni affinity column eluate after cleavage with SUMO hydrolase; lane 7, SUMO hydrolase-treated sample after dialysis; lane 8, second Ni affinity column flow-through; lane 9, second Ni affinity column eluate; lane 10, dialyzed sample from lane 8.

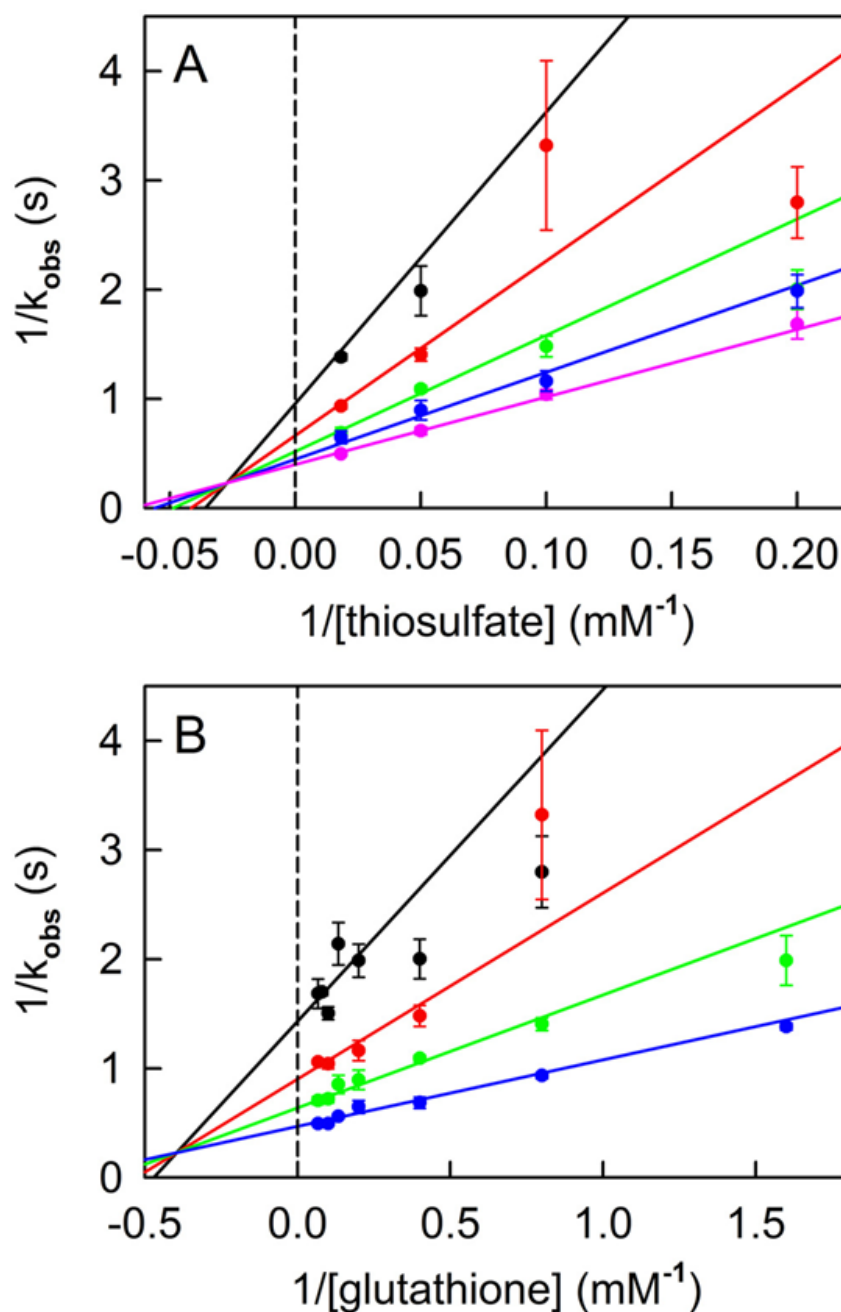


**Figure 3.4** Steady-state kinetic analysis of the thiosulfate:glutathione sulfurtransferase reaction catalyzed by recombinant human TSTD1. Reactions were conducted in 50 mM Tris-acetate buffer, pH 9.0 at 37°C. Panel A: Data obtained with 0.63, 1.25, 2.5, 5, and 15 mM glutathione are shown by the black, red, green, blue, and magenta circles, respectively. Panel B: Data obtained with 5, 10, 20, and 55 mM thiosulfate are shown by the black, red, green, and blue circles, respectively. The solid lines in panels A and B were obtained by fitting eq. 4 to the data.



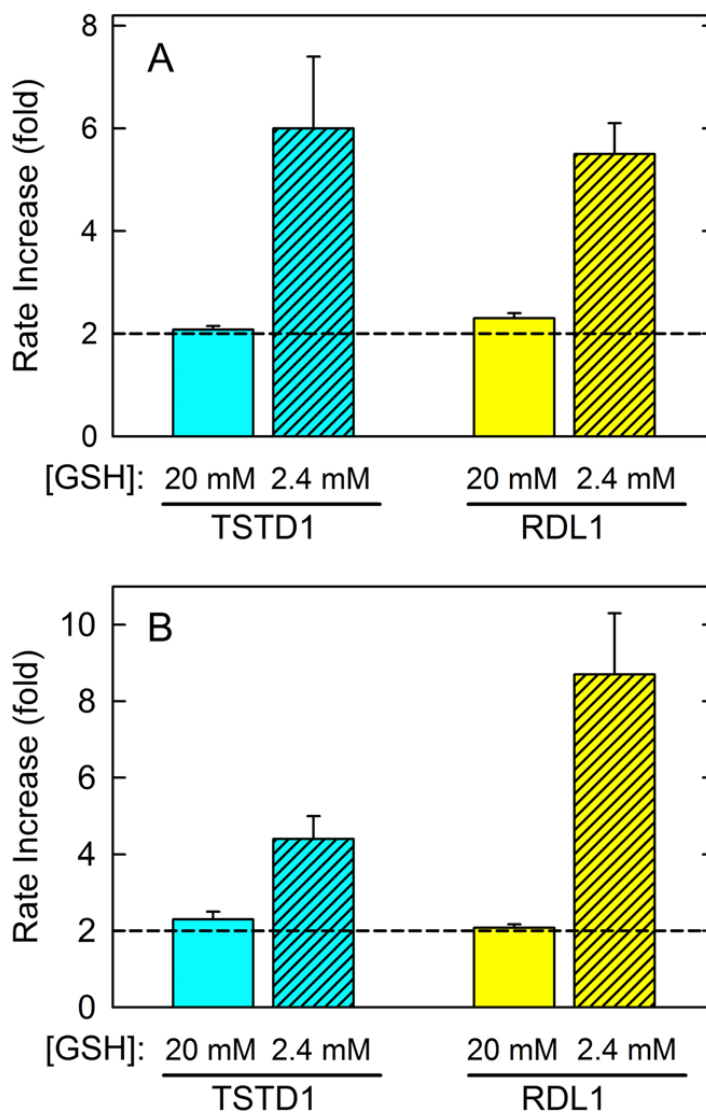


**Figure 3.5** Effect of human SDO on thiosulfate:glutathione sulfurtransferase reactions catalyzed by human TSTD1 or yeast RDL1. Reactions were conducted in 50 mM Tris-acetate buffer, pH 9.0, at 37°C (panel A) or 50 mM sodium/potassium phosphate, pH 8.0 at 25°C (panel B). Assays containing 20 mM thiosulfate, and 20 mM (solid filled bars) or 2.4 mM (diagonal stripped bars) glutathione were conducted in the absence or the presence of 4  $\mu$ M (panel A) or 800 nM (panel B) SDO. The bar graph shows the rate increase (fold) calculated by dividing values observed in the presence of SDO by those obtained for the same reaction in the absence of SDO.

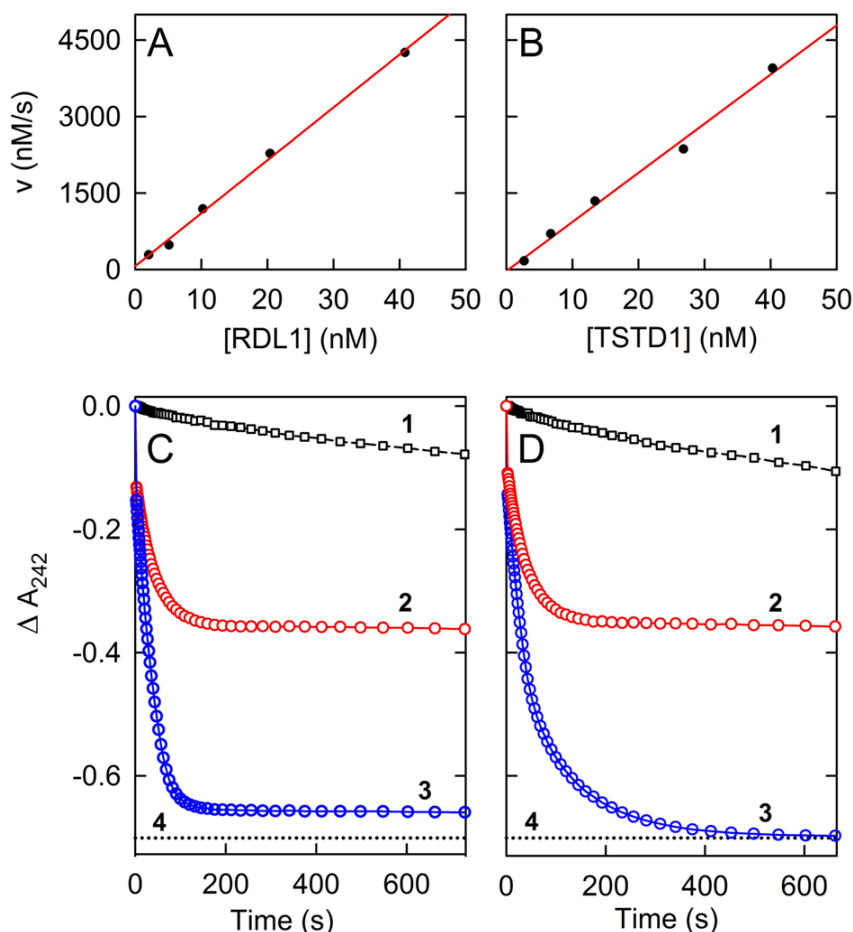
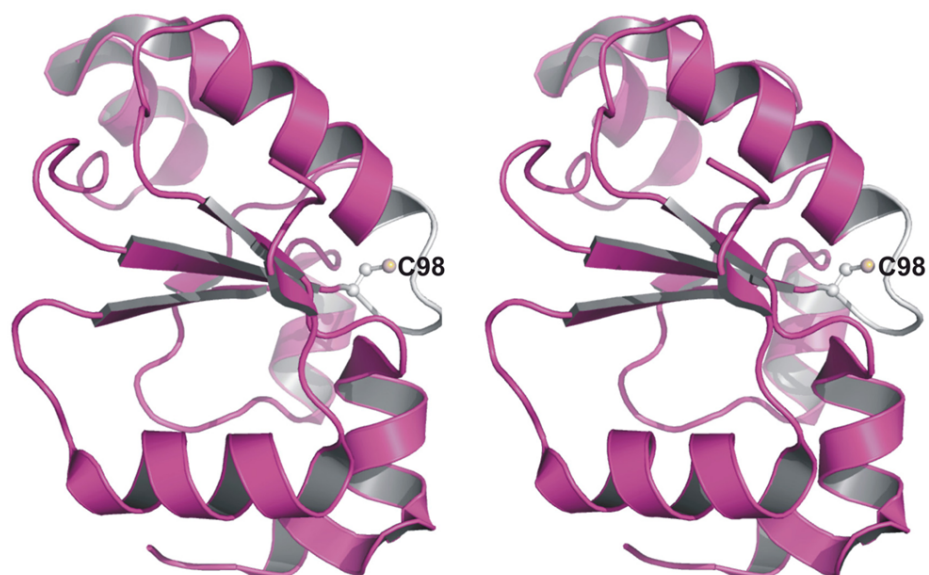


**Figure 3.6** Reaction of recombinant yeast RDL1 or human TSTD1 with *p*-toluenethiosulfonate (p-Tol-SO<sub>2</sub>S<sup>-</sup>) and glutathione as sulfane sulfur donor and acceptor, respectively. Reactions were conducted at 25 °C using 2 mm cuvettes in 50 mM potassium/sodium phosphate buffer, pH 8.0, containing 0.75 mM p-Tol-SO<sub>2</sub>S<sup>-</sup> and 2.4 mM glutathione, plus enzyme(s), as indicated. Panels A and B: The plots show the effect of the concentration of yeast RDL1 or human TSTD1 on the velocity observed during the initial 20 s of reactions conducted in the absence of SDO. The data are corrected for the blank rate observed in the absence of enzyme. Panels C and D show the effect of SDO (368 nM) on the extent of the reaction observed with 40.8 nM RDL1 and 80.3 nM TSTD1, respectively. In each panel: curve 1 is the blank reaction; curves 2 and 3 were obtained for the reactions with RDL1 or TSTD1 in the absence or presence of SDO, respectively; the dotted line (curve 4) shows the absorbance change calculated for 100% conversion of p-Tol-SO<sub>2</sub>S<sup>-</sup> to p-Tol-SO<sub>2</sub><sup>-</sup>. The first data point in curves 2 and 3 in panels C and D corresponds to the absorbance of p-Tol-SO<sub>2</sub>S<sup>-</sup>, observed immediately prior to enzyme addition. The apparent gap between the first and subsequent data points is due to the enzyme reaction that occurs during mixing (< 5 s), before readings can be made.



<b>RDL1</b>	<b>LIF</b> <b>C</b> <b>AS</b> <b>G</b> <b>K</b> <b>R</b> <b>G</b> <b>G</b> <b>E</b> <b>A</b> <b>Q</b> <b>K</b> <b>V</b> <b>A</b>	<b>111</b>
<b>TSTD1</b>	<b>L</b> <b>V</b> <b>F</b> <b>F</b> <b>C</b> <b>Q</b> <b>M</b> <b>G</b> <b>K</b> <b>R</b> <b>G</b> <b>L</b> <b>Q</b> <b>A</b> <b>T</b> <b>Q</b> <b>L</b> <b>A</b>	<b>92</b>
	<b>* : * : *</b> <b>*****</b> <b>: *</b> <b>: : *</b>	

**Figure 3.7** The active site loop and putative catalytic cysteine in RDL1 and TSTD1. The top panel is a stereo ribbon drawing of yeast RDL1 (3D1P.pdb), which is shown as a magenta ribbon, except for the white active site loop. Cys98 is shown in ball and stick. The bottom panel shows a region of a sequence alignment of RDL1 and TSTD1 around the putative catalytic cysteine (Cys98 and Cys79, respectively), which is located at the first position of the six-amino acid active site loop.

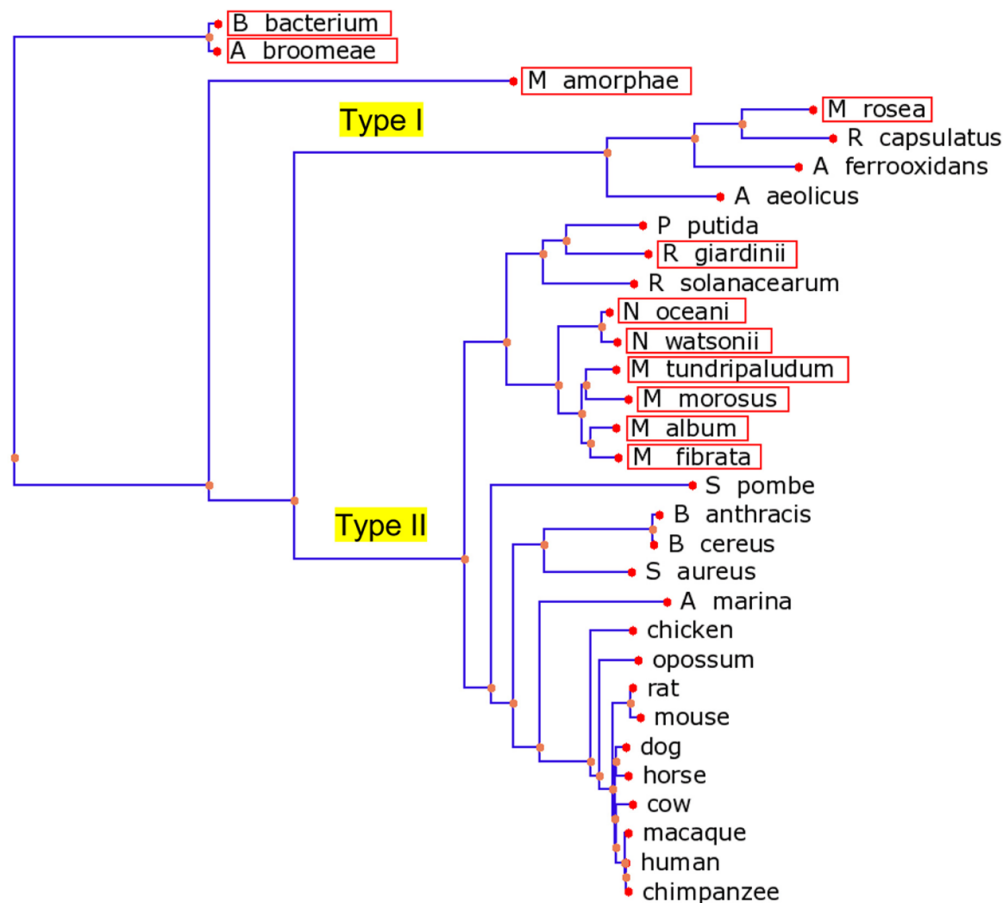


**Figure 3.8** Phylogenetic tree of SQOR homologs. A multiple sequence alignment of 31 homologs was performed using COBALT (<http://www.ncbi.nlm.nih.gov/tools/cobalt/>). The alignment included eleven SQORs produced in bacteria that express SDO-TSTD1 fusion proteins (see Appendix 2 Table 2) and twenty previously identified type I and type II SQORs<sup>25</sup>. The phylogenetic tree was rendered using the Newick file generated by COBALT and the online PHY-FI application<sup>63</sup>. The red boxes mark the eleven SQOR homologs found in bacteria that express SDO-TSTD1 fusion proteins. Starting from the upper left hand corner of the tree, the bacterial sequences include enzymes from: *Bradyrhizobiaceae bacterium*, *Afipia broomeae*, *Mesorhizobium amorphae*, *Methylocystis rosea*, *Rhodobacter capsulatus*, *Acidithiobacillus ferrooxidans*, *Aquifex aeolicus*, *Pseudomonas putida*, *Rhizobium giardinii*, *Ralstonia solanacearum*, *Nitrosococcus oceani*, *Nitrosococcus watsonii*, *Methylobacter tundripaludum*, *Methyloglobulus morosus*, *Methylomicrobium album*, *Methylosarcina fibrata*, *Bacillus anthracis*, *Bacillus cereus*, and *Staphylococcus aureus*. The eukaryotic sequences include SQORs from *Schizosaccharomyces pombe*, *Arenicola marina* (lugworm) and various higher eukaryotic animals, as indicated.

## Chapter 4: Characterization of the SDO-TSTD1 fusion enzyme from *Nitrosococcus oceanus*

### 4.1 Introduction

Hydrogen sulfide (H<sub>2</sub>S) is a gasotransmitter similar to nitric oxide and carbon monoxide. However, it is the only gasotransmitter that is enzymatically metabolized within the mitochondria. The first step is the two-electron oxidation of H<sub>2</sub>S catalyzed by SQOR to sulfane sulfur (S<sup>0</sup>) using coenzyme Q as an electron acceptor. In Chapter 2, we identified sulfite (SO<sub>3</sub><sup>2-</sup>) as the physiological acceptor of the sulfane sulfur. This reaction produces thiosulfate (SSO<sub>3</sub><sup>2-</sup>) (scheme 3.1, step 1), a known intermediate in the oxidation of H<sub>2</sub>S to sulfate (SO<sub>4</sub><sup>2-</sup>) (4, 6-11). By contrast, most bacterial SQORs do not require an acceptor of the sulfane sulfur. Instead, they produce polysulfide chains and cyclooctasulfur rings (S<sub>8</sub>, elemental sulfur). Our proposed scheme states that the thiosulfate produced by the SQOR reaction is a substrate for a glutathione-dependent thiosulfate sulfurtransferase (TST) (for more information on our proposed metabolic pathway of H<sub>2</sub>S see section 3.1) (Scheme 3.1, step 1) (2). In Chapter 3, we discovered a novel TST in humans, TSTD1, which transfers the sulfane sulfur in thiosulfate to glutathione (GS<sup>-</sup>), producing glutathione persulfide (GSS<sup>-</sup>) (eq. 10). In the presence of oxygen, human sulfur dioxygenase (SDO) will consume the GSS<sup>-</sup>, producing sulfite and regenerating the glutathione (scheme 3.1 step 3) (eq. 11).



As described in Chapter 3, we found phylogenetic evidence to further support the biochemical interaction of human TSTD1 and human SDO. A summary of this discovery

is below. Bioinformatic approaches were used to identify a possible fusion protein in bacteria containing two domains: a N-terminal SDO-like domain and a C-terminal TSTD1-like domain (186). The fusions are referred to as Rosetta stone proteins, which consist of two nonhomologous proteins that are found separately in another genome. It is postulated that the fusion is preserved by selection because it promotes a functional interaction, such as the kinetic coupling of consecutive enzymes in a pathway (170). Previously, six bacterial proteins were classified as fusions of SDO and rhodanese, which is a known thiosulfate:cyanide sulfurtransferase (22, 171). The functional interaction between TSTD1 and SDO that was observed in Chapter 3 brought into question the validity of this assignment. BLASTp searches of the human genome database were performed using each of the putative SDO-rhodanese fusion proteins as the query sequence. Our search results showed this to be an inaccurate label and more appropriately classified them as SDO-TSTD1 fusions.

We hypothesized that the six SDO-TSTD1 fusion proteins are part of a larger group of homologous Rosetta stone proteins. To evaluate this hypothesis, we used the fusion protein from *Methylobacter tundripaludum* as the query sequence in a BLASTp search against all non-redundant GenBank CDS translations. A selected subset of the hits obtained from the BLASTp search were used to further confirm that there was both a SDO and TSTD1 domain within the fusions. The selected hits were used as query sequences for BLASTp searches against the human genome. SDO and TSTD1 were indeed the highest scoring BLASTp hits obtained for the N- and C-terminal domains respectively in each tested query. *Nitrosococcus oceani* ATCC 19707 gene *Noc\_2007* had the lowest Expect (E) value ( $3 \times 10^{-11}$ ) with respect to the human *TSTD1* gene and

was chosen for biochemical studies (see Table 3.6). The E value is a parameter that is used in sequence alignments to determine if a hit is truly related to the query sequence (187-189). The lower the E value or closer to zero, the increased likelihood that the two are related (187-189). Operationally, the fusion is a glutathione-dependent thiosulfate dioxygenase (TSDO), which is the TST reaction (eq. 10) followed by the SDO reaction (eq. 11). The net reaction requires a catalytic amount of glutathione to facilitate the oxidation of one mole of thiosulfate in the presence of oxygen to two moles of sulfite (eq. 12).



*N. oceani* is an ammonia-oxidizing bacterium found in seawater (190). Ammonia-oxidizing bacteria are part of the nitrification process within the nitrogen cycle. The first step converts ammonia (NH<sub>3</sub>) or ammonium (NH<sub>4</sub><sup>+</sup>) into nitrite (NO<sub>2</sub><sup>-</sup>) and the second step converts the nitrite into nitrate (NO<sub>3</sub><sup>-</sup>). Within this process there is an intermediate, nitrous oxide (N<sub>2</sub>O), that is known to be a greenhouse gas (191). Therefore, *N. oceani* is indirectly related to the greenhouse effect and is why the whole genome was sequenced (190). The sequencing of this bacterium's genome enabled the discovery, through bioinformatics that there is a gene that encodes for a human-like SQOR the directly upstream. These genes are part of the same regulon, a gene cluster that is controlled by a regulatory protein. The fact that a human-like SQOR protein and the SDO-TSTD1 fusion are so close together suggests that at least some bacteria and mammals exhibit a similar pathway to metabolize H<sub>2</sub>S.

The goal of this chapter is to expand upon the phylogenetic evidence obtained in Chapter 3 by characterizing the SDO-TSTD1 fusion enzyme from *N. oceanii* (186). Furthermore, we wanted to determine whether the reaction of the fusion protein with  $\text{GSS}^-$  results in the consumption of a stoichiometric amount of oxygen (see eq. 11). Libiad et al. postulated that human TSTD1 could function in the reverse direction (eq. 13) (192). If a similar reaction occurred with the fusion protein, the TSTD1 domain would "compete" with the SDO domain for  $\text{GSS}^-$  by using the sulfite produced by the SDO domain to consume the  $\text{GSS}^-$  (eq. 13).



Our studies support the hypothesis that the *N. oceanii* gene, *Noc\_2007*, encodes for a fusion protein of SDO and TSTD1 and catalyzes the TSDO reaction. Additionally, the TSTD1 domain of the fusion enzyme does not compete with the SDO domain for  $\text{GSS}^-$ . Lastly, the TST reaction is the apparent rate-limiting step in the TSDO reaction.

## 4.2 Experimental procedure

### 4.2.1 Materials

Sodium sulfide was obtained from Alfa Aesar. Sodium thiosulfate pentahydrate was purchased from Sigma-Aldrich. Glutathione was obtained from Acros. Isopropyl- $\beta$ -D-thiogalactopyranoside (IPTG) was purchased from Gold Biotechnology. Restriction enzymes and T4 DNA ligase were obtained from New England Biolabs. PFU turbo was obtained from Agilent Technologies. Polymerase chain reaction mixture and oxidized glutathione (GSSG) were purchased from Amresco. A  $35 \pm 2\%$  oxygen (balanced with  $\text{N}_2$ ) tank was obtained from Airgas.



#### 4.2.2 Expression of wild type and mutant Noc\_2007

A synthetic version of the *N. oceani* *Noc\_2007* gene was obtained from GENEWIZ (South Plainfield, NJ) (see Appendix 3 figure 1). The synthetic version was optimized for expression in *E.coli* and was flanked by NdeI and XhoI sites. The synthetic gene was subcloned between the NdeI and XhoI sites in the pET23a plasmid to produce plasmid pET23a\_opzNoc\_2007. The resulting construct was used to transform *E. coli* BL21(DE3) cells to ampicillin resistance and sequenced across the insert (GENEWIZ, Inc.).

Mutant constructs of *Noc\_2007* were produced using PCR site-directed mutagenesis. An alignment with the N-terminus of the fusion protein and human SDO was performed to identify the iron-binding site residues for mutagenesis. An alignment with the C-terminus of the fusion protein and human TSTD1 was performed to identify the cysteine of the fusion protein required for TST activity. The amino acid sequence alignments with human SDO and TSTD1 to the N-terminus and C-terminus of *Noc\_2007* respectively are shown in figure 4.1. PCRs were conducted using pET23a\_opzNoc\_2007 as a template, PCR Mixture (Amresco), Pfu turbo DNA polymerase (Agilent Technologies), and the primers listed in Table 4.1. After treatment with DpnI (New England Bio Laboratories) to remove the template DNA, the PCR products were used to transform *E. coli* BL21(DE3) cells to ampicillin resistance and sequenced across the insert (Genewiz, Inc.). The constructs containing the SDO domain mutant plasmids were labeled as follows: pET23a\_opzNoc\_2007 His57Ala, pET23a\_opzNoc\_2007 His114Ala, and pET23a\_opzNoc\_2007 Asp131Ala. The constructs for the TSTD1 domain mutant

plasmids were labeled as follows: pET23a\_opzNoc\_2007 Cys322Ala and pET23a\_opzNoc\_2007 Cys322Ser.

For the expression of the wild type (WT) protein, a starter culture of *E.coli* BL21(DE3)/ pET23a\_opzNoc\_2007 cells was prepared by an overnight growth in LB medium at 37 °C containing ampicillin (200 µg/mL) and used to inoculate 2 L flasks containing 1 L of TB medium and ampicillin (100 µg/mL). Cells were grown with shaking at 25 °C. Iron(III)chloride (4 µM) was added to the medium 1 h prior to induction. Expression of the enzyme was induced with 0.1 mM IPTG when the cell density reached  $A_{595} \sim 1.7$ . Cells were harvested 18 h post induction (~10 g of cells from 1 L) and stored at -80 °C. The same method was used for the mutant constructs. Noteworthy, cells were not stored at -80 °C but used the same day when measuring the WT's SDO domain's activity.

#### **4.2.3 Purification of recombinant wild type and mutant fusion protein**

All steps were done at 4 °C. The protocol was modified from a previously described method (186). The same procedure was used to purify each construct, except as noted. 5 g of cells were suspended in 7.5 mL of buffer A [25 mM Tris-HCl (pH 8.0) containing 500 mM NaCl and 10 % (w/v) glycerol]. The cell suspension was mixed with a nuclease/protease inhibitor cocktail: 20 µg/mL DNAase, 20 µg/mL RNAase, 5 mM magnesium sulfate, 12.6 µg/mL soybean trypsin inhibitor, 2 µg/mL aprotinin, 25 µg/mL phenyl-methanesulfonyl fluoride, and 3 µg/mL tosyllysine chloromethyl ketone. The cells were disrupted by sonication. Cell debris was removed by centrifugation (10000 g for 10 min). The supernatant was loaded onto a 5 mL HisTrap IMAC column (GE Healthcare), previously equilibrated with buffer A.

Next, the column was washed with 5 column volumes of buffer B [25 mM Tris-HCl (pH 8.0) containing 500 mM NaCl, 10 % (w/v) glycerol, and 10 mM imidazole-HCl]. The fusion protein was eluted with a 90 mL linear gradient from 10-250 mM imidazole that was formed using buffer B and buffer C [25 mM Tris-HCl (pH 8.0) containing 500 mM NaCl, 10 % (w/v) glycerol, and 250 mM imidazole-HCl]. The eluate was dialyzed against 50 mM Tris-HCl (pH 8.0) containing 50 mM NaCl, and 5% (w/v) glycerol. Dialysis buffer for mutants His57Ala, His114Ala, Asp131Ala, and Cys322Ala was 25 mM Tris-HCl (pH 8.0) containing 10 % glycerol (w/v) and 125 mM imidazole-HCl. The sample was clarified (30000 g for 10 min) and the supernatant was stored in aliquots at -80 °C.

#### **4.2.4 Protein assay**

The protein concentration during enzyme purification was assessed by using a Nano Drop 2000 spectrometer (Thermo Scientific). The concentration of purified Noc\_2007 ( $\epsilon_{280} = 42860 \text{ M}^{-1} \text{ cm}^{-1}$ ) was determined using an extinction coefficient calculated using the ProParam tool (<http://web.expasy.org/protparam/>).

#### **4.2.5 Iron analysis**

Determination of the iron concentration was similar to, which was previously described (22, 193). First the sample was mixed with a final concentration of 5.94 mM sulfuric acid for a final ratio of 2:1 sample to sulfuric acid and boiled for 40 minutes. Afterwards, solutions were added to 75  $\mu\text{L}$  of boiled sample, in the following order at these final concentrations: (i) 968 mM sodium acetate (pH 7.5), (ii) 0.129 % hydroxylamine, and (iii) 0.039 % (w/v) bathophenanthroline disulfonic acid in a final

volume of 775  $\mu\text{L}$ . The color reaction went for 30 minutes at room temp. The color was read at 535 nm ( $\epsilon_{535} = 22100 \text{ M}^{-1} \text{ cm}^{-1}$ ).

#### **4.2.6 Producing glutathione persulfide**

$\text{GSS}^-$  was made via a reaction with sodium sulfide and GSSG in a quartz cuvette (Spectrocell) with a screw-cap equipped with a Teflon-silicon membrane. A stock solution of GSSG was made up with a pH of  $\sim 8.0$  and was stored in aliquots at  $-35^\circ\text{C}$ . An aliquot was diluted to 30 mM in 50 mM Tris-Acetate buffer (pH 7.5) and bubbled with argon for 30 min. Stock solutions of sodium sulfide were prepared as stated previously (158). 45 mM sodium sulfide was added to the 30 mM GSSG with an argon-purged gastight Hamilton syringe. Sodium sulfide was incubated with GSSG for 30 min. The  $\text{GSS}^-$  concentration was measured using a cold cyanolysis method as previously described (133). A typical final concentration of  $\text{GSS}^-$  was  $\sim 15 \text{ mM}$ .

#### **4.2.7 Catalytic assays of Noc\_2007 using an oxygen electrode**

Assays were conducted at  $25^\circ\text{C}$  using an Oxygraph (Hansatech) with continuous monitoring of oxygen consumption. Except where indicated, reactions were conducted in air-saturated buffer. Reaction rates were determined by monitoring the consumption of oxygen and were corrected for the corresponding blank rate observed in the absence of the enzyme.

TSDO activity was monitored using an assay that contained 50 mM sodium/potassium phosphate buffer (pH 8.0), 20 mM thiosulfate, and 20 mM glutathione and was initiated by the addition of the enzyme using a Hamilton syringe. To measure SDO activity,  $\text{GSS}^-$  was added to the above assay buffer using an argon-purged gastight Hamilton syringe at a final concentration of 280  $\mu\text{M}$  or 292  $\mu\text{M}$ , as indicated. For

reactions that required 35 % (450  $\mu\text{M}$ ) oxygen, the oxygen was bubbled for 30 min prior to the addition of  $\text{GSS}^-$ . It is noteworthy, that the maximal detectable limit of the oxygen electrode is 40 % oxygen. To be within the measurable range 35 % oxygen was chosen.

For some experiments, control studies using the oxygen electrode were conducted with human SDO. Recombinant human SDO was expressed in *E. coli* BL21(DE3)/pMW172ETHE and purified as previously described (22). Plasmid pMW172ETHE was obtained as a gift from V. Tiranti.

#### **4.2.8 TST catalytic assay of Noc\_2007 mutants using a sulfite discontinuous assay**

For mutants to the SDO domain (His57Ala, His 114Ala, and Asp131Ala) the TST activity of the TSTD1 domain was measured using a sulfite end point assay as previously described (163, 186). An assay containing 50 mM sodium/potassium phosphate buffer (pH 8.0), 20 mM thiosulfate, and enzyme were initiated by adding 20 mM glutathione (pH 8.0) at 25 °C in a final volume of 0.5 mL. Assays were quenched after 2 min by the addition of mercuric chloride to a final concentration of 115 mM and centrifuged. The supernatant was assayed for sulfite by using a pararosaniline colorimetric assay ( $\epsilon_{570} = 35300 \text{ M}^{-1} \text{ L}^{-1}$ ).

### **4.3 Results**

#### **4.3.1 Purification and iron analysis of recombinant *Nitrosococcus oceani* SDO-TSTD1 fusion protein**

*N. oceani* gene *Noc\_2007* was identified from a BLASTp search as a possible gene to encode for a fusion protein containing TSTD1-like and SDO-like domains connected with a linker region (Chapter 3) (186). We obtained a synthetic version of the DNA that was codon optimized for expression in *E. coli* and subcloned into a pET23a

expression vector that introduced a C-terminus (His)<sub>6</sub> tag. The resulting construct was used to transform *E.coli* BL21(DE3) cells. The purification strategy was modified from the purification for SUMO-TSTD1 (Chapter 3). The WT fusion protein was purified to greater than 95% homogeneity; a typical preparation yields approximately 70 mg of purified enzyme from 5 g of cells (figure 4.2).

Human SDO belongs to a superfamily of enzymes called dioxygen-activating mononuclear non-heme iron(II) enzymes that require a 2-His-1-carboxylate facial triad for iron binding (23, 24). The growth medium was supplemented with iron to ensure its incorporation into the SDO domain of the fusion enzyme. The mole ratio of iron to protein was  $0.45 \pm 0.04$  for the WT fusion enzyme (table 4.2).

The overall TSDO reaction (eq. 12) involves two consecutive reactions. The first step is a TST reaction, catalyzed by the TSTD1 domain, which requires thiosulfate and glutathione, producing sulfite and GSS<sup>-</sup> (eq. 10). The second step is a SDO reaction, catalyzed by the SDO domain requiring oxygen. This step consumes the GSS<sup>-</sup> formed in the first step, producing a second molecule of sulfite and regenerating glutathione (eq. 11). The WT enzyme is postulated to catalyze the formation of two moles of sulfite from one mole of thiosulfate and oxygen requires a catalytic amount of glutathione (eq. 12). For the WT enzyme, TSDO and SDO activity were determined by measuring oxygen consumption according to the assays described in the methods section (section 4.2.7). However, the TST activity with the WT enzyme could not be determined because sulfite is the product measured in determining TST activity, and both the TST and SDO reactions produce sulfite. As summarized in table 4.3, the TSDO activity of the WT fusion protein, is 15-fold slower than its SDO activity ( $k_{\text{cat,app}}$  of  $0.53 \pm 0.01 \text{ s}^{-1}$  versus 8.2

$\pm 0.5 \text{ s}^{-1}$ ). Because the SDO reaction is significantly faster than the TSDO reaction, we hypothesize that the TST reaction is the rate-limiting step. For comparison, the human SDO activity ( $20.4 \pm 0.6 \text{ s}^{-1}$ ) is 2.4-fold higher than the SDO activity of the WT fusion protein (table 4.3).

### 4.3.2 Mutagenesis of the TSTD1 Domain

We hypothesized that the TST activity of the WT enzyme required a catalytic cysteine. A sequence alignment of the C-terminus of the Noc\_2007 with human TSTD1 suggested that Cys322 is the catalytic cysteine residue in the fusion protein. Alanine and serine Cys322 mutant constructs were expressed, purified, and tested for SDO catalytic activity. Both mutations affected protein expression. The Cys322Ala mutant was purified to greater than 95% homogeneity; a typical preparation yields 8 mg of protein, which is significantly lower than the WT enzyme's yield (70 mg). The Cys322Ser mutant was purified to greater than 95% homogeneity; a typical preparation yields 173 mg of protein, which is 2.5-fold higher than the WT enzyme's yield (70 mg).

The mutation of Cys322 is not expected to affect the mole ratio of iron to protein because the binding site of iron is located in the SDO domain. This ratio was determined for the serine mutant only due to the low amount of purified alanine mutant. As expected, the ratio of  $0.62 \pm 0.04$  for the Cys322Ser mutant was similar to the  $0.45 \pm 0.04$  obtained for the WT enzyme (table 4.2). Both mutations were found to be catalytically inactive in the TSDO assay. As expected the SDO domain was still active. However, the observed SDO activity for the alanine and serine mutants was  $0.44 \pm 0.01 \text{ s}^{-1}$  and  $0.71 \pm 0.03 \text{ s}^{-1}$  respectively, and 19- and 12-fold slower respectively than the reaction catalyzed by the WT SDO domain ( $8.5 \pm 0.1 \text{ s}^{-1}$ ) (table 4.3). The slower rate with the mutants suggests

that the mutations affected the SDO domain's catalytic function. These results show that Cys322 is catalytically essential for the TST and TSDO reactions.

### 4.3.3 Mutagenesis of the SDO Domain

We hypothesized that the TST reaction in the TSDO reaction is the rate-limiting step, because with the WT enzyme the reaction catalyzed by the SDO domain is 15-fold faster than the rate of the overall TSDO reaction. With human SDO, iron is required to facilitate the catalytic formation of sulfite from  $\text{GSS}^-$  and oxygen (21). The iron is bound to a facial triad composed of two histidines and an aspartate. We expected that mutations of these amino acids would cause a decrease in the iron to protein ratio and render the SDO domain inactive. A sequence alignment of human SDO and the N-terminus of Noc\_2007 suggested that His57, His114, and Asp131, are the three residues that comprise the iron-binding site. All three mutants were purified to greater than 95% homogeneity. A typical preparation yielded, 93 mg, 23 mg, and 26 mg of protein for the His114Ala, His57Ala, and Asp131Ala mutations respectively. Compared to the amount of the WT enzyme (70 mg) the His114Ala mutant total protein was similar and the other two were significantly lower. All three mutants caused a greater than 50% decrease in bound iron (table 4.2). Neither TSDO nor SDO activity was detected with any of the three mutants (table 4.3).

To test the hypothesis that the loss of iron would not affect the TST reaction, we performed a TST assay by measuring the production of sulfite by each mutant. The results show that all three alanine mutants catalyzed the formation of sulfite with similar rates:  $0.44 \pm 0.00$ ,  $0.49 \pm 0.06$ , and  $0.46 \pm 0.03 \text{ s}^{-1}$  for His57Ala, His 114Ala and Asp131Ala respectively (table 4.3). The TST activity of the mutants was similar to the



WT's TSDO activity, which was  $0.53 \pm 0.01 \text{ s}^{-1}$  by measuring oxygen consumption. The TST catalytic activity of the three mutations was approximately 17-fold lower than the WT SDO activity. These results in conjunction with the SDO reaction being significantly faster than the TSDO reaction of the WT fusion protein, strongly suggests that the TST step is the rate-limiting step in the TSDO reaction.

#### **4.3.4 Is the TSTD1 domain of the fusion protein bidirectional?**

From our previous work (Chapter 3), we hypothesized that the TSTD1 domain functions in a single direction requiring glutathione and thiosulfate to produce  $\text{GSS}^-$  and sulfite (eq. 10). However, Libiad et al. postulated that human TSTD1 is a bidirectional enzyme that would also function in the reverse direction, requiring  $\text{GSS}^-$  and sulfite to produce glutathione and thiosulfate (eq. 13). If a similar reaction occurred with the fusion protein, the TSTD1 domain would "compete" with the SDO domain for  $\text{GSS}^-$  by consuming it and using the sulfite produced by the SDO domain.

If the TSTD1 domain functions bidirectionally, this would alter the mole ratio of oxygen consumed to the concentration of  $\text{GSS}^-$  in the SDO reaction. We would expect, for the SDO reaction that for every mole of oxygen consumed, an equal amount of  $\text{GSS}^-$  would be consumed for a ratio of one. However, if the TSTD1 domain does function in two directions, then the ratio of oxygen consumed to  $\text{GSS}^-$  would be less than one for the SDO reaction. We conducted the experiment with 35% oxygen ( $450 \mu\text{M}$ ) and  $292 \mu\text{M}$   $\text{GSS}^-$ , with the enzyme in excess.

Prior to testing the fusion enzyme, experiments were conducted with human SDO, as a control reaction. This would allow for the comparison of a known SDO to the human SDO-like domain in the fusion enzyme. The calculated mole ratio with human SDO was

not one as expected but  $0.37 \pm 0.1$  (table 4.4). The WT fusion enzyme's value was similar to that obtained with human SDO ( $0.39 \pm 0.01$  compared to  $0.37 \pm 0.1$ ) (table 4.4). The inactive TSTD1 domain (Cys332Ser mutant) had nearly an identical mole ratio of  $0.39 \pm 0.05$ , to the WT enzyme (table 4.4). These results provide definitive evidence that the TSTD1 domain within the fusion protein works in the single direction stated in eq. 1. A possibility for the ratio value being below one is that the reaction with oxidized glutathione and  $\text{H}_2\text{S}$  produces  $\text{GSS}^-$  (as described in section 4.2.6) along with polysulfides (ie.  $\text{GSS}_n^-$  or  $\text{GSS}_n\text{SG}^-$ ). These polysulfides along with  $\text{GSS}^-$  will react with cyanide forming thiocyanate, which is measured to determine the stock concentration of  $\text{GSS}^-$  (133). Human SDO and the human SDO-like domain of the fusion protein would consume only the  $\text{GSS}^-$ .

#### 4.4 Discussion

In Chapter 3, we presented phylogenetic evidence for the existence of bacterial fusion enzymes with a SDO-like and a TSTD1-like domain. In this chapter, we provide biochemical data to corroborate the phylogenetic evidence. The SDO-TSTD1 fusion enzyme from *N. oceani* was expressed in *E.coli* and purified using an immobilized metal ion affinity chromatography (IMAC) column. The SDO domain within the WT fusion protein is a mononuclear non-heme iron(II) enzyme. The ratio of iron to the WT fusion protein was similar to what was determined for human SDO (0.5) (22). Mutations that were introduced to the iron-binding center significantly decreased this ratio. A serine mutation to the catalytic cysteine (Cys322) in the fusion protein's TSTD1 domain did not affect this ratio.

The overall reaction catalyzed by the WT enzyme is a glutathione-dependent conversion of thiosulfate and oxygen to two moles of sulfite. The TSDO reaction consists of two steps: a TST reaction followed by a SDO reaction. We hypothesized that the TST reaction is the rate-limiting step. With the WT enzyme, the  $k_{\text{cat,app}}$  of the TSDO reaction was 15-fold slower than the  $k_{\text{cat,app}}$  for the SDO domain. The SDO domain mutants exhibited no TSDO or SDO activity. The  $k_{\text{cat,app}}$  for the TST reaction determined with the SDO domain mutants was similar to the  $k_{\text{cat,app}}$  for the WT enzyme's TSDO reaction. These results provide compelling evidence that the TST reaction is the rate-limiting step in the TSDO reaction.

To further support this conclusion, we wanted to test the SDO reaction catalyzed by the SDO domain with an inactive TSTD1 domain. To evaluate this hypothesis a sequence alignment identified Cys322 as the catalytic cysteine, which was subsequently mutated to alanine and serine. Instead of observing a rate for the SDO reaction similar to what was obtained with the WT enzyme, the  $k_{\text{cat,app}}$  for the alanine and serine mutants were 19- and 12-fold slower respectively. There are two possible explanations for this result: (i) mutation to the TSTD1 domain caused a conformational change to the SDO domain or the whole protein or (ii) the SDO domain is intrinsically unstable. Evidence that the SDO domain is unstable apart from its lower  $k_{\text{cat,app}}$  with the TSTD1 domain mutations, is that the  $k_{\text{cat,app}}$  obtained for the SDO activity of the WT enzyme was from unfrozen cells.

What is the overall importance of the  $\text{H}_2\text{S}$  metabolic pathway within *N. oceanii*? *N. oceanii* is an ammonia-oxidizing bacterium that produces all its energy from the oxidation of ammonia to nitrite (194).  $\text{H}_2\text{S}$  may regulate the nitrification process,

because studies have shown that  $H_2S$  can inhibit nitrification (195-197). This may explain why the genes that encode for the fusion and the human-like SQOR enzyme are located on the same regulon cluster. Further studies observing the role of  $H_2S$  in *N. oceanii* are required to better understand how it affects the organism. In turn, this could shed light on part of  $H_2S$ 's environmental impact, because ammonia-oxidizing bacteria are the rate-limiting step in the overall nitrification process (194).

In summary, we have described a novel TSDO fusion enzyme that contains SDO-like and TSTD1-like domains encoded by the gene, *Noc\_2007* in *N. oceanii*. The TSTD1 domain catalyzes a TST reaction, consuming thiosulfate and glutathione and producing sulfite and  $GSS^-$ . The SDO domain catalyzes a SDO reaction, consuming oxygen and the  $GSS^-$  from the TST reaction to produce a second molecule of sulfite and regenerate glutathione. Lastly, we observed that the TSTD1 domain does not “compete” with the SDO domain for  $GSS^-$  but rather functions only in the direction previously stated. In conclusion, these experiments support the functional interaction that was observed in Chapter 3 with human TSTD1 and SDO.

<b>Fusion Protein Mutant</b>	<b>Primer</b>	<b>Sequence 5' to 3'</b>
His57Ala	Forward	GAAATACAGCCTGGAGACCGCCGCCCATGCCGATC
	Reverse	GATCGGCATGGGCGGGCGGTCTCCAGGCTGTATTTC
His114Ala	Forward	GCCACACCGGGCGCCACCCCGGGTAGC
	Reverse	GCTACCCGGGGTGGCGCCCGGTGTGGC
Asp131Ala	Forward	CGTGTGTTTACCGGTGCAGCCCTGCTGATTAAC
	Reverse	GTTAATCAGCAGGGCTGCACCGGTAAACACACG
Cys322Ala	Forward	CCGATTATTCTGTACGCCAGACAGGTGGC
	Reverse	GCCACCTGTCTGGGCGTACAGAATAATCGG
Cys322Ser	Forward	CCGATTATTCTGTACAGCCAGACAGGTGGC
	Reverse	GCCACCTGTCTGGCTGTACAGAATAATCGG

<b>Sample</b>	<b>Ratio (iron: enzyme)</b>
WT	0.45 ± 0.04
His57Ala	0.18 ± 0.01
His114Ala	0.16 ± 0.02
Asp131Ala	0.21 ± 0.01
Cys322Ser	0.62 ± 0.04
Enzyme and iron concentrations were determined as described in Experimental Procedures.	

**Table 4.3** Rate of Wild Type and Mutant Noc\_2007 Compared to Human TSTD1 and SDO Enzymes

Sample	$k_{cat,app}$ ( $s^{-1}$ )		
	TSDO	TST	SDO
Wild Type	$0.53 \pm 0.01$	ND	$8.2 \pm 0.5$
His57Ala	0	$0.44 \pm 0.00^*$	0
His114Ala	0	$0.49 \pm 0.06$	0
Asp131Ala	0	$0.46 \pm 0.03$	0
Cys322Ala	0	0	$0.44 \pm 0.01$
Cys322Ser	0	0	$0.71 \pm 0.03$
Human TSTD1	0	$0.48 \pm 0.04$	0
Human SDO	0	0	$20.4 \pm 0.6$

Reactions were conducted as described in the Experimental Procedures. Values for  $k_{cat,app}$  are determined on the basis of the rate of oxygen consumption for the TSDO and SDO reactions and sulfite formation for the TST reactions. For the SDO reactions the GSS<sup>-</sup> was at a final concentration of 280  $\mu$ M.  
\*Reaction was done in duplicate with an identical value

**Table 4.4** SDO Reaction: Determining the Mole Ratio of a Mole of Oxygen Consumed to a Mole of Glutathione Persulfide for Human SDO and Wild Type and Cys322Ser of Noc\_2007

Enzyme	[GSS <sup>-</sup> ] ( $\mu$ M)	[Oxygen Consumed] ( $\mu$ M)	mol O <sub>2</sub> consumed/ mol of GSS <sup>-</sup>
Human SDO	$292 \pm 0$	$108 \pm 28$	$0.37 \pm 0.1$
WT Fusion Protein	$292 \pm 0$	$114 \pm 2$	$0.39 \pm 0.01$
Cys322Ser Fusion Protein	$292 \pm 0$	$114 \pm 16$	$0.39 \pm 0.05$

Reactions were initiated with an excess amount of enzyme and went to completion within 60 sec. Set up was conducted as described in the Experimental Procedures.

## A) N-terminal of SDO-like Domain

<b>N. oceani</b>	-----MIFRQLFDPESSYTYLIGDPATKEAVFIDPVNTRVDE	<b>38</b>
<b>ETHE1</b>	MAEAVLRVARRQLSQRGGSGAPILLRQMFEVPSCTFTYLLGDRESREAVLIDPVLETAPR	<b>60</b>
<b>N. oceani</b>	YLNLLNKYALKLKYSLET <b>H</b> AHADHITASGLLRQRT-GAKTGIGQACGAQYADYQLKDGVV	<b>97</b>
<b>ETHE1</b>	DAQLIKELGLRLLYAVNT <b>H</b> CHADHITGSGLLRSLLPQCQSVISRLSGAQ-ADLHIEDGDS	<b>119</b>
<b>N. oceani</b>	LAFGQGEEIKVLATPG <b>H</b> TPGSVSYLWRDR--VFTG <b>D</b> ALLINGCGRTDFQGGDPGVLYDSI	<b>155</b>
<b>ETHE1</b>	IRFGR-FALETRASP <b>G</b> HTPGCVTFVLNDHSMFT <b>G</b> DALLIRCGRTDFQGGCAKTLYHSV	<b>178</b>
<b>N. oceani</b>	TQKFLTLPGETIVYPGHYNGRWVSSIEQERTRNGRLAGK-TRSEFIEIMNNLNLKPKQR	<b>214</b>
<b>ETHE1</b>	HEKIFTLPGDCLIYPADHYHGFTVSTVVEERTLNPRL--TLSCEEVFKIMGNLNLKPKQQ	<b>236</b>
<b>N. oceani</b>	IIDEAVPANRRCG-----	<b>226</b>
<b>ETHE1</b>	IDFAVPANMRCGVQTPTA	<b>254</b>

## B) C-terminal of TSTD1-like Domain

<b>N. oceani</b>	-----EIDVATVKQRLGDGKTAIIDVREPEEFAAGHLPGAINVPRGVLEFRLGNTA--	<b>310</b>
<b>TSTD1</b>	MAGAPTVSLPELRSLLASGRARLFDVRSREAAAAGTIPGALNIPVSELESALQMEPAA	<b>58</b>
<b>N. oceani</b>	-----ELADPNVPIMLY <b>C</b> QTGGRAALAAWSLKCLGYTDAVLIAGGYDAWRAEQNAN	<b>362</b>
<b>TSTD1</b>	FQALYSAEKPKLEDEHLVFF <b>C</b> QMGKRGLQATQLARSLGYTGARNYAGAYREWLEKES---	<b>115</b>

**Figure 4.1** Sequence alignment of human SDO or human TSTD1 with the N-terminal SDO-like or the C-terminal TSTD1-like domain, respectively, in Noc\_2007. Panel A: Mutations made in Noc\_2007 are in bold and a larger font size corresponding to the iron-binding site, His57, His114, and Asp131. Panel B: Active site cysteine, Cys322, which was mutated in Noc\_2007, is bolded and a large font size.

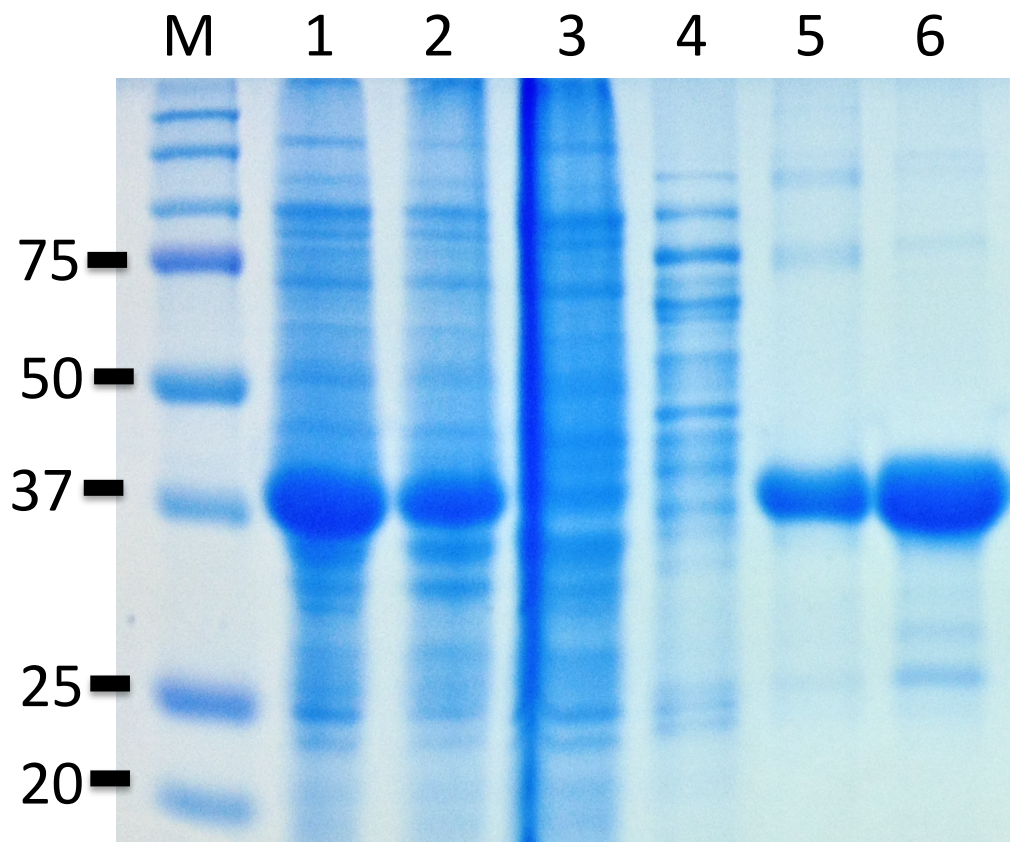


**Figure 4.2** Expression of recombinant *Nitrosococcus oceani* SDO-TSTD1 fusion protein. The SDS-12% polyacrylamide gel was stained for protein with ProSieve Blue Protein Staining Solution (Lonza); lane M, molecular markers; lane 1, whole cell lysate; lane 2, low-speed supernatant; lane 3, IMAC flow-through; lane 4 IMAC wash; lane 5, IMAC eluate; lane 6, dialyzed IMAC eluate from lane 5.



## Chapter 5: Conclusions and Future Directions

Hydrogen sulfide ( $\text{H}_2\text{S}$ ) is the newest member of the gasotransmitter family that includes nitric oxide and carbon monoxide. Although originally believed to be toxic to animals it is now understood that within a small concentration window it plays an important role within mammals ranging from high blood pressure to a neuroprotectant and modulator (93-95, 103). Outside of this range,  $\text{H}_2\text{S}$  is associated with pathological conditions, including hypertension, ethylmalonic encephalopathy, Down syndrome, ulcerative colitis, Alzheimer's disease, and Parkinson's disease (22, 25, 81, 90, 91, 95, 198). Importantly,  $\text{H}_2\text{S}$  is the only gasotransmitter that is enzymatically degraded. Studies involving the metabolic pathway of  $\text{H}_2\text{S}$  were lacking prior to our work. The goal of this thesis work was to improve the field's understanding of this pathway.

Prior to our work, Hildebrandt and Grieshaber proposed a pathway for the metabolism of  $\text{H}_2\text{S}$  to thiosulfate in mammals and invertebrates (14). The first enzyme in the proposed pathway is a membrane-associated enzyme called sulfide:quinone oxidoreductase (SQOR). They proposed that SQOR would catalyze the two-electron oxidation of  $\text{H}_2\text{S}$  to sulfane sulfur ( $\text{S}^0$ ) using coenzyme Q as the electron acceptor and glutathione as the physiological acceptor of the sulfane sulfur ( $\text{S}^0$ ) producing glutathione persulfide ( $\text{GSS}^{\cdot}$ ). It is note worthy, that at that time the physiological acceptor of the sulfane sulfur was unknown. In Chapter 2, we successfully purified and characterized human SQOR. Importantly, we determined that glutathione was not the physiological acceptor of the sulfane sulfur but rather sulfite, producing thiosulfate. The discovery of thiosulfate as the product was important, because thiosulfate is a known intermediate and

byproduct of H<sub>2</sub>S metabolism. Latter, Libiad et al. also showed that sulfite was an acceptor however, but they stated that glutathione would be the predominant acceptor within the cell (192). They reported a K<sub>m</sub> of 22 mM for glutathione, which is higher than the 1-8 mM concentration of glutathione found inside cells (180, 192). We have recently shown in assays with SQOR that Michaelis-Menten Kinetics are not observed at glutathione concentrations as high as 40 mM (199). The rate observed at glutathione concentrations found in cells is ≤ 2-fold faster than the slow rate of H<sub>2</sub>S oxidation observed in assays containing only sulfide and CoQ<sub>1</sub>.

A future experiment would be to determine the physiological concentration of sulfite within tissues and compare it to sulfite's K<sub>m</sub> (174 μM). If the tissue concentration of sulfite is close to its K<sub>m</sub>, it will provide further evidence supporting that sulfite is the predominant acceptor of the sulfane sulfur. Although, the concentration of sulfite in serum has been determined, it is important to determine the concentration in tissue, as SQOR is located in the mitochondria and is not present in serum (200, 201).

Another future experiment with SQOR would be to solve the crystal structure of the enzyme with and without a quinone. If solved, to our knowledge it would be the first structure of a Type II SQOR. This would allow us to compare it to the other known structures: (i) *A. aeolicus* SQOR (Type I), (ii) *A. ferrooxidans* SQOR (Type I), and (iii) *A. ambivalens* SQOR (Type V) and to our homology model (32-34, 202). Additionally, we could confirm that Cys201 and Cys379 comprise the redox-active disulfide bridge that is near the FAD. Moreover, the structure could provide insight to confirming our postulated catalytic mechanism for SQOR (Scheme 2.2). In conjunction to solving a crystal

structure, stopped-flow experiments could also be conducted to provide a detailed understanding of the mechanism.

Hildebrandt and Grieshaber postulated that the second enzyme in the metabolism of H<sub>2</sub>S is sulfur dioxygenase (SDO). SDO is a mitochondrial matrix enzyme, requiring oxygen to catalyze the four-electron oxidation of the sulfane sulfur in glutathione persulfide (GSS<sup>-</sup>) to produce sulfite and glutathione (14, 21, 22). In an alternate scenario, it has been suggested that SDO might directly oxidize the sulfane sulfur in the SQOR persulfide intermediate ( $\text{E-CysSS}^- + \text{O}_2 + \text{H}_2\text{O} \Rightarrow \text{E-CysS}^- + \text{SO}_3^{2-} + 2\text{H}^+$ ) (199). However, addition of human SDO to assays containing sulfide and CoQ<sub>1</sub> did not accelerate the rate of H<sub>2</sub>S oxidation (199). This result and the results obtained in Chapter 2 lead us to postulate a role for a thiosulfate sulfurtransferase (TST) in H<sub>2</sub>S metabolism. A TST requires thiosulfate and glutathione to produce GSS<sup>-</sup> and sulfite. We postulated that the TST reaction is the intermediate step that would consume the thiosulfate from the SQOR reaction and produce GSS<sup>-</sup>, a substrate required for the SDO reaction, linking the SQOR and SDO steps in H<sub>2</sub>S metabolism (Scheme 3.1).

Using bioinformatics in Chapter 3, we identified the yeast and human genes *RDL1* and *TSTD1* that encode for their respective TSTs. We discovered that GSS<sup>-</sup> was produced by both enzymes, released into solution, and a potent competitive inhibitor of the enzymes with respect to glutathione. The TST reaction is thermodynamically unfavorable because it produces GSS<sup>-</sup>, which is a highly reactive compound, compared to thiosulfate. On the other hand, the SDO reaction is thermodynamically favorable. We hypothesized that there is thermodynamic coupling between the enzymes. To test this we performed a continuous assay containing p-toluenethiosulfonate, a chromogenic substrate

that is a more reactive sulfane sulfur donor than thiosulfate. In assays containing only TST, the observed reaction reached an apparent equilibrium position when only approximately 50 % of the p-toluenethiosulfonate had been consumed. In the presence of excess SDO,  $GSS^-$  is oxidatively decomposed and 100 % of the p-toluenethiosulfonate was consumed. The observed ability of SDO to drive the TST reaction to completion provides a paradigm for proposed thermodynamic coupling of these reactions in cells. Additionally, this supports our hypothesis that the TST reaction is the missing link between the SQOR and SDO reactions in the  $H_2S$  metabolic pathway.

To confirm the roles of SQOR and TSTD1 in  $H_2S$  metabolism, it would be beneficial to perform protein knockdown experiments using clustered regularly interspaced short palindromic repeats-interference (CRISPRi) mediated transcriptional repression. A common method usually used to knockdown protein levels in cells is short hairpin RNA (shRNA). However, CRISPRi mediated transcriptional repression is a newer, more effective technique. This method decreases protein levels in a cell by affecting transcription instead of translation with shRNA (203). An expected result from SQOR knockdown would be an increase in the levels of  $H_2S$ . This increase would also be expected in experiments with TSTD1 knockdown. With either enzyme being knockdown sulfite would not be detected. SDO would not be able produce sulfite because  $GSS^-$ , a substrate for the reaction would not be produced (see Scheme 3.1 for proposed metabolic pathway of  $H_2S$ ). Our assumption that sulfite will not be detected is from the results obtained by Tiranti et al. that showed in *ETHE1*<sup>-/-</sup> (gene that encodes for human SDO) mice or individuals with ethylmalonic encephalopathy (disease associated with inactive SDO), that sulfite was undetectable (22).

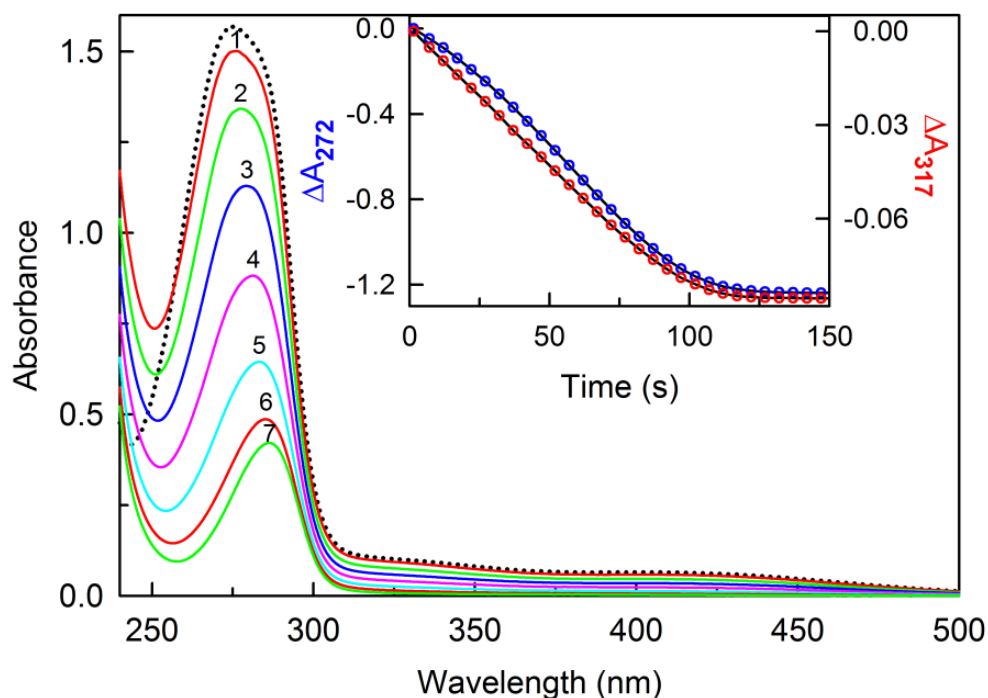
The thermodynamic coupling of human TSTD1 and SDO observed in Chapter 3 led us to inquire if there is phylogenetic evidence to support their interaction. From bioinformatic approaches we identified fusion proteins within bacteria that contain a human SDO-like and human TSTD1-like domain at the C- and N- terminal respectively connected with a variable-length linker region. Operationally, the fusion is a glutathione-dependent thiosulfate dioxygenase (TSDO), which has the combined functions, of a TST reaction followed by the SDO reaction. The net reaction requires a catalytic amount of glutathione to facilitate the oxidation of one mole of thiosulfate in the presence of oxygen, to two moles of sulfite. To confirm the results obtained from bioinformatics a fusion protein was expressed from *N. oceanus* that was encoded by the *Noc\_2007* gene (see Chapter 4). We determined that it is indeed a fusion of both enzymes and that the TST reaction is the apparent rate-limiting step in the TSDO reaction.

Libiad et al. postulated that human TSTD1 could function in the reverse direction (192). If a similar reaction occurred with the fusion protein, the TSTD1 domain would "compete" with the SDO domain for  $GSS^-$  by using the sulfite produced from the SDO reaction to consume  $GSS^-$ . We observed that the TSTD1 domain does not "compete" with the SDO domain for  $GSS^-$  and thus functions in one direction. A future experiment would be to obtain the crystal structure of the *N. oceanus* fusion protein. The structure would provide insight regarding the mechanism of catalysis by the fusion protein, including the possibility of substrate ( $GSS^-$ ) channeling between the two domains.

From our work we propose a newer model (Scheme 3.1) for the metabolic pathway of  $H_2S$  than previously described by Hildebrandt and Grieshaber (14). As the field of  $H_2S$  keeps expanding it is important that the metabolism of this gasotransmitter

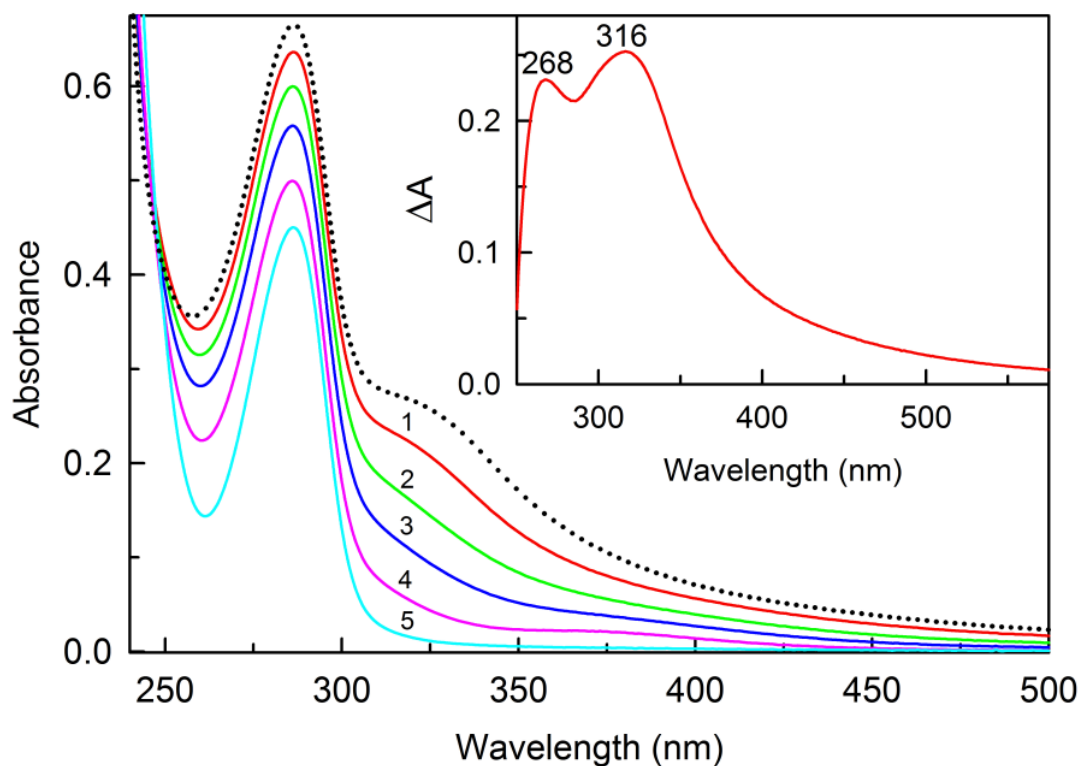
continues to be studied. Furthermore, understanding how this pathway is regulated could uncover key aspects related directly to H<sub>2</sub>S signaling.



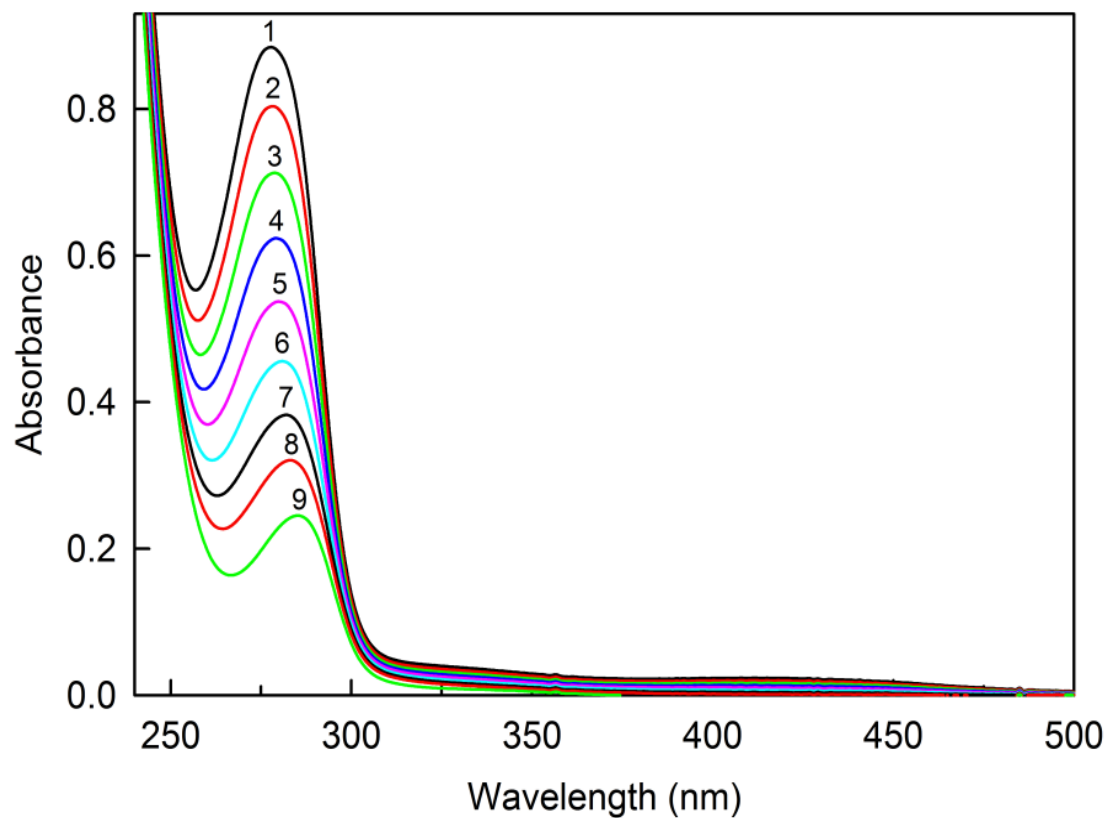


**Appendix 1 Figure 2** Spectral course of sulfide oxidation by SQOR in the presence of cyanide and CoQ<sub>1</sub>. The reaction was conducted at 25 °C in 100 mM potassium phosphate, pH 8.0, containing 0.5 mM EDTA. The dotted black line was recorded before addition of 300 μM sulfide to an assay mixture containing 158 μM CoQ<sub>1</sub>, 1.0 mM cyanide, and 9.3 nM SQOR. Curves 2 to 7 were recorded 1.4, 22, 42, 62, 82, 102, and 831 s, respectively, after sulfide addition. The inset shows the time course of absorbance changes at 272 and 317 nm plotted according to the left and right y-axes, respectively.

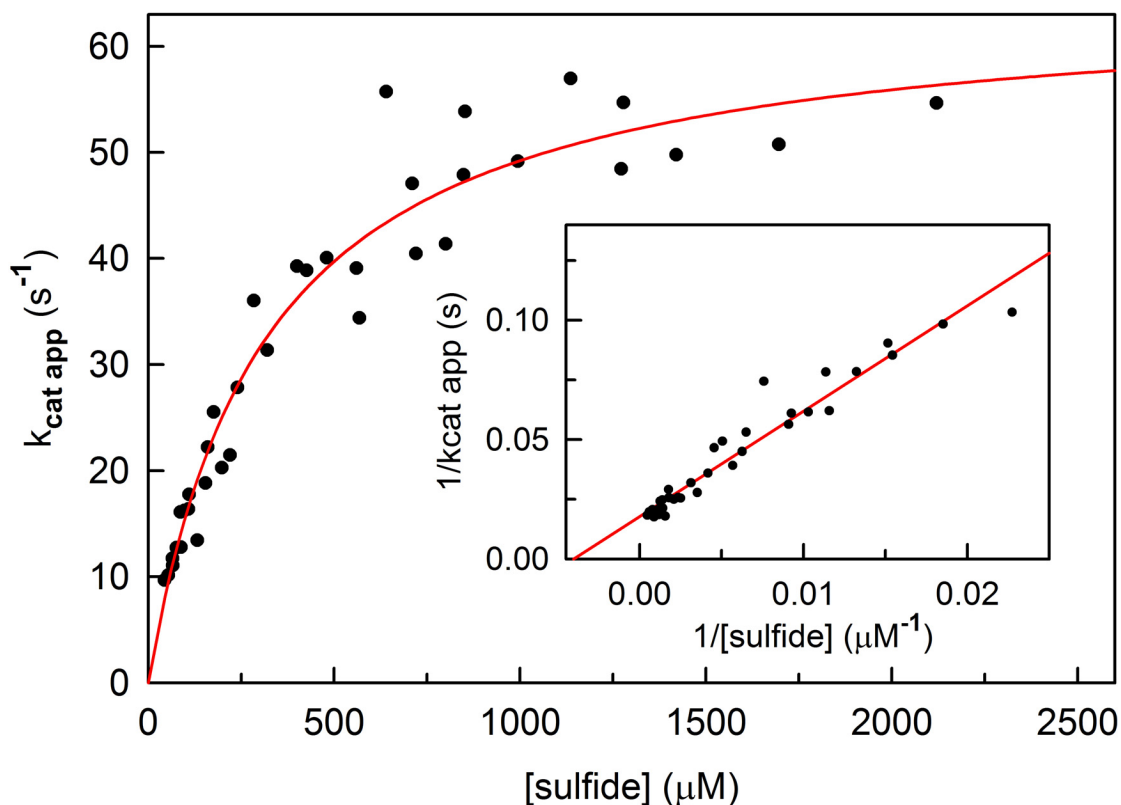




**Appendix 1 Figure 3** Reaction of dithiothreitol (DTT) with the sulfur oxidation product formed during the apparent “acceptor-free” oxidation of sulfide by SQOR. Reactions were conducted in 100 mM potassium phosphate, pH 8.0, containing 0.5 mM EDTA at 25 °C. The dotted black line was recorded after maximal formation of the sulfur oxidation product in an assay mixture containing 300  $\mu\text{M}$  sulfide, 158  $\mu\text{M}$  CoQ1 and 32.5 nM SQOR. Curves 1 to 5 were recorded 1.4, 17, 37, 117, and 831 s, respectively, after addition of 1.0 mM DTT. The inset shows a difference spectrum calculated by subtracting the spectrum observed at the end of the DTT reaction from the spectrum observed before DTT addition.



**Appendix 1 Figure 4** Spectral course of sulfide oxidation by SQOR in the presence of glutathione and CoQ<sub>1</sub>. The assay was conducted at 25 °C in 100 mM potassium phosphate buffer, pH 8.0, containing 0.5 mM EDTA, 200 μM sulfide, 83 μM CoQ<sub>1</sub>, 1.0 mM glutathione, and 36.2 nM SQOR. Curves 1 to 9 were recorded 1.4, 10, 20, 30, 40, 50, 60, 70, and 120 s, respectively, after sulfide addition.



**Appendix 1 Figure 5** Effect of sulfide concentration on the observed rate of reduction of CoQ<sub>1</sub>. Measurements were made at saturating CoQ<sub>1</sub> (66.2 μM) in 100 mM potassium phosphate buffer, pH 7.0, containing 0.5 mM EDTA at 25 °C. The red line was obtained by fitting a hyperbolic equation ( $k_{\text{cat app}} = k_{\text{cat}}[\text{sulfide}]/(K_m + [\text{sulfide}])$ ) to the data (black circles). The inset shows the corresponding double reciprocal plot. The red line was generated by linear regression analysis of the data ( $r^2 = 0.9443$ )

## Appendix 2: Supplemental Figures and Tables for Chapter 3

**Appendix 2 Table 1 Primers used for PCR reactions**

Reaction	Primers
Amplification of the <i>RDL1</i> gene from <i>S. cerevisiae</i> genomic DNA	5'- GCTAGCCATATGTGGAAGGCCGTGATGAATG-3' 5'- CCTAGAGTATACACTCGAGTAAGTCAAGTTTATCACCC-3'
Ligation-independent cloning of an optimized synthetic gene encoding human TSTD1 isoform 1	5'-AGATTGGTGGCATGGCCGGGCGCCG-3' 5'-GAGGAGAGTTTACTCAGACTCCTTCTCCAG-3'
Ligation-independent cloning of an optimized synthetic gene encoding human TSTD1 isoform 2	5'-AGATTGGTGGCATGGCAGGTGTTAGTG-3' 5'-GAGGAGAGTTTACTCAGGATTCTTTTTCTAAC-3'
Ligation-independent cloning of an optimized synthetic gene encoding human TSTD1 isoform 3	5'-AGATTGGTGGCATGGCCGGAGCCCC-3' 5'-GAGGAGAGTTTACTCAGCGACCTGCTAATAAC-3'
Mutation of Cys98 to Ala in yeast <i>RDL1</i>	5'-GGAGCTAATATTTTATGCTGCTTCTGGCAAACGCG-3' 5'-GCGTTTGCCAGAAGCAGCATAAAATATTAGCTCC-3'
Mutation of Cys98 to Ser in yeast <i>RDL1</i>	5'-GGAGCTAATATTTTATTGTGCTTCTGGCAAACGCG -3' 5'- GCGYYYYGCCAGAAGCACAATAAAATATTAGCTCC-3'
Mutation of Cys79 to Ala in human TSTD1 isoform 1	5'- CATCTGGTTTTTTTCGCACAGATGGGTAAACGC-3' 5'-GCGTTTACCCATCTGTGCGAAAAAACCAGATG-3'
Mutation of Cys79 to Ser in human TSTD1 isoform 1	5'- CATCTGGTTTTTTTCTCTCAGATGGGTAAACGC-3' 5'- GCGTTTACCCATCTGAGAGAAAAAACCAGATG-3'

<b>Appendix 2 Table 2</b> BLASTp Search of the Bacterial Proteomes that Contain SDO-TSTD1 Fusion Proteins Using Human SQOR as the Query Sequence						
Organism (Taxonomy ID)		Highest Scoring Blast Hit				
		GenBank accession number (remarks)	Query Cover (%)	E Value	Identity (%)	Distance (nucleotides) <sup>a</sup>
1	<i>Nitrosococcus oceani</i> (1229)	YP_343998.1	88	4e <sup>-144</sup>	42	73
2	<i>Nitrosococcus watsonii</i> (473531)	YP_003760988.1	88	5e <sup>-111</sup>	42	73
3	<i>Methylocella silvestris</i> (199596)	(no hit obtained)	-	-	-	-
4	<i>Methylobacter tundripaludum</i> (173365)	WP_006892758.1	87	1e <sup>-114</sup>	42	21
5	<i>Methylomicrobium album</i> (39775)	WP_005371245.1	87	4e <sup>-111</sup>	41	45
6	<i>Methyloglobulus morosus</i> (1410681)	WP_023495229.1	86	5e <sup>-115</sup>	42	113
7	<i>Methylocystis rosea</i> (173366)	WP_018406351.1	51	1e <sup>-10</sup>	27	nd
8	<i>Methylosarcina fibrata</i> (105972)	WP_020565271.1	87	7e <sup>-112</sup>	41	246
9	<i>Bradyrhizobiaceae bacterium</i> (709797)	WP_009735658.1	67	0.001	22	nd
10	<i>Afipia broomeae</i> (56946)	WP_006019594.1	65	3e <sup>-6</sup>	22	nd
11	<i>γ-proteobacterium HTCC2148</i> (247634)	(bacterial proteome unavailable)	-	-	-	-
12	<i>Rhizobium giardinii</i> (56731)	WP_018327723.1	86	5e <sup>-90</sup>	35	nd
13	<i>Mesorhizobium amorphae</i> (71433)	WP_006203294.1	79	2e <sup>-23</sup>	26	nd

<sup>a</sup>The indicated distance is determined based on the number of intervening nucleotides between the human SQOR homolog gene and the SDO-TSTD1 fusion protein gene in the bacterial chromosome. Complete genomic data are available only for *N. oceani* and *N. watsonii*. Genomic distances in other bacteria, where whole-genome shotgun contigs are available, could be determined when the genes for the SQOR homolog and the SDO-TSTD1 fusion protein were found in the same contig but not when the genes were located in different contigs (nd).



```
M A G V S E L E S A L Q M E P A A F Q A      20  
atggctggagtggtccgagttggagagtgctctgcagatggagccagctgccttccaggct  
||.|||.|||.|||.|||.|||.|||.|||.|||.|||.|||.|||.|||.|||.|||.|||  
ATGGCAGGTGTTAGTGAATTAGAATCCGCATTACAAATGGAACCGGCAGCATTTCAAGCT  
  
L Y S A E K P K L E D E H L V F F C Q M    40  
ttatattctgctgagaagccaaagctggaagatgagcatctcgttttcttctgtcagatg  
||.|||.|||.|||.|||.|||.|||.|||.|||.|||.|||.|||.|||.|||.|||.|||  
TTATACTCAGCAGAAAAACCGAAATTAGAAGATGAACACTTAGTATTTTTTTGTCAAATG  
  
G K R G L Q A T Q L A R S L G Y T G A R    60  
ggcaagcggggcctccaggccacgcagctggcccggagtcttggatacactggggctcgc  
||.|||.|||.|||.|||.|||.|||.|||.|||.|||.|||.|||.|||.|||.|||.|||  
GGAAAACGTGTTTTACAAGCAACTCAATTAGCACGCTCATTAGGATACACAGGCGCTCGG  
  
N Y A G A Y R E W L E K E S      74  
aactacgctggagcctatagagaatggttggagaaagagagt  
||.|||.|||.|||.|||.|||.|||.|||.|||.|||.|||.|||.|||.|||.|||.|||  
AATTATGCAGGGGCTTATCGCGAATGGTTAGAAAAAGAATCC
```

**Appendix 2 Figure 2** The nucleotide sequence of the synthetic gene used to express recombinant TSTD1 isoform 2 (upper case) is compared with the original gene sequence (lower case). The top line shows the amino acid sequence of isoform 2.

```

M A G A P T V S L P E L R S L L A S G R 20
atggctgggagcgcccacgggtctogcttctctgaactcogttcactcctagcctcgggacgg
|||||.|||||.|||||.|||||.|||||.|||||.|||||.|||||.|||||.|||||.
ATGGCCGGAGCCCTACAGTCTCTTTACCAGAATTACGCTCATTATTAGCATCAGGCCGT

A R L F D V R S R E E A A A G T I P G A 40
gccccggtctt cgacgtgcgctctcgcgaggaggcggcagctgggaccatcccagggcg
|||||.|||||.|||||.|||||.|||||.|||||.|||||.|||||.|||||.|||||.
GCCCGCCTTTTGAOGTACGTTCCCGCGAAGAAGCCGCAGCAGGAACCATCCCCGGAGCT

L N I P V S E L E S A L O M E P A A F O 60
ctcaacatcccgggtgtcgcgagttggagagtgctctcgcagatggagccagctgccttcag
.|.|||||.|||||.|||||.|||||.|||||.|||||.|||||.|||||.|||||.
TTAAACATCCCAGTCTCAGAATTAGAATCAGCATTACAAATGGAACCAGCAGCATTCAA

A L Y S A E K P K L E D E H L V F F C Q 80
gctttatattctgctgagaagccaaagctggaagatgagcatctcgttttcttctgtcag
|||.|||||.|||||.|||||.|||||.|||||.|||||.|||||.|||||.|||||.
GCACTTTACTCCGCOGAAAAACCAAACTTGAAGATGAACACTTAGTATTTTTTTGTCAA

M G K R G L Q A T Q L A R S L G Y T G Y 100
atgggcaagcggggcctccaggccacgcagctggc cgggagctcttggatacactgggtac
|||||.|||||.|||||.|||||.|||||.|||||.|||||.|||||.|||||.|||||.
ATGGGGAAACGTGGTTTACAAGCAACACAATTAGCTCGCAGCTTAGGTTATACAGGATAT

G E V W L L A G R 109
ggggaggtgtggctgctagctgggagg
|||.|||||.|||||.|||||.|||||.
GGAGAAGTTTGGTATTAGCAGGTGCG

```

**Appendix 2 Figure 3** The nucleotide sequence of the synthetic gene used to express recombinant TSTD1 isoform 3 (upper case) is compared with the original gene sequence (lower case). The top line shows the amino acid sequence of isoform 3.



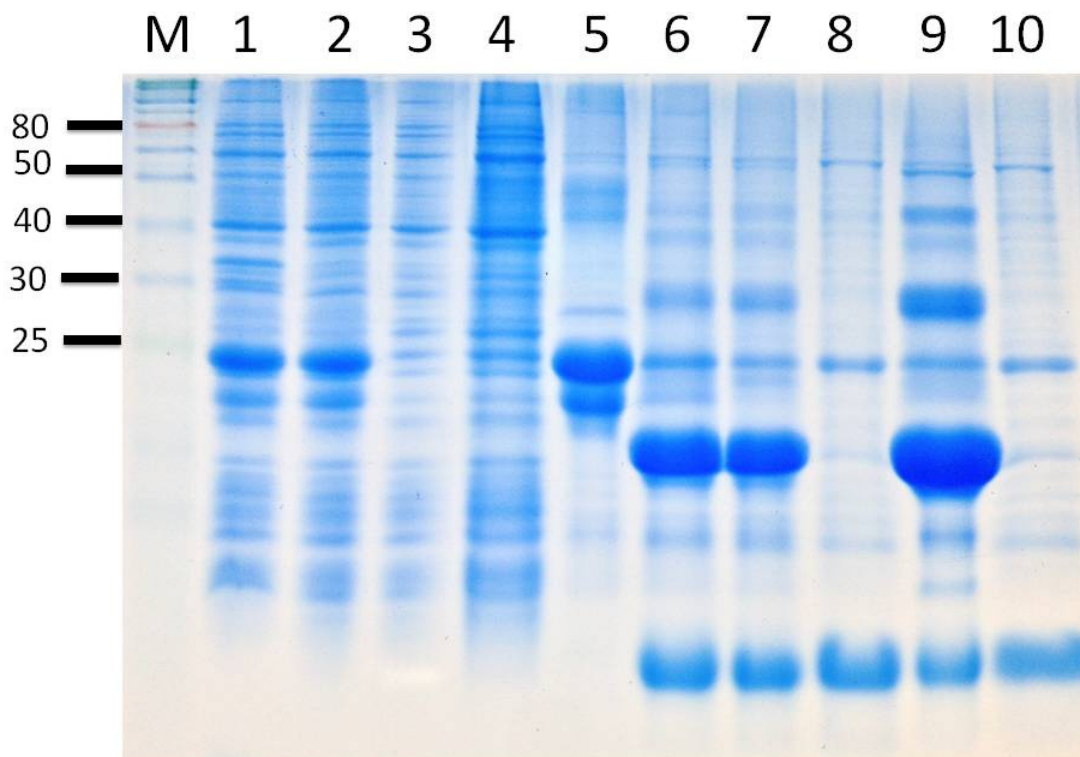
```

1  MAGAPTYVSYLPYELYRSLLASGRARLFDVRSREEAAAGTIPGALNIPYVSELESALQMEPAAFQ 60
3  MAGAPTYVSYLPYELYRSLLASGRARLFDVRSREEAAAGTIPGALNIPYVSELESALQMEPAAFQ 60
2  MAG-----VSELESALQMEPAAFQ 19
   ***                                     *****

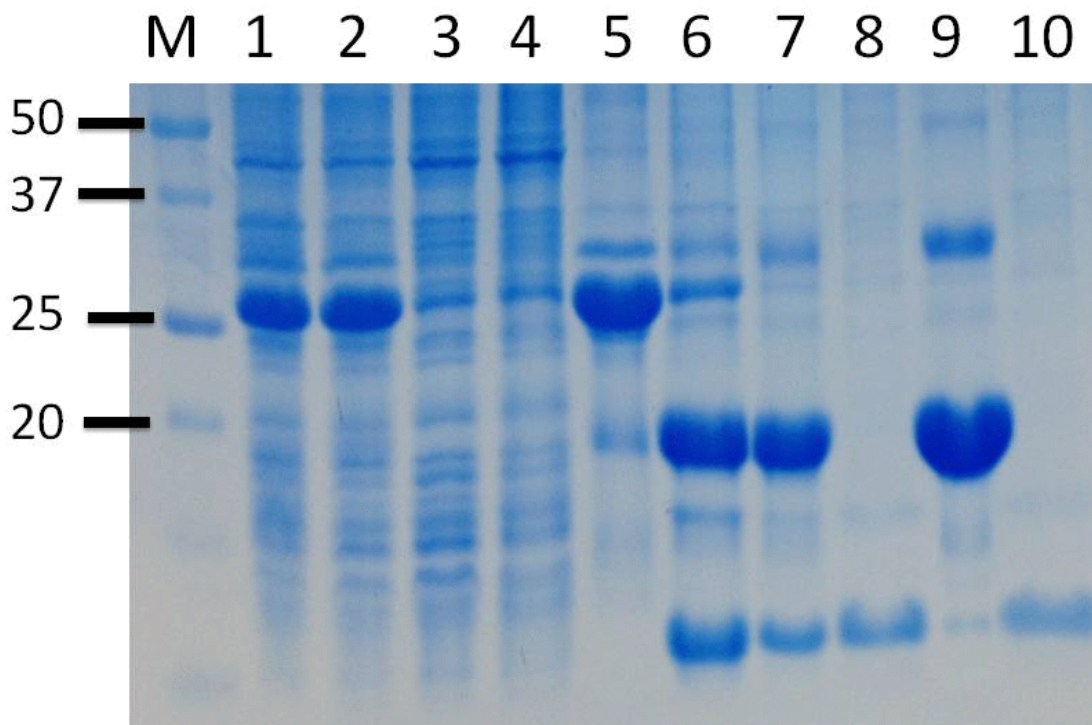
1  ALYSAEKPKLEDEHLVFFCQMGKRGLQATQLARSLGYTYGARNYAGAYREWLEKES 115
3  ALYSAEKPKLEDEHLVFFCQMGKRGLQATQLARSLGYTG-----YGEVWLLAGR 109
2  ALYSAEKPKLEDEHLVFFCQMGKRGLQATQLARSLGYTYGARNYAGAYREWLEKES 74
   *****                                     **

```

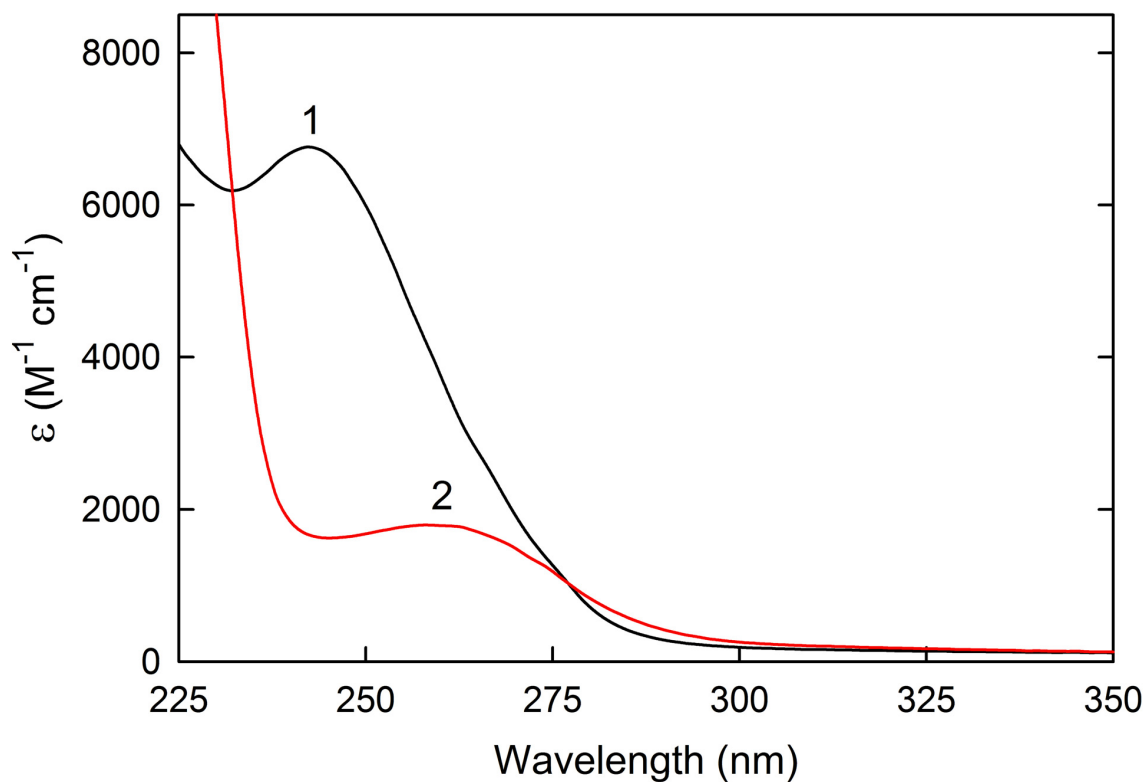
**Appendix 2 Figure 4** Alignment of human TSTD1 isoforms. Amino acids encoded across a splice junction and cysteines are highlighted in yellow and red, respectively. All isoforms contain a tripeptide at the N-terminus and a central core of 55 amino acids that are encoded by exons 1 and 3, respectively. The N-terminal tripeptide in isoforms 1 and 3 is followed by a stretch of 41 amino acids (encoded by exon 2) that is absent in isoform 2. The 16 amino acids at the C-terminus of isoforms 1 and 2 (encoded by exon 4) are replaced by a decapeptide in isoform 3 (encoded by retained intron 3).



**Appendix 2 Figure 5** Purification of recombinant human TSTD1 isoform 2 with a cleavable N-terminal His-SUMO tag. The SDS 15% polyacrylamide gel was stained for protein with ProSieve Blue Protein Staining Solution (Lonza); lane M, molecular markers; lane 1, whole cell lysate; lane 2, low speed supernatant; lane 3, Ni affinity column flow-through; lane 4, Ni affinity column wash; lane 5, Ni affinity column eluate; lane 6, Ni affinity column eluate after cleavage with SUMO hydrolase; lane 7, SUMO hydrolase-treated sample after dialysis; lane 8, second Ni affinity column flow-through; lane 9, second Ni affinity column eluate; lane 10, dialyzed sample from lane 8.



**Appendix 2 Figure 6** Purification of recombinant human TSTD1 isoform 3 with a cleavable N-terminal His- SUMO tag. The SDS 15% polyacrylamide gel was stained for protein with ProSieve Blue Protein Staining Solution (Lonza); lane M, molecular markers; lane 1, whole cell lysate; lane 2, low speed supernatant; lane 3, Ni affinity column flow-through; lane 4, Ni affinity column wash; lane 5, Ni affinity column eluate; lane 6, Ni affinity column eluate after cleavage with SUMO hydrolase; lane 7, SUMO hydrolase-treated sample after dialysis; lane 8, second Ni affinity column flow-through; lane 9, second Ni affinity column eluate; lane 10, dialyzed sample from lane 8.



**Appendix 2 Figure 7** Spectral properties of p-toluenethiosulfonate (p-Tol-SO<sub>2</sub>S<sup>-</sup>) and p-toluenesulfonite (p-Tol-SO<sub>2</sub><sup>-</sup>). Spectra were recorded at 25 EC using a 2 mm cuvette. Curve 1 is the absorption spectrum of p-Tol-SO<sub>2</sub>S<sup>-</sup> in 50 mM potassium/sodium phosphate buffer, pH 8.0, recorded 2 s after addition of 1.6 mM potassium cyanide. Curve 2 is the absorption spectrum of p-Tol-SO<sub>2</sub><sup>-</sup> in the same buffer, recorded 190 s after addition of 60 nM human rhodanese, an enzyme previously shown to catalyze the transfer of the sulfane sulfur from p-Tol-SO<sub>2</sub>S<sup>-</sup> to cyanide (Sorbo, B. (1953) *Acta Chem. Scand.* 7, 32-37).

N. oceani	MIFRQLFDPESSITYTLLIGDPATKEAVFIDPVNTRVDEYLNLLNKYNLKLKYSLETHAHA	60
M. silvestris	MIFRQLFDHVSQTYTYLLASRPGGEALIDPVLEKVDRYLQFLDELDVKLVKAVDTHLHA	60
M. tundripaludum	MLFKQLFDQETWYTYTYLIADPVSKDAILIDPVNTHIDEYIELLAHGLQLKYSLETHVHA	60
M. album	MIFKQLFDPEWTWYTYFIADTDAKEAVLIDPVKSHIDEYIALLDEHGLKLYTLETHVHA	60
M. morosus	MLFKQLFDQETWYTYTYLIADPANKEAVLIDPVNTHIDDYLAMLTEQGLQLKYYTLETHVHA	60
	*:*:**** : ****:.. :*:**** :* * : : :* :*:** *	
N. oceani	DHITASGLLRQHTGAKTGIQACGAQYADYQLKDGVVLAFFGQGEIKVLATPGHTPGSIS	120
M. silvestris	DHVTGLGALDRTHCITVMEQTKADVSMRVADGDRIDIE-GLSLEALFTPGHTDSSYS	119
M. tundripaludum	DHITASGLLRQRLGAQTAVSGLCGAESADIQIQDGDIFKFAGDEQIKVIATPGHTRGSIS	120
M. album	DHITASGLLRQKLGAEETGVQLCGAIGADLQLQDGDVLEFGNGEKIKVIATPGHTQGSVS	120
M. morosus	DHITASGLLRQKLSQTGVGALCGAETADFQMKDGDLSFTNGEQIKVIATPGHTKGSMS	120
	**:* . * ** : . * : . * .. : * : : . : : : **** * *	
N. oceani	YLWRDRVFTGDALLINGCGRTDFQGGDPGLYDSVTQKLFLLPGETIVYPGHYNGRWVS	180
M. silvestris	FLLEGRVFTGDTLLIRGTGRDFQNGDPRAQYHSIFDRLLKLPDETLVYPAHDYKGDTVS	179
M. tundripaludum	FLWRDRVFTGDSLLIGGCGRTDFQGGDAGALYDCITQRLFTLTPDETLYVPGHDYQQRVVS	180
M. album	FLWRDRVFTGDSLFIQGGCGRTDFQSGDAGALYDCITRKLFTLTPDETLYVPGHDYQQRVVS	180
M. morosus	FLWRDRVFTGDSLFIQGGCGRTDFQGGDAGALYDCITQRLFTLTPDDTLVYPGHYQQRVVS	180
	:* . * :****:* * * ***** * * : * .. : * : ** * : * : * : * : *	
N. oceani	SVEQERTGNRRLAGKTRAEFFIEIMNNLNLPKPRLIDEAVPANRRCGLTEEE-----IRQD	238
M. silvestris	TIGERLRFNRLKVRSDVEYVDLNNLNLPNPKMDDVAVPANMRVGFHQDE-----IARKG	239
M. tundripaludum	SIMQERTTNPRLAGKTRQEFIEIMNNLNLPKPRLIDEAVPANRYCGLENERQDAVALRD	240
M. album	SIMQERITNPRLAGKTRAEFFIEIMNNLNLPKPRLIDEAVPANRYCGLEDEDERQDAVARRD	240
M. morosus	NIVQERTTNPRLAGKTRDEFITIMNNLNLPKPKLIDEAVPANRYCGLENERQDAVAHRE	240
	. : * * * * * : : : : * : * : * : * : * : * : * : * : * : * : *	
N. oceani	TMMG-----EKRIVSTPQDLVQEARKQVREIDVATVKQRLGDKTAIID	278
M. silvestris	WAAQ-----AAEALALFGRPDIAIVD	256
M. tundripaludum	A-----SLPVRATTRTEDMVAEAKQHIVEIDVAKSKQLLTGNNVLVD	283
M. album	STR-----PERAMISAQDLVSAAKERITEIGIDKARQLLNQSGVAVVD	283
M. morosus	TVRESAKPGDVPVNCGGMPKSGGMTVQDLVAAKQQITEVNEKAKQLIVQGSITVID	300
	: : * : *	
N. oceani	VREPEEFAA-GHLPGAINVPRGVLEFRLG--NTAELADPNIPILIYCQTGGRALAAS	334
M. silvestris	LREKREREKQGIIPGSLHAPYDRLRESIGPGGALHELAAGKTIIFYCAFGERSAMAVQA	316
M. tundripaludum	TREESEYAA-GHVDGALLVPRGMLEFKIG--NMPELADKSKAVLIYCRNLGRSALAAQT	339
M. album	VRESEYAA-GHIDNALPIPRGVLEFKVG--ATPELADKSKTUVVYCRGTGGRALAASQT	339
M. morosus	TREESEYAA-GHIDNAVLLPRGVLEFRIN--TIPELADKAKPVLIYCRGTGGRALAASQS	356
	** * * : : * * : * * : * * : * * : * * : * * : * * : * * : *	
N. oceani	LKCLGYTDATLIAGGYDAWRAAKQAD-	361
M. silvestris	AQDAGFKSARHIAGGFDAWKKENGAVAP	344
M. tundripaludum	LQQLGYSNVLVSMAGGFDAWKKSQEAE--	365
M. album	LQNLGYSNVLVSIAGGYEAWQKSL-----	362
M. morosus	LKTLGYTNVLSIAGGYETWQKGN-----	379
	: * : * : * : * : * : * : * : * : * : *	

**Appendix 2 Figure 8** Multiple sequence alignment of selected SDO-TSTD1 bacterial fusion proteins. The black box marks a poorly conserved, variable length linker (9 to 52 amino acids) between the N-terminal SDO-like domain (230 or 231 amino acids) and the C-terminal TSTD1-like domain (96 to 105 amino acids). GenBank accession numbers: *Nitrosococcus oceani* (WP\_013220760.1); *Methylocella silvestris* (WP\_012591638.1); *Methylobacter tundripaludum* (WP\_006892756.1); *Methylomicrobium album* (WP\_005371248.1); *Methyloglobulus morosus* (WP\_023495230.1).







**A N R R C G L T E E E I R Q D T M M G E** 720  
gcaaataggcgctgtggcttaaccgaggaagaaattcgccaggatactatgatgggcgag  
|||||.|.|.|.|.|.|.|.|.|.|.|.|.|.|.|.|.|.|.|.|.|.|.|.|.|.|.|.  
GCAAATCGCCGTTGCGGTCTGACCGAAGAAGAGATTCGCCAGGACACCATGATGGGCGAA

**K R V S T P Q D L V Q E A R K Q V R E I** 780  
aaacgcgtcagcagccacaggatttagtacaggaggccaggaagcagggtccgtgaaatt  
|||||.|.|.|.|.|.|.|.|.|.|.|.|.|.|.|.|.|.|.|.|.|.|.|.|.|.|.|.  
AAACGCGTTAGTACCCCGCAGGATCTGGTGCGGAAGCACGCAAACAAGTGCCTGAGATC

**D V A T V K Q R L G D G K T A I I D V R** 840  
gacgttgccaccggtgaagcaaaggtggcgatggtaaaacagccatcattgatgtgcgg  
||.|.|.|.|.|.|.|.|.|.|.|.|.|.|.|.|.|.|.|.|.|.|.|.|.|.|.|.|.  
GATGTTGCCACCGTGAAACAGCGTCTGGGTGATGGCAAACCGCCATTATCGACGTGCGT

**E P E E F A A G H L P G A I N V P R G V** 900  
gagcgggaagaattcgcgggcggtcatctgcctggcgctatcaatgtaccacgtgggtg  
|||||.|.|.|.|.|.|.|.|.|.|.|.|.|.|.|.|.|.|.|.|.|.|.|.|.|.|.|.  
GAGCCGGAAGAATTTGCCCGCAGGCCATCTGCCGGGTGCCATTAATGTGCCCGTGCTGTT

**L E F R L G N T A E L A D P N I P I I L** 960  
ttagagtttgccttaggtaataactgaggagctggctgacctaataatccctattattctg  
.|.|.|.|.|.|.|.|.|.|.|.|.|.|.|.|.|.|.|.|.|.|.|.|.|.|.|.|.|.  
CTGGAATTTGCGCTGGGCAACACCGCCGAACACTGGCCGATCCGAATATTCCGATTATTCTG

**Y C Q T G G R A A L A A W S L K C L G Y** 1020  
tactgccaacaggtgggcgcgagcattggctgcctggctcgctcaaatgccttgggtat  
|||||.|.|.|.|.|.|.|.|.|.|.|.|.|.|.|.|.|.|.|.|.|.|.|.|.|.|.|.  
TACTGCCAGACAGGTGGCCGCGCCGATTAGCAGCCTGGAGCCTGAAATGCTTAGGCTAT

**T D A T L I A G G Y D A W R A A K Q N A D** 1083  
actgatgcaacgctaataagcggggcggttatgacgcatggcgagcagccaagcagaacgctgat  
||.|.|.|.|.|.|.|.|.|.|.|.|.|.|.|.|.|.|.|.|.|.|.|.|.|.|.|.|.|.  
ACCGATGCCACCCTGATTGCGGGGTTATGATGCGCTGGCGTCCCGCAAACAGAATGCCGAT

**Appendix 3 Figure 1** The nucleotide sequence of the synthetic gene used to express recombinant Noc\_2007 (upper case) is compared with the original gene sequence (lower case). The top line shows the amino acid sequence of Noc\_2007.



### List of References

1. Kabil, O, Banerjee, R. Redox biochemistry of hydrogen sulfide. *J. Biol. Chem.* 2010; 285: 21903-21907.
2. Hancock, JT, Whiteman, M. Hydrogen sulfide and cell signaling: Team player or referee? *Plant Physiology and Biochemistry.* 2014; 78: 37-42.
3. Gunina, A. The metabolism of hydrogen sulfide ( $\text{H}_2\text{S}^{35}$ ) injected subcutaneously. *Bulletin of Experimental Biology and Medicine.* 1957; 43: 176-179.
4. Beauchamp, R, Bus, JS, Popp, JA, Boreiko, CJ, Andjelkovich, DA, Leber, P. A critical review of the literature on hydrogen sulfide toxicity. *Crit Rev Toxicol.* 1984; 13: 25-97.
5. Garrett, RM, Johnson, JL, Graf, TN, Feigenbaum, A, Rajagopalan, K. Human sulfite oxidase R160Q: identification of the mutation in a sulfite oxidase-deficient patient and expression and characterization of the mutant enzyme. *PNAS.* 1998; 95: 6394-6398.
6. Szabó, C. Hydrogen sulphide and its therapeutic potential. *Nature Reviews Drug Discovery.* 2007; 6: 917-935.
7. Koj, A, Frendo, J, Janik, Z. [ $^{35}\text{S}$ ]Thiosulphate oxidation by rat liver mitochondria in the presence of glutathione. *Biochem. J.* 1967; 103: 791-795.
8. Szczepkowski, TW, Skarzynski, B., and Weber, M. . The metabolic state of thiosulphate. *Nature.* 1961; 198: 1007-1008.
9. Bartholomew, TC, Dodgson, KS, Curtis, CG. Oxidation of sodium sulphide by rat liver, lungs and kidney. *Biochem. Pharm.* 1980; 29: 2431-2437.
10. Sorbo, B. On the metabolism of thiosulfate esters. *Acta chem. scand.* 1958; 12: 1990-1996.

11. Völkel, S, Grieshaber, M. Oxygen dependent sulfide detoxification in the lugworm *Arenicola marina*. *Mar Biol.* 1994; 118: 137-147.
12. Levitt, MD, Furne, J, Springfield, J, Suarez, F, DeMaster, E. Detoxification of hydrogen sulfide and methanethiol in the cecal mucosa. *J Clin Invest.* 1999; 104: 1107-1114.
13. Furne, J, Springfield, J, Koenig, T, DeMaster, E, Levitt, MD. Oxidation of hydrogen sulfide and methanethiol to thiosulfate by rat tissues: a specialized function of the colonic mucosa. *Biochem. Pharm.* 2001; 62: 255-259.
14. Hildebrandt, TM, Grieshaber, MK. Three enzymatic activities catalyze the oxidation of sulfide to thiosulfate in mammalian and invertebrate mitochondria. *FEBS J.* 2008; 275: 3352-3361.
15. Marcia, M, Ermler, U, Peng, G, Michel, H. A new structure-based classification of sulfide:quinone oxidoreductases. *Proteins.* 2010; 78: 1073-1083.
16. Lagoutte, E, Mimoun, S, Andriamihaja, M, Chaumontet, C, Blachier, F, Bouillaud, F. Oxidation of hydrogen sulfide remains a priority in mammalian cells and causes reverse electron transfer in colonocytes. *Biochimica et Biophysica Acta (BBA)-Bioenergetics.* 2010; 1797: 1500-1511.
17. Powell, MA, Somero, GN. Hydrogen sulfide oxidation is coupled to oxidative phosphorylation in mitochondria of *Solemya reidi*. *Science.* 1986; 233: 563-566.
18. Shahak, Y, Hauska, G. Sulfide oxidation from cyanobacteria to humans: sulfide:quinone oxidoreductase (SQR). *Advances in Photosynthesis and Respiration* Springer; 2008. p. 319-335.
19. Theissen, U, Martin, W. Sulfide: quinone oxidoreductase (SQR) from the lugworm *Arenicola marina* shows cyanide- and thioredoxin-dependent activity. *FEBS J.* 2008; 275: 1131-1139.
20. Sorbo, B. Rhodanese. *Methods Enzymol.* 1955; 2: 334-337.
21. Kabil, O, Banerjee, R. Characterization of patient mutations in human persulfide dioxygenase (ETHE1) involved in H<sub>2</sub>S catabolism. *J. Biol. Chem.* 2012; 287: 44561-44567.

22. Tiranti, V, Viscomi, C, Hildebrandt, T, Di Meo, I, Mineri, R, Tiveron, C, Levitt, MD, Prella, A, Fagiolari, G, Rimoldi, M. Loss of ETHE1, a mitochondrial dioxygenase, causes fatal sulfide toxicity in ethylmalonic encephalopathy. *Nat. Med.* 2009; 15: 200-205.
  
23. Hegg, EL. The 2-His-1-Carboxylate Facial Triad—An Emerging Structural Motif in Mononuclear Non-Heme Iron (II) Enzymes. *Eur J Biochem.* 1997; 250: 625-629.
  
24. Koehntop, KD, Emerson, JP, Que Jr, L. The 2-His-1-carboxylate facial triad: a versatile platform for dioxygen activation by mononuclear non-heme iron (II) enzymes. *J. Biol. Inorg. Chem.* 2005; 10: 87-93.
  
25. Tiranti, V, D'Adamo, P, Briem, E, Ferrari, G, Mineri, R, Lamantea, E, Mandel, H, Balestri, P, Garcia-Silva, M-T, Vollmer, B. Ethylmalonic encephalopathy is caused by mutations in ETHE1, a gene encoding a mitochondrial matrix protein. *Am J Hum Genet.* 2004; 74: 239-252.
  
26. Rohwerder, T, Sand, W. The sulfane sulfur of persulfides is the actual substrate of the sulfur-oxidizing enzymes from *Acidithiobacillus* and *Acidiphilium* spp. *Microbiology.* 2003; 149: 1699-1710.
  
27. Rohwerder, T, Sand, W. Oxidation of inorganic sulfur compounds in acidophilic prokaryotes. *Engineering in Life Sciences.* 2007; 7: 301-309.
  
28. Arieli, B, Shahak, Y, Taglicht, D, Hauska, G, Padan, E. Purification and characterization of sulfide-quinone reductase, a novel enzyme driving anoxygenic photosynthesis in *Oscillatoria limnetica*. *J. Biol. Chem.* 1994; 269: 5705-5711.
  
29. Arieli, B, Padan, E, Shahak, Y. Sulfide-induced sulfide-quinone reductase activity in thylakoids of *Oscillatoria limnetica*. *J. Biol. Chem.* 1991; 266: 104-111.
  
30. Shahak, Y, Arieli, B, Binder, B, Padan, E. Sulfide-dependent photosynthetic electron flow coupled to proton translocation in thylakoids of the cyanobacterium *Oscillatoria limnetica*. *Arch. Biochem. Biophys.* 1987; 259: 605-615.
  
31. Weghe, JGV, Ow, DW. A fission yeast gene for mitochondrial sulfide oxidation. *J. Biol. Chem.* 1999; 274: 13250-13257.

32. Brito, JA, Sousa, FL, Stelter, M, Bandejas, TM, Vorrhein, C, Teixeira, M, Pereira, MM, Archer, M. Structural and functional insights into sulfide: quinone oxidoreductase. *Biochemistry*. 2009; 48: 5613-5622.
  
33. Cherney, MM, Zhang, Y, Solomonson, M, Weiner, JH, James, MN. Crystal Structure of Sulfide: Quinone Oxidoreductase from *Acidithiobacillus ferrooxidans*: Insights into Sulfidotrophic Respiration and Detoxification. *J. Mol. Biol.* 2010; 398: 292-305.
  
34. Marcia, M, Ermler, U, Peng, G, Michel, H. The structure of Aquifex aeolicus sulfide: quinone oxidoreductase, a basis to understand sulfide detoxification and respiration. *PNAS*. 2009; 106: 9625-9630.
  
35. Heuts, DP, Scrutton, NS, McIntire, WS, Fraaije, MW. What's in a covalent bond? *FEBS J.* 2009; 276: 3405-3427.
  
36. Argyrou, A, Blanchard, JS. Flavoprotein disulfide reductases: advances in chemistry and function. *Prog Nucleic Acid Res Mol Biol.* 2004; 78: 89-142.
  
37. Theissen, U, Hoffmeister, M, Grieshaber, M, Martin, W. Single eubacterial origin of eukaryotic sulfide: quinone oxidoreductase, a mitochondrial enzyme conserved from the early evolution of eukaryotes during anoxic and sulfidic times. *Molecular biology and evolution*. 2003; 20: 1564-1574.
  
38. Pham, VH, Yong, J-J, Park, S-J, Yoon, D-N, Chung, W-H, Rhee, S-K. Molecular analysis of the diversity of the sulfide: quinone reductase (sqr) gene in sediment environments. *Microbiology*. 2008; 154: 3112-3121.
  
39. Shibata, H, Kobayashi, S. Characterization of a HMT2-like enzyme for sulfide oxidation from *Pseudomonas putida*. *Canadian journal of microbiology*. 2006; 52: 724-730.
  
40. Shibata, H, Suzuki, K, Kobayashi, S. Menaquinone reduction by an HMT2-like sulfide dehydrogenase from *Bacillus stearothermophilus*. *Canadian journal of microbiology*. 2007; 53: 1091-1100.
  
41. Griesbeck, C, Schütz, M, Schödl, T, Bathe, S, Nausch, L, Mederer, N, Vielreicher, M, Hauska, G. Mechanism of sulfide-quinone reductase investigated using site-directed mutagenesis and sulfur analysis. *Biochemistry*. 2002; 41: 11552-11565.

42. Wakai, S, Tsujita, M, Kikumoto, M, Manchur, MA, Kanao, T, Kamimura, K. Purification and characterization of sulfide: quinone oxidoreductase from an acidophilic iron-oxidizing bacterium, *Acidithiobacillus ferrooxidans*. *Biosci Biotechnol Biochem*. 2007; 71: 2735-2742.
43. Chan, L-K, Morgan-Kiss, RM, Hanson, TE. Functional analysis of three sulfide: quinone oxidoreductase homologs in *Chlorobaculum tepidum*. *J Bacteriol*. 2009; 191: 1026-1034.
44. Zhang, Y, Cherney, MM, Solomonson, M, Liu, J, James, MN, Weiner, JH. Preliminary X-ray crystallographic analysis of sulfide: quinone oxidoreductase from *Acidithiobacillus ferrooxidans*. *Acta Crystallographica Section F: Structural Biology and Crystallization Communications*. 2009; 65: 839-842.
45. Zhang, Y, Weiner, JH. Characterization of the kinetics and electron paramagnetic resonance spectroscopic properties of *Acidithiobacillus ferrooxidans* sulfide: quinone oxidoreductase (SQR). *Arch. Biochem. Biophys*. 2014; 564: 110-119.
46. Nübel, T, Klughammer, C, Huber, R, Hauska, G, Schütz, M. Sulfide: quinone oxidoreductase in membranes of the hyperthermophilic bacterium *Aquifex aeolicus* (VF5). *Archives of microbiology*. 2000; 173: 233-244.
47. Kelly, DP. Thermodynamic aspects of energy conservation by chemolithotrophic sulfur bacteria in relation to the sulfur oxidation pathways. *Archives of Microbiology*. 1999; 171: 219-229.
48. Wakai, S, Kikumoto, M, Kanao, T, Kamimura, K. Involvement of sulfide: quinone oxidoreductase in sulfur oxidation of an acidophilic iron-oxidizing bacterium, *Acidithiobacillus ferrooxidans* NASF-1. *Biosci Biotechnol Biochem*. 2004; 68: 2519-2528.
49. Marcia, M, Langer, JD, Parcej, D, Vogel, V, Peng, G, Michel, H. Characterizing a monotopic membrane enzyme. Biochemical, enzymatic and crystallization studies on *Aquifex aeolicus* sulfide: quinone oxidoreductase. *Biochimica et Biophysica Acta (BBA)-Biomembranes*. 2010; 1798: 2114-2123.
50. Peng, G, Fritsch, G, Zickermann, V, Schägger, H, Mentele, R, Lottspeich, F, Bostina, M, Radermacher, M, Huber, R, Stetter, KO. Isolation, characterization and electron microscopic single particle analysis of the NADH: ubiquinone oxidoreductase

(complex I) from the hyperthermophilic eubacterium *Aquifex aeolicus*. *Biochemistry*. 2003; 42: 3032-3039.

51. Marcia, M. Functional and structural characterization of *Aquifex aeolicus* sulfide: quinone oxidoreductase: Johann Wolfgang Goethe Universität 2010.
52. Zillig, W, Yeats, S, Holz, I, Böck, A, Rettenberger, M, Gropp, F, Simon, G. *Desulfurolobus ambivalens*, gen. nov., sp. nov., an autotrophic archaebacterium facultatively oxidizing or reducing sulfur. *Systematic and Applied Microbiology*. 1986; 8: 197-203.
53. Gomes, CM, Backgren, C, Teixeira, M, Puustinen, A, Verkhovskaya, ML, Wikström, M, Verkhovsky, MI. Heme-copper oxidases with modified D-and K-pathways are yet efficient proton pumps. *FEBS letters*. 2001; 497: 159-164.
54. Gomes, CM, Bandejas, TM, Teixeira, M. A new type-II NADH dehydrogenase from the archaeon *Acidianus ambivalens*: characterization and in vitro reconstitution of the respiratory chain. *Journal of bioenergetics and biomembranes*. 2001; 33: 1-8.
55. Müller, FH, Bandejas, TM, Urich, T, Teixeira, M, Gomes, CM, Kletzin, A. Coupling of the pathway of sulphur oxidation to dioxygen reduction: characterization of a novel membrane-bound thiosulphate: quinone oxidoreductase. *Mol Microbiol*. 2004; 53: 1147-1160.
56. Brito, JA, Bandejas, TM, Teixeira, M, Vorrhein, C, Archer, M. Crystallisation and preliminary structure determination of a NADH: quinone oxidoreductase from the extremophile *Acidianus ambivalens*. *Biochimica et Biophysica Acta (BBA)-Proteins and Proteomics*. 2006; 1764: 842-845.
57. Steudel, R. Mechanism for the formation of elemental sulfur from aqueous sulfide in chemical and microbiological desulfurization processes. *Industrial & engineering chemistry research*. 1996; 35: 1417-1423.
58. van Gemerden, H. Production of elemental sulfur by green and purple sulfur bacteria. *Archives of microbiology*. 1986; 146: 52-56.
59. Shahak, Y, Klughammer, C, Schreiber, U, Padan, E, Herrman, I, Hauska, G. Sulfide-quinone and sulfide-cytochrome reduction in *Rhodobacter capsulatus*. *Photosynthesis research*. 1994; 39: 175-181.

60. Brune, DC. Sulfur oxidation by phototrophic bacteria. *Biochimica et Biophysica Acta (BBA)-Bioenergetics*. 1989; 975: 189-221.
61. Schütz, M, Maldener, I, Griesbeck, C, Hauska, G. Sulfide-quinone reductase from *Rhodobacter capsulatus*: requirement for growth, periplasmic localization, and extension of gene sequence analysis. *J Bacteriol*. 1999; 181: 6516-6523.
62. Driessche, GV, Koh, M, Van Beeumen, JJ, Chen, ZW, Mathews, FS, Meyer, TE, Bartsch, RG, Cusanovich, MA. Covalent structure of the flavoprotein subunit of the flavocytochrome c: sulfide dehydrogenase from the purple phototrophic bacterium *Chromatium vinosum*. *Protein science*. 1996; 5: 1753-1764.
63. Rich, P, Heathcote, P. Quinone binding sites in membrane proteins: structure, function and applied aspects: Portland Press; 1999.
64. Bronstein, M, Schütz, M, Hauska, G, Padan, E, Shahak, Y. Cyanobacterial sulfide-quinone reductase: cloning and heterologous expression. *J Bacteriol*. 2000; 182: 3336-3344.
65. Coorevits, A, Dinsdale, AE, Halket, G, Lebbe, L, De Vos, P, Van Landschoot, A, Logan, NA. Taxonomic revision of the genus *Geobacillus*: emendation of *Geobacillus*, *G. stearothermophilus*, *G. jurassicus*, *G. toebii*, *G. thermodenitrificans* and *G. thermoglucosidans* (nom. corrig., formerly 'thermoglucosidasius'); transfer of *Bacillus thermantarcticus* to the genus as *G. thermantarcticus* comb. nov.; proposal of *Caldibacillus debilis* gen. nov., comb. nov.; transfer of *G. tepidamans* to *Anoxybacillus* as *A. tepidamans* comb. nov.; and proposal of *Anoxybacillus caldiproteolyticus* sp. nov. *International journal of systematic and evolutionary microbiology*. 2012; 62: 1470-1485.
66. Nazina, T, Tourova, T, Poltarau, A, Novikova, E, Grigoryan, A, Ivanova, A, Lysenko, A, Petrunyaka, V, Osipov, G, Belyaev, S. Taxonomic study of aerobic thermophilic bacilli: descriptions of *Geobacillus subterraneus* gen. nov., sp. nov. and *Geobacillus uzenensis* sp. nov. from petroleum reservoirs and transfer of *Bacillus stearothermophilus*, *Bacillus thermocatenulatus*, *Bacillus thermoleovorans*, *Bacillus kaustophilus*, *Bacillus thermodenitrificans* to *Geobacillus* as the new combinations *G. stearothermophilus*, *G. th*. *International Journal of Systematic and Evolutionary Microbiology*. 2001; 51: 433-446.
67. Chung, YC, Huang, C, Tseng, CP. Biodegradation of Hydrogen Sulfide by a Laboratory-Scale Immobilized *Pseudomonas putida* CH11 Biofilter. *Biotechnology Progress*. 1996; 12: 773-778.

68. Vande Weghe, JG, Ow, DW. Accumulation of metal-binding peptides in fission yeast requires hmt2+. *Mol Microbiol.* 2001; 42: 29-36.
69. Völkel, S, Grieshaber, MK. Mitochondrial sulfide oxidation in *Arenicola marina*. *Eur J Biochem.* 1996; 235: 231-237.
70. Mustafa, AK, Gadalla, MM, Sen, N, Kim, S, Mu, W, Gazi, SK, Barrow, RK, Yang, G, Wang, R, Snyder, SH. H<sub>2</sub>S signals through protein S-sulfhydration. *Sci. Signaling.* 2009; 2: ra72.
71. Sen, N, Paul, BD, Gadalla, MM, Mustafa, AK, Sen, T, Xu, R, Kim, S, Snyder, SH. Hydrogen Sulfide-Linked Sulfhydration of NF- $\kappa$ B Mediates Its Antiapoptotic Actions. *Mol Cell.* 2012; 45: 13-24.
72. Mustafa, AK, Sikka, G, Gazi, SK, Stepan, J, Jung, SM, Bhunia, AK, Barodka, VM, Gazi, FK, Barrow, RK, Wang, R. Hydrogen Sulfide as Endothelium-Derived Hyperpolarizing Factor Sulfhydrates Potassium Channels. *Circ Res.* 2011; 109: 1259-1268.
73. Krishnan, N, Fu, C, Pappin, DJ, Tonks, NK. H<sub>2</sub>S-Induced sulfhydration of the phosphatase PTP1B and its role in the endoplasmic reticulum stress response. *Science Signalling.* 2011; 4: ra86.
74. Nichols, CG. KATP channels as molecular sensors of cellular metabolism. *Nature.* 2006; 440: 470-476.
75. Weber, RE, Vinogradov, SN. Nonvertebrate hemoglobins: functions and molecular adaptations. *Physiol Rev.* 2001; 81: 569-628.
76. Suzuki, T, Takagi, T, Ohta, S. Primary structure of a constituent polypeptide chain (AIII) of the giant haemoglobin from the deep-sea tube worm *Lamellibrachia*. A possible H<sub>2</sub>S-binding site. *Biochem. J.* 1990; 266: 221-225.
77. Nagy, P. Mechanistic Chemical Perspective of Hydrogen Sulfide Signaling. *Methods Enzymol.* 2015; 554: 3-29.
78. Babidge, W, Millard, S, Roediger, W. Sulfides impair short chain fatty acid beta-oxidation at acyl-CoA dehydrogenase level in colonocytes: Implications for ulcerative colitis. *Mol. Cell Biochem.* 1998; 181: 117-124.



79. Rowan, F, Docherty, N, Coffey, J, O'Connell, P. Sulphate-reducing bacteria and hydrogen sulphide in the aetiology of ulcerative colitis. *Br. J. Surg.* 2009; 96: 151-158.
80. Fite, A, Macfarlane, G, Cummings, J, Hopkins, M, Kong, S, Furrie, E, Macfarlane, S. Identification and quantitation of mucosal and faecal desulfovibrios using real time polymerase chain reaction. *Gut.* 2004; 53: 523-529.
81. Ichinohe, A, Kanaumi, T, Takashima, S, Enokido, Y, Nagai, Y, Kimura, H. Cystathionine  $\beta$ -synthase is enriched in the brains of Down's patients. *Biochem. Biophys. Res. Commun.* 2005; 338: 1547-1550.
82. Kamoun, P, Belardinelli, M-C, Chabli, A, Lallouchi, K, Chadeaux-Vekemans, B. Endogenous hydrogen sulfide overproduction in Down syndrome. *Am J Med Genet Part A.* 2003; 116: 310-311.
83. Belardinelli, M-C, Chabli, A, Chadeaux-Vekemans, B, Kamoun, P. Urinary sulfur compounds in Down syndrome. *Clin Chem.* 2001; 47: 1500-1501.
84. Ichinohe, A, Kanaumi, T, Takashima, S, Enokido, Y, Nagai, Y, Kimura, H. Cystathionine beta-synthase is enriched in the brains of Down syndrome patients. *Biochem. Biophys. Res. Commun.* 2005; 338: 1547-1550.
85. Kamoun, P. Mental retardation in Down syndrome: a hydrogen sulfide hypothesis. *Med Hypotheses.* 2001; 57: 389-392.
86. Selkoe, DJ. Alzheimer's disease is a synaptic failure. *Science.* 2002; 298: 789-791.
87. Malenka, RC, Bear, MF. LTP and LTD: an embarrassment of riches. *Neuron.* 2004; 44: 5-21.
88. Kimura, H. Hydrogen sulfide induces cyclic AMP and modulates the NMDA receptor. *Biochem. Biophys. Res. Commun.* 2000; 267: 129-133.
89. Abe, K, Kimura, H. The possible role of hydrogen sulfide as an endogenous neuromodulator. *J Neurosci.* 1996; 16: 1066-1071.

90. Lee, M, Schwab, C, Yu, S, McGeer, E, McGeer, PL. Astrocytes produce the antiinflammatory and neuroprotective agent hydrogen sulfide. *Neurobiol Aging*. 2009; 30: 1523-1534.
91. Eto, K, Asada, T, Arima, K, Makifuchi, T, Kimura, H. Brain hydrogen sulfide is severely decreased in Alzheimer's disease. *Biochem. Biophys. Res. Commun*. 2002; 293: 1485-1488.
92. Giuliani, D, Ottani, A, Zaffe, D, Galantucci, M, Strinati, F, Lodi, R, Guarini, S. Hydrogen sulfide slows down progression of experimental Alzheimer's disease by targeting multiple pathophysiological mechanisms. *Neurobiology of learning and memory*. 2013; 104: 82-91.
93. Zhang, X, Bian, J-S. Hydrogen sulfide: A neuromodulator and neuroprotectant in the central nervous system. *ACS Chem. Neurosci*. 2014; 5: 876-883.
94. Kimura, H. Hydrogen sulfide as a neuromodulator. *Mol. Neurobiol*. 2002; 26: 13-19.
95. Yang, G, Wu, L, Jiang, B, Yang, W, Qi, J, Cao, K, Meng, Q, Mustafa, AK, Mu, W, Zhang, S. H<sub>2</sub>S as a physiologic vasorelaxant: Hypertension in mice with deletion of cystathionine gamma-lyase. *Sci STKE*. 2008; 322: 587-590.
96. Predmore, BL, Lefer, DJ. Hydrogen sulfide-mediated myocardial pre-and post-conditioning. *Expert Rev Clin Pharmacol*. 2011; 4: 83-96.
97. Papapetropoulos, A, Pyriochou, A, Altaany, Z, Yang, G, Marazioti, A, Zhou, Z, Jeschke, MG, Branski, LK, Herndon, DN, Wang, R. Hydrogen sulfide is an endogenous stimulator of angiogenesis. *PNAS*. 2009; 106: 21972-21977.
98. Lynn, EG, Austin, RC. Hydrogen sulfide in the pathogenesis of atherosclerosis and its therapeutic potential. *Expert Rev Clin Pharmacol*. 2011; 4: 97-108.
99. Yan, H, Du, J, Tang, C. The possible role of hydrogen sulfide on the pathogenesis of spontaneous hypertension in rats. *Biochem. Biophys. Res. Commun*. 2004; 313: 22-27.
100. Elrod, JW, Calvert, JW, Morrison, J, Doeller, JE, Kraus, DW, Tao, L, Jiao, X, Scalia, R, Kiss, L, Szabo, C. Hydrogen sulfide attenuates myocardial ischemia-

reperfusion injury by preservation of mitochondrial function. *PNAS*. 2007; 104: 15560-15565.

101. Lobb, I, Davison, M, Lan, Z, Jian, J, Sener, A. P31 Hydrogen sulfide treatment improves graft function and survival following prolonged cold ischemia and allogeneic renal transplantation. *Nitric Oxide*. 2014; 39: S25.

102. Xie, H, Xu, Q, Jia, J, Ao, G, Sun, Y, Hu, L, Alkayed, NJ, Wang, C, Cheng, J. Hydrogen sulfide protects against myocardial ischemia and reperfusion injury by activating AMP-activated protein kinase to restore autophagic flux. *Biochem. Biophys. Res. Commun*. 2015.

103. Zhao, W, Ndisang, JF, Wang, R. Modulation of endogenous production of H<sub>2</sub>S in rat tissues. *Can J Physiol Pharmacol*. 2003; 81: 848-853.

104. Zhao, W, Zhang, J, Lu, Y, Wang, R. The vasorelaxant effect of H<sub>2</sub>S as a novel endogenous gaseous K<sub>ATP</sub> channel opener. *The EMBO journal*. 2001; 20: 6008-6016.

105. Cheng, Y, Ndisang, JF, Tang, G, Cao, K, Wang, R. Hydrogen sulfide-induced relaxation of resistance mesenteric artery beds of rats. *Am J Physiol Heart Circ Physiol*. 2004; 287: H2316-H2323.

106. Liu, MYH, Lu, MM, Hu, LF, Wong, PTH, Webb, GD, Bian, JS. Hydrogen sulfide in the mammalian cardiovascular system. *Antioxid. Redox Signaling*. 2012; 17: 141-185.

107. Cai, W-J, Wang, M-J, Moore, PK, Jin, H-M, Yao, T, Zhu, Y-C. The novel proangiogenic effect of hydrogen sulfide is dependent on Akt phosphorylation. *Cardiovasc Res*. 2007; 76: 29-40.

108. Mani, S, Li, H, Untereiner, A, Wu, L, Yang, G, Austin, RC, Dickhout, JG, Lhoták, Š, Meng, QH, Wang, R. Decreased endogenous production of hydrogen sulfide accelerates atherosclerosis. *Circulation*. 2013; 127: 2523-2534.

109. Xu, S, Liu, Z, Liu, P. Targeting hydrogen sulfide as a promising therapeutic strategy for atherosclerosis. *Int J Cardiol*. 2014; 172: 313-317.

110. Mani, S, Untereiner, A, Wu, L, Wang, R. Hydrogen sulfide and the pathogenesis of atherosclerosis. *Antioxid. Redox Signaling*. 2014; 20: 805-817.

111. Peng, YJ, Nanduri, J, Raghuraman, G, Souvannakitti, D, Gadalla, MM, Kumar, GK, Snyder, SH, Prabhakar, NR. H<sub>2</sub>S mediates O<sub>2</sub> sensing in the carotid body. PNAS. 2010; 107: 10719-10724.
112. Li, Q, Sun, B, Wang, X, Jin, Z, Zhou, Y, Dong, L, Jiang, L-H, Rong, W. A crucial role for hydrogen sulfide in oxygen sensing via modulating large conductance calcium-activated potassium channels. Antioxid. Redox Signaling. 2010; 12: 1179-1189.
113. Prabhakar, NR. Oxygen sensing by the carotid body chemoreceptors. J Appl Physiol. 2000; 88: 2287-2295.
114. Olson, KR. Hydrogen sulfide as an oxygen sensor. Clin Chem Lab Med. 2013; 51: 623-632.
115. Lee, Z-W, Teo, X-Y, Moore, PK, Tan, C-H, Deng, L-W. P18 Effects of hydrogen sulfide on cancer cell growth and metastasis. Nitric Oxide. 2014; 39: S21.
116. Lee, ZW, Teo, XY, Tay, EW, Tan, CH, Hagen, T, Moore, P, Deng, LW. Utilizing hydrogen sulfide as a novel anti-cancer agent by targeting cancer glycolysis and pH imbalance. Br J Pharmacol. 2014; 171: 4322-4336.
117. Szabo, C, Coletta, C, Chao, C, Módis, K, Szczesny, B, Papapetropoulos, A, Hellmich, MR. Tumor-derived hydrogen sulfide, produced by cystathionine- $\beta$ -synthase, stimulates bioenergetics, cell proliferation, and angiogenesis in colon cancer. PNAS. 2013; 110: 12474-12479.
118. Chattopadhyay, M, Kodela, R, Nath, N, Dastagirzada, YM, Velázquez-Martínez, CA, Boring, D, Kashfi, K. Hydrogen sulfide-releasing NSAIDs inhibit the growth of human cancer cells: a general property and evidence of a tissue type-independent effect. Biochem. Pharm. 2012; 83: 715-722.
119. Kodela, R, Chattopadhyay, M, Kashfi, K. NOSH-Aspirin: A novel nitric oxide-hydrogen sulfide-releasing hybrid: A new class of anti-inflammatory pharmaceuticals. ACS medicinal chemistry letters. 2012; 3: 257-262.
120. Kashfi, K. Anti-cancer activity of new designer hydrogen sulfide-donating hybrids. Antioxid. Redox Signaling. 2014; 20: 831-846.

121. Muniraj, N, Ang, AD, Badiei, A, Rivers-Auty, J, Bhatia, M. Hydrogen Sulfide: A New Tool to Design and Develop Drugs. *Clinical Anti-Inflammatory & Anti-Allergy Drugs*. 2014; 1: 57-66.
122. Hine, C, Harputlugil, E, Zhang, Y, Ruckenstuhl, C, Lee, BC, Brace, L, Longchamp, A, Treviño-Villarreal, JH, Mejia, P, Ozaki, CK. Endogenous Hydrogen Sulfide Production Is Essential for Dietary Restriction Benefits. *Cell*. 2015; 160: 132-144.
123. Predmore, BL, Alendy, MJ, Ahmed, KI, Leeuwenburgh, C, Julian, D. The hydrogen sulfide signaling system: changes during aging and the benefits of caloric restriction. *Age*. 2010; 32: 467-481.
124. Miller, DL, Roth, MB. Hydrogen sulfide increases thermotolerance and lifespan in *Caenorhabditis elegans*. *PNAS*. 2007; 104: 20618-20622.
125. Zhang, Y, Tang, Z-H, Ren, Z, Qu, S-L, Liu, M-H, Liu, L-S, Jiang, Z-S. Hydrogen sulfide, the next potent preventive and therapeutic agent in aging and age-associated diseases. *Mol Cell Biol*. 2013; 33: 1104-1113.
126. Yong, R, Searcy, DG. Sulfide oxidation coupled to ATP synthesis in chicken liver mitochondria. *Comp. Biochem. Physiol. part B*. 2001; 129: 129-137.
127. Griesbeck, C, Hauska, G, Schütz, M. Biological sulfide oxidation: sulfide-quinone reductase (SQR), the primary reaction. *Recent research developments in microbiology*. 2000; 4: 179-203.
128. Kvalnes-Krick, K, Jorns, MS. Bacterial sarcosine oxidase: comparison of two multisubunit enzymes containing both covalent and noncovalent flavin. *Biochemistry*. 1986; 25: 6061-6069.
129. Wagner, MA, Khanna, P, Jorns, MS. Structure of the flavocoenzyme of two homologous amine oxidases: Monomeric sarcosine oxidase and N-methyltryptophan oxidase. *Biochemistry*. 1999; 38: 5588-5595.
130. Hughes, MN, Centelles, MN, Moore, KP. Making and working with hydrogen sulfide: the chemistry and generation of hydrogen sulfide in vitro and its measurement in vivo: a review. *Free Radical Biol. Med*. 2009; 47: 1346-1353.

131. Degli Esposti, M, Ferri, E, Lenaz, G. Spectroscopic properties of ubiquinones in model systems. *Ital. J. Biochem.* 1980; 30: 437-452.
132. Sörbo, B. A colorimetric method for the determination of thiosulfate. *Bioenergetics.* 1957; 23: 412-416.
133. Wood, JL. Sulfane sulfur. *Methods Enzymol.* 1987; 143: 25-29.
134. Ferrer, M, Chernikova, TN, Yakimov, MM, Golyshin, PN, Timmis, KN. Chaperonins govern growth of *Escherichia coli* at low temperatures. *Nat. Biotechnol.* 2003; 21: 1266-1267.
135. Kessi, J, Poirée, J-C, Wehrli, E, Bachofen, R, Semenza, G, Hauser, H. Short-chain phosphatidylcholines as superior detergents in solubilizing membrane proteins and preserving biological activity. *Biochemistry.* 1994; 33: 10825-10836.
136. Schwarzenbach, G, and Fischer, A. . Der Acidität der Sulfane and die Zusammensetzung wässriger Polysulfidlösungen. *Helv. Chim. Acta.* 1960; 43: 1365-1390.
137. Franzehör, F, Münzner, H. Beiträge zur Chemie des Schwefels, 62. Ultraviolett-Absorptionsspektren kettenförmiger Schwefelverbindungen. *Z. Anorg. Allg. Chem.* 1963; 96: 1131-1149.
138. Giggenbach, W. Optical spectra and equilibrium distribution of polysulfide ions in aqueous solution at 20°. *Inorg. Chem.* 1972; 11: 1201-1207.
139. Schneider, JF, Westley, J. Metabolic interrelations of sulfur in proteins, thiosulfate, and cystine. *J. Biol. Chem.* 1969; 244: 5735-5744.
140. LaRonde-LeBlanc, N, Resto, M, Gerratana, B. Regulation of active site coupling in glutamine-dependent NAD<sup>+</sup> synthetase. *Nature structural & molecular biology.* 2009; 16: 421-429.
141. Jarret, C, Stauffer, F, Henz, ME, Marty, M, Lüönd, RM, Bobálová, J, Schürmann, P, Neier, R. Inhibition of *Escherichia coli* porphobilinogen synthase using analogs of postulated intermediates. *Chem. Bio.* 2000; 7: 185-196.

142. Neuhaus, FC. The Enzymatic Synthesis of d-Alanyl-d-alanine II. Kinetic Studies on d-alanyl-d-alanine synthetase. *J. Biol. Chem.* 1962; 237: 3128-3135.
143. Huang, J, Khan, S, O'Brien, PJ. The glutathione dependence of inorganic sulfate formation from L-or D-cysteine in isolated rat hepatocytes. *Chem-Biol Interact.* 1998; 110: 189-202.
144. Koj, A, Frendo, J. Oxidation of thiosulphate to sulphate in animal tissues. *Folia Biol. (Krakow).* 1967; 15: 49-65.
145. Steiner, H, Jonsson, BH, Lindskog, S. The catalytic mechanism of carbonic anhydrase. *Eur J Biochem.* 1975; 59: 253-259.
146. Linden, D, Furne, J, Stoltz, G, Abdel-Rehim, M, Levitt, M, Szurszewski, J. Sulphide quinone reductase contributes to hydrogen sulphide metabolism in murine peripheral tissues but not in the CNS. *Br J Pharmacol.* 2012; 165: 2178-2190.
147. Viscomi, C, Burlina, AB, Dweikat, I, Savoiaro, M, Lamperti, C, Hildebrandt, T, Tiranti, V, Zeviani, M. Combined treatment with oral metronidazole and N-acetylcysteine is effective in ethylmalonic encephalopathy. *Nat. Med.* 2010; 16: 869-871.
148. Johnson-Winters, K, Nordstrom, AR, Emesh, S, Astashkin, AV, Rajapakshe, A, Berry, RE, Tollin, G, Enemark, JH. Effects of interdomain tether length and flexibility on the kinetics of intramolecular electron transfer in human sulfite oxidase. *Biochemistry.* 2010; 49: 1290-1296.
149. Kangas, J, Savolainen, H. Urinary thiosulphate as an indicator of exposure to hydrogen sulphide vapour. *Clinica chimica acta.* 1987; 164: 7-10.
150. Stipanuk, MH. Metabolism of sulfur-containing amino acids. *Annu. Rev. Nutr.* 1986; 6: 179-209.
151. Chen, ZW, Koh, M, Van Driessche, G, Van Beeumen, JJ, Bartsch, RG, Meyer, TE, Cusanovich, MA, Mathews, FS. The structure of flavocytochrome c sulfide dehydrogenase from a purple phototrophic bacterium. *Science.* 1994; 266: 430-432.
152. Williams Jr, CH. Lipoamide dehydrogenase, glutathione reductase, thioredoxin reductase, and mercuric ion reductase- a family of flavoenzyme transhydrogenases. In:

Muller F, editor. Chemistry and biochemistry of flavoenzymes. Boca Raton: CRC Press; 1992. p. 121-211.

153. Müller, F, Brüstlein, M, Hemmerich, P, Massey, V, Walker, WH. Light-Absorption Studies on Neutral Flavin Radicals. *Eur J Biochem.* 1972; 25: 573-580.

154. Ghisla, S, Thorpe, C. Acyl-CoA dehydrogenases-- A mechanistic overview. *Eur J Biochem.* 2004; 271: 494-508.

155. Wagner, MA, Trickey, P, Chen, Z-w, Mathews, FS, Jorns, MS. Monomeric sarcosine oxidase: 1. Flavin reactivity and active site binding determinants. *Biochemistry.* 2000; 39: 8813-8824.

156. Stewart, RC, Massey, V. Potentiometric studies of native and flavin-substituted Old Yellow Enzyme. *J. Biol. Chem.* 1985; 260: 13639-13647.

157. Williamson, G, Engel, PC, Mizzer, JP, Thorpe, C, Massey, V. Evidence that the greening ligand in native butyryl-CoA dehydrogenase is a CoA persulfide. *J. Biol. Chem.* 1982; 257: 4314-4320.

158. Jackson, MR, Melideo, SL, Jorns, MS. Human Sulfide: Quinone Oxidoreductase Catalyzes the First Step in Hydrogen Sulfide Metabolism and Produces a Sulfane Sulfur Metabolite. *Biochemistry.* 2012; 51: 6804-6815.

159. Grings, M, Moura, AP, Parmeggiani, B, Marcowich, GF, Amaral, AU, de Souza Wyse, AT, Wajner, M, Leipnitz, G. Disturbance of brain energy and redox homeostasis provoked by sulfite and thiosulfate: Potential pathomechanisms involved in the neuropathology of sulfite oxidase deficiency. *Gene.* 2013; 531: 191-198.

160. Kage, S, Ikeda, H, Ikeda, N, Tsujita, A, Kudo, K. Fatal hydrogen sulfide poisoning at a dye works. *Legal medicine.* 2004; 6: 182-186.

161. Chauncey, TR, Westley, J. The catalytic mechanism of yeast thiosulfate reductase. *J. Biol. Chem.* 1983; 258: 15037-15045.

162. Chauncey, TR, Westley, J. Improved purification and sulfhydryl analysis of thiosulfate reductase. *Biochim. Biophys. Acta.* 1983; 744: 304-311.



163. Uhteg, LC, Westley, J. Purification and steady-state kinetic analysis of yeast thiosulfate reductase. *Arch. Biochem. Biophys.* 1979; 195: 211-222.
164. Koj, A. Enzymic reduction of thiosulphate in preparations from beef liver. *Acta Biochim Pol.* 1968; 15: 161-169.
165. Foster, MW, Forrester, MT, Stamler, JS. A protein microarray-based analysis of S-nitrosylation. *PNAS.* 2009; 106: 18948-18953.
166. Weeks, SD, Drinker, M, Loll, PJ. Ligation independent cloning vectors for expression of SUMO fusions. *Protein Express Purif.* 2007; 53: 40-50.
167. Seelan, RS, Lakshmanan, J, Casanova, MF, Parthasarathy, RN. Identification of myo-Inositol-3-phosphate Synthase Isoforms Characterization, Expression and Putative Role of a 16-kDa  $\gamma$ c Isoform. *J. Biol. Chem.* 2009; 284: 9443-9457.
168. Mintel, R, Westley, J. The Rhodanese Reaction Mechanism of Sulfur-Sulfur Bond Cleavage. *J. Biol. Chem.* 1966; 241: 3381-3385.
169. Sorbo, B. On the acceptor specificity of rhodanese. *Acta Chem. Scand.* 1962; 16.
170. Galperin, MY, Koonin, EV. Who's your neighbor? New computational approaches for functional genomics. *Nat. Biotechnol.* 2000; 18: 609-613.
171. Zhang, L, Liu, X, Liu, J, Zhang, Z. Characteristics and function of sulfur dioxygenase in echiuran worm *Urechis unicinctus*. *PloS one.* 2013; 8: e81885.
172. Bamford, VA, Bruno, S, Rasmussen, T, Appia-Ayme, C, Cheesman, MR, Berks, BC, Hemmings, AM. Structural basis for the oxidation of thiosulfate by a sulfur cycle enzyme. *The EMBO journal.* 2002; 21: 5599-5610.
173. Kolker, E, Higdon, R, Haynes, W, Welch, D, Broomall, W, Lancet, D, Stanberry, L, Kolker, N. MOPED: model organism protein expression database. *Nucleic Acids Res.* 2012; 40: D1093-D1099.
174. Wang, M, Weiss, M, Simonovic, M, Haertinger, G, Schrimpf, SP, Hengartner, MO, von Mering, C. PaxDb, a database of protein abundance averages across all three domains of life. *Molecular & Cellular Proteomics.* 2012; 11: 492-500.

175. Wenzel, K, Felix, SB, Flachmeier, C, Heere, P, Schulze, W, Grunewald, I, Pankow, H, Hewelt, A, Scherneck, S, Bauer, D. Identification and characterization of KAT, a novel gene preferentially expressed in several human cancer cell lines. *Biol Chem.* 2003; 384: 763-775.
176. Finazzi Agrò, A, Federici, G, Giovagnoli, C, Cannella, C, Cavallini, D. Effect of sulfur binding on rhodanese fluorescence. *Eur J Biochem.* 1972; 28: 89-93.
177. Ploegman, JH, Drent, G, Kalk, KH, Hol, WG. The structure of bovine liver rhodanese: II. The active site in the sulfur-substituted and the sulfur-free enzyme. *J. Mol. Biol.* 1979; 127: 149-162.
178. Cipollone, R, Ascenzi, P, Visca, P. Common themes and variations in the rhodanese superfamily. *IUBMB life.* 2007; 59: 51-59.
179. Yadav, PK, Yamada, K, Chiku, T, Koutmos, M, Banerjee, R. Structure and kinetic analysis of H<sub>2</sub>S production by human mercaptopyruvate sulfurtransferase. *J. Biol. Chem.* 2013; 288: 20002-20013.
180. Griffith, OW. Biologic and pharmacologic regulation of mammalian glutathione synthesis. *Free Radical Biol. Med.* 1999; 27: 922-935.
181. Leonardi, R, Zhang, Y-M, Rock, CO, Jackowski, S. Coenzyme A: back in action. *Prog. Lipid Res.* 2005; 44: 125-153.
182. Tateishi, N, Higashi, T, Shinya, S, Naruse, A, Sakamoto, Y. Studies on the regulation of glutathione level in rat liver. *Journal of biochemistry.* 1974; 75: 93-103.
183. Ida, T, Sawa, T, Ihara, H, Tsuchiya, Y, Watanabe, Y, Kumagai, Y, Suematsu, M, Motohashi, H, Fujii, S, Matsunaga, T. Reactive cysteine persulfides and S-polythiolation regulate oxidative stress and redox signaling. *PNAS.* 2014; 111: 7606-7611.
184. Greiner, R, Pálinkás, Z, Bäsell, K, Becher, D, Antelmann, H, Nagy, P, Dick, TP. Polysulfides link H<sub>2</sub>S to protein thiol oxidation. *Antioxid. Redox Signaling.* 2013; 19: 1749-1765.
185. Francoleon, NE, Carrington, SJ, Fukuto, JM. The reaction of H<sub>2</sub>S with oxidized thiols: Generation of persulfides and implications to H<sub>2</sub> S biology. *Arch. Biochem. Biophys.* 2011; 516: 146-153.

186. Melideo, SL, Jackson, MR, Jorns, MS. Biosynthesis of a Central Intermediate in Hydrogen Sulfide Metabolism by a Novel Human Sulfurtransferase and its Yeast Ortholog. *Biochemistry*. 2014; 53: 4739-4753.
187. Kyle, C, Wilson, C. Mitochondrial DNA identification of game and harvested freshwater fish species. *Forensic Sci Int*. 2007; 166: 68-76.
188. Kramer, KJ, Kanost, MR, Hopkins, TL, Jiang, H, Zhu, YC, Xu, R, Kerwin, J, Turecek, F. Oxidative conjugation of catechols with proteins in insect skeletal systems. *Tetrahedron*. 2001; 57: 385-392.
189. Altschul, SF, Madden, TL, Schäffer, AA, Zhang, J, Zhang, Z, Miller, W, Lipman, DJ. Gapped BLAST and PSI-BLAST: a new generation of protein database search programs. *Nucleic Acids Res*. 1997; 25: 3389-3402.
190. Klotz, MG, Arp, DJ, Chain, PS, El-Sheikh, AF, Hauser, LJ, Hommes, NG, Larimer, FW, Malfatti, SA, Norton, JM, Poret-Peterson, AT. Complete genome sequence of the marine, chemolithoautotrophic, ammonia-oxidizing bacterium *Nitrosococcus oceanus* ATCC 19707. *Appl Environ Microbiol*. 2006; 72: 6299-6315.
191. Nevison, C, Butler, JH, Elkins, J. Global distribution of  $N_2O$  and the  $\Delta N_2O$ -AOU yield in the subsurface ocean. *Global Biogeochemical Cycles*. 2003; 17.
192. Libiad, M, Yadav, PK, Vitvitsky, V, Martinov, M, Banerjee, R. Organization of the human mitochondrial  $H_2S$  oxidation pathway. *J. Biol. Chem*. 2014; 289: 30901-30910.
193. Pierce, BS, Gardner, JD, Bailey, LJ, Brunold, TC, Fox, BG. Characterization of the nitrosyl adduct of substrate-bound mouse cysteine dioxygenase by electron paramagnetic resonance: electronic structure of the active site and mechanistic implications. *Biochemistry*. 2007; 46: 8569-8578.
194. Kowalchuk, GA, Stephen, JR. Ammonia-oxidizing bacteria: a model for molecular microbial ecology. *Annual Reviews in Microbiology*. 2001; 55: 485-529.
195. Joye, SB, Hollibaugh, JT. Influence of sulfide inhibition of nitrification on nitrogen regeneration in sediments. *Science*. 1995; 270: 623-625.

196. Bremner, J, Bundy, L. Inhibition of nitrification in soils by volatile sulfur compounds. *Soil Biology and Biochemistry*. 1974; 6: 161-165.
197. Berg, C, Vandieken, V, Thamdrup, B, Jürgens, K. Significance of archaeal nitrification in hypoxic waters of the Baltic Sea. *The ISME journal*. 2014.
198. Wang, M, Zhu, J, Pan, Y, Dong, J, Zhang, L, Zhang, X, Zhang, L. Hydrogen sulfide functions as a neuromodulator to regulate striatal neurotransmission in a mouse model of Parkinson's disease. *J Neurosci Res*. 2015; 93: 487-494.
199. Jackson, MR, Melideo, SL, Jorns, MS. Role of Human Sulfide: Quinone Oxidoreductase in H<sub>2</sub>S Metabolism. *Methods Enzymol*. 2015; 554: 255-270.
200. Togawa, T, Ogawa, M, Nawata, M, Ogasawara, Y, Kawanabe, K, Tanabe, S. High performance liquid chromatographic determination of bound sulfide and sulfite and thiosulfate at their low levels in human serum by pre-column fluorescence derivatization with monobromobimane. *Chemical & pharmaceutical bulletin*. 1992; 40: 3000-3004.
201. Ji, AJ, Savon, SR, Jacobsen, DW. Determination of total serum sulfite by HPLC with fluorescence detection. *Clin Chem*. 1995; 41: 897-903.
202. White, MM, Jorns, MS. Homology model of human sulfide:quinone oxidoreductase created using MODELLER 9.10 with flavocytochrome C sulfide dehydrogenase holoenzyme (1FCD.pdb) as template and refined using SCWRL4. unpublished results. 2012.
203. Gilbert, LA, Larson, MH, Morsut, L, Liu, Z, Brar, GA, Torres, SE, Stern-Ginossar, N, Brandman, O, Whitehead, EH, Doudna, JA. CRISPR-mediated modular RNA-guided regulation of transcription in eukaryotes. *Cell*. 2013; 154: 442-451.

## Vita

Scott L. Melideo

### Education

Drexel University College of Medicine, Philadelphia, PA  
Ph.D. Biochemistry, 2015

The University of Scranton, Scranton, PA  
Bachelor of Science Degree, Biochemistry, 2010

### Publications (\*co-first authors)

- S.L. Melideo\*, Jackson, M.R.\*, and M.S. Jorns. (2014). Biosynthesis of a Central Intermediate in Hydrogen Sulfide Metabolism by a Novel Human Sulfurtransferase and its Yeast Ortholog. *Biochemistry*, 53 4739-4753.
- Jackson, M.R.\*, S.L. Melideo\*, and M.S. Jorns. (2012). Human Sulfide: Quinone Oxidoreductase Catalyzes the First Step in Hydrogen Sulfide Metabolism and Produces a Sulfane Sulfur Metabolite. *Biochemistry*, 51 6804-6815.
- Jackson, M.R., S.L. Melideo, and M.S. Jorns. (2015). Chapter Fourteen – Role of Human Sulfide: Quinone Oxidoreductase in H<sub>2</sub>S Metabolism. *Methods of Enzymology*, 554 255-270.
- P. Loll, P. Xu, J. Schmidt and S.L. Melideo (2014). Enhancing ubiquitin crystallization through surface entropy reduction. *Acta Cryst*, F70 1434-1442.
- Foley, T.D., S.L. Melideo, A.E Healey, E.J. Lucas, & J.A. Koval (2011). Phenylarsine Oxide Binding Reveals Redox-Active and Potential Regulatory Vicinal Thiols on the Catalytic Subunit of Protein Phosphatase 2A. *Neurochemical research*, 36 232-240.

### HONORS AND AWARDS

- Co-President of Drexel University Graduate Student Association (2013-2014)
- Who's Who Among College Students, Drexel University (2013)
- Father Fitzpatrick Award (2010)
- Landmark Conference Academic honor roll (2010)
- President of The University of Scranton University Student-Athlete Advisory Committee (2009-2010)
- Vice-President of The University Scranton Chemistry/Biochemistry club (2009-2010)
- Landmark Conference Student-Athlete Advisory Committee (2007-2010)
- Captain of The University of Scranton men's tennis team (2007-2010)

